

Cardiomyocyte Survival Pathways

Intracellulaire signaalwegen ter overleving van de cardiomyocyt

(with a summary in English)

Proefschrift ter verkrijging van de graad van doctor aan de Universiteit Utrecht op gezag van de Rector magnificus, Prof.dr. W.H. Gispen, ingevolge het besluit van het College voor Promoties in het openbaar te verdedigen op dinsdag 18 mei 2004 des ochtends te 10:30 uur

door Daniel Jozef Lips
geboren op 15 oktober 1978 te Hwidiem (Ghana)

Promotores:

Prof. A. Brutel de la Rivière, Hart-Long Instituut Utrecht

Prof. H.J.J. Wellens, emeritus-hoogleraar Universiteit Maastricht

Co-promotor:

Dr. P.A.F.M. Doevendans, Hart-Long Instituut Utrecht

Het verschijnen van dit proefschrift werd mede mogelijk gemaakt door steun van de Nederlandse Hartstichting en Medtronic – Bakken Research Center.

Financial support by the Netherlands Heart Foundation and Medtronic – Bakken Research Center for the publication of this thesis is gratefully acknowledged.

Contents

Preface

Chapter 1 The use of transgenic animals to assess cardiac remodeling

Chapter 2 Molecular determinants of myocardial hypertrophy and failure

Chapter 3 Left ventricular pressure-volume measurements in mice

Chapter 4 The MEK1-ERK2 signaling pathway protects the myocardium from ischemic damage in vivo

Chapter 5 Calcineurin A β gene targeting predisposes the myocardium to acute stress-induced apoptosis and dysfunction

Chapter 6 GSK-3 β overexpression attenuates hypertrophy and sensitizes the heart to ischemic damage and dysfunction

Chapter 7 Discussion

Summary

Samenvatting

Curriculum vitae

List of publications

Acknowledgements / Dankbetuigingen

Preface

Cardiovascular diseases account for the majority of disease-related deaths in the modern Western world. Coronary artery disease causes up to 66% of these cases. The typical patient at risk presents with the signs of an acute myocardial infarction due to progressive coronary atherosclerosis. The patient endures large scale loss of ventricular myocardium through cell death during this medical emergency. Current therapeutic tools for the treatment of myocardial infarction include reperfusion by thrombolytic therapy or revascularization through balloon angioplasty or bypass surgery. The majority of patients admitted for acute myocardial infarction will not only suffer from the detrimental effects of ischemia, but also from those of additional reperfusion related injury. Despite improved treatment modalities, the prevention of atherosclerosis and myocardial infarction is obviously the main target. Therefore, the policy of governmental and healthcare institutions shifts towards preventive medicine. In the meantime it is of the utmost importance to develop strategies to limit myocardial damage due to ischemia and reperfusion. The scientific work performed on human stem cells could provide a spectacular breakthrough in daily practice. However, standard therapeutic implications are not expected in the nearby future.

Another branch of experimental cardiology focuses on molecular interventions. Through direct intervention in active and vital intracellular signaling cascades beneficial cellular responses could be stimulated, while maladaptive responses could be inhibited. The experiments described in this thesis explore the possibility to intervene in the intracellular signaling cascades involved in apoptotic cell death during myocardial ischemia-reperfusion. The aims of the studies presented here were defined as follows:

Aim 1: *to investigate the possibility of inhibiting the process of ischemia-reperfusion induced cardiomyocyte apoptosis through molecular intervention, by genetic modification, in the MEK1-ERK1/2 and calcineurin-NFAT pathways.*

Aim 2: A. *to develop a protocol for in vivo closed-chest left ventricular pressure-volume (PV) assessment.*

B. *to determine the effects of molecular intervention in ischemia-reperfusion induced apoptosis on cardiac performance by closed-chest PV relationship measurements.*

Chapter one reviews the contribution of genetically engineered mice in the elucidation of molecular pathways in cardiac remodeling. The concept of murine genome engineering enabled researchers to investigate the spectrum of functions of various proteins involved in the intracellular signaling pathways mediating processes as hypertrophy and apoptosis. The techniques of gene targeting have been improved allowing inducible, cell type specific gene deletion and overexpression experiments. Furthermore, the tools to measure murine cardiac function have been extended with pressure volume (PV-loop) relationship recordings and magnetic resonance imaging. This chapter reviews the contribution of genetically engineered mice to the elucidation of molecular pathways in cardiac remodeling.

Chapter two reviews the molecular pathways active at the onset and during development of hypertrophy, and the progression into heart failure. Conventional views identify myocardial hypertrophy as a compensatory response to increased workload, prone to evoke end-stage heart disease. Recent findings in genetic models of myocardial hypertrophy and human studies have provided the molecular basis for a novel concept, which favors the existence of either compensatory or maladaptive forms of hypertrophy, of which only the latter leads to cardiac failure. Furthermore, the concept that hypertrophy compensates for

augmented wall stress is probably outdated. Here we have been able to provide the molecular pathways that can distinguish beneficial from maladaptive hypertrophy.

Genetically engineered mice are extensively used in cardiovascular research. The *in vivo* assessment of cardiac performance demands accurate measuring methods. *In vivo* left ventricular PV-loop measurements provide an essential tool in the assessment of cardiac function in genetically modified mice. PV-loops adequately represent cardiac function and provide load and heart rate independent parameters of intrinsic myocardial contractility and relaxation. Changes in ventricular contractility are best detected by PV derived parameters in comparison to other methods of cardiac function determination. The concept of *in vivo* open- and closed-chest left ventricular PV-loops is highlighted in chapter three.

The results from studies concerning the mitogen-activated protein kinase kinases (MEK)1- extracellular signal-regulated kinases (ERK)1/2 pathway in genetically modified mice are discussed in chapter four. While MEK1-ERK1/2 signaling is thought to protect the myocardium from apoptotic insults, definitive genetic data demonstrating a necessary function for MEK1-ERK1/2 signaling have not been reported. Here we analyzed deficiency of the ERK 1 and 2 gene, in *Erk1*^{-/-} and *Erk2*^{+/-} gene targeted mice, as well as MEK1 transgenic mice to evaluate both gain- and loss-of-function phenotypes in relation to cardiomyocyte cell survival. *Erk2* heterozygote mice showed enhanced apoptosis following ischemia-reperfusion injury, while transgenic mice expressing activated MEK1 in the heart were significantly protected. These results provide definitive genetic data implicating ERKs as beneficial effectors of myocyte survival following myocardial stress stimulation.

The calcineurin-nuclear factor of activated T-cells (NFAT) pathway in cardiomyocyte apoptosis is the main subject of chapter five. In this chapter, we discuss the role of calcium calmodulin-activated protein phosphatase calcineurin (PP2B) in modulating cardiac apoptosis after acute ischemia-reperfusion injury to the heart. *Calcineurin A β* gene-targeted mice

showed a greater loss of viable myocardium, enhanced DNA degradation and a greater loss in functional performance compared with strain-matched wild-type control mice after ischemia-reperfusion injury. These results represent the first genetic loss-of-function data showing a prosurvival role of calcineurin-NFAT signaling in the heart.

Another approach to investigate the role of calcineurin-NFAT in ischemia-induced cardiomyocyte apoptosis, focusing on the endogenous inhibitor of the calcineurin-NFAT pathway, i.e. glycogen synthase kinase (GSK)-3 β , is described in chapter six. In *GSK-3 β* transgenic mice ischemia-reperfusion led to an 85% enlargement of the infarct areas compared to wildtype littermates. Hypertrophic growth was attenuated in transgenic animals following I/R. Finally, as a result of ischemia, cardiac functional deterioration was more pronounced in *GSK-3 β* transgenic mice than in wildtype mice. GSK-3 β acts as a central modifier in antihypertrophic and proapoptotic signaling pathways. Future research should be performed to elucidate the possible clinical value of GSK-3 β in cardiac hypertrophy and ischemia.

In chapter seven the findings of our studies are positioned within current knowledge concerning ischemia-induced apoptosis and molecular cardiomyocyte survival pathways. Here the clinical relevance of our findings for the daily cardiology clinic is discussed, and directions are provided for future reference.

Chapter 1. Transgenic mice and cardiac remodeling

The use of transgenic animals to assess cardiac remodeling

Daniel J. Lips, Rutger Hassink, Aart Brutel de la Rivière and Pieter A. Doevendans

In modified version published in textbook *Myocardial Remodeling*, ed. B.H.

Greenberg.

Abstract

Cardiac remodeling is defined by structural, electrical and concomitant functional alterations in the heart upon specific extrinsic and intrinsic stimuli. Pathophysiological situations as hypertension, volume-overload and especially myocardial ischemia induce the process of cardiac remodeling characterized by hypertrophic growth, global or local ventricular dilatation, deposition of collagen and apoptosis of cardiomyocytes. Cardiac remodeling has been investigated extensively in animal and human studies. The concept of genetic engineering of murine DNA enabled researchers to investigate the spectrum of specific functions of proteins in the intracellular signaling pathways mediating processes as hypertrophy and apoptosis. The techniques of gene targeting have been improved allowing inducible, cell type specific gene deletion experiments. Furthermore the tools to measure murine cardiac function have been extended with pressure volume relationship recording and magnetic resonance imaging. This chapter reviews the contribution of genetically engineered mice in the elucidation of molecular pathways in cardiac remodeling.

Introduction

Cardiac remodeling describes the adaptive response of the myocardium in response to pathophysiological changes. The remodeling process can be measured at different levels. First of all, the composition of myocardial tissue will change in response to injury. Concomitantly, the left ventricular contractile function and relaxation pattern adapt. The mechanism of remodeling, albeit adaptive or maladaptive, can be studied at the organ, cellular or molecular level. To unravel the importance of various signaling pathways and specific proteins, often gene targeting studies are being performed in rodents, predominantly mice.(1) In mice, the plain effect of transgenesis (adding genes) or gene targeting (replacing genes) on left ventricular morphology and function can be assessed. (2-4) Specific alterations in individual genes result in (A) the absence of selected proteins (i.e. knockout); (B) abundance of a selected protein (i.e. overexpression); (C) truncated and/or dysfunctional proteins with a potential dominant-negative effect (D) introduction of constitutively active proteins (dominant-positive). Because single genes are targeted, it is possible to elucidate the specific functions of the corresponding protein in intracellular signaling pathways. All aspects of cardiac remodeling can be investigated through this approach. In addition, surgical interventions can be applied to induce pathology, including aortic banding, myocardial infarction (MI) or ischemia/reperfusion (I/R). By systematic application of these surgical interventions to various recently generated mouse lines, several crucial pathways have been recognized and subsequently unraveled step by step. (5) The importance of genes involved in post-ischemic cardiac remodeling, hypertrophy and heart failure, and pro- and anti-apoptotic pathways have been studied. A fascinating observation is the close relationship between various intracellular signaling events during distinct pathogenic conditions. For instance the family of mitogen-activated protein kinases (MAPK) was described as a group of crucial molecules for the development of hypertrophy in the heart. (6-8) More recent studies outlined their protective role

Chapter 1. Transgenic mice and cardiac remodeling

in ischemia-induced apoptosis. (9,10) The reverse is true for the Akt protein. Initially identified as a prosurvival protein (11), a potential role in ischemic heart disease and even dilated cardiomyopathy has been proposed recently.(12) The conclusion can be drawn that intracellular pathways may result in distinct cellular outcomes depending on the specific pathophysiological situation. Moreover, the myocyte response is not solely determined by activation of a single pathway, but by the relative activity of various simultaneous acting signaling molecules. Part of the complexity involved can be elucidated by using more advanced genetic models in the adult mouse where genes can be activated or repressed at will by the investigator. For example the tamoxifen-induced cardiomyocyte-specific and temporally regulated gene-expression in a Mer-Cre-Mer based mouse model, can be used to delete a floxed gene. (13) This is an example of an inducible tissue specific knock-out approach. Here we will focus on the most recent information available on cardiac remodeling. The most important aspect of remodeling is its effect on cardiac function, as the morphological changes are less crucial for the final outcome or prognosis compared to functional changes in man and mouse alike.

Figure 1

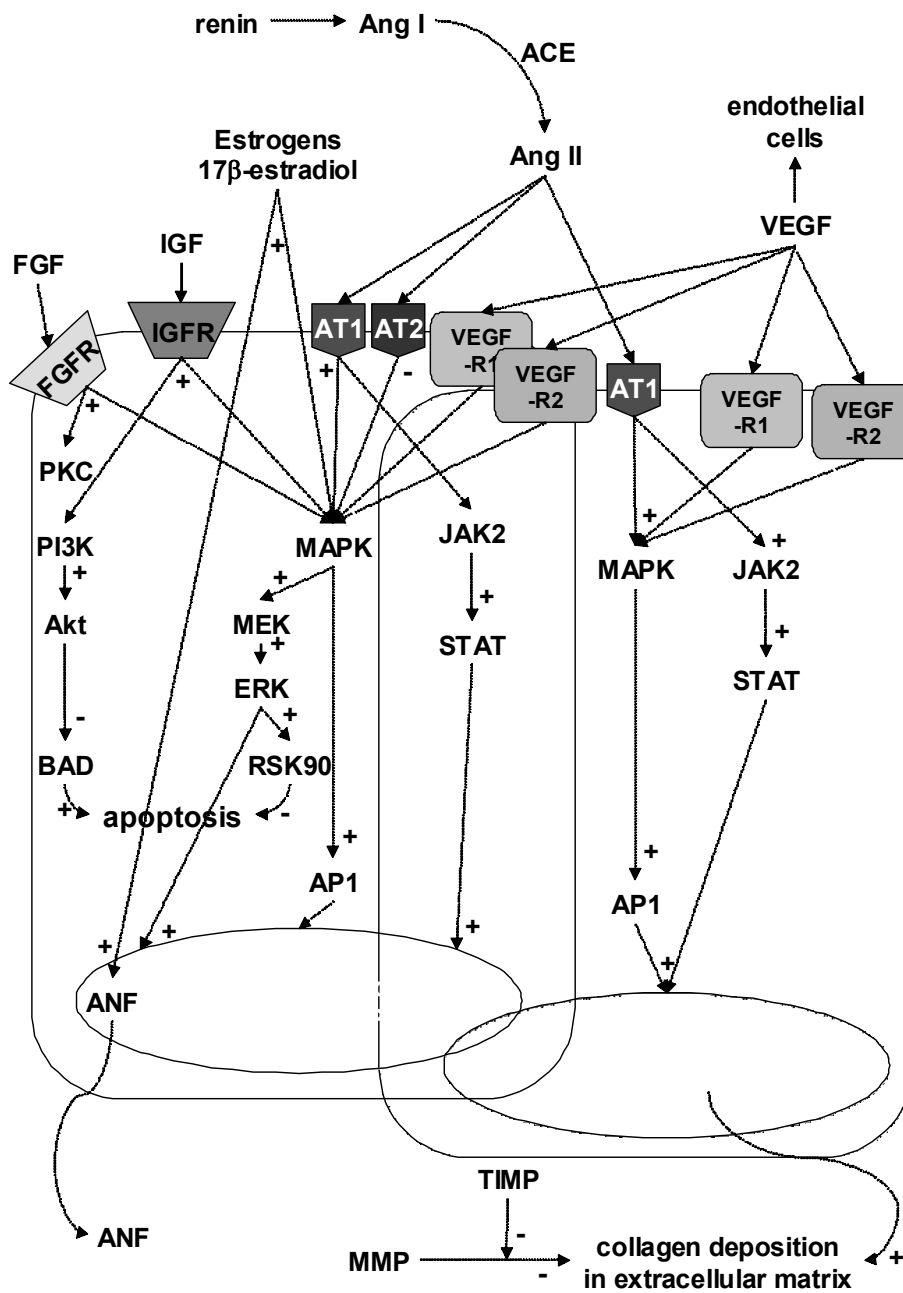


Fig. 1: Signaling pathways in cardiac remodeling. Several intracellular signaling pathways involved in the cellular adaptation of cardiac remodeling are shown. The figure presents the signaling pathways as discussed in the text. Activation or inhibition of single molecules are indicated by respectively (+) and (-).

Cardiac remodeling and myocardial ischemia

Cardiac remodeling is defined by the structural and concomitant functional alterations in the heart after an ischemic event. The ischemia-induced architectural remodeling encompasses ventricular dilatation, myocardial hypertrophy, deposition of collagen and apoptosis in the area-at-risk-(for-ischemia) and the remote myocardium. Cardiac remodeling in man occurs classically within 2 to 4 weeks following the ischemic event, characterized by an enlargement of ventricular dimensions or volumes (end-diastolic and –systolic dimensions) combined with a decrease in left ventricular ejection fraction and increase in mass-index. Even nowadays, in the era of aggressive medical therapy for ischemic heart disease and during acute myocardial infarction, cardiac remodeling remains important for long term cardiac function. (14) Current therapy of acute myocardial infarction in the human can attenuate ventricular volume enlargement and dilation at 1 month following the ischemic event, coinciding with improvement of left ventricular geometry and cardiac function as defined by left ventricular ejection fraction. (14) But more importantly, cardiac death and hospitalization for clinical heart failure are still significantly higher in patients with left ventricular remodeling following ischemia as compared to patients without. (15) Thorough investigation into the prevention of adverse effects of cardiac remodeling has become vital in daily cardiological practice.

Cardiac remodeling has been investigated extensively in animals (16-18) and humans, using imaging techniques such as echocardiography (19), computer tomography (CT) (20), radionuclide ventriculography (21) and recently magnetic resonance imaging (MRI) (14,22). With the development of genetically altered mice an intense interest arose for murine models of I/R and MI. (16,23) Through genetic engineering it is possible to elucidate the spectrum of specific functions of single proteins in the intracellular signaling pathways involved in ischemia(-reperfusion) injury. Mouse models of ischemia following the occlusion of the left anterior

Chapter 1. Transgenic mice and cardiac remodeling

descending coronary artery permanently (MI) or temporarily (I/R), allow assessment of the process of cardiac remodeling. These experimental studies showed the important roles of the renin-angiotensin-system (RAS), androgenic hormones, growth factors, and tissue-matrix components in both acute and chronic remodeling (figure 1).

The importance of the renin-angiotensin axis originates from its role in cardiomyocyte hypertrophy and induction of fibrosis. The effector protein of the RAS is angiotensin II (Ang II). All the components necessary to generate Ang II are present in the myocardium and cardiac Ang II formation, from angiotensin I by angiotensin converting enzyme (ACE), appears to be regulated independent of the systemically circulating ACE. (24) Ang II induces hypertrophic growth mostly through the angiotensin 1 (AT1) receptor. (25) Activation of this G-protein coupled receptor initiates the expression of growth-related genes through mitogen-activated protein kinases (MAPK) and the family of Janus kinase /signal transducer and activator of transcription (JAK/STAT) proteins dependent pathways. (26) Most prohypertrophic stimuli mediated by Ang II are also instigators of cardiac fibroblasts proliferation leading to formation of excessive collagen in the myocardial interstitium. (27) The remodeling process is dependent on the amount of collagen deposition in both the ischemic area and the remote myocardium. Inhibition of Ang II reduces the amount of collagen deposition and improves cardiac function during the remodeling phase. Genetically altered mouse models have been the key in elucidating the specific roles for the RAS components. For instance, AT1a receptor knockout mice displayed less left ventricular remodeling and improved survival after MI. (28) In contrast to the AT1 receptor, the AT2 receptor has an inhibitory regulatory effect on MAPK and JAK/STAT activity. Therefore, cardiac AT2 receptor overexpression led to preservation of left ventricular performance during post-MI remodeling thereby reducing early mortality after MI. (24,29)

Chapter 1. Transgenic mice and cardiac remodeling

Growth factors stimulate various cell types into hyperplastic or hypertrophic responses, and initiate angiogenesis. These cellular functions enable growth factors to protect the heart from deleterious remodeling and impaired cardiac performance. An important role for these factors could have been anticipated as ischemia results in the loss of significant amounts of cardiomyocytes, providing a trigger for regeneration and growth. Insulin-like growth factor (IGF) is an endogenous protector of cardiomyocytes and induces prosurvival processes *ex* and *in vivo*. In IGF-1 knockout mice myocardial ischemia resulted in the attenuation of DNA synthesis and an augmentation of apoptosis rates. (30) Mice lacking isoforms of the vascular endothelial growth factor (VEGF) showed impaired angiogenesis and worsened cardiac performance following myocardial ischemia. (31,32) The fibroblast growth factor (FGF) is produced by cardiomyocytes and fibroblasts. FGF mainly stimulates cellular proliferation and deposition of collagen. The degradation of collagen is started within minutes from the start of ischemia, mainly of collagen type 1. Loss of the myocardial collagen-network thins the infarcted myocardium that expands during systole and promotes cardiac rupture and dilation of the left ventricle. After 5 days the initial degradation of collagen is followed by the deposition of newly formed collagen produced by the cardiac fibroblasts stimulated by FGF. Cardiac-specific overexpression of human FGF delays infarct development due to a higher expression of prosurvival ERK1/2 signaling pathways. (33) These studies therefore demonstrate the importance of growth factors during the remodeling phase as they mediate proliferative processes.

Both the RAS and growth factors are involved in the induction of fibrosis and highlight extracellular collagen organization as an important feature of cardiac remodeling. These extracellular matrix degrading enzymes, belonging to the families of serine and matrix metalloproteinases (MMP), are activated following MI. (34) MMP's belong to the only proteinase enzymes capable of degrading collagen. Targeted deletion of MMP-9 attenuated left

Chapter 1. Transgenic mice and cardiac remodeling

ventricular enlargement and increased myocardial collagen content following infarction, leading to a decreased incidence of cardiac rupture. (35,36) Moreover, uncontrolled MMP activity as seen by tissue-inhibitor of MMP (TIMP)-1 deficient mice, demonstrated amplified adverse left ventricular remodeling (i.e. significant loss of fibrillar collagen) following MI, thereby emphasizing the importance of local endogenous control of cardiac MMP activity. (37) Adequate control of collagen organization is reflected by the main physiological functions of the interstitial collagen network: to retain tissue integrity and cardiac pump function. (34) The RAS, growth factors and extracellular matrix molecules are of vital importance in maintaining these functions following an ischemic event.

Several other intriguing factors have been shown to be involved in post-ischemic remodeling. Interesting data suggest that estrogens prevent deterioration of cardiac function and remodeling after MI, while testosterone on the other hand worsened cardiac dysfunction and remodeling. (38) Moreover, estrogen replacement therapy reduces infarct size and cardiomyocyte apoptosis in mice. (39) In accordance with the beneficial effects post-ischemia, estrogens are also believed to mediate hypertrophy reducing effects predominantly by the estrogen- β receptor. (40,41) Survival pathways mediated by estrogens involve probably atrial natriuretic peptide (ANP) expression. (42) Molecular substrates are now uncovered through studies in gene targeted mice missing specific sex hormone receptors. Newly detected substrate or molecular interactions could provide the biological explanations for the generally observed sex differences in cardiovascular response to pathological conditions.

Figure 2

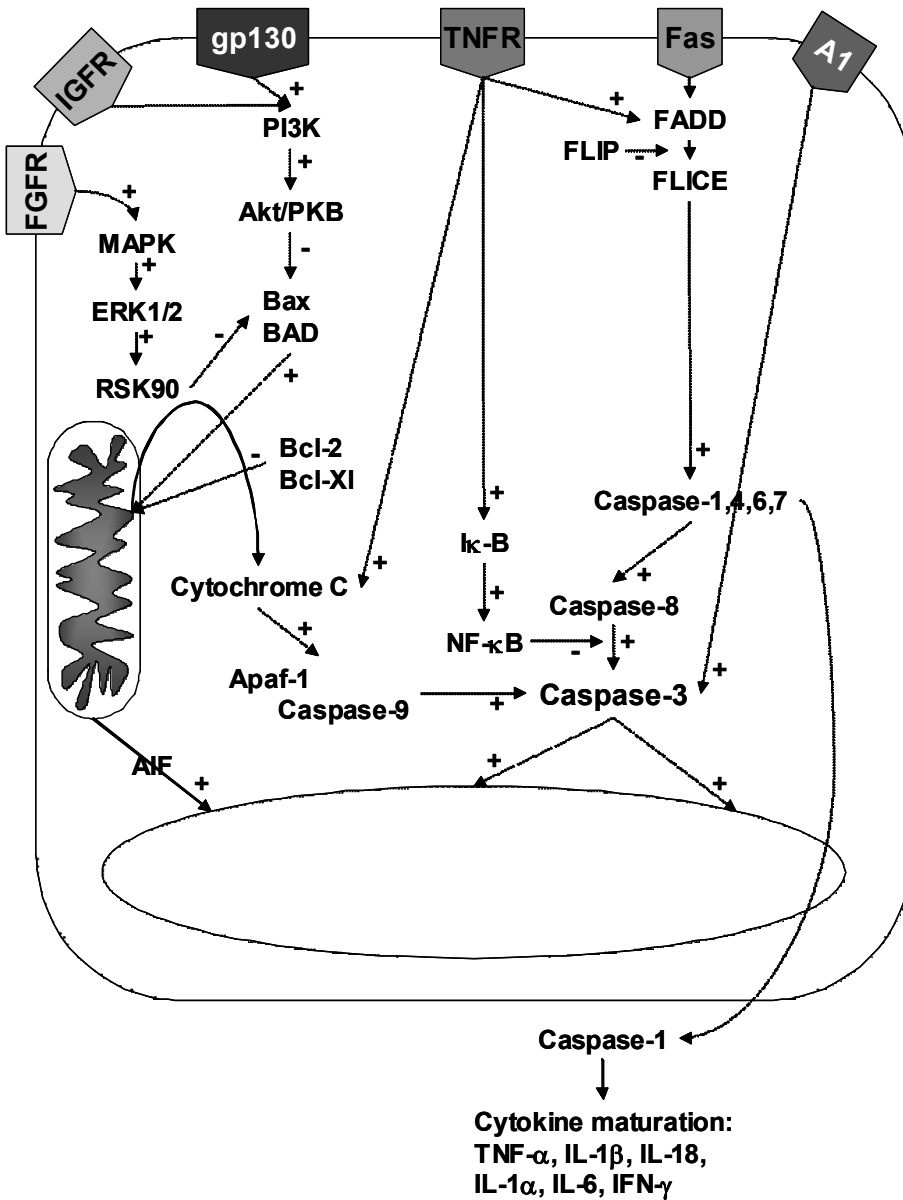


Fig. 2: Signaling pathways in cardiomyocyte apoptosis. The figure presents the signaling pathways as discussed in the text. Activation or inhibition of single molecules are indicated by respectively (+) and (-).

Myocardial ischemia and apoptosis

Myocardial ischemia will lead to the loss of cardiomyocytes by three different mechanisms: necrosis, apoptosis and autophagic cell death. Necrosis is well characterized by cell swelling, disruption of cell organelles and cell membranes, and an inflammatory tissue reaction. In apoptosis (i.e. programmed cell death) the cell undergoes shrinkage, nuclear chromatin condensation and formation of apoptotic bodies, which are removed by macrophages without eliciting inflammation. (43) In contrast to necrosis, apoptosis is an energy-requiring and multiprotein involving process. Various molecular cascades lead to the degradation of nuclear DNA. Autophagic cell death is another form of programmed cell death and seems to be of importance in heart failure. (44) Like apoptosis, autophagic cell death is regulated and associated with DNA fragmentation. Unlike apoptosis, it is caspase-independent and morphologically it resembles necrosis.

Many proteins and enzymes have been linked to the regulation of programmed cell death under pathological conditions (figure 2). Deprivation of serum and glucose, hallmark of ischemia *in vivo*, results in cardiomyocyte apoptosis. (45) Ischemia-induced apoptosis is characterized by cytochrome C release from the mitochondria into the cytosol after 30-60 minutes by the opening of the mitochondrial permeability transition (MPT) pores. (46,47) Cytochrome C release can be inhibited by anti-apoptotic members of the Bcl-2 family, such as Bcl-2 and Bcl-xL, or stimulated by pro-apoptotic members like Bad and Bax. Once released into the cytosol, cytochrome C binds to the apoptotic protease-activating factor (Apaf)-1. (47) The cytochrome C/Apaf-1 complex activates pro-apoptotic molecules like caspase-9 eventually leading to the activation of the main effector caspase, caspase-3. Caspases are the specialized cysteine-dependent proteases that cleave major structural proteins of the cytoplasm and nucleus. (47) Secondly, apoptosis can be induced via so-called death receptors (Fas and TNF- α), resulting in the recruitment of a death domain and

Chapter 1. Transgenic mice and cardiac remodeling

activation of caspase-8 and effector-caspases. Fas activation induces apoptosis in cardiac myocytes. Lymphoproliferative (lpr) mice that lack functional Fas exhibit smaller infarcts with concomitant linear decrements in myocyte apoptosis. (48) Repressor domains and other inhibitory proteins like FLIP (Fas-associated death domain protein -like interleukin 1 β -converting enzyme [FLICE]/caspase-8-inhibitory protein), are able to block apoptosis via the death receptors. The two pathways come together downstream as a common pathway at the level of the effector caspases, such as caspase-3. The generation of caspase-knockout mice by homologous recombination provided the possibility to study the role of individual caspase proteins. (49)

Apoptosis can be assessed by several methods, like electron microscopy, terminal deoxynucleotidyl transferase-mediated dUTP nick end labeling (TUNEL) or in situ end labeling (ISEL) methods for identification of DNA fragments, Annexin-V staining (50), or by the appearance of DNA laddering in gel electrophoresis. Technical and experimental difficulties, however, have to be taken into account, since overestimation of the number of apoptotic cardiomyocytes (false-positives) and misinterpretation of electron microscopic photos are pitfalls in these studies.

Table 1. Mouse models used in cardiac remodeling.

Molecular target	Genetic modification	Phenotype	Reference
<i>CARDIAC REMODELING</i>			
AT1a receptor	Knockout	Less LV remodeling, improved survival	Harada K, et al. Circulation 1999 ²⁸
AT2 receptor	Overexpression	Less LV remodeling, improved survival	Oishi Y, et al. Hypertension 2003 ²⁹
	Knockout	No different cardiac remodeling	Xu J, et al. Hypertension 2002 ²⁵
IGF-1	Knockout	Attenuation DNA synthesis, higher apoptosis rates	Palmen M, et al. Cardiovasc Res 2001 ³⁰
	Overexpression	Smaller infarctions, lower apoptosis rates	Li O, et al. JCI 1997 ⁷⁰
VEGF	Knockout	Deterioration cardiac function, impaired angiogenesis	Carmeliet P, et al. Nat Med 1999 ³¹
FGF-1	Overexpression	Delayed infarct development, prosurvival cellular signaling	Buehler A, et al. Cardiovasc Res 2002 ³³
MMP-9	Knockout	Attenuated LV enlargement, augmented collagen deposition	Ducharme A, et al. J Clin Invest 2000 ³⁵
TIMP-1	Knockout	Loss of fibrillar collagen	Creemers E, et al. AJP 2003 ³⁷
<i>APOPTOSIS AND HYPERTROPHY</i>			
Fas	Non-functional	Smaller infarction, lower apoptosis rate	Lee P, et al. AJP 2003 ⁴⁸
Caspase-3	Overexpression	Larger infarction, higher apoptosis rate	Condorelli G, et al. PNAS 2001 ⁵⁵
Bax	Knockout	Smaller infarction, lower apoptosis rate	Hochhauser E, et al. AJP 2003 ⁵⁶
Mst1	Overexpression	Higher apoptosis rate, abolishment cardiac hypertrophy	Yamamoto S, et al. JCI 2003 ⁵⁷
	Dominant-negative overexpression	Smaller infarction, lower apoptosis rate	
A1 adenosine receptor	Overexpression	Smaller infarction, lower apoptosis rate	Regan S, et al. AJP 2003 ⁵⁸
Caspase-1	Knockout	Smaller infarction, lower apoptosis rate	Frantz S, et al. JMCC 2003 ⁶²

Chapter 1. Transgenic mice and cardiac remodeling

TNF receptor	Knockout	Larger infarction, higher apoptosis rate	Kurrelmeyer K, et al. PNAS 2000 ⁶⁵
TNF- α	Knockout	Smaller infarction	Maekawa N, et al. JACC 2002 ⁶⁶
gp130	Overexpression	Cardiac hypertrophy	Hirota H, et al. PNAS 1995 ⁷⁶
	Dominant-negative overexpression	Attenuated hypertrophic response	Uozumi H, et al. JBC 2001 ⁷⁷
	Knockout	Progressive pressure-induced cardiomyopathy, augmented apoptosis rates	Hirota H, et al. Cell 1999 ¹¹³
STAT3	Overexpression	Cardiac hypertrophy	Kunisada K, et al. PNAS 2000 ⁸⁰
MEKK1	Knockout	Abolishment of cardiac hypertrophy, attenuated hypertrophic response	Minamino T, et al. PNAS 2002 ⁸¹ Sadoshima J, et al. JCI 2002 ⁸⁸
MKP-1	Overexpression	Diminished developmental myocardial growth, attenuated hypertrophic response	Bueno O, et al. Circ Res 2001 ⁸⁴
MEK1	Overexpression	Concentric cardiac hypertrophy	Bueno O, et al. EMBO J 2000 ⁶
		Smaller infarction, lower apoptosis rate	Lips D, et al. 2003 ¹⁰
MEK5	Overexpression	Eccentric cardiac hypertrophy, sudden death	Nicol R, et al. EMBO J 2001 ⁸⁵
JNK	Inducible overexpression of MKK7D	Progressive cardiomyopathy	Petrich B, et al. FASEB J 2003 ¹³
p38	Inducible overexpression of MKK3bE or MKK6bE	Restrictive cardiomyopathy, heterogeneous myocyte atrophy	Liao P, et al. PNAS 2001 ⁷
p38 α	Dominant-negative overexpression	Hypertrophic cardiomyopathy	Braz J, et al. JCI 2003 ⁹²
Calcineurin	Overexpression	Cardiac hypertrophy	Molkentin J, et al. Cell 1998 ⁹⁴
		Sudden cardiac death	Dong D, et al. CVR 2003 ⁹⁵
		Smaller infarction, lower apoptosis rate	De Windt, et al. Circ Res 2000 ⁹⁶
	Dominant-negative overexpression	Attenuated adrenergic-stimulated hypertrophic response	Zou Y, et al. Circ 2001 ⁹⁷

Chapter 1. Transgenic mice and cardiac remodeling

		Attenuated pressure-induced hypertrophic response	Zou Y, et al. <i>Circ</i> 2001 ⁹⁸
Calcineurin A β	Knockout	Larger infarction, higher apoptosis rate	Bueno O, et al. 2003 ¹¹⁶
NFAT3c	Knockout	Abolishment of cardiac hypertrophy, attenuated hypertrophic response	Wilkins B, et al. <i>MCB</i> 2002 ¹⁰⁰
MCIP-1	Overexpression	Attenuated hypertrophic response	Rothermel B, et al. <i>PNAS</i> 2001 ¹⁰³
	Knockout	Exacerbated hypertrophic response	Vega R, et al. <i>PNAS</i> 2003 ¹⁰⁵
GSK-3 β	Overexpression	Abolishment of cardiac hypertrophy	Antos C, et al. <i>PNAS</i> 2002 ¹⁰⁶
Cain/cabin	Overexpression	Attenuated hypertrophic response	De Windt, et al. <i>PNAS</i> 2001 ¹⁰⁷
A-kinase anchoring protein	Overexpression	Attenuated hypertrophic response	De Windt, et al. <i>PNAS</i> 2001 ¹⁰⁷

Mouse models in cardiac remodeling as discussed in the text and figures. Abbreviations used are explained in the text. Models are listed in order of appearance in the text.

Apoptosis in ischemia-reperfusion

Notwithstanding cell necrosis being pathognomic for acute MI, apoptosis represents the major form of cell death in continuing ischemia. (51) Prolonged periods of myocardial ischemia are causing an increase in the rate of necrosis, whereas, reperfusion leads to an enhancement in apoptosis. (52) Essentials for the survival of viable cells are provided when reperfusion restores oxygen and glucose supply, thereby delivering the required energy for apoptosis and restarting or accelerating the apoptotic process compared with the situation in continuously ischemic myocardium. (53) Reports by Kajstura et al (51) and Fliss and Gattinger (53) described apoptosis to be induced following 2 hours of coronary occlusion and accelerated after 45 min of ischemia followed by 1 hour of reperfusion. Gottlieb found apoptosis in the ischemic myocardium after 30

Chapter 1. Transgenic mice and cardiac remodeling

minutes of ischemia and 4 hours of reperfusion in the rabbit (52), but not in the permanently-ischemic areas, suggesting that apoptosis can only start during reperfusion. Also in a more recent study in dogs, apoptosis appeared in myocardium subjected to a brief period of ischemia followed by reperfusion, and not in ischemic tissue without reperfusion. (54) Whether apoptosis can be triggered during ischemia or predominantly during reperfusion remains controversial.

Current clinical reperfusion techniques, including thrombolytic therapy and primary percutaneous transluminal coronary angioplasty (PTCA) or on pump coronary artery bypass grafting (CABG), make inhibition of reperfusion-induced apoptosis a clinically relevant issue with potential therapeutic possibilities. In the experimental setting pharmacological intervention and genetic modification of the heart provide interesting tools to block or just activate apoptotic signaling pathways. The application of such pharmacologic or genetic interventions makes it possible to study the effects of individual molecules in the apoptotic and cardiac remodeling process. Accordingly, the role of caspase-3 in apoptotic signaling has been revealed through such a strategy. Cardiac-specific overexpression of caspase-3 driven by the rat alpha-myosin heavy chain promoter in mice resulted in increased infarct size and higher mortality when exposed to myocardial ischemia-reperfusion and demonstrated caspase-3 to be a pro-apoptotic regulator. (55) Gene-targeting of Bax in mice inhibited caspase-3 activity and consequently decreased TUNEL-positive cardiomyocytes and improved cardiac function of the Bax null hearts following ischemia-reperfusion. (56) Transgenic mice have clarified that the α MHC promoter-Mst1 cDNA construct is an efficient mediator of apoptosis through the activation of caspase-3. In this model stimulation of cardiomyocyte apoptosis and the development of dilated cardiomyopathy was found. (57) Overexpression of the dominant negative Mst1 transgene significantly decreased the rate of apoptosis and the extent of myocardial loss in mice following I/R. The activity of caspase-

Chapter 1. Transgenic mice and cardiac remodeling

3 could also be reduced by overexpressing the cardiac A1 adenosine receptors. (58)

Consequently, induction of apoptosis was attenuated in transgenic hearts exposed to I/R injury.

The discussed studies present evident genetic proof defining caspase-3 as an important determinant in I/R induced apoptotic signaling.

Apoptosis in myocardial infarction

As stated above, reperfusion accelerates the myocardial apoptotic process. Nevertheless, the total amount of dead cardiomyocytes is maximal in the permanently occluded myocardium. (53)

Persistence of ischemia leads to irreversible loss of cells.

The apoptotic hallmark of DNA fragmentation has not exclusively been observed during the acute stages of infarction. (53) Heightened rates of cardiomyocyte apoptosis are continuously present in the border zones of the infarct-area and the remote myocardium over a time-period of 12 weeks following MI. (59) This extended period designates apoptosis to be a key-player in post-infarction cardiac remodeling. Similar findings have been reported from human studies where the presence of high grades of apoptosis have been observed in human hearts of patients dying within 12 to 62 days following acute MI. (60) Blockade of the apoptotic process by a caspase-inhibitor during the subacute stage of MI has recently been shown to have beneficial effects on persistent apoptosis rates and cardiac remodeling in rats. (61)

The application of transgenic animals has been extremely useful in elucidating molecular mechanisms in apoptosis and cardiac remodeling following MI. The proapoptotic active caspase-1 is known to be important for the production of various cytokines such as IFN γ and TNF- α which contribute to the cardiac remodeling process after MI. Knockout mice lacking the caspase-1 gene showed significant reduction in apoptosis rates at day 1 post infarction and decreased

Chapter 1. Transgenic mice and cardiac remodeling

ventricular dilatation as assessed by echocardiography. (62) Tumor necrosis factor (TNF) itself may have anti-apoptotic and subsequent beneficial effects on the cell survival of myocytes injured by ischemia. (63,64) Post-infarction remodeling in TNF-receptor knockout mice was characterized by significantly greater infarct-areas and accelerated rates of apoptosis. (65) In knockout mice for TNF-receptors-1 and -2 the peak frequency and extent of apoptosis were significantly elevated in response to I/R. (65) These data suggest that TNF signaling gives rise to one or more cytoprotective signals that prevent and/or delay the development of cardiac myocyte apoptosis after acute ischemic injury. In contrast, the infarct size in TNF- α knockout mice was significantly reduced compared with wildtype littermates. (66) The systemic release of TNF- α in the early course of acute MI contributes to myocardial injury by promoting leukocyte infiltration of the myocardium, and TNF- α induces apoptosis in cardiomyocytes. (67) The systemic TNF- α concentration during ischemia correlates with the size of myocardial infarction in for example rabbits. (68) The use of TNF- α antibodies in ischemic-preconditioning studies reduces infarct extent significantly. (68,69) Currently clinical trials are in progress to investigate the protective effect of TNF-antibodies during myocardial ischemia.

The growth promoting peptide IGF-1 contributes *in vivo* to the protection of cardiomyocytes against apoptosis. IGF-1 deficient mice appeared to develop increased amounts of cardiomyocyte apoptosis 1 week post-infarction, affecting cardiac remodeling by thinning of the ventricular walls. (30) The IGF-1 protective effect on apoptosis was confirmed by the report that overexpression of the peptide in mice with chronic MI reduced myocyte death by blocking apoptosis rates. (70) This resulted in preserved wall thickness and decreased ventricular dilatation. IGF-1 induces anti-apoptotic signals in cardiomyocytes through PI3K-dependent Akt activation (figure 1). (71,72) Transgenic mice with cardiac-specific overexpression of human

Chapter 1. Transgenic mice and cardiac remodeling

FGF-1 showed delayed first signs of myocardial damage and postponing maximal infarction extension compared to wildtype animals. (33) FGF-1 provides cardioprotection at the level of the cardiac myocyte and is at least partially mediated via activation of the mitogen activated protein kinase (MAP) ERK-1 and -2. The presence of growth promoting peptides as IGF and FGF in the acute and chronic phase of myocardial ischemia is beneficial for the morphological and functional outcome.

The presented studies underscore the importance in future therapy of directly attenuating cell death in the infarct-area border zones and the remote myocardium to prevent adverse cardiac remodeling (i.e. wall thinning, ventricular dilatation and deteriorating cardiac performance) following MI.

Hypertrophy

The hypertrophic response of cardiomyocytes has been studied extensively during the past decade using genetically modified mouse models and *in vitro* models. Cardiomyocyte hypertrophic growth *in vivo* is triggered by various stimuli such as ventricular pressure- or volume-overload, ischemia-(reperfusion) or drug induced. (73) Furthermore, analogues to human hypertrophic cardiomyopathies the possibility arose to evoke hypertrophy by engineering mutations in the sarcomeric genes of mice. Many aspects of cardiac hypertrophic growth have been investigated with these techniques. Hypertrophy is characterized by cardiomyocyte growth, myofibrillar disarray, fibrosis, apoptosis, arrhythmias, elevated filling and end-diastolic pressures, decline in systolic function, cellular and mitochondrial energy inefficiency, alterations in calcium handling and eventually transition towards heart failure. (73) The single most powerful predictor for the development of heart failure is the presence of left ventricular hypertrophy. (74) For this reason, much effort is currently undertaken to investigate the etiology of molecular hypertrophic mechanisms and to unravel the signaling pathways underlying this process (figure 3).

To date, more than 100 genetically altered mouse models of hypertrophic cardiomyopathy, myocardial hypertrophy and heart failure have been engineered. (75) Because of the variety of genes involved numerous molecular mechanisms in the development of hypertrophy have been investigated. Proposed molecular mechanisms in the development of hypertrophy include abnormalities in contractile, cytoskeletal, and intracellular calcium (Ca^{2+})-regulatory proteins, alterations in excitation-contraction coupling, signal transduction system, cardiac metabolism or myocyte apoptosis and many others. (75) All hypertrophic stimuli (i.e. myocyte stretch, hemodynamic stress, ischemia, hormones, vasoactive peptides or neurotransmitters) converge in several intracellular signaling cascades mediating these extrinsic

Chapter 1. Transgenic mice and cardiac remodeling

and intrinsic growth signals into co-ordinated alterations of genetic profiles, and increments in the overall rate of RNA transcription and protein synthesis.

An important signaling pathway in cardiomyocyte hypertrophy is initiated by the gp130 cytokine receptor. Transgenic mice expressing constitutively active gp130 protein in the heart were created by mating mice from interleukin (IL)-6 and IL-6-receptor transgenic mouse lines. The continuous activation of the gp130 signaling pathways in these mice led to overt cardiac hypertrophy. (76) In transgenic mice overexpressing a dominant-negative mutant of gp130 pressure-overload induced smaller increments in heart-to-body weight ratios, ventricular wall thickness and cross-sectional areas of cardiomyocytes than in wildtype littermates. (77) The gp130 protein induced hypertrophic gene program could be antagonized by monoclonal anti-gp130 antibodies. (78) Investigations in cultured murine cardiomyocytes infected with adenoviruses suggested that mainly the STAT3-dependent signaling pathway downstream of gp130 promoted cardiac myocyte hypertrophy. (79) Pressure-overload activated ERKs and STAT3 in the heart of wildtype mice, whereas pressure overload-induced activation of STAT3, but not of ERKs, was suppressed in transgenic mice overexpressing dominant-negative gp130. (77) Moreover, transgenic mice with cardiac-specific overexpression of the STAT3 gene manifested myocardial hypertrophy at the age of 12 weeks. (80) These results suggest that gp130 plays a critical role in stimulus-induced cardiac hypertrophy possibly through the STAT3 signaling pathway.

ERK belongs to another important pathway through which extracellular stimuli induce hypertrophy. Hypertrophic stimuli induce the activation of the mitogen-activated protein kinase (MAPK) superfamily cascades. MAPKs are a widely distributed group of intracellular proteins composed of three terminal MAPK branches; (A) the extracellular signal-regulated kinases (ERKs); (B) c-Jun NH(2)-terminal kinases (JNKs) and (C) the stress-induced p38 MAPKs.

Chapter 1. Transgenic mice and cardiac remodeling

Hypertrophic stimuli induce the activation of MAPKs through G-protein coupled receptors (81) and low molecular weight GTP binding proteins Ras and Rho depending pathways (figure 3).

(82,83) A family of MAPK phosphatases (MKPs) act as the critical counteracting factors of p38, JNK and ERK. (84) Selective ERK1/2 stimulation by cardiac specific overexpression of MEK1 (endogenous kinase activator of ERK1/2) demonstrated concentric hypertrophy without signs of cardiomyopathy combined with improved cardiac function. (6) On the contrary, cardiac-specific expression of activated MEK5 in transgenic mice resulted in eccentric cardiac hypertrophy that progressed to dilated cardiomyopathy and sudden death. (85)

JNK MAPK contributes to the pressure-overload and catecholamine-induced hypertrophic response. (82,86) Prevention of JNK activity through JNK-interacting protein 1 (JIP-1), a cytosolic scaffolding protein, results in reduced cellular growth in response to G-protein coupled receptor agonists. (87) Pressure-overload however caused significant levels of cardiac hypertrophy coinciding with signs of clinical heart failure and higher mortality in mice deficient for MEKK1 (mitogen-activated protein kinase kinase kinase; mediates JNK activation). (88) Direct JNK-gene overexpression or deficiency in cardiomyocytes has not been published so far. However, through an ingenious mouse model using tamoxifen-inducible cardiac-specific-gene expression, a constitutively activated upstream activator of JNK was investigated in the adult mouse heart. (13) Prolonged activation of JNK resulted in progressive cardiomyopathy adding molecular proof for a regulatory role of JNK in maladaptive cardiac growth.

Stress-induced p38 MAPK activity increases significantly in mouse hearts after chronic transverse aortic constriction, coinciding with the onset of ventricular hypertrophy. Adenoviral overexpression of wild type p38 β or a dominant-negative p38 β variant respectively enhanced and suppressed the hypertrophic response following aortic constriction. (89) p38 Activity has also

Chapter 1. Transgenic mice and cardiac remodeling

been associated with catecholamine-induced hypertrophy. (90) Transgenic male and female mice with fourfold phospholamban (PLB) overexpression exhibited enhanced circulating catecholamines concurrent with p38 MAPK activation levels.(90) However, *in vivo* cardiac overexpression of p38 MAPK activation resulted in varying degrees of myocyte atrophy. This was shown using a transgenic gene-switch strategy with activated mutants of well-established upstream activators of the p38, namely MKK3bE and MKK6bE. (7) The gene-switch strategy is based on cre/loxP-mediated DNA recombination to restrict transgene expression to ventricular myocytes and avoid potential adverse effects of transgene expression on the survival of the founder transgenic animals. (91) Moreover, dominant-negative p38 α transgenic mice showed enhanced cardiac hypertrophy following both pressure-overload and catecholamine drug infusion. (92) Further investigations in these mice revealed an enhancement of calcineurin-NFAT signaling following reduced p38 activity, providing a possible explanation for the contradicting results in the studies presented. However, probably both p38 and JNK MAPK activation are directly associated with a failing cardiac phenotype. In longstanding hypertrophy only p38 and JNK MAPKs are activated, associated with progressive deterioration to maladaptive chronic hypertrophy and congestive heart failure. (86,93)

The calcium/calmodulin-dependent protein phosphatase calcineurin is important in cardiac hypertrophy in response to numerous stimuli. Transgenic mice overexpressing the activated form of calcineurin exhibited a severe form of cardiac hypertrophy with concurrent transition towards apoptosis-independent heart failure and sudden death due to lethal arrhythmias. (94-96) Besides the ability of calcineurin itself to provoke hypertrophic growth of the heart, it may play a significant role in pressure-overload-induced and isoproterenol-induced cardiac hypertrophy in transgenic mice overexpressing a dominant negative mutant of

Chapter 1. Transgenic mice and cardiac remodeling

calcineurin. (97,98) Calcineurin was shown to dephosphorylate the transcription factor NFAT3, enabling it to translocate to the nucleus, where NFAT interacted mainly with transcription factor GATA4, resulting in synergistic activation of cardiac transcription. (94) NFAT3 appeared to be required for calcineurin mediated hypertrophic signaling based on reduced cardiac growth upon calcineurin stimulation in NFAT3 knockout mice. (99,100) Transgenic mice expressing the activated form of calcineurin showed interaction with other developmental pathways by inactivation of p38 and increased MKP-1 expression. (101) Calcineurin hypertrophic signaling was furthermore interconnected with PKC α , theta, and JNK in the heart. (102) Endogenous myocyte-enriched calcineurin-interacting protein (MCIP) counteracts calcineurin through a negative feedback loop. Cardiac-specific expression of human MCIP1 in mice inhibited cardiac hypertrophy provoked by constitutively active calcineurin. (103) Even hypertrophy induced by catecholamines, exercise training or pressure-overload was attenuated, without deterioration of ventricular performance. (103,104) Even so, the lack of MCIP1 in homozygous knock-out mice exacerbated the hypertrophic response to activated calcineurin. (105) Another endogenous inhibiting protein of the calcineurin-dependent hypertrophic signaling pathway is glycogen synthase kinase (GSK)-3 β . Transgenic mice that express a constitutively active form of GSK-3 β showed a significant ability to attenuate the hypertrophic response to calcineurin activation. (106) GSK-3 β mice expressing the calcineurin inhibitory domains of Cain/Cabin-1 and A-kinase anchoring protein 79 demonstrated reduced cardiac calcineurin activity and reduced hypertrophy in response to catecholamine infusion and pressure overload. (107) The calcium/calmodulin-dependent protein phosphatase calcineurin is therefore an importantly regulator of cardiac hypertrophy induced by various stimuli as shown by multiple studies in genetically engineered mice.

Chapter 1. Transgenic mice and cardiac remodeling

Apoptosis and its relation to cardiac hypertrophy

Cardiac hypertrophy may occur to compensate for the loss of viable cells after myocardial ischemia. (108) Cardiomyopathy in transgenic mice is related to increased apoptosis rates. Nix/Bnip3L, one of the mitochondrial death proteins, was shown to be upregulated in cardiac hypertrophy, but also to play a major role in the apoptotic process. (109) As reported earlier, the cardiac-specific overexpression of Mst1 resulted in activation of caspases and an increase of apoptosis. Interestingly, Mst1 also prevents cardiac myocyte elongation and hypertrophy despite increased wall stress. (57) Mst1 may inhibit signaling molecules causing hypertrophy.

However, several molecular effectors in hypertrophic signaling have been proven to be important in anti-apoptotic signaling also, as part of the second leg of cardiomyocyte survival pathways. For instance, the MEK1-ERK1/2 signaling pathway stimulates cardiac hypertrophic growth associated with augmented cardiac function (i.e. adaptive hypertrophy) combined with partial resistance to apoptosis. (10,110) The gp130 protein, another potent cardiac survival factor, mediates cardiotrophin-1 (CT-1)-induced cardiac hypertrophy and is capable of inhibiting cardiomyocyte apoptosis also. (111,112) In gp130 knockout mice, the application of pressure overload by aortic banding resulted in massive apoptosis rates plus reduced cardiac hypertrophy. (113) To date, the role of the calcineurin-NFAT pathway in pro- or anti-apoptotic responses is not clear. (114) For instance, adrenergic stimulation led to calcineurin mediated cardiomyocyte apoptosis (115), while other investigations found myocardial protection against I/R induced apoptosis through calcineurin *in vitro* and *in vivo*. (96,116) It seems that NFAT activity is the critical component mediating effects of calcineurin stimulation resulting in the activation of pro- or antiapoptotic pathways in cardiomyocytes. (116,117) Selective NFAT inhibition during phenylephrine stimulation prevented calcineurin mediated hypertrophy but resulted in increased cardiomyocyte apoptosis. (117) Therefore, certain prohypertrophic and antiapoptotic pathways

Chapter 1. Transgenic mice and cardiac remodeling

can come together as a common survival pathway, suggesting interplay between cellular pathways in adaptive myocyte responses.

Figure 3

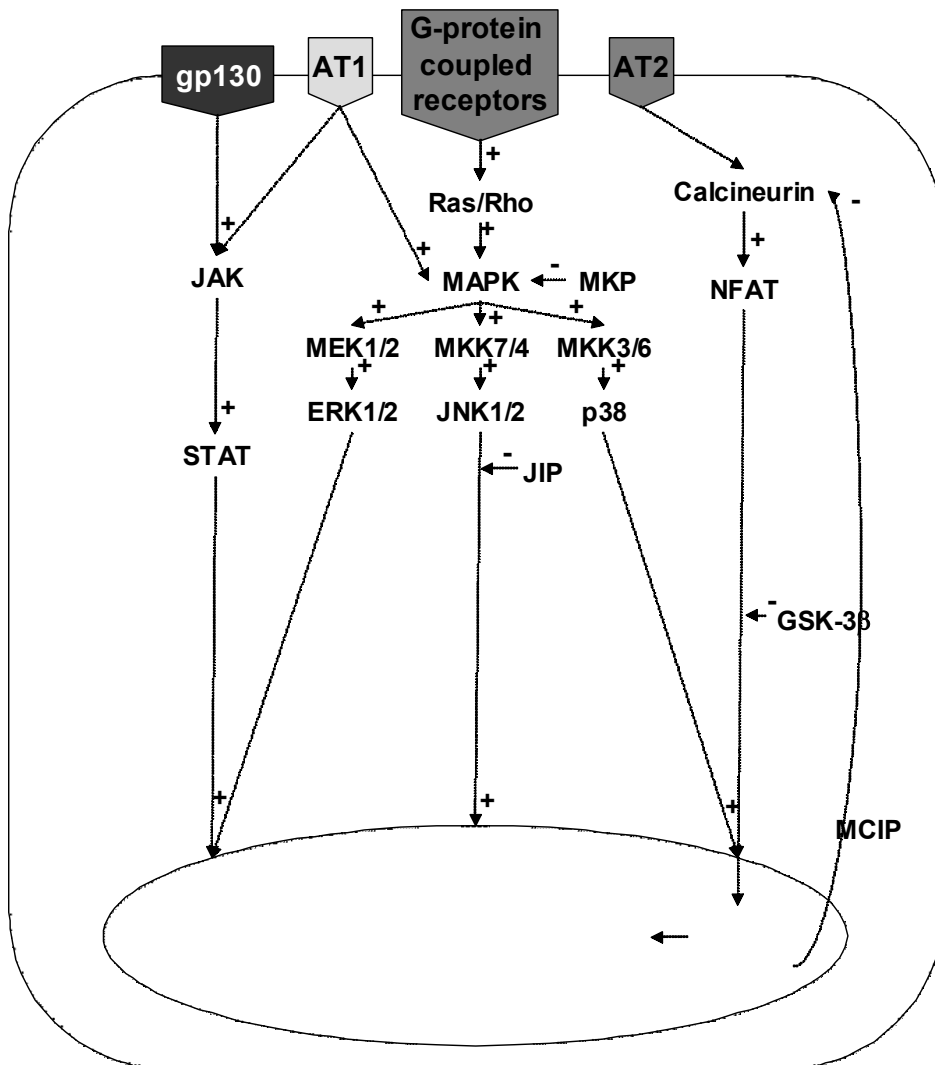


Fig. 3: Signaling pathways in cardiomyocyte hypertrophy. Activation or inhibition of single molecules are indicated by respectively (+) and (-).

Hemodynamics

The use of genetically engineered mice rendered vital information about the precise role various proteins play in the diversity of intracellular signaling pathways in the event of cellular hypertrophy or apoptosis. The link between the genotype of the mouse and the concurrent phenotype is investigated with the use of sophisticated molecular and cellular techniques. An equally important aspect of the resultant phenotype is cardiac function. Genetic engineering provides the possibility to probe the precise mechanism by which specific proteins exert their effects on plain cardiac function, or in the process of remodeling. The small size of the murine heart and the rapid pace at which it contracts makes measurements of cardiac performance difficult. Various techniques have been used to assess murine cardiac function, such as transthoracic ultrasonography (118), Langendorff perfusion systems (119), aortic flow probes (120) and micromanometers (121). Those techniques have been and are being used extensively in mouse studies, notwithstanding their relative inaccuracy and lack of total cardiac performance assessment. This could theoretically be obtained by measuring cardiac pressure and volume simultaneously. The development of new cardiac function techniques such as magnetic resonance imaging (MRI) (122) and conductance-micromanometers (123) provide new tools for accurate and total cardiac performance assessment.

The concept of simultaneous *in vivo* pressure and volume measurements in the left ventricle was developed by Baan et al in the early 1980's. (124) The volume-signal is derived in accordance with Ohm's Law, depending on the varying amount of ventricular bloodvolume during the cardiac cycle. An electrical current is produced by an intraventricular catheter to measure conductance, which is directly related to the varying bloodvolume. The pressure- and volume signals produced by the conductance-micromanometer catheter are displayed in a two-dimensional diagram. This presentation results in pressure-volume loops representing cardiac

Chapter 1. Transgenic mice and cardiac remodeling

performance, which can be analyzed accurately. The pressure-volume technique originates from large animal and human studies, but has recently been miniaturized and made available for mouse studies. (123) Pressure-volume assessment protocols have been developed (125) and hemodynamic studies have been successfully performed in genetically engineered mice. (10,126)

The use of MRI in mice is another relatively new concept in the studies of murine hemodynamics. (122) The noninvasive technique of MRI enables the investigator to study *in vivo* murine cardiac metabolism, morphology, and function under (patho)physiological conditions. To quantify left ventricular function high-resolution (HR) MRI is used. To date, MRI studies have been successfully implemented in cardiac phenotyping. Evaluation of cardiac mass and function in post-MI remodeling was performed by MRI studies in mice overexpressing the AT2 receptor. (24) Serial MRI studies in transgenic mice overexpressing TNF- α demonstrated increased ventricular mass and deteriorating cardiac function over time in this murine model of dilating cardiomyopathy. (127)

To stress the importance of accurate phenotyping of cardiac performance in (genetically altered) mice some relevant studies will be discussed in more detail. In accordance with the general consensus hypertrophy is the increase in cardiac mass as a compensating mechanism to withstand augmented hemodynamic stress. Cardiac hypertrophy can be defined as the increase in myocardial mass in an effort to alleviate the elevation in wall stress according to LaPlace's principle. Studies using a heart size-independent analysis for *in vivo* murine cardiac function determination suggested that the development of cardiac hypertrophy is associated with a heightened contractile state, perhaps as an early compensatory response to pressure overload. (128) The systolic wall stress increases significantly in the early response to pressure-overload concomitant with ejection fraction and fractional shortening attenuation. In time a gradual

Chapter 1. Transgenic mice and cardiac remodeling

normalization of wall stress and cardiac performance is seen with serial measurements. (129)

Pharmacological inhibition of hypertrophic growth in pressure-overloaded mice showed

maintenance of normal LV size and systolic function, as measured by echocardiography, (130)

without reducing left ventricular wall stress. (131) Moreover, two genetically altered mouse

models (mice with myocardial expression of a carboxyl terminal peptide of G_{α_q} [TgGqI] that

specifically inhibits G_q -mediated signaling and genetically altered mice that lack endogenous

norepinephrine and epinephrine created by disruption of the dopamine β -hydroxylase gene [Dbh^{-/-}

]) have a blunted hypertrophic response to pressure-overload and show inadequacy to normalize

the 2-fold increased wall stress. Despite the increase in wall stress cardiac function as measured

by serial echocardiography showed little deterioration in these pressure-overloaded genetic

mouse strains. (132) In contrast, wild-type mice with similar pressure overload showed a

significant increase in chamber dimensions and progressive deterioration in cardiac function.

These data suggest that under conditions of pressure overload, the development of cardiac

hypertrophy and normalization of wall stress may not be necessary to preserve cardiac function,

as previously hypothesized. The data suggest that cardiac hypertrophic growth is not mandatory

to maintain ventricular wall stress at normal levels, as augmented wall stress is not a predictor of

cardiac function decline.

Conclusion

Genetic modification of murine DNA provides the possibility to elucidate the spectrum of specific functions of a single molecule and its corresponding intracellular signaling pathways in specific pathophysiological situations such as myocardial ischemia. Cardiac remodeling is defined by the ischemia-induced structural and concomitantly functional alterations in the heart. Murine models of I/R and MI mimic the pathophysiological changes observed in man. Cell death, deposition of collagen and myocardial hypertrophy are the characteristics of cardiac remodeling in man and mouse alike. The predominant factor in determining the severity of the resultant cardiac phenotype is ventricular function (figure 4), which is best assessed by the use of *in vivo* pressure-volume measurements in mice. The use of genetically modified murine models in ischemia(-reperfusion) studies led to new knowledge about the molecular processes involved in these processes. In spite of this, intracellular signaling is still a mystery as we lack the tools to study several pathways simultaneously and maybe even more importantly the temporal changes in signaling cascade interactions.

Figure 4

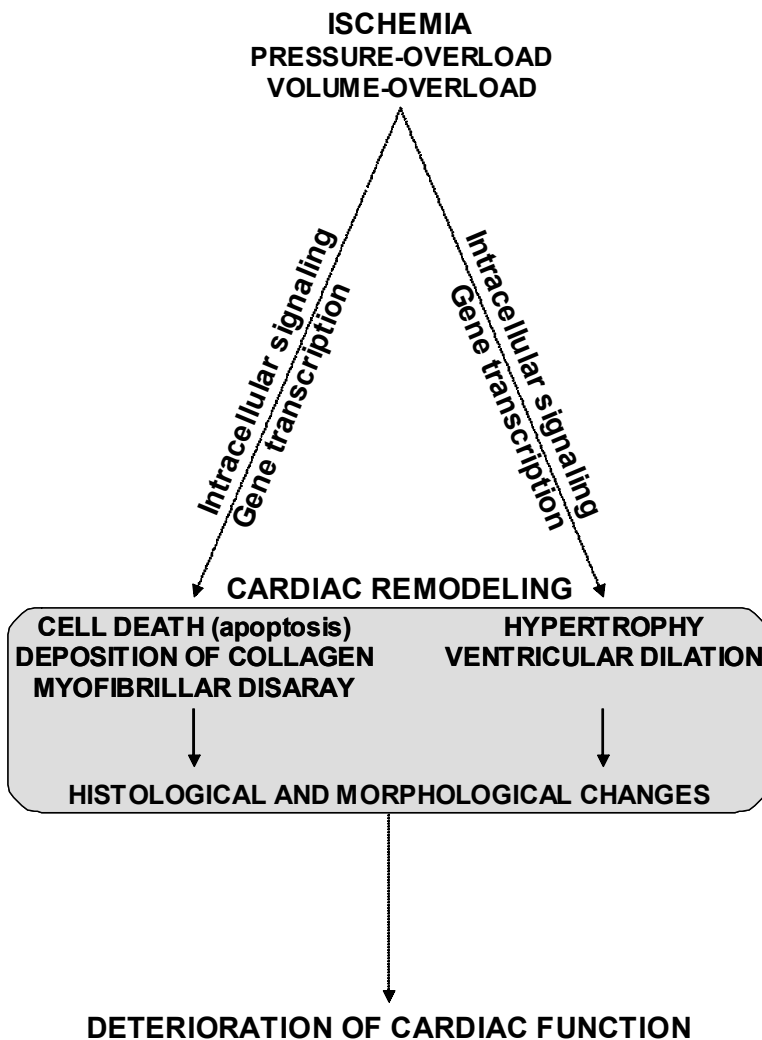


Fig. 4: The development of adverse cardiac remodeling in human heart disease. Presented is a scheme of deteriorating cardiac function, mediated by the characteristics of cardiac remodeling. Cardiac remodeling is initiated by several pathophysiological situations such as myocardial ischemia. Activated molecular pathways and newly expressed gene transcription profiles are the basis of cellular, histological and morphological alterations leading to the development of clinical heart disease.

References

1. Bueno OF, van Rooij E, Molkentin JD, Doevendans PA, De Windt LJ. Calcineurin and hypertrophic heart disease: novel insights and remaining questions. *Cardiovasc Res* 2002;53:806-21.
2. Doevendans PA, Hunter JJ, Lembo G, al. e. Strategies for studying cardiovascular diseases in transgenic mice and gene-targeted mice. In: Monastersky GM RJ, ed. *Strategies in transgenic animal science*. Washington: American Society for Microbiology, 1995:107-44.
3. Doevendans PA, Daemen M, de Muinck E, Smits JF. Cardiovascular phenotyping in mice. *Cardiovasc Res* 1998;39:34-49.
4. Kubalak S, Doevendans PA, Rockman H, al. e. Molecular analysis of cardiac muscle diseases based on mouse genetics. In: Adolph KW, ed. *Human molecular genetics*. Orlando: Academic Press, 1996:470-87.
5. Bueno OF, van Rooij E, Lips DJ, Doevendans PA, De Windt LJ. Cardiac hypertrophic signaling: the Good, the Bad and the Ugly. In: Doevendans PA, Kaab S, eds. *Cardiovascular Genomics: new insights into pathophysiology*. Dordrecht: Kluwer, 2002:131-55.
6. Bueno OF, De Windt LJ, Tymitz KM, et al. The MEK1-ERK1/2 signaling pathway promotes compensated cardiac hypertrophy in transgenic mice. *Embo J* 2000;19:6341-50.
7. Liao P, Georgakopoulos D, Kovacs A, et al. The in vivo role of p38 MAP kinases in cardiac remodeling and restrictive cardiomyopathy. *Proc Natl Acad Sci U S A* 2001;98:12283-8.
8. Zhang D, Gaussin V, Taffet GE, et al. TAK1 is activated in the myocardium after pressure overload and is sufficient to provoke heart failure in transgenic mice. *Nat Med* 2000;6:556-63.
9. Eefting F, Rensing B, Wigman J, et al. Apoptosis in reperfusion injury. In press *Cardiovasc Res* 2003.
10. Lips DJ, Bueno OF, Wilkins BJ, et al. The MEK1-ERK2 signaling pathway protects the myocardium from ischemic damage in vivo. Submitted 2003.
11. Camper-Kirby D, Welch S, Walker A, et al. Myocardial Akt activation and gender: increased nuclear activity in females versus males. *Circ Res* 2001;88:1020-7.
12. Haq S, Choukroun G, Lim H, et al. Differential activation of signal transduction pathways in human hearts with hypertrophy versus advanced heart failure. *Circulation* 2001;103:670-7.
13. Petrich BG, Molkentin JD, Wang Y. Temporal activation of c-Jun N-terminal kinase in adult transgenic heart via cre-loxP-mediated DNA recombination. *FASEB J* 2003;17:749-51.
14. Bellenger NG, Swinburn JM, Rajappan K, Lahiri A, Senior R, Pennell DJ. Cardiac remodelling in the era of aggressive medical therapy: does it still exist? *Int J Cardiol* 2002;83:217-25.
15. Bolognese L, Neskovic AN, Parodi G, et al. Left ventricular remodeling after primary coronary angioplasty: patterns of left ventricular dilation and long-term prognostic implications. *Circulation* 2002;106:2351-7.
16. Lutgens E, Daemen MJ, de Muinck ED, Debets J, Leenders P, Smits JF. Chronic myocardial infarction in the mouse: cardiac structural and functional changes. *Cardiovasc Res* 1999;41:586-93.

Chapter 1. Transgenic mice and cardiac remodeling

17. Eaton LW, Bulkley BH. Expansion of acute myocardial infarction: its relationship to infarct morphology in a canine model. *Circ Res* 1981;49:80-8.
18. Holmes JW, Yamashita H, Waldman LK, Covell JW. Scar remodeling and transmural deformation after infarction in the pig. *Circulation* 1994;90:411-20.
19. Eaton LW, Weiss JL, Bulkley BH, Garrison JB, Weisfeldt ML. Regional cardiac dilatation after acute myocardial infarction: recognition by two-dimensional echocardiography. *N Engl J Med* 1979;300:57-62.
20. Rumberger JA, Behrenbeck T, Breen JR, Reed JE, Gersh BJ. Nonparallel changes in global left ventricular chamber volume and muscle mass during the first year after transmural myocardial infarction in humans. *J Am Coll Cardiol* 1993;21:673-82.
21. Gaudron P, Eilles C, Kugler I, Ertl G. Progressive left ventricular dysfunction and remodeling after myocardial infarction. Potential mechanisms and early predictors. *Circulation* 1993;87:755-63.
22. Nahrendorf M, Wiesmann F, Hiller KH, et al. In vivo assessment of cardiac remodeling after myocardial infarction in rats by cine-magnetic resonance imaging. *J Cardiovasc Magn Reson* 2000;2:171-80.
23. Michael LH, Entman ML, Hartley CJ, et al. Myocardial ischemia and reperfusion: a murine model. *Am J Physiol Heart Circ Physiol* 1995;269:H2147-54.
24. Yang Z, Bove CM, French BA, et al. Angiotensin II type 2 receptor overexpression preserves left ventricular function after myocardial infarction. *Circulation* 2002;106:106-11.
25. Xu J, Carretero OA, Liu YH, et al. Role of AT2 receptors in the cardioprotective effect of AT1 antagonists in mice. *Hypertension* 2002;40:244-50.
26. Bader M. Role of the local renin-angiotensin system in cardiac damage: a minireview focussing on transgenic animal models. *J Mol Cell Cardiol* 2002;34:1455-62.
27. Booz GW, Baker KM. Molecular signalling mechanisms controlling growth and function of cardiac fibroblasts. *Cardiovasc Res* 1995;30:537-43.
28. Harada K, Sugaya T, Murakami K, Yazaki Y, Komuro I. Angiotensin II type 1A receptor knockout mice display less left ventricular remodeling and improved survival after myocardial infarction. *Circulation* 1999;100:2093-9.
29. Oishi Y, Ozono R, Yano Y, et al. Cardioprotective role of AT2 receptor in postinfarction left ventricular remodeling. *Hypertension* 2003;41:814-8.
30. Palmén M, Daemen MJ, Bronsær R, et al. Cardiac remodeling after myocardial infarction is impaired in IGF-1 deficient mice. *Cardiovasc Res* 2001;50:516-24.
31. Carmeliet P, Ng YS, Nuyens D, et al. Impaired myocardial angiogenesis and ischemic cardiomyopathy in mice lacking the vascular endothelial growth factor isoforms VEGF164 and VEGF188. *Nat Med* 1999;5:495-502.
32. Bellomo D, Headrick JP, Silins GU, et al. Mice lacking the vascular endothelial growth factor-B gene (*Vegfb*) have smaller hearts, dysfunctional coronary vasculature, and impaired recovery from cardiac ischem. *Circ Res* 2000;86:E29-35.
33. Buehler A, Martire A, Strohm C, et al. Angiogenesis-independent cardioprotection in FGF-1 transgenic mice. *Cardiovasc Res* 2002;55:768-77.
34. Cleutjens JP, Creemers EE. Integration of concepts: cardiac extracellular matrix remodeling after myocardial infarction. *J Card Fail* 2002;8:S344-8.
35. Ducharme A, Frantz S, Aikawa M, et al. Targeted deletion of matrix metalloproteinase-9 attenuates left ventricular enlargement and collagen accumulation after experimental myocardial infarction. *J Clin Invest* 2000;106:55-92.

36. Heymans S, Luttun A, Nuyens D, et al. Inhibition of plasminogen activators or matrix metalloproteinases prevents cardiac rupture but impairs therapeutic angiogenesis and causes cardiac failure. *Nat Med* 1999;5:1135-42.
37. Creemers EE, Davis JN, Parkhurst AM, et al. Deficiency of TIMP-1 exacerbates LV remodeling after myocardial infarction in mice. *Am J Physiol Heart Circ Physiol* 2003;284:H364-71.
38. Cavaasin MA, Sankey SS, Yu AL, Menon S, Yang XP. Estrogen and testosterone have opposing effects on chronic cardiac remodeling and function in mice with myocardial infarction. *Am J Physiol Heart Circ Physiol* 2003;284:H1560-9.
39. Van Eickels M, Patten RD, Aronovitz MJ, et al. 17-beta-estradiol increases cardiac remodeling and mortality in mice with myocardial infarction. *J Am Coll Cardiol* 2003;41:2084-92.
40. Van Eickels M, Grohe C, Cleutjens JPM, Janssen BJ, Wellens HJJ, Doevendans PA. 17beta-Estradiol attenuates the development of pressure-overload hypertrophy. *Circulation* 2001;104:1419-1423.
41. Babiker FA, Lips DJ, Delvaux E, et al. ERbeta protects the murine heart against left ventricular hypertrophy. Submitted 2003.
42. Babiker FA, De Windt LJ, Van Eickels M, et al. 17{beta}-Estradiol Antagonizes Cardiomyocyte Hypertrophy by Autocrine/Paracrine Stimulation of a Guanylyl Cyclase A Receptor-Cyclic Guanosine Monophosphate-Dependent Protein Kinase Pathway. *Circulation* 2004;[Epub ahead of print].
43. Majno G, Joris I. Apoptosis, oncosis, and necrosis. An overview of cell death. *Am J Pathol* 1995;146:3-15.
44. Knaapen MW, Davies MJ, De Bie M, Haven AJ, Martinet W, Kockx MM. Apoptotic versus autophagic cell death in heart failure. *Cardiovasc Res* 2001;51:304-12.
45. Bialik S, Cryns VL, Drincic A, et al. The mitochondrial apoptotic pathway is activated by serum and glucose deprivation in cardiac myocytes. *Circ Res* 1999;85:403-14.
46. Li P, Nijhawan D, Budihardjo I, et al. Cytochrome c and dATP-dependent formation of Apaf-1/caspase-9 complex initiates an apoptotic protease cascade. *Cell* 1997;91:479-89.
47. Borutaite V, Brown GC. Mitochondria in apoptosis of ischemic heart. *FEBS Lett* 2003;541:1-5.
48. Lee P, Sata M, Lefer DJ, Factor SM, Walsh K, Kitsis RN. Fas pathway is a critical mediator of cardiac myocyte death and MI during ischemia-reperfusion in vivo. *Am J Physiol Heart Circ Physiol* 2003;284:H456-63.
49. Zheng TS, Hunot S, Kuida K, Flavell RA. Caspase knockouts: matters of life and death. *Cell Death Differ* 1999;6:1043-53.
50. Dumont EA, Reutelingsperger CP, Smits JF, et al. Real-time imaging of apoptotic cell-membrane changes at the single-cell level in the beating murine heart. *Nat Med* 2001;7:1352-5.
51. Kajstura J, Cheng W, Reiss K, et al. Apoptotic and necrotic myocyte cell deaths are independent contributing variables of infarct size in rats. *Lab Invest* 1996;74:86-107.
52. Gottlieb RA, Burlison KO, Kloner RA, Babior BM, Engler RL. Reperfusion injury induces apoptosis in rabbit cardiomyocytes. *J Clin Invest* 1994;94:1621-8.
53. Fliss H, Gattinger D. Apoptosis in ischemic and reperfused rat myocardium. *Circ Res* 1996;79:949-56.
54. Zhao ZQ, Nakamura M, Wang NP, et al. Reperfusion induces myocardial apoptotic cell death. *Cardiovasc Res* 2000;45:651-60.

Chapter 1. Transgenic mice and cardiac remodeling

55. Condorelli G, Roncarati R, Ross JJ, et al. Heart-targeted overexpression of caspase3 in mice increases infarct size and depresses cardiac function. *Proc Natl Acad Sci U S A* 2001;98:9977-82.
56. Hochhauser E, Kivity S, Offen D, et al. Bax ablation protects against myocardial ischemia-reperfusion injury in transgenic mice. *Am J Physiol Heart Circ Physiol* 2003;284:H2351-9.
57. Yamamoto S, Yang G, Zablocki D, et al. Activation of Mst1 causes dilated cardiomyopathy by stimulating apoptosis without compensatory ventricular myocyte hypertrophy. *J Clin Invest* 2003;111:1463-74.
58. Regan SE, Broad M, Byford AM, et al. A1 adenosine receptor overexpression attenuates ischemia-reperfusion-induced apoptosis and caspase 3 activity. *Am J Physiol Heart Circ Physiol* 2003;284:H859-66.
59. Palojoki E, Saraste A, Eriksson A, et al. Cardiomyocyte apoptosis and ventricular remodeling after myocardial infarction in rats. *Am J Physiol Heart Circ Physiol* 2001;280:H2726-31.
60. Baldi A, Abbate A, Bussani R, et al. Apoptosis and post-infarction left ventricular remodeling. *J Mol Cell Cardiol* 2002;34:165-74.
61. Hayakawa K, Takemura G, Kanoh M, et al. Inhibition of granulation tissue cell apoptosis during the subacute stage of myocardial infarction improves cardiac remodeling and dysfunction at the chronic stage. *Circulation* 2003;108:104-9.
62. Frantz S, Ducharme A, Sawyer D, et al. Targeted deletion of caspase-1 reduces early mortality and left ventricular dilatation following myocardial infarction. *J Mol Cell Cardiol* 2003;35:685-94.
63. Beg AA, Baltimore D. An essential role for NF-kappaB in preventing TNF-alpha-induced cell death. *Science* 1996;274:782-4.
64. Garg AK, Aggarwal BB. Reactive oxygen intermediates in TNF signaling. *Mol Immunol* 2002;39:509-17.
65. Kurrelmeyer KM, Michael LH, Baumgarten G, et al. Endogenous tumor necrosis factor protects the adult cardiac myocyte against ischemic-induced apoptosis in a murine model of acute myocardial infarction. *Proc Natl Acad Sci U S A* 2000;97:5456-61.
66. Maekawa N, Wada H, Kanda T, et al. Improved myocardial ischemia/reperfusion injury in mice lacking tumor necrosis factor-alpha. *J Am Coll Cardiol* 2002;39:1229-35.
67. Sugano M, Koyanagi M, Tsuchida K, Hata T, Makino N. In vivo gene transfer of soluble TNF-alpha receptor 1 alleviates myocardial infarction. *FASEB J* 2002;16:1421-2.
68. Belosjorow S, Bolle I, Duschin A, Heusch G, Schulz R. TNF-alpha antibodies are as effective as ischemic preconditioning in reducing infarct size in rabbits. *Am J Physiol Heart Circ Physiol* 2003;284:H927-30.
69. Yamashita N, Hoshida S, Otsu K, Taniguchi N, Kuzuya T, Hori M. The involvement of cytokines in the second window of ischaemic preconditioning. *Br J Pharmacol* 2000;131:415-22.
70. Li Q, Li B, Wang X, et al. Overexpression of insulin-like growth factor-1 in mice protects from myocyte death after infarction, attenuating ventricular dilation, wall stress, and cardiac hypertrophy. *J Clin Invest* 1997;100:1991-9.
71. Kuwahara K, Saito Y, Kishimoto I, et al. Cardiotrophin-1 phosphorylates akt and BAD, and prolongs cell survival via a PI3K-dependent pathway in cardiac myocytes. *J Mol Cell Cardiol* 2000;32:1385-94.

72. Wu W, Lee WL, Wu YY, et al. Expression of constitutively active phosphatidylinositol 3-kinase inhibits activation of caspase 3 and apoptosis of cardiac muscle cells. *J Biol Chem* 2000;275:40113-9.
73. Lips DJ, Van Kraaij DL, De Windt LJ, Doevendans PA. Molecular determinants of myocardial hypertrophy and failure: alternative pathways for beneficial and maladaptive hypertrophy. *Eur Heart J* 2003;24:883-896.
74. Maron BJ. Hypertrophic cardiomyopathy. *Lancet* 1997;350:127-33.
75. Chu G, Haghighi K, Kranias EG. From mouse to man: understanding heart failure through genetically altered mouse models. *J Card Fail* 2002;8:S432-39.
76. Hirota H, Yoshida K, Kishimoto T, Taga T. Continuous activation of gp130, a signal-transducing receptor component for interleukin 6-related cytokines, causes myocardial hypertrophy in mice. *Proc Natl Acad Sci U S A* 1995;92:4862-6.
77. Uozumi H, Hiroi Y, Zou Y, et al. gp130 plays a critical role in pressure overload-induced cardiac hypertrophy. *J Biol Chem* 2001;276:23115-9.
78. Wollert KC, Taga T, Saito M, et al. Cardiotrophin-1 activates a distinct form of cardiac muscle cell hypertrophy. Assembly of sarcomeric units in series VIA gp130/leukemia inhibitory factor receptor-dependent pathways. *J Biol Chem* 1996;271:9535-45.
79. Kunisada K, Tone E, Fujio Y, Matsui H, Yamauchi-Takahara K, Kishimoto T. Activation of gp130 transduces hypertrophic signals via STAT3 in cardiac myocytes. *Circulation* 1998;98:346-52.
80. Kunisada K, Negoro S, Tone E, et al. Signal transducer and activator of transcription 3 in the heart transduces not only a hypertrophic signal but a protective signal against doxorubicin-induced cardiomyopathy. *Proc Natl Acad Sci U S A* 2000;97:315-9.
81. Minamino T, Yujiri T, Terada N, et al. MEKK1 is essential for cardiac hypertrophy and dysfunction induced by Gq. *Proc Natl Acad Sci U S A* 2002;99:3866-71.
82. Ramirez MT, Sah VP, Zhao XL, Hunter JJ, Chien KR, Brown JH. The MEKK-JNK pathway is stimulated by alpha1-adrenergic receptor and ras activation and is associated with in vitro and in vivo cardiac hypertrophy. *J Biol Chem* 1997;272:14057-61.
83. Thorburn J, Xu S, Thorburn A. MAP kinase- and Rho-dependent signals interact to regulate gene expression but not actin morphology in cardiac muscle cells. *EMBO J* 1997;16:1888-900.
84. Bueno OF, De Windt LJ, Lim HW, et al. The dual-specificity phosphatase MKP-1 limits the cardiac hypertrophic response in vitro and in vivo. *Circ Res* 2001;88:88-96.
85. Nicol RL, Frey N, Pearson G, Cobb M, Richardson J, Olson EN. Activated MEK5 induces serial assembly of sarcomeres and eccentric cardiac hypertrophy. *Embo J* 2001;20:2757-67.
86. Esposito G, Prasad SV, Rapacciuolo A, Mao L, Koch WJ, Rockman HA. Cardiac overexpression of a G(q) inhibitor blocks induction of extracellular signal-regulated kinase and c-Jun NH(2)-terminal kinase activity in in vivo pressure overload. *Circulation* 2001;103:1453-8.
87. Finn SG, Dickens M, Fuller SJ. c-Jun N-terminal kinase-interacting protein 1 inhibits gene expression in response to hypertrophic agonists in neonatal rat ventricular myocytes. *Biochem J* 2001;358:489-95.
88. Sadoshima J, Montagne O, Wang Q, et al. The MEKK1-JNK pathway plays a protective role in pressure overload but does not mediate cardiac hypertrophy. *J Clin Invest* 2002;110:271-9.

Chapter 1. Transgenic mice and cardiac remodeling

89. Wang Y, Huang S, Sah VP, et al. Cardiac muscle cell hypertrophy and apoptosis induced by distinct members of the p38 mitogen-activated protein kinase family. *J Biol Chem* 1998;273:2161-8.
90. Dash R, Schmidt AG, Pathak A, et al. Differential regulation of p38 mitogen-activated protein kinase mediates gender-dependent catecholamine-induced hypertrophy. *Cardiovasc Res* 2003;57:704-14.
91. Rajewsky K, Gu H, Kuhn R, et al. Conditional gene targeting. *J Clin Invest* 1996;98:600-3.
92. Braz JC, Bueno OF, Liang Q, et al. Targeted inhibition of p38 MAPK promotes hypertrophic cardiomyopathy through upregulation of calcineurin NFAT signaling. *J Clin Invest* 2003;111:1475-86.
93. Hayashida W, Kihara Y, Yasaka A, Inagaki K, Iwanaga Y, Sasayama S. Stage-specific differential activation of mitogen-activated protein kinases in hypertrophied and failing rat hearts. *J Mol Cell Cardiol* 2001;33:733-44.
94. Molkentin JD, Lu JR, Antos CL, et al. A calcineurin-dependent transcriptional pathway for cardiac hypertrophy. *Cell* 1998;93:215-28.
95. Dong D, Duan Y, Guo J, et al. Overexpression of calcineurin in mouse causes sudden cardiac death associated with decreased density of K⁺ channels. *Cardiovasc Res* 2003;57:320-32.
96. De Windt LJ, Lim HW, Taigen T, et al. Calcineurin-mediated hypertrophy protects cardiomyocytes from apoptosis in vitro and in vivo: An apoptosis-independent model of dilated heart failure. *Circ Res* 2000;86:255-63.
97. Zou Y, Hiroi Y, Uozumi H, et al. Calcineurin plays a critical role in the development of pressure overload-induced cardiac hypertrophy. *Circulation* 2001;104:97-101.
98. Zou Y, Yao A, Zhu W, et al. Isoproterenol activates extracellular signal-regulated protein kinases in cardiomyocytes through calcineurin. *Circulation* 2001;104:102-8.
99. Van Rooij E, Doevendans PA, de Theije CC, Babiker FA, Molkentin JD, de Windt LJ. Requirement of nuclear factor of activated T-cells in calcineurin-mediated cardiomyocyte hypertrophy. *J Biol Chem* 2002;277:48617-26.
100. Wilkins BJ, De Windt LJ, Bueno OF, et al. Targeted disruption of NFATc3, but not NFATc4, reveals an intrinsic defect in calcineurin-mediated cardiac hypertrophic growth. *Mol Cell Biol* 2002;22:7603-13.
101. Lim HW, New L, Han J, Molkentin JD. Calcineurin enhances MAPK phosphatase-1 expression and p38 MAPK inactivation in cardiac myocytes. *J Biol Chem* 2001;276:15913-9.
102. De Windt LJ, Lim HW, Haq S, Force T, Molkentin JD. Calcineurin promotes protein kinase C and c-Jun NH₂-terminal kinase activation in the heart. Cross-talk between cardiac hypertrophic signaling pathways. *J Biol Chem* 2000;275:13571-9.
103. Rothermel BA, McKinsey TA, Vega RB, et al. Myocyte-enriched calcineurin-interacting protein, MCIP1, inhibits cardiac hypertrophy in vivo. *Proc Natl Acad Sci U S A* 2001;98:3328-33.
104. Hill JA, Rothermel B, Yoo KD, et al. Targeted inhibition of calcineurin in pressure-overload cardiac hypertrophy. Preservation of systolic function. *J Biol Chem* 2002;277:10251-5.
105. Vega RB, Rothermel BA, Weinheimer CJ, et al. Dual roles of modulatory calcineurin-interacting protein 1 in cardiac hypertrophy. *Proc Natl Acad Sci U S A* 2003;100:669-74.

Chapter 1. Transgenic mice and cardiac remodeling

106. Antos CL, McKinsey TA, Frey N, et al. Activated glycogen synthase-3 beta suppresses cardiac hypertrophy in vivo. *Proc Natl Acad Sci U S A* 2002;99:907-12.
107. De Windt LJ, Lim HW, Bueno OF, et al. Targeted inhibition of calcineurin attenuates cardiac hypertrophy in vivo. *Proc Natl Acad Sci U S A* 2001;98:3322-7.
108. Adams JW, Sakata Y, Davis MG, et al. Enhanced Galphaq signaling: a common pathway mediates cardiac hypertrophy and apoptotic heart failure. *Proc Natl Acad Sci U S A* 1998;95:10140-5.
109. Yussman MG, Toyokawa T, Odley A, et al. Mitochondrial death protein Nix is induced in cardiac hypertrophy and triggers apoptotic cardiomyopathy. *Nat Med* 2002;8:725-30.
110. Bueno OF, Molkentin JD. Involvement of extracellular signal-regulated kinases 1/2 in cardiac hypertrophy and cell death. *Circ Res* 2002;91:776-81.
111. Pennica D, King KL, Shaw KJ, et al. Expression cloning of cardiotrophin 1, a cytokine that induces cardiac myocyte hypertrophy. *Proc Natl Acad Sci U S A* 1995;92:1142-6.
112. Sheng Z, Knowlton K, Chen J, Hoshijima M, Brown JH, Chien KR. Cardiotrophin 1 (CT-1) inhibition of cardiac myocyte apoptosis via a mitogen-activated protein kinase-dependent pathway. Divergence from downstream CT-1 signals for myocardial cell hypertrophy. *J Biol Chem* 1997;272:5783-91.
113. Hirota H, Chen J, Betz UA, et al. Loss of a gp130 cardiac muscle cell survival pathway is a critical event in the onset of heart failure during biomechanical stress. *Cell* 1999;97:189-98.
114. Lotem J, Kama R, Sachs L. Suppression or induction of apoptosis by opposing pathways downstream from calcium-activated calcineurin. *Proc Natl Acad Sci USA* 1999;96:12016-20.
115. Saito S, Hiroi Y, Zou Y, et al. beta-Adrenergic pathway induces apoptosis through calcineurin activation in cardiac myocytes. *J Biol Chem* 2000;275:34528-33.
116. Bueno OF, Lips DJ, Kaiser RA, et al. Calcineurin Abeta gene targeting predisposes the myocardium to stress-induced apoptosis and dysfunction. *Circ Res*. 2003 Nov 13 [Epub ahead of print] 2003.
117. Pu WT, Ma Q, Izumo S. NFAT transcription factors are critical survival factors that inhibit cardiomyocyte apoptosis during phenylephrine stimulation in vitro. *Circ Res* 2003;92:725-31.
118. Tanaka N, Dalton N, Mao L, et al. Transthoracic echocardiography in models of cardiac disease in the mouse. *Circulation* 1996;94:1109-17.
119. De Windt LJ, Willems J, Reneman RS, Van der Vusse GJ, Arts T, Van Bilsen M. An improved isolated, left ventricular ejecting, murine heart model. Functional and metabolic evaluation. *Pflugers Arch* 1999;437:182-90.
120. Palmén M, Daemen MJ, Buehler A, et al. Impaired cardiac remodeling and function after myocardial infarction in FGF-1 transgenic mice. *Circulation* 1999;100:250.
121. Rockman HA, Hamilton RA, Jones LR, Milano CA, Mao L, Lefkowitz RJ. Enhanced myocardial relaxation in vivo in transgenic mice overexpressing the beta2-adrenergic receptor is associated with reduced phospholamban protein. *J Clin Invest* 1996;97:1618-23.
122. Chacko VP, Aresta F, Chacko SM, Weiss RG. MRI/MRS assessment of in vivo murine cardiac metabolism, morphology, and function at physiological heart rates. *Am J Physiol Heart Circ Physiol* 2000;279:H2218-24.

Chapter 1. Transgenic mice and cardiac remodeling

123. Georgakopoulos D, Mitzner WA, Chen CH, et al. In vivo murine left ventricular pressure-volume relations by miniaturized conductance micromanometry. *Am J Physiol* 1998;274:H1416-22.
124. Baan J, van der Velde ET, de Bruin HG, et al. Continuous measurement of left ventricular volume in animals and humans by conductance catheter. *Circulation* 1984;70:812-23.
125. Lips DJ, Van der Nagel T, Steendijk P, et al. Left ventricular pressure-volume measurements in mice: A comparative study between a closed-chest versus open-chest approach. Submitted 2003.
126. Georgakopoulos D, Christe ME, Giewat M, Seidman CM, Seidman JG, Kass DA. The pathogenesis of familial hypertrophic cardiomyopathy: early and evolving effects from an alpha-cardiac myosin heavy chain missense mutation. *Nat Med* 1999;5:327-30.
127. Franco F, Thomas GD, Giroir B, et al. Magnetic resonance imaging and invasive evaluation of development of heart failure in transgenic mice with myocardial expression of tumor necrosis factor-alpha. *Circulation* 1999;99:448-54.
128. Takaoka H, Esposito G, Mao L, Suga H, Rockman HA. Heart size-independent analysis of myocardial function in murine pressure overload hypertrophy. *Am J Physiol Heart Circ Physiol* 2002;282:H2190-7.
129. Nakamura A, Rokosh DG, Paccanaro M, et al. LV systolic performance improves with development of hypertrophy after transverse aortic constriction in mice. *Am J Physiol Heart Circ Physiol* 2001;281:H1104-12.
130. Hill JA, Karimi M, Kutschke W, et al. Cardiac hypertrophy is not a required compensatory response to short-term pressure overload. *Circulation* 2000;101:2863-9.
131. Kai T, Ishikawa K. Lisinopril reduces left ventricular hypertrophy and cardiac polyamine concentrations without a reduction in left ventricular wall stress in transgenic Tsukuba hypertensive mice. *Hypertens Res* 2000;23:625-31.
132. Esposito G, Rapacciuolo A, Naga Prasad SV, et al. Genetic alterations that inhibit in vivo pressure-overload hypertrophy prevent cardiac dysfunction despite increased wall stress. *Circulation* 2002;105:85-92.

Chapter 2. Molecular aspects of cardiac failure

Molecular determinants of myocardial hypertrophy and failure

Daniel J. Lips., Leon J. de Windt, Dave J.W. van Kraaij and Pieter A.

Doevendans

Published in European Heart Journal 2003, volume 24, issue 10, pages 883-96

Abstract

The implementation of molecular biological approaches has led to the discovery of single genetic variations that contribute to the development of cardiac failure. In the present review characteristics that are invariably associated with the development of failure in experimental animals and clinical studies are discussed, which may provide attractive biological targets in the treatment of human heart failure. Findings from the Framingham studies have provided evidence that the presence of left ventricular hypertrophy is the main risk factor for subsequent development of heart failure in man. Conventional views identify myocardial hypertrophy as a compensatory response to increased workload, prone to evoke disease. Recent findings in genetic models of myocardial hypertrophy and human studies have provided the molecular basis for a novel concept, which favors the existence of either compensatory or maladaptive forms of hypertrophy, of which only the latter leads the way to cardiac failure. Furthermore, the concept that hypertrophy compensates for augmented wall stress is probably outdated. Here we provide the molecular pathways that can distinguish beneficial from maladaptive hypertrophy.

Introduction

Heart failure is associated with high morbidity and mortality rates in modern Western societies and can be viewed upon as the end-stage form of various forms of heart disease.(1) The prognosis for patients with heart failure is poor and is in fact even worse than the survival chances in patients suffering from various malignancies.(2,3) In community studies, the annual mortality was found to be 10-20% in patients with mild-moderate symptoms requiring hospital admission and this figure can be as high as 40-60% in patients with severe heart failure.(4) The single most powerful predictor for the development of heart failure is the presence of left ventricular hypertrophy.(5) For this reason, much effort is currently undertaken to investigate the etiology of hypertrophic mechanisms and to unravel the molecular pathways underlying this affliction. These efforts are part of an ongoing search to find novel treatment modalities to prevent or even reverse human heart failure. Heart failure is one of the most challenging diseases of the future due to the heterogeneous cardiac response especially in its final stages. In addition, it is still under-represented in the public and political attention.

A powerful tool in the hands of cardiovascular researchers is the implementation of molecular biological approaches to investigate the role of single modifier genes on the development of cardiac disease. Accordingly, the number of transgenic and knockout models of hypertrophy and failure has grown exponentially in recent years, and this has provided us with novel genetic cues about the human etiology of this affliction. The aim of the present review is to give a brief summary of the current status of our knowledge on cardiac hypertrophy and failure and to discuss novel biological targets that have been demonstrated to be critical in the development of the disease in genetic models. These targets may become key players in future treatment of human heart failure.

Figure 1

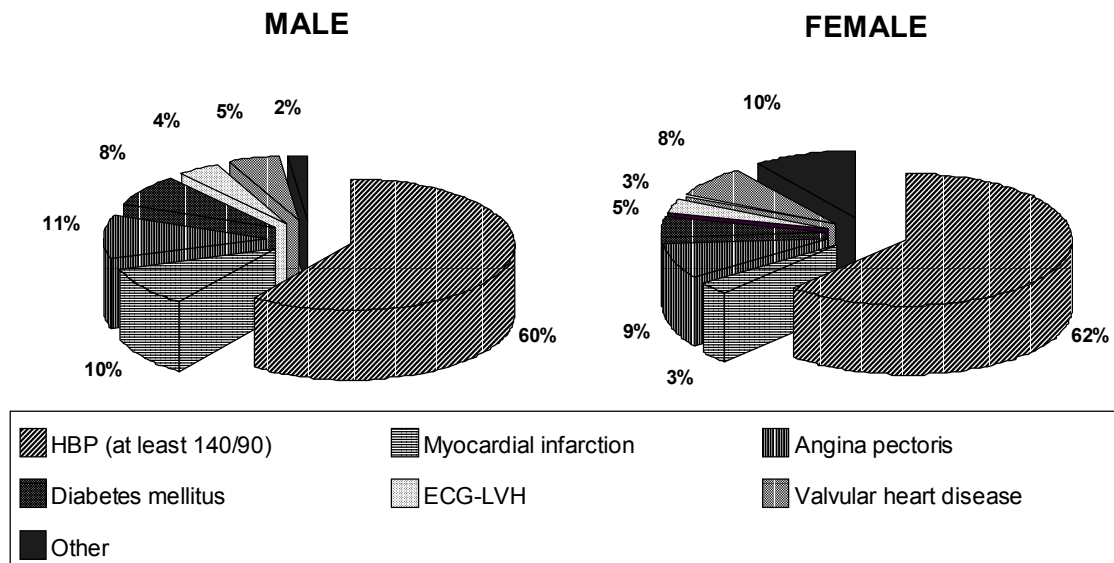


Fig. 1: Percentages of risk-factors for male and female patients for the development of subsequent heart failure. The pie-diagrams are representative for Dutch males and females with a mean age of 69 years. The percentages of risk-factors are rather similar distributed between sexes, the percentage myocardial infarctions being the only significant difference between males and females. High blood pressure is the far most common risk factor for developing heart failure. (With permission derived from Mosterd et al. Prevalence of heart failure and left ventricular dysfunction in the general population: the Rotterdam Study. Eur Heart J 1999;20(6):447-55).

Heart failure

Heart failure in humans is characterized by low cardiac output due to systolic and/or diastolic dysfunction.(6) When depending on increased ventricular performance, for example during physical exercise, heart failure patients typically present with acute symptoms of clinical cardiac failure, e.g. fatigue, dyspnea and sometimes anginal pain, and palpitations (Table 1). For the diagnosis of heart failure the clinical criteria from the European Society of Cardiology are being used.(7) The diagnosis heart failure is made confidently in the presence of multiple symptoms and signs, combined with objective evidence of cardiac dysfunction, usually through echocardiography (Table 1). Echocardiography is essential for both systolic and diastolic failure.(6) In cases where the diagnosis is in doubt, the diagnosis can be stated by an additional positive response to treatment directed towards heart failure. The degree of cardiovascular disability is distinguished by The New York Heart Association Functional Classification (class I–IV) or the classification of symptoms in mild, moderate and severe. Both represent the degree of functional impairment in these patients.

Table 1. Criteria for diagnosing human heart failure

DIAGNOSTIC CRITERIA
<p>1. Symptoms of heart failure (at rest or during exercise)</p> <p style="text-align: center;"><i>Symptoms</i></p> <ul style="list-style-type: none"> • breathlessness • ankle swelling • fatigue <p style="text-align: center;"><i>Signs</i></p> <ul style="list-style-type: none"> • displaced heart beat • pitting edema • raised venous pressure • third heart sound
<p>2. Objective evidence of cardiac dysfunction (at rest)</p>
<p>3. Response to treatment directed towards heart failure</p>

The clinical criteria for the diagnosis of heart failure are divided into three parts: (1) the presence of symptoms of heart failure; (2) evidence of cardiac dysfunction as measured by echocardiography; (3) in case of doubt of the diagnosis, a positive response towards heart failure treatment. Patients are subject to heart failure, when at least criteria 1 and 2 are evidently present.

Chapter 2. Molecular aspects of cardiac failure

From a clinical point of view three broad categories of heart failure have been proposed (see table 1). In this view, heart failure can originate from (1) increased hemodynamic burden, by far the most common cause; (2) inherited mutations in genes encoding structural components which affect contraction and relaxation, and (3) precipitating causes initiating episodes of clinical heart failure.(8) A general misconception states that ischemic heart disease (e.g. acute myocardial infarction (MI) or coronary artery disease) is the most common underlying and precipitating cause of heart failure in prevalence. Instead, heart failure in Western societies most often results from progressive hypertensive heart disease (Figure 1).(1) Patients who survived MI have, however, a significant higher relative risk to develop subsequent heart failure than patients with any other cardiac disease.(1-3,5)

Multiple studies have described the contribution of several characteristic changes that are encountered in the end-stage failing heart, which distinguishes it from the non-diseased state. The best documented characteristics on the intracellular, stromal or organ level are (1) a genetic reprogramming which resembles the genetic expression profile of the fetal heart; differing degrees of cardiomyocyte hypertrophy and concomitant activation of intracellular signaling molecules; mitochondrial dysfunction; alterations at the level of the sarcomeric and cytoskeletal architecture; aberrant intracellular calcium handling; unfavorable myofibrillar architecture; (2) increased vulnerability or presence of necrotic or programmed cell death; excess extracellular matrix formation; (3) a reduction of organ capillarisation and presence of regional ischemia; evidence of systemic and myocardial (neuro)humoral stimulation; vulnerability to (supra)ventricular dysrhythmias, and, most notably, hemodynamic dysfunction at the systolic and/or diastolic level. Although each of these characteristic alterations appear to form independent entities, presence of any of the above mentioned characteristics is sufficient, at least in experimental models, to set in motion a sequence of

Chapter 2. Molecular aspects of cardiac failure

events invariably resulting in organ failure, characterized by a phenotype encompassing some or even all of the above abnormalities.

Table 2. Characteristics of cardiac hypertrophy in transition to failure

<i>Morphology</i>	
Heart weight/body weight	↑
Concentric hypertrophy	Pronounced increase wall thickness
Eccentric hypertrophy	Pronounced ventricular dilation
<i>Histology</i>	
Apoptosis	↑
Necrosis	↑
Fibrosis	↑
Thrombosis	↑
<i>Cellular</i>	
Myocyte hypertrophy	↑
Protein synthesis	↑
ANF excretion	↑
Gene-expression	
c-Fos	↑
c-Jun	↑
c-Myc	↑
ANF	↑
BNP	↑
β-MHC	↑
α-skeletal actin	↑
MLC-2a	↓
Calcium handling	↓
<i>Cardiac function</i>	
Systolic function	↓
End-systolic pressure	↓
Diastolic function	↓
End-diastolic pressure	↑
Contractility	↓
Relaxation	↓
β-Adrenergic response	↓
Arrhythmias	↑
<i>Signaling pathways</i>	
MAPK:	
ERK 1/2	Concentric hypertrophy
JNK	Eccentric hypertrophy; severe dilation
p38	Eccentric hypertrophy; severe dilation

JAK/STAT	Concentric hypertrophy; compensating
CaMK/calcineurin	Cardiac hypertrophy and heart failure

Distinctive features are detected in the transition towards heart failure. Histologic analyses proved increase of apoptosis, necrosis, fibrosis and thrombosis. At the cellular level, well-known hypertrophic markers remain elevated or increase, while the cellular calcium handling attenuates in efficiency. All these features have their effects on cardiac function, such as decreased contractility and relaxation, elevated end-diastolic pressure and arrhythmias. Animal research led to the discovery of several possible causative cellular signaling pathways, such as MAPK, JAK/STAT and CaMK/Calcineurin pathways.

Hypertrophy

Current conceptualization states that the heart is able to augment output in the face of increased hemodynamic demands by means of growth of cardiomyocytes. In that view, cardiac hypertrophy can be defined as the increase in myocardial mass in an effort to alleviate the elevation in wall stress according to LaPlace's principle (Figure 2).(9) To execute this response, the myocardium is equipped with a host of conserved neurohumoral and intracellular reactive cascade systems. Since the proliferative capacity of the cardiac myocyte is absent or at best limited, the heart reduces wall stress by myocyte growth (hypertrophy), during which process the nucleus of human cardiomyocytes undergoes polyploidy.(10,11) The diploid set (2c) of the myocyte proliferates during this growth process to tetraploid (4c), octoploid (8c) sets of chromosomes, or even more. The polyploidization probably enables the cardiomyocyte to hypertrophy without losing its normal cell volume/DNA content ratio, but the functional significance of this adaptation still remains obscure. The myocardial cell types that do respond with proliferation (hyperplasia) in response to mitogenic stimuli, are non-muscle cells, most notably fibroblasts, and this event does not lead to the required reduction of wall stress.

Figure 2

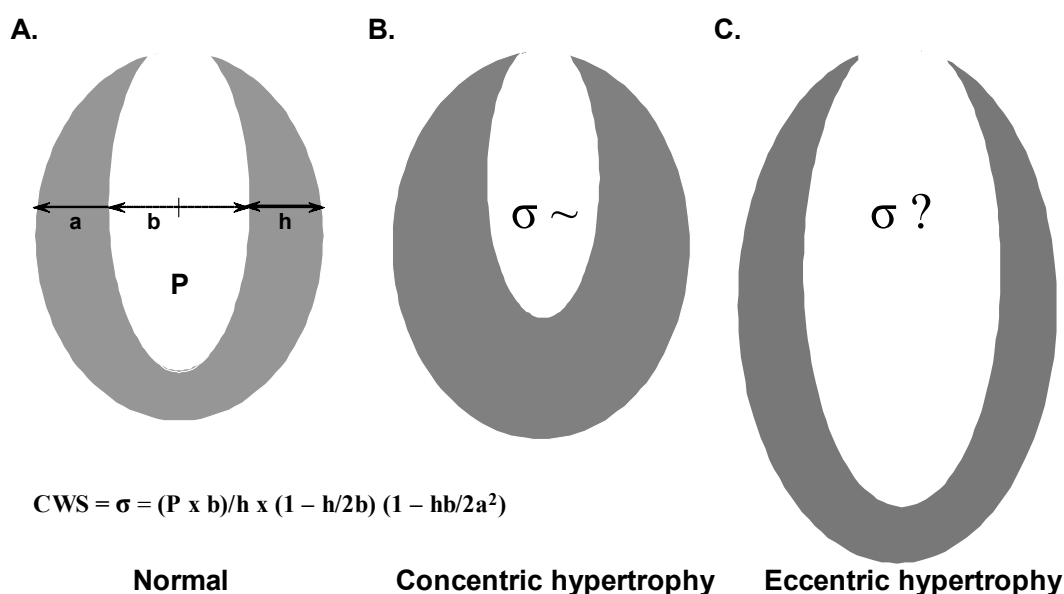


Fig. 2: Morphology of the left ventricle: differences between normal and hypertrophic hearts.

The schematic presentation of concentric and eccentric hypertrophy clearly shows the morphologic features, which generally are detected during echocardiographic analysis. A. Also depicted are the elements which determine circumferential wall stress (CWS) in the left ventricle, the strongest force generated within the ventricular wall. P indicates intraventricular pressure, a and b are the major and minor semiaxes and h is left ventricular wall thickness. These assumptions are only correct in those situations where left ventricular function is relatively uniform. B. Wall stress (σ) increases at any LV radius when LV pressure (e.g. afterload) rises, for example in case of systemic hypertension or aortic stenosis. Hypertrophy is thought to balance the augmented pressure by increasing wall thickness. C. In dilated cardiomyopathy the enlarged ventricular diameter results in a greater wall stress.

Data derived from mouse studies, however, cast doubt on the idea that a reduction of wall stress is required for preserving hemodynamic functioning during the development of hypertrophy.(12) In gene-targeted mice, where Gq signaling pathway is genetically blocked, with blunted hypertrophy after experimentally pressure-overload, maintenance of cardiac function was observed, despite an inadequate normalization of left ventricular wall stress. The mice with blunted hypertrophy fared better than their wild-type littermates in response to long-term load, as shown by the absence of progressive LV dilatation and dysfunction on serial echocardiography. (12) The observation underscores the importance of preventing or inhibiting hypertrophic growth in the human heart as ventricular hypertrophy is proven to be a risk factor for cardiovascular mortality in humans. (13) Not only leads hypertrophic growth of the heart in time to increased morbidity and mortality, also the early correction of wall stress seems unnecessary to maintain cardiac function on the long-term. Thereby, a commonly accepted hypothesis should probably be reconsidered.

Defined extrinsic hypertrophic stimuli consist of conditions of increased resistance to left ventricular afterload, resulting from outflow obstructions such as aortic stenosis and systemic hypertension. These conditions produce a state of pressure-overload. The morphological adaptation to pressure-overload consists of concentric hypertrophy, characterized by thickening of the myocardial walls without a significant LV lumen dilation (Figure 2). Other defined extrinsic stimuli include volume-overload, which occurs in the clinical setting of aortic valve regurgitation, mitral valve regurgitation, anemia or other situations in which cardiac output is increased at normotensive pressures. Volume-overload specifically leads to eccentric hypertrophy defined by thickening of the free walls in conjunction with LV cavity diameter increase.(14) Ischemia, myocardial infarction and episodes of atrial fibrillation also act as extrinsic hypertrophic stimuli.

Intrinsic stimuli involve genetic abnormalities (mutations) in sarcomeric motor protein genes or in genes that encode components of the cytoskeletal architecture and metabolic (mitochondrial) disorders.(5,15) Genetic mutations in sarcomeric proteins are the basis of congenital human heart disease such as hypertrophic cardiomyopathy (HCM), with a prevalence of 1 in 500 patients.(5,16) Characteristic myocardial changes in HCM include a non-dilated left ventricular chamber with thickened walls, reminiscent of a concentric hypertrophy.(5) HCM is a Mendelian trait with an autosomal dominant pattern of inheritance.(5) Currently, mutations have been found in the human genes coding for β -myosin heavy chain, cardiac troponin T, α -tropomyosin, myosin-binding protein C, myosin light chain 1 and 2, cardiac α -actin genes, titin and mitochondrial DNA.(5,17-19) Mutated cytoskeletal genes are not able to handle the mechanical workload that is required, causing mechanical dysfunction of myocytes, thus provoking a hypertrophic response.

During both pressure and volume overload defined systemic and local neurohumoral changes take place. The best characterized example is the renin-angiotensin-aldosterone system

(RAAS). Rise of systemic and myocardial angiotensin II (Ang II), acting through the angiotensin (AT)-1 and AT-2 receptors, promotes fibroblast proliferation and collagen production which is usually extensive enough to produce macroscopically visible fibrosis that contribute to increased left ventricular stiffness and reduced compliance.(20) Independent of the systemic influences on vascular resistance and cardiac afterload, Ang II is prominently involved in promoting cardiomyocyte hypertrophy.(20-25) Endothelin-1 (ET-1) is another humoral factor with systemic and local actions sufficient to induce a hypertrophic response in cardiomyocytes.(23) ET-1 has been proven to be a local contributor to pressure-overload or mechanical-stretch induced hypertrophy.(20,26,27) Finally, sympathetic activation is thought to be the cause of β -adrenergic desensitization in heart failure, a consequence of downregulation of β 1-receptors and uncoupling of the β 2-receptors.(28) The downregulation and desensitization of β -adrenergic receptors is more prominent in failing than in hypertrophied myocardium.(29) This uncoupling is thought to be caused by increased activity of a β -adrenergic receptor kinase (β ARK) and an increase in inhibitory G-protein alpha subunits ($G_{i\alpha}$) which depress adenylyl cyclase activity.(30) The attenuation in adenylyl cyclase activity is thought to be a causal link in the transition from cardiac hypertrophy to cardiac failure.(29,31)

ACE-inhibition is currently accepted as a valuable therapeutic approach in the management of heart failure.(32) Specific AT-1 antagonists overcome the potential limitations of the use of ACE-inhibitors, such as insufficient suppression of tissue ANG II production and bradykinin-related side effects.(33)

Numerous animal studies and clinical trials have convincingly demonstrated that beta-blockade improves functional capacity, ventricular function and decreases mortality in patients with heart failure of various etiologies. Amongst the effects of beta-blockers are improvement in function of failing myocardium, decrease in dilation and hypertrophy, and

reduction in LV wall stress. Recent evidence indicates that beta-blockers can also inhibit the RAAS and in this role limit progressive chamber stiffening, thereby attenuating chamber remodeling and diastolic dysfunction in heart failure.(34)

Controversy exists as to whether LV hypertrophy should be considered either as a pathological condition that invariably evokes disease by transforming in failure, or as fundamentally different forms of cardiomyocyte growth exist. For example, a profound increase in myocardial mass is observed shortly after birth due to hemodynamic demands on the neonatal heart. Also, increased demands for cardiac work e.g. during athletic exercise or during pregnancy evokes a considerable hypertrophic response, which is not associated with risk for the development of decompensation and failure. In view of recent experimental observations and the distinctive phenotypic observations in humans, we rather favor a distinction between *compensatory* versus *maladaptive* forms of hypertrophy (Table 2). Since the morphological and hemodynamic characteristics associated with beneficial hypertrophic growth are fundamentally different from those following hypertension or MI, it seems feasible to reason that fundamentally different molecular programs underlie beneficial and maladaptive hypertrophy. In our view, maladaptive hypertrophy is invariably associated with activation of a molecular program involving persistent activation of unfavorable intracellular signaling modules, an increased rate of cardiomyocyte apoptosis, profound extracellular matrix deposition leading to reduced diastolic compliance and aberrant intracellular Ca^{2+} handling. In the following sections these aspects are further delineated.

Current molecular investigations

In recent years, much research has focused on the identification of intracellular signaling cascades which mediate extrinsic and intrinsic growth signals into co-ordinated alterations of genetic profiles. In addition to causing changes in gene expression, hypertrophic stimuli increase the overall rate of RNA transcription and protein synthesis, both leading to hypertrophic growth of cardiomyocytes. In the transition from compensating to decompensating hypertrophy several intracellular molecules have found to be up- or down-regulated and therefore thought to be mediators of this pathologic process. Preventing the development of maladaptive hypertrophy is the ultimate goal of research into these molecules.

Hypertrophy is initiated and maintained *in vitro* and *in vivo* by several factors, such as vasoactive peptides, peptide growth factors, hormones and neurotransmitters (i.e. ET-1, α_1 -adrenergic agonists, Ang II, fibroblast growth factors (FGF), insulin-like growth factor (IGF)-1 and cardiotrophin (CT)-1).(24,35-43) Estrogens on the other side are believed to have hypertrophy reducing effects(44-48), which are probably mediated via increased atrial natriuretic factor (ANF) expression. (49) The hypertrophic factors stimulate intracellular signaling cascades which initiate a hypertrophic, fetal-like gene-program. In pathological conditions ANF is produced by ventricular cells as part of the newly expressed ventricular fetal gene-program. The effect of ANF on blood pressure, but also direct cellular effects could explain the beneficial aspects of ANF. (49,50)

Most of the agonists bind to G protein coupled receptors, from which G_q/G_{11} and G_i/G_o are involved in the hypertrophic response.(51-53) Protein kinases (PKs) are located downstream from these receptors, from which protein kinase C (PKC) is strongly implicated in hypertrophic signaling.(35,54) The small GTP binding proteins (Ras and Rho families) play important roles in the hypertrophic response through mediating the activation of the mitogen-activated protein kinase (MAPK) superfamily cascades following PKC activation.(55,56)

MAPKs are a widely distributed group of enzymes ending in three terminal MAPK branches [p38-MAPKs, the extracellular signal-regulated kinases (ERKs), c-Jun NH(2)-terminal kinases (JNKs). Figure 3]. The family of MAPKs has been shown to play causal roles in the development of cardiac hypertrophy and the transition towards heart failure.(54,57-59)

Differential activation of single terminal branches of the MAPK families results in specific cardiac morphologic and functional phenotypes.(57) (60) For example, ERK1/2 MAPK activation leads to a concentric form of hypertrophy with enhanced cardiac function.(57) In contrast single activation of ERK5 MAPK leads to eccentric cardiac hypertrophy and rapid transition towards heart failure.(60) Furthermore, p38-MAPK and JNK activation lead to maladaptive hypertrophy.(61-65) Like ERK1/2 overexpression, another example of beneficial hypertrophic phenotypic alterations is observed upon activation of the phosphoinositide 3-kinase (PI3K), which lies downstream of many receptor tyrosine kinases. Furthermore, recent studies have indicated that pathways employing the gp130 receptor might be of benefit to the heart. Well-known intracellular mediators of gp130 signaling include the family of Janus Kinase (JAK), which activate the family of the Signal Transducer and Activator of Transcription (STAT) proteins. The JAK/STAT pathway, which is activated by CT-1, leukemia inhibitory factor (LIF) and Angiotensin II, is implicated in the hypertrophic response, but its role is still obscure.(66-68)

Figure 3

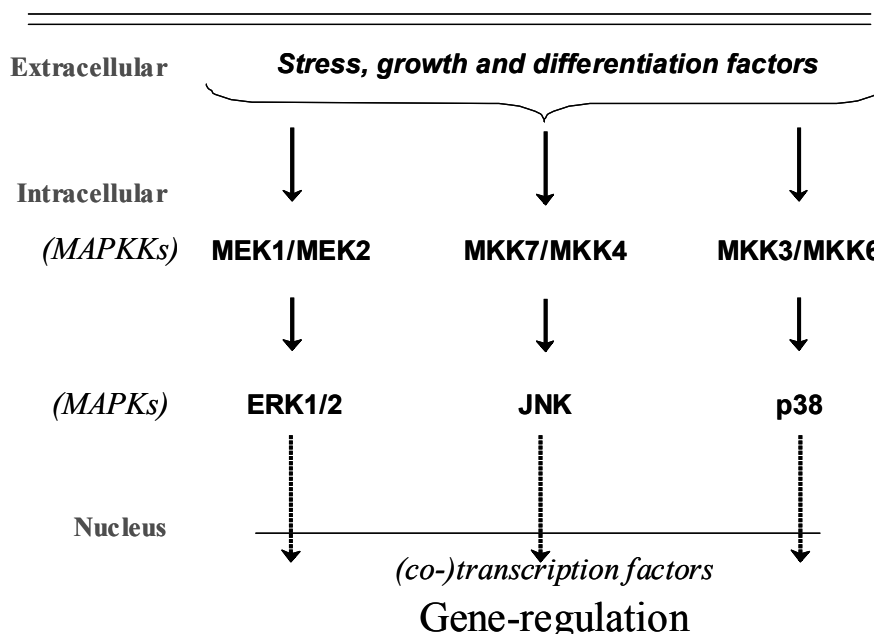


Fig. 3: Simple presentation of the three kinase modules and MAPK subfamilies. The mitogen-activated protein kinase (MAPK) pathways consist of three separate terminal branches: the extracellular signal-regulated kinases (ERK), c-Jun NH(2)-terminal kinases (JNKs) and the p38 MAPK pathways. These translocate to the nucleus after activation and set gene transcription. The MAPKs are activated by MAPK kinases (MAPKKs) upon extracellular stimulation. The MAPKK differ per kinase module. MEK1 and MEK2 MAPKKs activate ERK MAPKs; MKK7 and MKK4 activate JNK and MKK3/MKK6 are upstream of p38 MAPKs.

Because of these findings, it has been hypothesized that specific intracellular protein activation programs lead to specific cardiac phenotypes. Similar results are presented in human studies.⁽⁶⁵⁾ For example, involving the MAPK-family, the activation of JNK and p38-MAPKs is augmented in failing human hearts, while ERK activation remains on a physiologic level. This finding indicates an association between p38-MAPK, JNKs and a failing cardiac phenotype in human. Further understanding of the mechanisms, through which differential activation of MAPKs may lead to distinctive cardiac phenotypes, is essential for future clinical therapy.

Intracellular calcium handling

Intracellular Ca^{2+} concentrations and handling are also involved in the hypertrophic response. The Ca^{2+} /calmodulin-dependent protein kinase II and the Ca^{2+} /calmodulin-dependent protein phosphatase (calcineurin), from which the activity is Ca^{2+} dependent, are involved in the cardiac hypertrophic response.(69-74) Activated calcineurin promotes the dephosphorylation of the transcription factor NF-AT3, which sequentially migrates into the nucleus and interacts with the transcription factor GATA4 to induce hypertrophic gene-program expression.

Figure 4

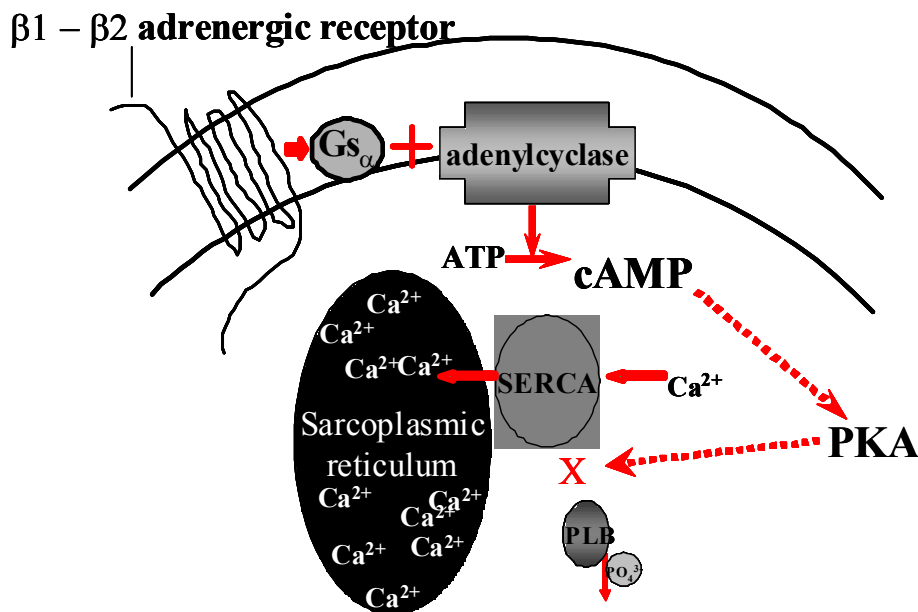


Fig. 4 The β -adrenergic pathway leading to SR Ca^{2+} uptake. Following β -adrenergic stimulation of the adrenergic G-protein, coupled receptors the Gs_α - and $\text{Gs}_{\beta\gamma}$ -subunits detach from each other. The Gs_α -subunit stimulates the membrane bound adenylylase to form cyclic AMP (cAMP). The cAMP stimulates protein kinase A (PKA) to dephosphorylate the phospholamban protein (PLB) attached to the sarcoplasmic reticulum

Ca²⁺-ATPase (SERCA). Upon dephosphorylation PLB loses its ability to bind SERCA. SERCA, without the PLB binding, increases actively the sarcoplasmic reticulum Ca²⁺-uptake, which directly increases relaxation and indirectly increases contractility.

In pressure-overload ventricular hypertrophy, after the early-response phase, a reduction in the expression of sarcoplasmic reticulum Ca²⁺ ATPase (SERCA) mRNA and protein were shown (Figure 4).(75-81) This seems in contradiction with the situation in the early-response phase. During the catecholamine mediated early-response phase the up-regulation of SERCA is needed to maintain cardiac output. The assumption is that when increased amounts of sarcomeric proteins start to stabilize cardiac function, SERCA is downregulated. Within 72-96 hours the SERCA-levels already return to base-line and they will decline even further in the progress of the hypertrophic process.(82) The consequence is a downregulated sarcoplasmic reticulum calcium uptake in the hypertrophic cardiomyocyte, resulting in a smaller amplitude and slower decline of the cellular [Ca²⁺]_i transient.(75-81) In dilated and failing human hearts, no differences in protein levels of SERCA, phospholamban and calsequestrin have been detected compared to non-failing controls.(83-87) Although no reduction in protein levels was detected, there were alterations found in the calcium handling, i.e. an attenuation in the sensitivity of SERCA develops.(87) A possible explanation for the alterations in calcium handling is provided by the phospholamban-sarcoplasmic reticulum calcium pump interaction.(59,88-92) The protein phospholamban is the inhibitor of SERCA in the reticular membrane.(93-99) SERCA functions at the end of contraction of the heart. It pumps calcium out of the cytosol into the sarcoplasmic reticulum. During contraction phospholamban is bound to SERCA thereby decreasing the SERCA affinity for Ca²⁺.(93) In this manner phospholamban inhibits the function of SERCA. It is also possible to improve cardiac function by inhibiting phospholamban interaction with SERCA.(98) An alternative mechanism was proposed by Esposito et al(59), stating that the calcium homeostasis in the

Chapter 2. Molecular aspects of cardiac failure

myocytes of diseased murine hearts is altered, leading to decreased intracellular $[Ca^{2+}]$ transients and contractile responses caused by a dysfunctional excitation-contraction coupling, identified as a decreased sensitivity of the SR Ca^{2+} release mechanism to triggering Ca^{2+} . The question remains, which molecular process essential is in the transition from hypertrophy to failure. Nevertheless, the importance of the intracellular calcium milieu has been proven unequivocally.

Apoptosis

The programmed cell death process (apoptosis) can be divided in several biochemical and morphological distinct phases.(100) In the initiation phase pro-apoptotic stimuli trigger the onset of molecular changes leading to apoptosis. The apoptotic process is working on its full capacity during the effector phase, in which nucleic degradation takes place. In the degradation phase the hallmarks of apoptosis, such as membrane markers and morphologic changes, become evident. However, the point of no return occurs several hours before the appearance of the morphologic features.(101) Some morphologic features are the shrinkage of the cell at the onset of apoptosis accompanied by nuclear chromatin condensation. The nucleus eventually breaks up, a process called karyorrhexis. The apoptotic cell detaches from neighboring cells and surrounding extracellular matrix and forms extensions on its membrane. The extensions detach from the apoptotic cell (i.e. budding) and form apoptotic bodies. The bodies are rapidly phagocytosed by all sorts of neighboring cells without associated inflammation, which could be the consequence of releasing intracellular contents in cardiac tissue.

The chronic exposure to catecholamines can exert a toxic effect on the myocardium, by increasing the number of apoptotic myocytes mediated by the beta1-adrenergic receptor. Furthermore, angiotensin II type 1 receptor pathways, nitric oxide and natriuretic peptides are involved in the induction of apoptosis in these cells, while alpha1- and beta2- adrenergic receptors, endothelin-1 receptor type A pathways and gp130- activating cytokines are anti-apoptotic. The myocardial protection of the latter is mediated, at least in part, through MAPK-dependent pathways (especially ERK MAPK), compatible with the findings in other cell types.(57,102,103) In contrast, in some cases signaling pathways leading to apoptosis in cardiac myocytes are distinct from those in other cell types. The cAMP/PKA pathway induces apoptosis in cardiac myocytes and blocks apoptosis in other cell types. The p300 protein, a

co-activator of p53, mediates apoptosis in fibroblasts, but appears to play a protective role in differentiated cardiac myocytes.(104)

Figure 5

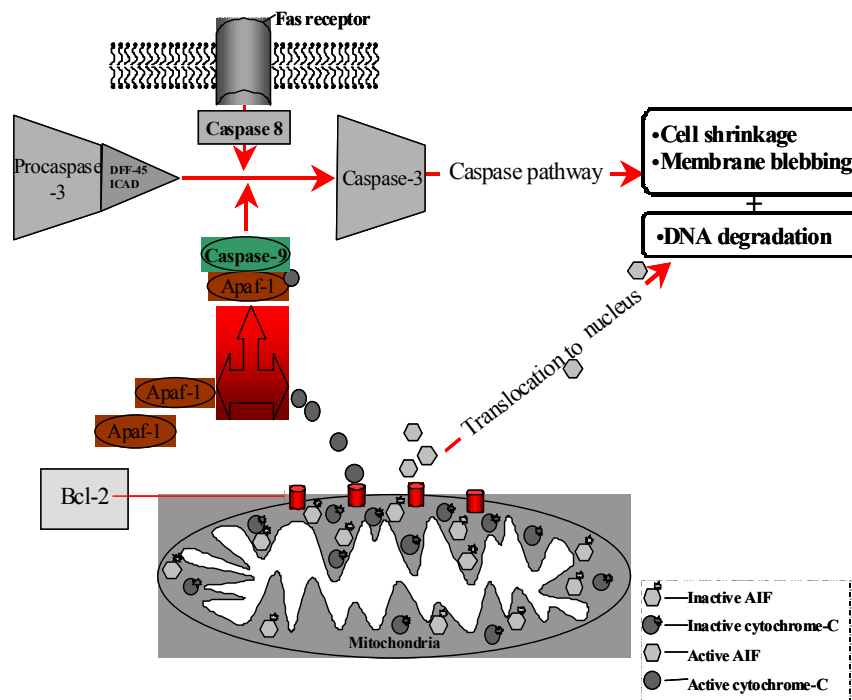


Fig. 5: Apoptosis pathways in cardiomyocytes. Several pathways leading to apoptosis have been identified in cardiomyocytes. Cell shrinkage, membrane blebbing and DNA degradation are followed upon stimulation by death receptors, for instance Fas-receptors, or mitochondrial proteins, such as cytochrome-C and apoptosis inducing factor (AIF). Fas-receptor activation leading to caspase 8 activation which induces the translation of procaspase-3 to caspase-3, the critical caspase. Caspase can also be activated by cytochrome-C. Cytochrome C is normally present in the outerlayer of the mitochondrial membranes in an inactive state. Upon stimulation it travels through protein-pores into the sarcoplasm and simultaneously gets activated. In the sarcoplasm cytochrome-C induces the activation of caspase-3, while AIF directly translocates to the nucleus and degradates the present DNA.

Initiation of apoptosis is associated with activation of different cascades, including the release of cytochrome C and the apoptosis inducing factor (AIF) from mitochondria into the cytoplasm and the processing of proteolytic caspases.(105-108) The activation of the caspases leads to fragmentation of various proteins, including cytoplasmic structural proteins, contractile proteins, proteins at the cell-to-cell and cell-to-matrix attachment sites and nuclear envelope proteins. At this time-point apoptotic cells can be visualized by labeled Annexin-V *in vivo*.(109,110) AIF, in contrast, translocates to the nucleus and initiates the fragmentation of nuclear DNA. This process results in the cleavage of chromatin into oligonucleosome-length DNA fragments, which is supported by endogenous DNA caspases, DNases like DNA fragmentation factor (DFF40) and caspase activated DNase (CAD). Caspases are cysteine proteases that cleave their substrate proteins specifically behind an aspartate residue.(111) They are formed constitutively in the non-apoptotic cell and remain inactive by dimerization with inhibitory proteins DFF45 and Inhibitor of CAD until stimulation by one of two major pathways. The first pathway is initiated by ligation of the death receptors, Fas and TNF receptors.(112) The mitochondrial pathway is the other and integrates apoptotic signals. This pathway is regulated by the Bcl-2 protein family.(113,114) When the mitochondrial pathway is activated permeability transition associated pores in the outer membrane of the mitochondria are opened, and this enables cytochrome C and AIF to be released from the mitochondrial transmembrane space.(115,116) In its turn cytochrome C activates apoptosis protease-activating factor (Apaf-1) and dATP, which lead to caspase activation. DNases cut the internucleosomal regions into double-stranded DNA fragments of 180-200 base pairs (bp).(100,117,118) This DNA fragmentation can be demonstrated by a characteristic laddering pattern on DNA agarose gel electrophoresis (DNA laddering) and terminal deoxynucleotidyltransferase-mediated dUTP nick end labeling (TUNEL) assay. Formation of

large size (50-300 Kilobp) DNA fragments precedes internucleosomal fragmentation, which is dependent of AIF activity (Figure 5).(106-108)

Apoptosis plays a role in the pathophysiology of several cardiac diseases such as maladaptive hypertrophy and heart failure.(105,119,120) Apoptosis is found to be increased in the remote myocardium after MI in animals and humans. Also, significantly more apoptotic cells are found in end-stage cardiomyopathy compared to control hearts. It has been proposed that ventricular dilatation and neurohumoral activation during heart failure lead to upregulation of transcription factors and prepare the cell for re-entry into the cell cycle, which fails and induces apoptosis.(105) The functional relevance of apoptosis though, is still obscure.

The question remains, if the frequency of apoptosis found in failing hearts is sufficient to explain a deterioration of cardiac function. Moreover, the question remains if apoptosis precedes the transition towards heart failure or only accompanies this process. Interpretation of the rate of apoptosis in diseased hearts is hampered by the fact that the time course of the apoptotic cascade in adult cardiomyocytes is unknown.(121) Results from animal studies indicate tight regulation of the different steps of the apoptotic cascade, which are time-dependent.(121) Furthermore, apoptosis seems to be a general muscular phenomenon.(122) Myocyte apoptosis occurs also in the skeletal muscle of patients with chronic heart failure, and its magnitude is associated with the severity of exercise capacity limitation and the degree of muscle atrophy. Muscle atrophy contributes to the limitation of exercise capacity, together with the increased synthesis of fast, more fatigable myosin heavy chains.(122)

If apoptosis accompanies heart failure and could lead to deterioration of cardiac function, beneficial effects could be expected from blockade of the process. Although studies in rats revealed a reduction of apoptosis after caspase blockade, the rate of necrosis subsequently increased.(121) This suggests that the cells are destined to die once the caspases

Chapter 2. Molecular aspects of cardiac failure

are activated, for example by mitochondrial damage. Blockade of apoptosis would therefore not be beneficial, because necrosis is accompanied with secondary morbidity, i.e. inflammation and extensive fibrosis.

Myocyte replacement could explain the discrepancy between extensive collagen accumulation and the modest reduction in the number of ventricular myocytes and the occasional detection of nuclear mitotic divisions in the pathologic heart. These findings led to the suggestion that myocytes are not terminally differentiated and cell proliferation may be stimulated in cardiomyopathies. Recent data indicated an increase in myocytes in the diseased and decompensated human heart by myocyte division.(123,124) Although these results appear very convincing, many cardiovascular researchers remain skeptic towards the rate and therefore the importance of cardiomyocyte division.

Fibrosis

Extracellular fibrillar collagen functions as scaffolding tissue to maintain cardiac structure and stiffness. An adverse accumulation of extracellular matrix structural protein compromises tissue stiffness and adversely affects myocardial viscoelasticity.(125)

Accumulation of fibrillar collagen leads to diastolic and systolic ventricular dysfunction. The increased amounts of myocardial fibrillar collagen in the setting of hypertrophy and heart failure are accompanied by elevated levels of circulating Ang II and aldosterone.(125) There is sufficient evidence for a major role of the RAAS-system with autocrine and paracrine actions in the process mentioned. Augmented systemic and tissue angiotensin formation are observed in hypertrophy and heart failure as already stated. These augmented hormone levels influence the progressive nature of heart failure. Normal cardiac tissue contains mineralocorticoid receptors (MR) and high affinity MRs are localized on cardiomyocytes.(126) High levels of aldosterone promote accumulation of interstitial collagen in the heart. This process is dependent on the salt status. (126) Aldosterone promotes the reabsorption of sodium in the distal tubule of the nephrons, mostly in exchange for potassium and hydrogen excretion. The secretion of aldosterone in response to Ang II is negatively controlled by salt-losing hormones as atrial natriuretic peptide and dopamine. Also, the adrenal response is enhanced following poor dietary sodium and potassium intake. The involvement of upregulated AT-1 receptors for Ang II, which are targets for aldosterone, is proposed.(126,127) Ang II induces cardiac fibroblast proliferation, synthesis and secretion of adhesion molecules and extracellular matrix proteins, and expression of integrin adhesion receptors.(127,128) Ang II stimulates cardiac fibroblasts also to adhere more vigorously to defined matrixes.(128) The ability of Ang II to induce collagen synthesis may be mediated by increased TGF- β 1 production, from which the expression is markedly increased in infarcted hearts and has shown to induce myocardial fibrosis.(127,129) Either type I or type II Ang II receptor antagonists or the competitive

aldosterone antagonist spironolactone completely abolish the increased collagen deposition.

(130)

The increased cardiac fibrosis in heart failure is not related to the augmented rates of apoptotic cell death, because dying myocytes are removed from neighboring cells in the absence of an inflammatory reaction and responsive fibrosis.(131)

The maladaptive fibrosis could be the target of pharmacologic intervention. Such cardioprotective strategies could be based on inhibiting the generation of these hormones or interfering with their receptor-ligand binding.(125)

Arrhythmias are common in heart failure and related to extensive cardiac fibrosis. In one half of heart failure patients tachyarrhythmias lead to sudden death.(132) Re-entrance mechanisms around scar tissue, afterdepolarizations, and triggered activity due to changes in calcium metabolism significantly contribute to the etiology of arrhythmias.(132)

Conclusion

Causal factors for the transition from hypertrophy to heart failure are detected in animal and human studies: 1 the changes in cellular signaling molecules; 2 the increased degree of myocyte apoptosis; 3 the accelerated deposition of collagen; 4 and arrhythmogenicity and the alterations in intracellular calcium handling and excitation contraction coupling are all contributing to this transition. However, the relative importance of the processes remains to be resolved. Certain is their relevance for the transition from hypertrophy to failure and they explain largely the distinction between beneficial and maladaptive hypertrophy. Contributors to maladaptive hypertrophy lead to heart failure and eventually death. Our future challenge will be to allow compensatory hypertrophy and block maladaptive processes in the human heart.

References

1. Mosterd A, Hoes AW, de Bruyne MC, et al. Prevalence of heart failure and left ventricular dysfunction in the general population; The Rotterdam Study. *Eur Heart J* 1999;20:447-55.
2. Murray CJ, Lopez AD. Global mortality, disability, and the contribution of risk factors: Global Burden of Disease Study. *Lancet* 1997;349:1436-42.
3. Murray CJ, Lopez AD. Mortality by cause for eight regions of the world: Global Burden of Disease Study. *Lancet* 1997;349:1269-76.
4. Dargie HJ, McMurray JJ, McDonagh TA. Heart failure--implications of the true size of the problem. *J Intern Med* 1996;239:309-15.
5. Maron BJ. Hypertrophic cardiomyopathy [published erratum appears in *Lancet* 1997 Nov 1;350(9087):1330]. *Lancet* 1997;350:127-33.
6. Van Kraaij D, Van Pol P, Ruiters AW, et al. Diagnosing diastolic heart failure. *Eur J Heart Fail* 2002;4:419-430.
7. Remme WJ, Swedberg K. Guidelines for the diagnosis and treatment of chronic heart failure. *Eur Heart J* 2001;22:1527-1560.
8. Braunwald E. *Heart Disease: A Textbook of Cardiovascular Medicine*. 5th edition ed. Philadelphia: W.B. Saunders Company, 1997.
9. James MA, Saadeh AM, Jones JV. Wall stress and hypertension. *J Cardiovasc Risk* 2000;7:187-90.
10. Rockman HA, Ross RS, Harris AN, et al. Segregation of atrial-specific and inducible expression of an atrial natriuretic factor transgene in an in vivo murine model of cardiac hypertrophy [published erratum appears in *Proc Natl Acad Sci U S A* 1991 Nov 1;88(21):9907]. *Proc Natl Acad Sci U S A* 1991;88:8277-81.
11. Van der laarse A RC, Van Wamel JET, Van Gilst WH, Doevendans PAFM, Van Bilsen M. Molecular aspects of cardiac hypertrophy and heart failure. *Cardiologie* 1998.
12. Esposito G, Rapacciuolo A, Prasad SV, et al. Genetic alterations that inhibit in vivo pressure-overload hypertrophy prevent cardiac dysfunction despite increased wall stress. *Circulation* 2002;105:85-92.
13. Mathew J, Sleight P, Lonn E, et al. Reduction of cardiovascular risk by regression of electrocardiographic markers of left ventricular hypertrophy by the angiotensin-converting enzyme inhibitor ramipril. *Circulation* 2001;104:1615-21.
14. Lorell BH, Carabello BA. Left ventricular hypertrophy: pathogenesis, detection, and prognosis. *Circulation* 2000;102:470-9.
15. Obayashi T, Hattori K, Sugiyama S, et al. Point mutations in mitochondrial DNA in patients with hypertrophic cardiomyopathy. *Am Heart J* 1992;124:1263-1269.
16. Maron BJ, Gardin JM, Flack JM, Gidding SS, Kurosaki TT, Bild DE. Prevalence of hypertrophic cardiomyopathy in a general population of young adults. Echocardiographic analysis of 4111 subjects in the CARDIA Study. Coronary Artery Risk Development in (Young) Adults. *Circulation* 1995;92:785-9.
17. Olson TM, Michels VV, Thibodeau SN, Tai YS, Keating MT. Actin mutations in dilated cardiomyopathy, a heritable form of heart failure. *Science* 1998;280:750-2.
18. Satoh M, Takahashi M, Sakamoto T, Hiroe M, Marumo F, Kimura A. Structural analysis of the titin gene in hypertrophic cardiomyopathy: identification of a novel disease gene. *Biochem Biophys Res Commun* 1999;262:411-7.
19. Watkins H, Seidman JG, Seidman CE. Familial hypertrophic cardiomyopathy: a genetic model of cardiac hypertrophy. *Hum Mol Genet* 1995;4:1721-7.

20. Yamazaki T, Komuro I, Yazaki Y. Role of the renin-angiotensin system in cardiac hypertrophy. *Am J Cardiol* 1999;83:53H-57H.
21. Baker KM, Chernin MI, Wixson SK, Aceto JF. Renin-angiotensin system involvement in pressure-overload cardiac hypertrophy in rats. *Am J Physiol* 1990;259:H324-32.
22. Kijima K, Matsubara H, Murasawa S, et al. Mechanical stretch induces enhanced expression of angiotensin II receptor subtypes in neonatal rat cardiac myocytes. *Circ Res* 1996;79:887-97.
23. Mascareno E, Dhar M, Siddiqui MA. Signal transduction and activator of transcription (STAT) protein- dependent activation of angiotensinogen promoter: a cellular signal for hypertrophy in cardiac muscle. *Proc Natl Acad Sci U S A* 1998;95:5590-4.
24. Sadoshima J, Izumo S. Molecular characterization of angiotensin II--induced hypertrophy of cardiac myocytes and hyperplasia of cardiac fibroblasts. Critical role of the AT1 receptor subtype. *Circ Res* 1993;73:413-23.
25. Sadoshima J, Xu Y, Slayter HS, Izumo S. Autocrine release of angiotensin II mediates stretch-induced hypertrophy of cardiac myocytes in vitro. *Cell* 1993;75:977-84.
26. Arai M, Yoguchi A, Iso T, et al. Endothelin-1 and its binding sites are upregulated in pressure overload cardiac hypertrophy. *Am J Physiol* 1995;268:H2084-91.
27. Ito H, Hiroe M, Hirata Y, et al. Endothelin ETA receptor antagonist blocks cardiac hypertrophy provoked by hemodynamic overload. *Circulation* 1994;89:2198-203.
28. Murphree SS, Saffitz JE. Distribution of beta-adrenergic receptors in failing human myocardium. Implications for mechanisms of down-regulation. *Circulation* 1989;79:1214-25.
29. Tse J, Huang MW, Leone RJ, Weiss HR, He YQ, Scholz PM. Down regulation of myocardial beta1-adrenoceptor signal transduction system in pacing-induced failure in dogs with aortic stenosis-induced left ventricular hypertrophy. *Mol Cell Biochem* 2000;205:67-73.
30. Rockman HA, Choi DJ, Akhter SA, et al. Control of myocardial contractile function by the level of beta- adrenergic receptor kinase 1 in gene-targeted mice. *J Biol Chem* 1998;273:18180-4.
31. Bohm M, Flesch M, Schnabel P. Beta-adrenergic signal transduction in the failing and hypertrophied myocardium. *J Mol Med* 1997;75:842-8.
32. Rush JE, Rajfer SI. Theoretical basis for the use of angiotensin II antagonists in the treatment of heart failure. *J Hypertens Suppl* 1993;11:S69-71.
33. Regitz-Zagrosek V, Neuss M, Fleck E. Effects of angiotensin receptor antagonists in heart failure: clinical and experimental aspects. *Eur Heart J* 1995;16 Suppl N:86-91.
34. Senzaki H, Paolocci N, Gluzband YA, et al. beta-blockade prevents sustained metalloproteinase activation and diastolic stiffening induced by angiotensin II combined with evolving cardiac dysfunction. *Circ Res* 2000;86:807-15.
35. Bogoyevitch MA, Glennon PE, Andersson MB, et al. Endothelin-1 and fibroblast growth factors stimulate the mitogen- activated protein kinase signaling cascade in cardiac myocytes. The potential role of the cascade in the integration of two signaling pathways leading to myocyte hypertrophy. *J Biol Chem* 1994;269:1110-9.
36. Kaddoura S, Firth JD, Boheler KR, Sugden PH, Poole-Wilson PA. Endothelin-1 is involved in norepinephrine-induced ventricular hypertrophy in vivo. Acute effects of bosentan, an orally active, mixed endothelin ETA and ETB receptor antagonist. *Circulation* 1996;93:2068-79.
37. Pennica D, King KL, Shaw KJ, et al. Expression cloning of cardiotrophin 1, a cytokine that induces cardiac myocyte hypertrophy. *Proc Natl Acad Sci U S A* 1995;92:1142-6.
38. Parker TG, Chow KL, Schwartz RJ, Schneider MD. Positive and negative control of the skeletal alpha-actin promoter in cardiac muscle. A proximal serum response

- element is sufficient for induction by basic fibroblast growth factor (FGF) but not for inhibition by acidic FGF. *J Biol Chem* 1992;267:3343-50.
39. Parker TG, Packer SE, Schneider MD. Peptide growth factors can provoke "fetal" contractile protein gene expression in rat cardiac myocytes. *J Clin Invest* 1990;85:507-14.
 40. Ito H, Hiroe M, Hirata Y, et al. Insulin-like growth factor-I induces hypertrophy with enhanced expression of muscle specific genes in cultured rat cardiomyocytes. *Circulation* 1993;87:1715-21.
 41. Ito H, Hirata Y, Adachi S, et al. Endothelin-1 is an autocrine/paracrine factor in the mechanism of angiotensin II-induced hypertrophy in cultured rat cardiomyocytes. *J Clin Invest* 1993;92:398-403.
 42. Kim NN, Villarreal FJ, Printz MP, Lee AA, Dillmann WH. Trophic effects of angiotensin II on neonatal rat cardiac myocytes are mediated by cardiac fibroblasts. *Am J Physiol* 1995;269:E426-37.
 43. Lavandero S, Foncea R, Perez V, Sapag-Hagar M. Effect of inhibitors of signal transduction on IGF-1-induced protein synthesis associated with hypertrophy in cultured neonatal rat ventricular myocytes. *FEBS Lett* 1998;422:193-6.
 44. Van Eickels M, Grohe C, Cleutjens JPM, Janssen BJ, Wellens HJJ, Doevendans PA. 17beta-estradiol attenuates the development of pressure-overload hypertrophy. *Circulation* 2001;104:1419-1423.
 45. Hayward CS, Webb CM, Collins P. Effect of sex hormones on cardiac mass. *Lancet* 2001;357:1354-6.
 46. Nuedling S, Kahlert S, Loebbert K, Meyer R, Vetter H, Grohe C. Differential effects of 17beta-estradiol on mitogen-activated protein kinase pathways in rat cardiomyocytes. *FEBS Lett* 1999;454:271-6.
 47. Grohe C, Kahlert S, Lobbert K, Vetter H. Expression of oestrogen receptor alpha and beta in rat heart: role of local oestrogen synthesis. *J Endocrinol* 1998;156:R1-7.
 48. Grohe C, Kahlert S, Lobbert K, et al. Cardiac myocytes and fibroblasts contain functional estrogen receptors. *FEBS Lett* 1997;416:107-12.
 49. Babiker FA, De Windt LJ, Van Eickels M, et al. 17{beta}-Estradiol Antagonizes Cardiomyocyte Hypertrophy by Autocrine/Paracrine Stimulation of a Guanylyl Cyclase A Receptor-Cyclic Guanosine Monophosphate-Dependent Protein Kinase Pathway. *Circulation* 2004;[Epub ahead of print].
 50. Lin KF, Chao J, Chao L. Atrial natriuretic peptide gene delivery attenuates hypertension, cardiac hypertrophy, and renal injury in salt-sensitive rats. *Hum Gene Ther* 1998;9:1429-38.
 51. Hilal-Dandan R, Ramirez MT, Villegas S, et al. Endothelin ETA receptor regulates signaling and ANF gene expression via multiple G protein-linked pathways. *Am J Physiol* 1997;272:H130-7.
 52. Milano CA, Dolber PC, Rockman HA, et al. Myocardial expression of a constitutively active alpha 1B-adrenergic receptor in transgenic mice induces cardiac hypertrophy. *Proc Natl Acad Sci U S A* 1994;91:10109-13.
 53. D'Angelo DD, Sakata Y, Lorenz JN, et al. Transgenic Galphaq overexpression induces cardiac contractile failure in mice. *Proc Natl Acad Sci U S A* 1997;94:8121-6.
 54. Clerk A, Bogoyevitch MA, Anderson MB, Sugden PH. Differential activation of protein kinase C isoforms by endothelin-1 and phenylephrine and subsequent stimulation of p42 and p44 mitogen- activated protein kinases in ventricular myocytes cultured from neonatal rat hearts. *J Biol Chem* 1994;269:32848-57.

55. Denhardt DT. Signal-transducing protein phosphorylation cascades mediated by Ras/Rho proteins in the mammalian cell: the potential for multiplex signalling. *Biochem J* 1996;318:729-47.
56. Thorburn J, Xu S, Thorburn A. MAP kinase- and Rho-dependent signals interact to regulate gene expression but not actin morphology in cardiac muscle cells. *Embo J* 1997;16:1888-900.
57. Bueno OF, De Windt LJ, Tymitz KM, et al. The MEK1-ERK1/2 signaling pathway promotes compensated cardiac hypertrophy in transgenic mice. *Embo J* 2000;19:6341-50.
58. Bueno OF, De Windt LJ, Lim HW, et al. The dual-specificity phosphatase MKP-1 limits the cardiac hypertrophic response in vitro and in vivo. *Circ Res* 2001;88:88-96.
59. Esposito G, Santana LF, Dilly K, et al. Cellular and functional defects in a mouse model of heart failure. *Am J Physiol Heart Circ Physiol* 2000;279:H3101-12.
60. Nicol RL, Frey N, Pearson G, Cobb M, Richardson J, Olson EN. Activated MEK5 induces serial assembly of sarcomeres and eccentric cardiac hypertrophy. *Embo J* 2001;20:2757-67.
61. Zhang D, Gaussin V, Taffet GE, et al. TAK1 is activated in the myocardium after pressure overload and is sufficient to provoke heart failure in transgenic mice. *Nat Med* 2000;6:556-63.
62. Ng DC, Long CS, Bogoyevitch MA. A role for the ERK and p38 MAPKs in Interleukin-1beta-stimulated delayed STAT3 activation, ANF expression and cardiac myocyte morphology. *J Biol Chem* 2001;29:29.
63. Hayashida W, Kihara Y, Yasaka A, Inagaki K, Iwanaga Y, Sasayama S. Stage-specific differential activation of mitogen-activated protein kinases in hypertrophied and failing rat hearts. *J Mol Cell Cardiol* 2001;33:733-44.
64. Fischer TA, Ludwig S, Flory E, et al. Activation of Cardiac c-Jun NH(2)-Terminal Kinases and p38-Mitogen- Activated Protein Kinases With Abrupt Changes in Hemodynamic Load. *Hypertension* 2001;37:1222-8.
65. Cook SA, Sugden PH, Clerk A. Activation of c-Jun N-terminal kinases and p38-mitogen-activated protein kinases in human heart failure secondary to ischaemic heart disease. *J Mol Cell Cardiol* 1999;31:1429-34.
66. Sheng Z, Knowlton K, Chen J, Hoshijima M, Brown JH, Chien KR. Cardiotrophin 1 (CT-1) inhibition of cardiac myocyte apoptosis via a mitogen-activated protein kinase-dependent pathway. Divergence from downstream CT-1 signals for myocardial cell hypertrophy. *J Biol Chem* 1997;272:5783-91.
67. Kodama H, Fukuda K, Pan J, et al. Biphasic activation of the JAK/STAT pathway by angiotensin II in rat cardiomyocytes. *Circ Res* 1998;82:244-50.
68. Pan J, Fukuda K, Kodama H, et al. Role of angiotensin II in activation of the JAK/STAT pathway induced by acute pressure overload in the rat heart. *Circ Res* 1997;81:611-7.
69. De Windt LJ, Lim HW, Haq S, Force T, Molkentin JD. Calcineurin promotes protein kinase C and c-Jun NH2-terminal kinase activation in the heart. Cross-talk between cardiac hypertrophic signaling pathways. *J Biol Chem* 2000;275:13571-9.
70. De Windt LJ, Lim HW, Taigen T, et al. Calcineurin-mediated hypertrophy protects cardiomyocytes from apoptosis in vitro and in vivo: An apoptosis-independent model of dilated heart failure. *Circ Res* 2000;86:255-63.
71. Lim HW, De Windt LJ, Steinberg L, et al. Calcineurin expression, activation, and function in cardiac pressure- overload hypertrophy. *Circulation* 2000;101:2431-7.
72. Lim HW, De Windt LJ, Mante J, et al. Reversal of cardiac hypertrophy in transgenic disease models by calcineurin inhibition. *J Mol Cell Cardiol* 2000;32:697-709.

73. Ramirez MT, Zhao XL, Schulman H, Brown JH. The nuclear deltaB isoform of Ca²⁺/calmodulin-dependent protein kinase II regulates atrial natriuretic factor gene expression in ventricular myocytes. *J Biol Chem* 1997;272:31203-8.
74. Taigen T, De Windt LJ, Lim HW, Molkentin JD. Targeted inhibition of calcineurin prevents agonist-induced cardiomyocyte hypertrophy. *Proc Natl Acad Sci U S A* 2000;97:1196-201.
75. Maier LS, Brandes R, Pieske B, Bers DM. Effects of left ventricular hypertrophy on force and Ca²⁺ handling in isolated rat myocardium. *Am J Physiol* 1998;274:H1361-70.
76. Moore RL, Yelamarty RV, Misawa H, et al. Altered Ca²⁺ dynamics in single cardiac myocytes from renovascular hypertensive rats. *Am J Physiol* 1991;260:C327-37.
77. Qi M, Shannon TR, Euler DE, Bers DM, Samarel AM. Downregulation of sarcoplasmic reticulum Ca(2+)-ATPase during progression of left ventricular hypertrophy. *Am J Physiol* 1997;272:H2416-24.
78. Kiss E, Ball NA, Kranias EG, Walsh RA. Differential changes in cardiac phospholamban and sarcoplasmic reticular Ca(2+)-ATPase protein levels. Effects on Ca²⁺ transport and mechanics in compensated pressure-overload hypertrophy and congestive heart failure. *Circ Res* 1995;77:759-64.
79. de la Bastie D, Levitsky D, Rappaport L, et al. Function of the sarcoplasmic reticulum and expression of its Ca²⁺-ATPase gene in pressure overload-induced cardiac hypertrophy in the rat. *Circ Res* 1990;66:554-64.
80. Bailey BA, Houser SR. Sarcoplasmic reticulum-related changes in cytosolic calcium in pressure-overload-induced feline LV hypertrophy. *Am J Physiol* 1993;265:H2009-16.
81. Arai M, Matsui H, Periasamy M. Sarcoplasmic reticulum gene expression in cardiac hypertrophy and heart failure. *Circ Res* 1994;74:555-64.
82. Nediani C, Formigli L, Perna AM, et al. Early changes induced in the left ventricle by pressure overload. An experimental study on swine heart. *J Mol Cell Cardiol* 2000;32:131-42.
83. Movsesian MA, Schwinger RH. Calcium sequestration by the sarcoplasmic reticulum in heart failure. *Cardiovasc Res* 1998;37:352-9.
84. Munch G, Bolck B, Hoischen S, et al. Unchanged protein expression of sarcoplasmic reticulum Ca²⁺-ATPase, phospholamban, and calsequestrin in terminally failing human myocardium. *J Mol Med* 1998;76:434-41.
85. Schwinger RH, Bohm M, Schmidt U, et al. Unchanged protein levels of SERCA II and phospholamban but reduced Ca²⁺ uptake and Ca(2+)-ATPase activity of cardiac sarcoplasmic reticulum from dilated cardiomyopathy patients compared with patients with nonfailing hearts. *Circulation* 1995;92:3220-8.
86. Schwinger RH, Bolck B, Munch G, Brixius K, Muller-Ehmsen J, Erdmann E. cAMP-dependent protein kinase A-stimulated sarcoplasmic reticulum function in heart failure. *Ann N Y Acad Sci* 1998;853:240-50.
87. Schwinger RH, Munch G, Bolck B, Karczewski P, Krause EG, Erdmann E. Reduced Ca(2+)-sensitivity of SERCA 2a in failing human myocardium due to reduced serin-16 phospholamban phosphorylation. *J Mol Cell Cardiol* 1999;31:479-91.
88. Arber S, Halder G, Caroni P. Muscle LIM protein, a novel essential regulator of myogenesis, promotes myogenic differentiation. *Cell* 1994;79:221-31.
89. Arber S, Caroni P. Specificity of single LIM motifs in targeting and LIM/LIM interactions in situ. *Genes Dev* 1996;10:289-300.

90. Arber S, Hunter JJ, Ross J, Jr., et al. MLP-deficient mice exhibit a disruption of cardiac cytoarchitectural organization, dilated cardiomyopathy, and heart failure. *Cell* 1997;88:393-403.
91. Kong Y, Flick MJ, Kudla AJ, Konieczny SF. Muscle LIM protein promotes myogenesis by enhancing the activity of MyoD. *Mol Cell Biol* 1997;17:4750-60.
92. Schneider AG, Sultan KR, Pette D. Muscle LIM protein: expressed in slow muscle and induced in fast muscle by enhanced contractile activity. *Am J Physiol* 1999;276:C900-6.
93. Mahaney JE, Autry JM, Jones LR. Kinetics studies of the cardiac Ca-ATPase expressed in Sf21 cells: new insights on Ca-ATPase regulation by phospholamban. *Biophys J* 2000;78:1306-23.
94. Luo W, Grupp IL, Harrer J, et al. Targeted ablation of the phospholamban gene is associated with markedly enhanced myocardial contractility and loss of beta-agonist stimulation. *Circ Res* 1994;75:401-9.
95. Luo W, Chu G, Sato Y, Zhou Z, Kadambi VJ, Kranias EG. Transgenic approaches to define the functional role of dual site phospholamban phosphorylation. *J Biol Chem* 1998;273:4734-9.
96. Hoit BD, Khoury SF, Kranias EG, Ball N, Walsh RA. In vivo echocardiographic detection of enhanced left ventricular function in gene-targeted mice with phospholamban deficiency. *Circ Res* 1995;77:632-7.
97. Kadambi VJ, Ponniah S, Harrer JM, et al. Cardiac-specific overexpression of phospholamban alters calcium kinetics and resultant cardiomyocyte mechanics in transgenic mice. *J Clin Invest* 1996;97:533-9.
98. Minamisawa S, Hoshijima M, Chu G, et al. Chronic phospholamban-sarcoplasmic reticulum calcium ATPase interaction is the critical calcium cycling defect in dilated cardiomyopathy. *Cell* 1999;99:313-22.
99. Schwinger RH, Brixius K, Savvidou-Zaroti P, et al. The enhanced contractility in phospholamban deficient mouse hearts is not associated with alterations in (Ca²⁺)-sensitivity or myosin ATPase- activity of the contractile proteins. *Basic Res Cardiol* 2000;95:12-8.
100. Saraste A, Pulkki K. Morphologic and biochemical hallmarks of apoptosis. *Cardiovasc Res* 2000;45:528-37.
101. Brunet CL, Gunby RH, Benson RS, Hickman JA, Watson AJ, Brady G. Commitment to cell death measured by loss of clonogenicity is separable from the appearance of apoptotic markers. *Cell Death Differ* 1998;5:107-15.
102. Foncea R, Galvez A, Perez V, et al. Extracellular regulated kinase, but not protein kinase C, is an antiapoptotic signal of insulin-like growth factor-1 on cultured cardiac myocytes. *Biochem Biophys Res Commun* 2000;273:736-44.
103. Lips DJ, Bueno OF, Wilkins BJ, et al. The MEK1-ERK2 signaling pathway protects the myocardium from ischemic damage in vivo. Submitted 2003.
104. Hasegawa K, Iwai-Kanai E, Sasayama S. Neurohormonal regulation of myocardial cell apoptosis during the development of heart failure. *J Cell Physiol* 2001;186:11-8.
105. Narula J, Kolodgie FD, Virmani R. Apoptosis and cardiomyopathy. *Curr Opin Cardiol* 2000;15:183-8.
106. Susin SA, Zamzami N, Castedo M, et al. Bcl-2 inhibits the mitochondrial release of an apoptogenic protease. *J Exp Med* 1996;184:1331-41.
107. Joza N, Susin SA, Daugas E, et al. Essential role of the mitochondrial apoptosis-inducing factor in programmed cell death. *Nature* 2001;410:549-54.

108. Hisatomi T, Sakamoto T, Murata T, et al. Relocalization of apoptosis-inducing factor in photoreceptor apoptosis induced by retinal detachment in vivo. *Am J Pathol* 2001;158:1271-8.
109. Hofstra L, Liem IH, Dumont E, et al. Visualisation of cell death in vivo in patients with acute myocardial infarction. *Lancet* 2000;356:209-12.
110. Dumont E, Reutelingsperger CP, Smits JF, et al. Real-time imaging of apoptotic cell-membrane changes at the single-cell level in the beating murine heart. *Nat Med* 2001;7:1352-5.
111. Thornberry NA, Lazebnik Y. Caspases: enemies within. *Science* 1998;281:1312-6.
112. Ashkenazi A, Dixit VM. Death receptors: signaling and modulation. *Science* 1998;281:1305-8.
113. Chen Z, Chua CC, Ho YS, Hamdy RC, Chua BH. Overexpression of Bcl-2 attenuates apoptosis and protects against myocardial I/R injury in transgenic mice. *Am J Physiol Heart Circ Physiol* 2001;280:H2313-20.
114. Condorelli G, Morisco C, Stassi G, et al. Increased cardiomyocyte apoptosis and changes in proapoptotic and antiapoptotic genes bax and bcl-2 during left ventricular adaptations to chronic pressure overload in the rat. *Circulation* 1999;99:3071-8.
115. Fearnhead HO, Rodriguez J, Govek EE, et al. Oncogene-dependent apoptosis is mediated by caspase-9. *Proc Natl Acad Sci U S A* 1998;95:13664-9.
116. Soengas MS, Alarcon RM, Yoshida H, et al. Apaf-1 and caspase-9 in p53-dependent apoptosis and tumor inhibition. *Science* 1999;284:156-9.
117. Liu X, Li P, Widlak P, et al. The 40-kDa subunit of DNA fragmentation factor induces DNA fragmentation and chromatin condensation during apoptosis. *Proc Natl Acad Sci U S A* 1998;95:8461-6.
118. Enari M, Sakahira H, Yokoyama H, Okawa K, Iwamatsu A, Nagata S. A caspase-activated DNase that degrades DNA during apoptosis, and its inhibitor ICAD. *Nature* 1998;391:43-50.
119. Narula J, Pandey P, Arbustini E, et al. Apoptosis in heart failure: release of cytochrome c from mitochondria and activation of caspase-3 in human cardiomyopathy. *Proc Natl Acad Sci U S A* 1999;96:8144-9.
120. Narula J, Hajjar RJ, Dec GW. Apoptosis in the failing heart. *Cardiol Clin* 1998;16:691-710.
121. Suzuki K, Kostin S, Person V, Elsasser A, Schaper J. Time course of the apoptotic cascade and effects of caspase inhibitors in adult rat ventricular cardiomyocytes. *J Moll Cell Cardiol* 2001;33:983-94.
122. Vescovo G, Volterrani M, Zennaro R, et al. Apoptosis in the skeletal muscle of patients with heart failure: investigation of clinical and biochemical changes. *Heart* 2000;84:431-7.
123. Kajstura J, Leri A, Finato N, Di Loreto C, Beltrami CA, Anversa P. Myocyte proliferation in end-stage cardiac failure in humans. *Proc Natl Acad Sci U S A* 1998;95:8801-5.
124. Beltrami AP, Urbanek K, Kajstura J, et al. Evidence that human cardiac myocytes divide after myocardial infarction. *N Engl J Med* 2001;344:1750-7.
125. Burlew BS, Weber KT. Connective tissue and the heart. Functional significance and regulatory mechanisms. *Cardiol Clin* 2000;18:435-42.
126. Lijnen P, Petrov V. Induction of cardiac fibrosis by aldosterone. *J Mol Cell Cardiol* 2000;32:865-79.
127. Lijnen PJ, Petrov VV, Fagard RH. Induction of cardiac fibrosis by angiotensin II. *Methods Find Exp Clin Pharmacol* 2000;22:709-23.

Chapter 2. Molecular aspects of cardiac failure

128. Schnee JM, Hsueh WA. Angiotensin II, adhesion, and cardiac fibrosis. *Cardiovasc Res* 2000;46:264-8.
129. Lijnen PJ, Petrov VV, Fagard RH. Induction of cardiac fibrosis by transforming growth factor-beta(1). *Mol Genet Metab* 2000;71:418-35.
130. Brilla CG, Zhou G, Matsubara L, Weber KT. Collagen metabolism in cultured rat cardiac fibroblasts: response to angiotensin II and aldosterone. *J Mol Cell Cardiol* 1994;26:809-20.
131. MacLellan WR, Schneider MD. Death by design. Programmed cell death in cardiovascular biology and disease. *Circ Res* 1997;81:137-44.
132. Eckardt L, Haverkamp W, Johna R, et al. Arrhythmias in heart failure: current concepts of mechanisms and therapy. *J Cardiovasc Electrophysiol* 2000;11:106-17.

Left ventricular pressure-volume measurements in mice

Daniel J. Lips, Theo van der Nagel, Paul Steendijk, Meindert Palmen, Ben Janssen, Jan-Melle van Dantzig, Leon J. de Windt and Pieter A. Doevendans

In modified version in press Basic Res Cardiol.

Abstract

Genetically engineered mice are used in experiments in cardiovascular research. The *in vivo* assessment of cardiac performance demands accurate methods. Overall cardiac performance can be acquired by simultaneous and continuous left ventricular pressure and volume (PV) measurements through the use of an intraventricular 1.4 F ultraminiature conductance-micromanometer catheter positioned in the left ventricular cavity of intact mice. Cardiac performance is represented in the two-dimensional graph plotting pressure and volume into PV-loops. PV-loops adequately represent cardiac function and provide load and heart rate independent parameters of intrinsic myocardial contractility and relaxation. All sorts of cardiopathological situations can be investigated thoroughly with the use of PV-measurements.

Introduction

The use of murine transgenic and gene-targeted models in the field of cardiovascular research has shown an exponential growth, since this approach provides essential genetic and molecular insight into human congenital and acquired heart disease. By manipulating and investigating cardiac gene expression by means of accurate techniques to analyze the resultant phenotype, the molecular basis for cardiac dysfunction may be uncovered.

To date, multiple techniques allow assessment of murine left ventricular hemodynamic behavior(1,2), such as MRI (3), transthoracic ultrasonography (4), Langendorff perfusion systems (5), aortic flow probes (6), micromanometers (7) and, more recently, conductance-micromanometers (8). The use of conductance-micromanometers allows generation of instantaneous pressure and volume signals to create pressure-volume (PV) relations for highly accurate assessment of left ventricular performance. The PV-loop method is regarded as the golden standard for assessment of intrinsic myocardial function in large animals (9) and humans (10). Recently, the development of miniaturized PV-catheters has made this methodology applicable to small animals such as mice. (8)

The method of PV-loop assessment will be discussed in the following paragraphs. More detailed information about the acquisition of left ventricular volume will be provided, and the concepts of parallel conductance and volume correction factors are introduced. The surgical protocols for open-chest and closed-chest PV measurements and the difference in cardiac performance between these two protocols are part of the discussion. How to read PV-loops completes the chapter.

Figure 1

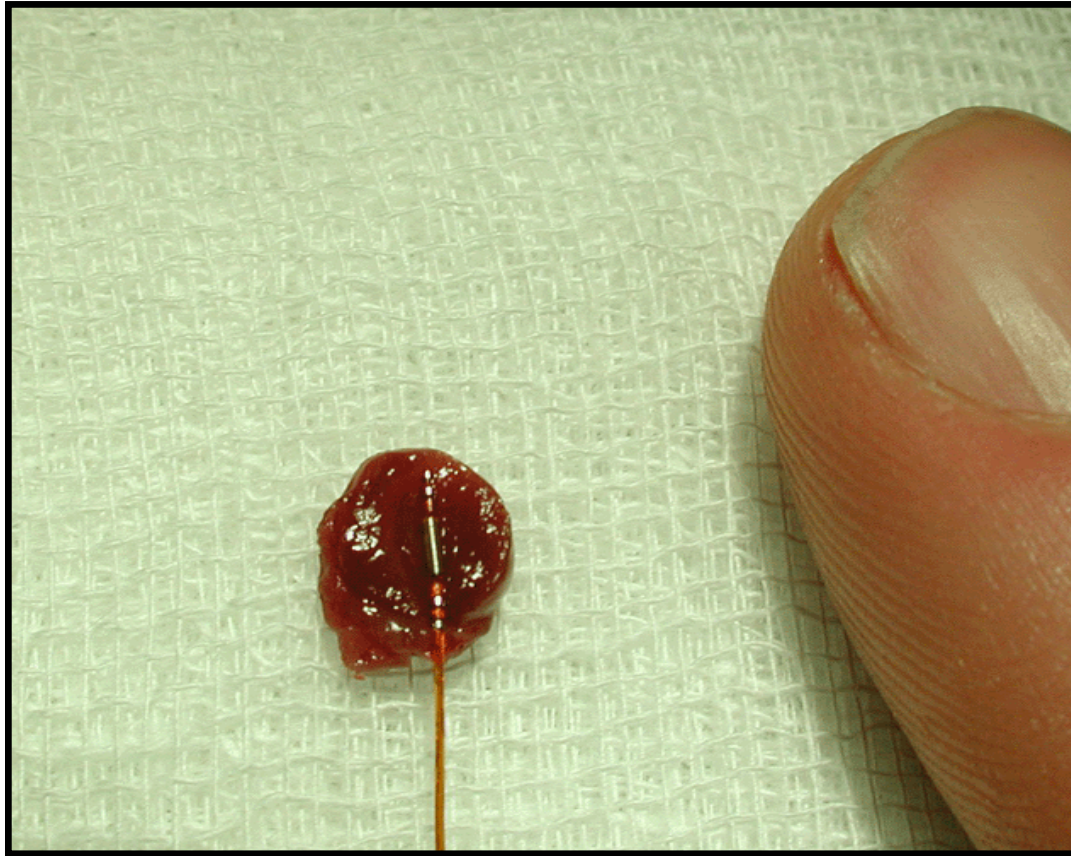


Fig. 1: Presentation of the size of the Millar conductance-micromanometer. The catheter is placed in the left ventricle from a longitudinal sliced murine heart. The tip of the catheter is placed in the apex of the heart, while the proximal part runs through the aortic valves. From top to bottom are seen two volume electrodes, the pressure sensor and at the bottom two volume electrodes. An index finger indicates the miniature size of the catheter.

The assessment of pressure-volume loops

PV loops are obtained by the conductance-micromanometer, miniaturized for invasive use in rodents (figure 1). (11) The volume-signal is derived in accordance with Ohm's Law: "The amount of current flowing in a circuit made up of pure resistances is directly proportional to the electromotive forces impressed on the circuit and inversely proportional to the total resistance of the circuit". In the setting of a mouse heart is *the circuit of pure resistances* an analogue for ventricular bloodvolume, *the electromotive forces* for the applied voltage and *the amount of current* for plain current. Voltage and current are constant during bloodvolume measurements in the heart. Bloodvolume itself, however, is not. It varies according to the cardiac cycle. The varying ventricular bloodvolume of the mouse heart is inversely proportional with the measured **resistance/impedance**. Or, ventricular bloodvolume is direct proportional with the measured electrical **conductance** of the blood (figure 2).

Figure 2

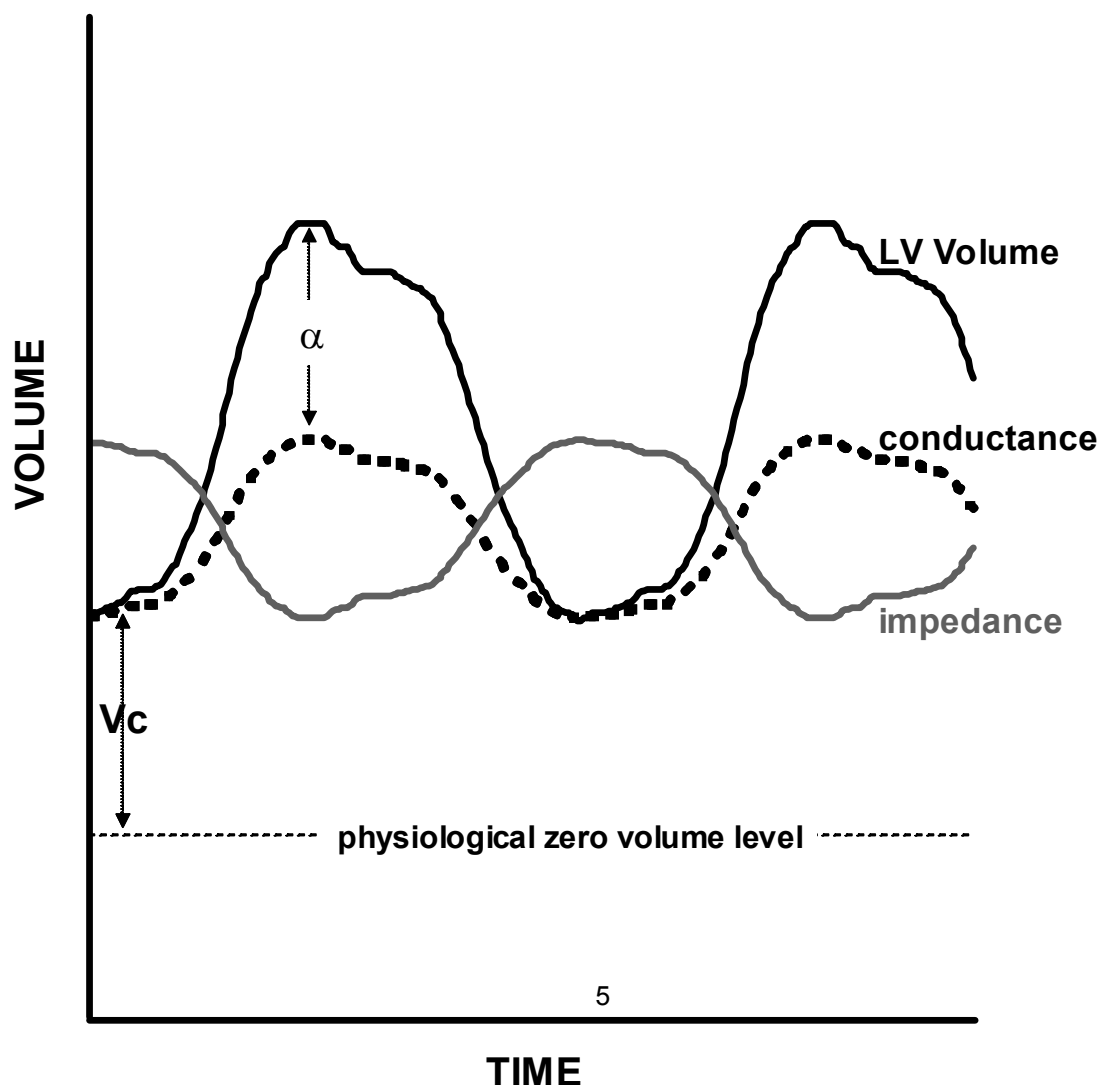


Fig. 2: The concept of conductance derived left ventricular volume. Left ventricular blood volume is linear proportional with the time-varying conductance signal, which correlates with the level of resistance/impedance of the blood volume on the electric current produced by the catheter. The conductance-catheter underestimates the volume-signal due to inhomogeneity of the electrical field. The slope factor α corrects for this underestimation. The offset volume that arises from the protrusion of the electrical current in tissues besides blood (parallel conductance), is corrected by the correction volume V_c .

The conductance catheter is equipped with four electrodes (figure 3): two current electrodes and two sensor electrodes. The current electrodes produce an electric field with a magnitude of $30 \mu\text{A}$.

Figure 3

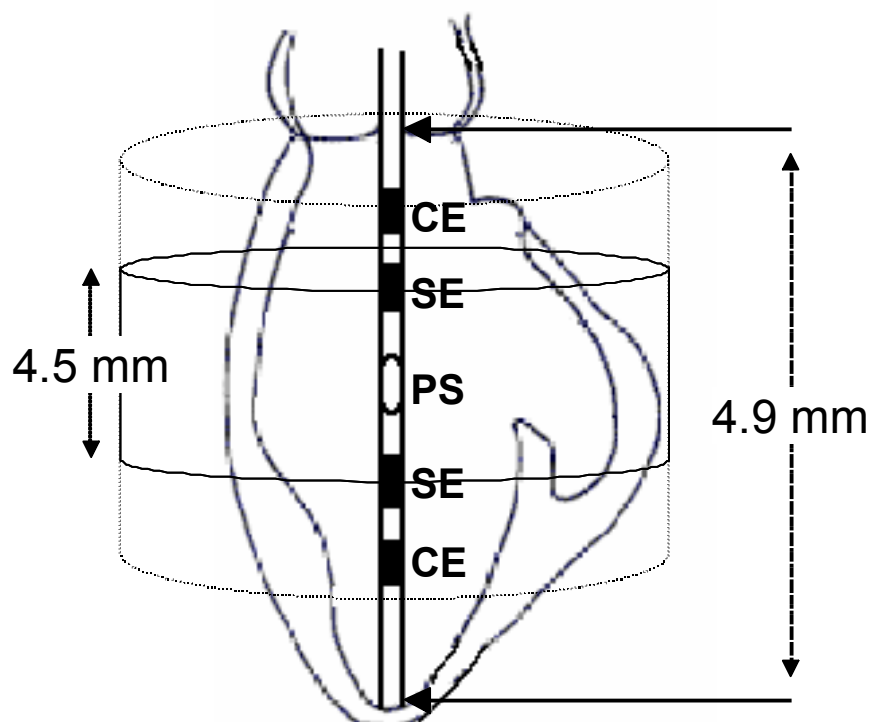


Fig. 3: Position of the conductance catheter in the left ventricle. The catheter is retrogradely inserted in the left ventricle. The catheter consists of one pressure sensor and four volume

Chapter 3. Murine left ventricular pressure-volume loops

electrodes: two current electrodes and two sensor electrodes. The height of the measured volume segment depends on the distance between the sensing electrodes, i.e. 4.5 mm. The mean length of the longitudinal axis of the heart from adult mice is approximately 4.9 mm. CE indicates current electrode, SE sensing electrode and PS pressure sensor.

This specific current is chosen to prevent interaction with the murine endogenous conduction system of the heart. The catheter measures conductance, which is translated into left ventricular volume by a software program. Cycle-varying conductance correlates with time-varying ventricular volume $V(t)$ according to the following formula:

$$V(t) = \rho L^2 [G(t) - G^p]$$

where ρ (rho) is the mouse specific blood resistivity, L indicates the distance between the sensor electrodes (i.e. 4.5 mm), $G(t)$ the instantaneous conductance and G^p parallel conductance. The mouse specific blood resistance is determined using a Rho-cuvette, with a length of 0.5 cm and a diameter of 0.2 cm resulting in a content of 150 μ l. G^p is the offset in the volume signal that originates from an additional conductance signal. Shortly, an electric field broadens theoretically without end and protrudes through the ventricular wall into other intrathoracic structures and organs. Therefore, the ventricular-derived conductance signal originates partly from lungs, mediastinum, and most notably from the left ventricular myocardium. All have a relative contribution to the addition in ventricular-derived conductance signal. This offset-volume is referred to as the correction volume V_c (figure 2). Several methods are used to acquire G^p and subsequent V_c . One method calculates G^p from the differences between myocardial and blood conductances at catheter excitation frequencies of 2 and 10 kHz. (12) The second method estimates G^p by exploiting the differential frequency-induced conductivity of myocardium and blood. (13) In our experiments we used the hypertonic saline injection (HSI) method. The method comprises of the infusion of 4 μ l

hypertonic (30% NaCl) saline solution into the external jugular vein (~ 15% of left ventricular absolute end-diastolic volume). The saline mixes with the murine blood and increases conductance of blood through its high content of electrolytes. The result is a volume increase as shown by figure 4, a representative figure of a common HSI procedure. The amount of saline infusion is limited to 4 μL to prevent hemodynamic changes due to the fluid injection. As shown in figure 4 there is no influence on pressure. The correction volume V_c is derived via computerized algorithms.

Figure 4

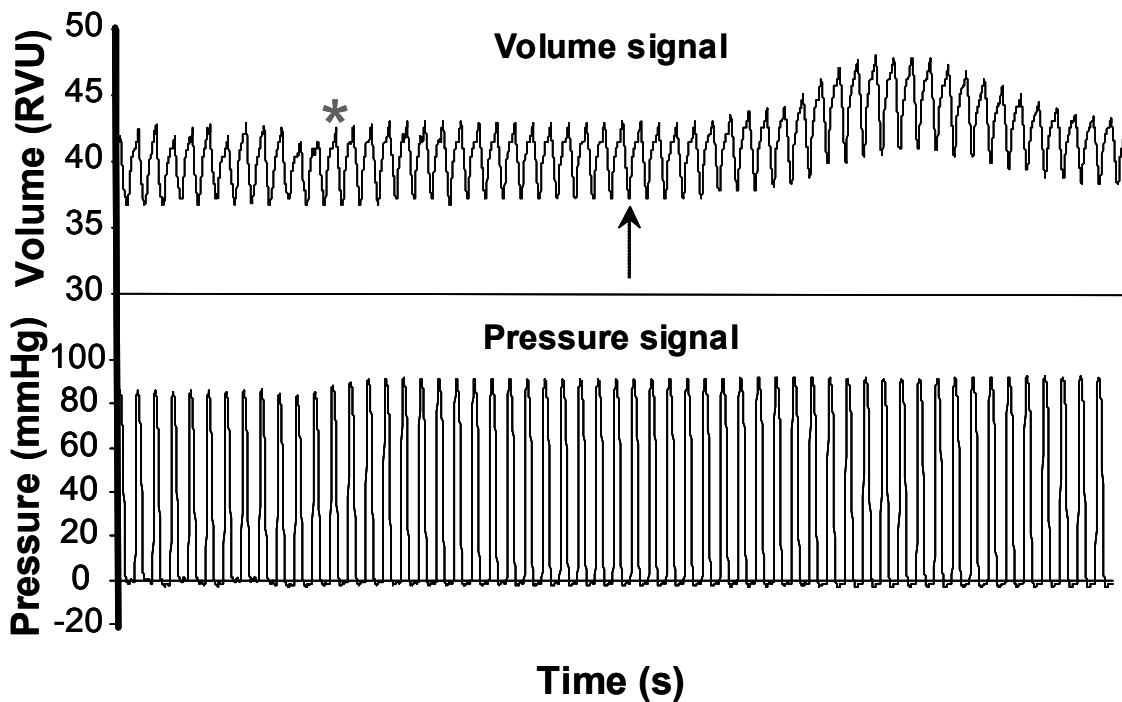


Fig. 4: Conductance and pressure signals during hypertonic saline injection. The total acquired time period was 5.84 seconds. Ventilation was stopped at the mark (*), after which 4 μL of 30% saline was injected (arrow) into the external jugular vein. The conductivity of blood was increased by the hypertonic saline infusion as demonstrated by the increase in the conductance signal. Parallel conductance is calculated by analyzing the conductance signal

Chapter 3. Murine left ventricular pressure-volume loops

obtained during wash-in of the saline. The unchanged pressure indicates that hemodynamics are stable.

In practice the conductance-catheter tends to constantly underestimate the left ventricular bloodvolume. The slope factor α should be calculated to correct for this discrepancy (figure 2). For this purpose an independent volume measurement is needed, obtained in mice by blood flow measurements or echocardiography. The slope factor α then follows from the ratio *conductance volume/independent measured volume*. Table 1 shows the results of α determination by echocardiography. Slope factor α varied from 0.3 - 0.5, depending on the moment of measurement within the cardiac cycle. The variance could be due to the relative inaccuracy of ultrasonographic analyses. It could also be inherent to conductance measurements in the manner as performed. Slope factor α deviates from 1 primarily due to the dependency of G^P on left ventricular volume. (14) G^P should therefore be measured continuously within the cardiac cycle to be able to correct adequately for the variance of α . However, as the result of technical limitations continuous G^P acquisition is not yet possible. Whenever echocardiography is used, end-diastolic volume EDV should be used for α determination. The variance of this calculated α is minor (SEM = 0.02) and the correlation relatively high (adjusted $R^2 = 0.65$).

Surgical protocols for PV-loops acquisition

The Sigma SA (CDLeycom, Zoetermeer, the Netherlands) single segment data acquisition module was used for assessment of PV-loops. The system operated on a constant excitation current of 30 μ A to prevent interaction with the murine cardiac conduction system. determined by hypertonic saline injection and subtracted offline. CONDUCT 2000 software (CDLeycom, Zoetermeer, The Netherlands) was used for data acquisition and Circlab software (LUMC, Leiden, The Netherlands) was used for offline data analysis.

Invasive hemodynamic measurements of the murine left ventricle can theoretically be performed by several ways for. To date, the most frequently reported method is an open-chest (OC) approach. (8) In brief, mice are anaesthetized and the anterior thorax and the neck of the mouse are shaved. The animals are fixed on a warming plate. Care is taken to maintain body temperature constant at 37° Celsius. The neck skin of the mouse is opened by a sagittal incision. The trachea is exposed to visually guide the intratracheal cannula (20-Gauge), where after the cannula is connected to a mouse ventilator, Minivent type 845 (Hugo Sachs Electronics, Germany), set at 150 strokes per minute and a tidal volume of 250 μ l. The external jugular veins are cannulated with a flame-stretched PE-50 catheter for infusion of saline and drugs. The abdomen is opened subcostally. The diaphragm is incised by a transverse substernal approach leaving the pericardium intact. The micromanometer is calibrated with a mercury manometer by placing the sensor in 37° Celsius normal saline. The left ventricle is entered through an apical stab with a 25 1/2 G needle, immediately followed by the Millar conductance-micromanometer. The catheter is positioned correctly in the left ventricle under guidance of the online pressure and volume signals. The combination of pressure and volume signals allows accurate positioning of the catheter in the left ventricle. Ventilation is stopped during data acquisition to avoid influence from ventilation of the lungs on the pressure and volume signals. The acquisition protocol consists of measurements of

Chapter 3. Murine left ventricular pressure-volume loops

baseline cardiac function, hypertonic saline injection (3x), inferior caval vein occlusions with and without β -adrenergic stimulation (isoproterenol, 1000 pg).

This method is theoretically disadvantageous, since collapse of the lungs and destruction of myocardial integrity are induced through the relatively large surgical trauma. Furthermore, in myocardial infarction studies the open-chest approach is hampered by extensive left ventricular remodeling, since the scar tissue is not accessible for the conductance catheter and fails to provide a stable position.

A closed-chest (CC) approach would theoretically circumvent several of these disadvantages. Firstly, in a closed-chest the lungs remain untouched. Secondly, the cardiac position and myocardial structures remain intact. Thirdly, surgical trauma and hemodynamic stress would be reduced to a minimum. Finally, a closed-chest approach would allow accurate assessment of left ventricular (LV) hemodynamic behavior in mice which underwent transient or permanent occlusion of the left anterior descending coronary artery. The surgical procedure is similar to the open-chest approach, except for the insertion of the conductance catheter into the left ventricle. In brief, mice are anaesthetized and the neck and abdomen are shaved. Care is taken to maintain body temperature and ventilation support is provided as above. Venous catheters are placed, after which the right common carotid is prepared for insertion of the ultraminiature conductance-micromanometer. The catheter is calibrated and subsequently inserted into the left ventricle under guidance of the online pressure signal. A transverse abdominal incision without opening the thorax is performed to expose the inferior caval vein. The acquisition protocol is similar as in the open-chest approach.

Explanation of the pressure-volume loop

The left ventricular PV loop is a two-dimensional representation of a single cardiac cycle (figure 5). Beginning at end-diastole, when the mitral valve closes, the ejection phase starts with pressure build up without actual volume ejection, i.e. the isovolumic contraction phase. Blood is ejected out of the ventricle into the aorta upon opening of the aortic valve and, subsequently, left ventricular volume decreases. The end of ejection is defined by aortic valve closure and followed by myocardial relaxation characterized by pressure decrease without volume change, i.e. the isovolumic relaxation phase. The filling phase is initiated with opening of the mitral valve and rise of ventricular volume. The technique of simultaneous left ventricular pressure and volume measurements provides continuous assessment of cardiac function.

Figure 5

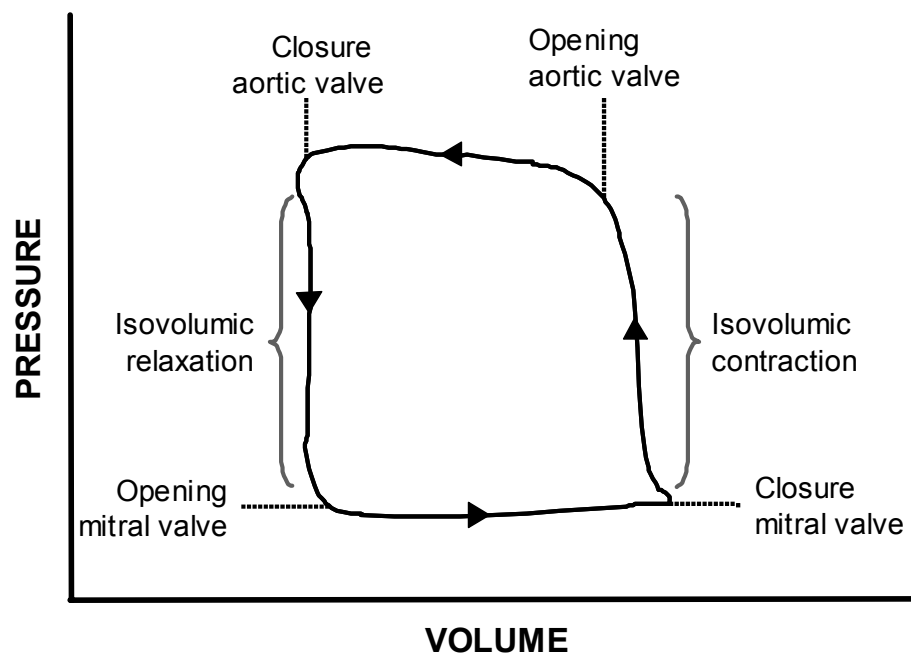


Fig. 5: The cardiac cycle in a single pressure-volume loop. End-diastole is marked by the closure of the mitral valves. The hearts starts to build up pressure while all valves are closed (isovolumetric contraction phase), before actual ejection begins following the opening of the aortic valve. Volume decreases while ejection progresses until the aortic valves close (end-

systole) and relaxation starts. Aortic and mitral valves are closed during relaxation (isovolumic relaxation phase). The filling phase follows upon the opening of the mitral valve and volume increase while pressure build up is minor.

PV loops reveal in first instance the standard functional parameters (figure 6).

Figure 6

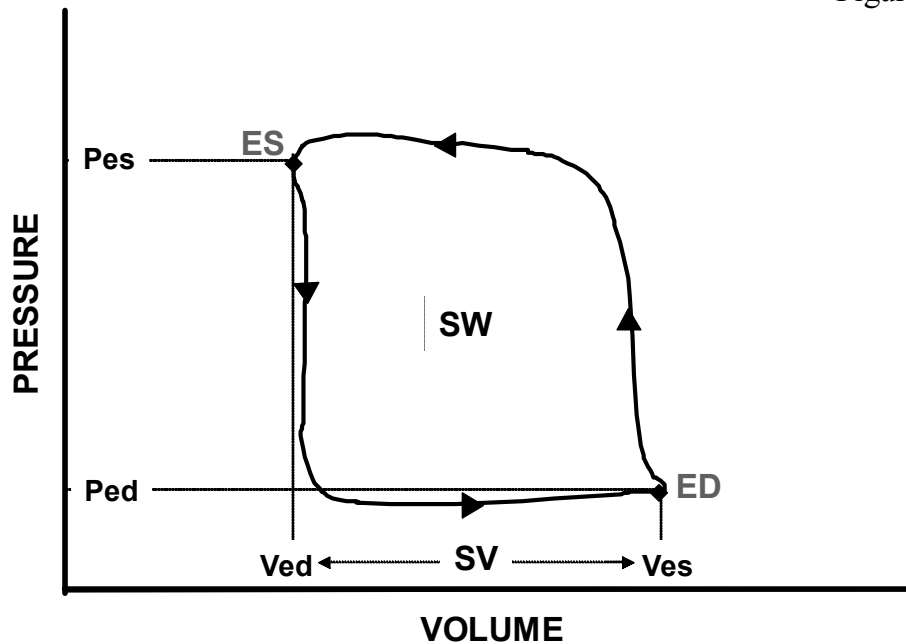


Fig. 6: Cardiac performance parameters in the pressure-volume loop. ED indicates end-diastole; ES: end-systole; Ved: end-diastolic volume; Ves: end-systolic volume; Ped: end-diastolic pressure; Pes: end-systolic pressure. The area of the PV loop resembles stroke work (SW). Stroke volume SV can be derived by subtracting Ves from Ved.

However, specific PV relationships are acquired too (table 2, figure 7). These relationships describe the contractile and relaxative capabilities of the heart independent of preload, afterload or heart rate. Transient occlusion of the inferior caval vein in mice is performed to obtain these relationships. Caval vein occlusion leads to a decrease in venous return and thereby in preload of the left ventricle. The response of the heart is typical, as

presented in figure 7, and shows the PV correlations. Contractile parameters derived from PV-correlations best detect small alterations in contractility in mice. (15)

Figure 7

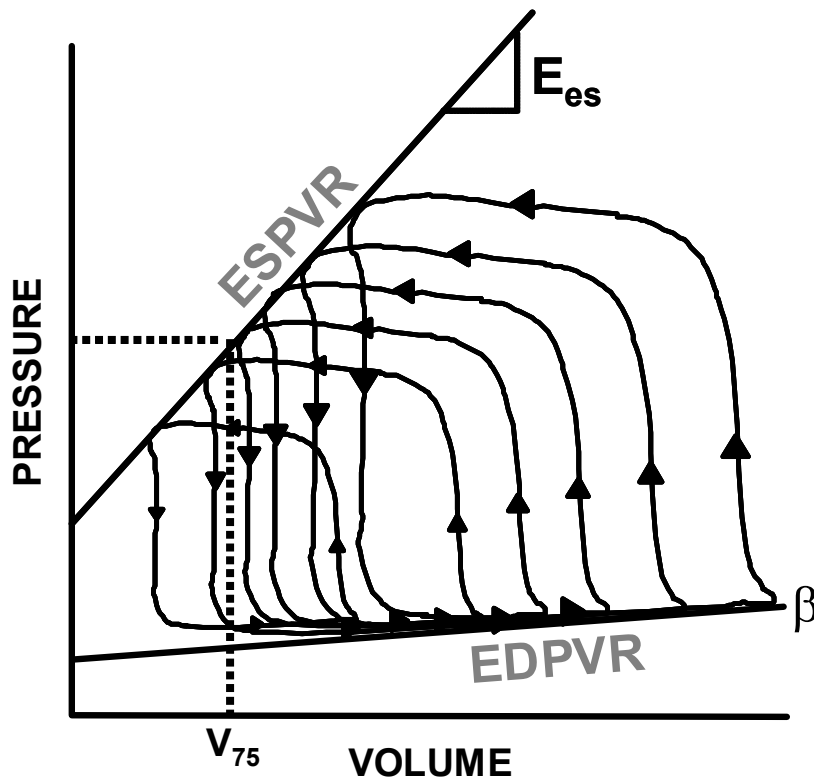


Fig. 7: Pressure-volume relationships. Variably loaded PV loops are used to define several PV relationships. The variable loading is derived by occluding the inferior caval vein and thereby reducing venous return. The end-systolic PV relationship (ESPVR) describes the contractile performance of the left ventricle. Contractility is linear correlated with the steepness of the ESPVR slope, i.e. E_{es} . The end-diastolic PV relationship (EDPVR) describes diastolic performance, for instance diastolic distensibility. The slope of the EDPVR (β) indicates the passive chamber stiffness.

The end-systolic PV relationship (ESPVR) describes the relation between volume and pressure changes in systole. Within the physiological range, this relationship approximates a straight line. The relationship can be described in terms of its slope, which reflects myocardial contractility, and its volume axis intercept V_0 . The volume intercept from the ESPVR line

could better be taken at a constant pressure level in the physiological range, for example between 50 and 100 mm Hg. (16) The volume intercept at a constant pressure (e.g. V_{75}) reflects myocardial contractility as it indicates the extent of contraction. Increased myocardial contractility, for instance during beta-adrenergic stimulation with isoprenaline, results in a steeper ESPVR-slope and a leftward shift on the volume axis, while attenuated contractility, for example during clinical heart failure, results in a concomitantly plain slope and a rightward shift on the volume axis. The slope of the ESPVR (E_{es}) is used to describe the left ventricular elastance. Arterial elastance (E_a), a measure for ventricular afterload, is described by the slope of the relationship between stroke volume and end-systolic pressure (figure 8).

Figure 8

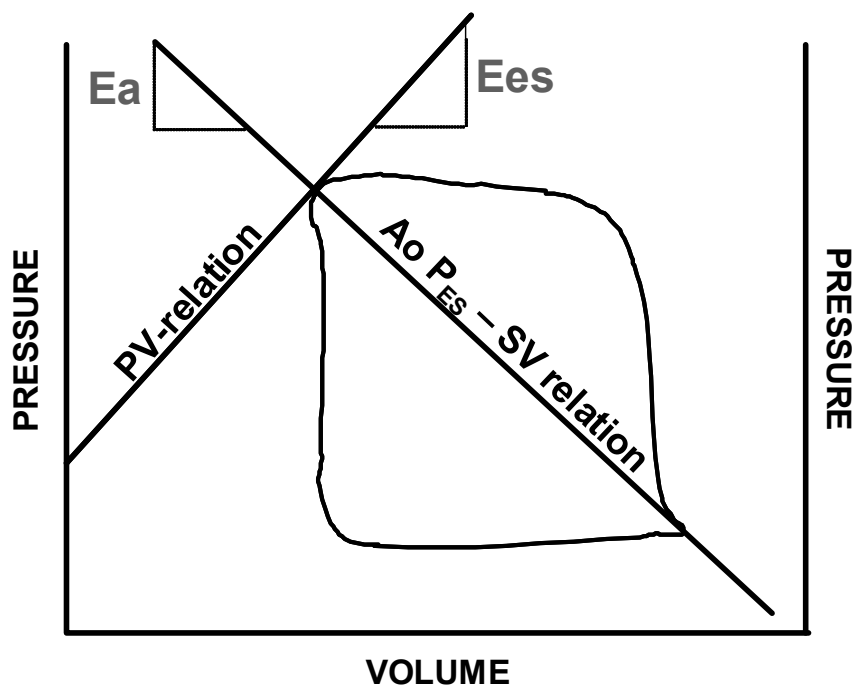


Fig. 8: Arterial-ventricular coupling. Ventricular elastance is estimated from the end-systolic PV relationship (ESPVR) slope, E_{es} . Arterial elastance (E_a) is approximated by the stroke volume/end-systolic pressure ratio ($Ao P_{ES} - SV$ relationship). The between E_a and E_{es} reflects the coupling between the left ventricle and the arterial circulation. The production of stroke work is maximal when the E_a and E_{es} are approximately equal.

Chapter 3. Murine left ventricular pressure-volume loops

The production of stroke work is maximal when the E_{es} and E_a are approximately equal. Stroke work attenuates substantially in relation to its maximal value, whenever E_a and E_{es} differ markedly. (17,18) The preload-recruitable stroke work (PRSW) is the relationship between end-diastolic volume and performed stroke work by the ventricle. It is a load-independent measure of contractility related to preload. The contractile state of the heart is resembled by the steepness of the PRSW-slope. In a high contractile state the heart is able to perform more stroke work at a constant end-diastolic volume, for instance by augmenting the ejection fraction.

Diastolic function is derived from the end-diastolic PV relationship (EDPVR), which correlates with the compliance of the ventricular myocardium. Diastolic dysfunctioning or failure is observed by an inappropriate upward shift of the ESPVR. The slope of the EDPVR (β) increases during augmented stiffness of the ventricular wall, when pressure rises progressively more during ventricular filling. The opposite occurs in case of increased compliance. Certain cardiac diseases and remodeling processes are correlated with increased stiffness of the ventricular wall by collagen deposition, resulting in an increase of the EDPVR-slope. (19)

Numerous other relationships can be assessed. The limits are determined by the interests and the creativity of the investigator.

Results of PV-measurements with the open- (OC) and closed-chest (CC) approach

A comparative study was performed to determine scientifically based arguments for the choice between open- (OC) or closed-chest (CC) PV measurements to examine murine cardiac function. Comparing cardiac performance between OC and CC protocols revealed overall relatively similar values for the investigated parameters (table 3). The values for LV volumes were corrected for ρ , determined at $124 \Omega \cdot \text{cm}$ in the used setup ($N = 10$, $123.52 \pm 0.88 \Omega \cdot \text{cm}$), α ($N = 13$, 0.30) and V_c . V_c was determined during all PV experiments by the hypertonic saline injection method. No significant differences could be detected between CC and OC instrumentation ($94.69 \pm 4.83 \mu\text{l}$ versus $92.72 \pm 2.05 \mu\text{l}$, respectively; N.S.). The $4 \mu\text{l}$ 30% saline demonstrated to be sufficient to change blood conductivity. Moreover, as this volume encompasses only 15% of the normal murine end-diastolic volume, it proved to be too small to influence LV end-diastolic and end-systolic pressures (figure 4) in either OC or CC mice.

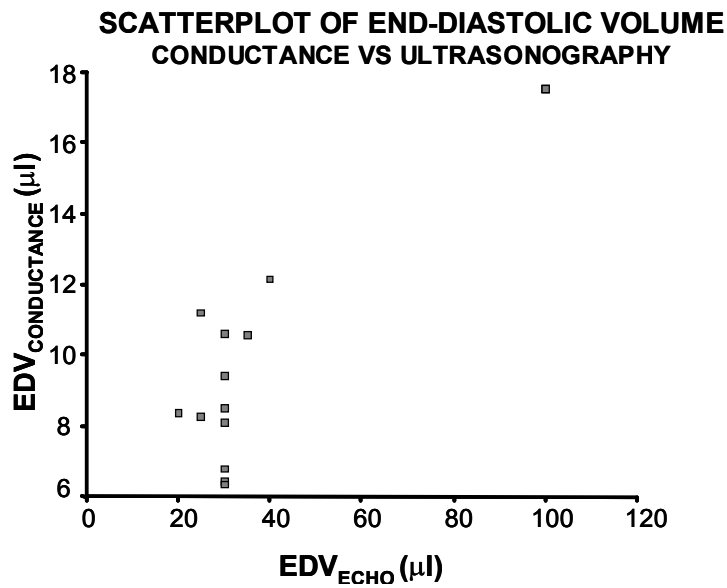
Several differences were found between the OC and CC approaches (table 3). Cardiac function in the OC approach was characterized by higher ejection fractions (EF 69 versus 48% respectively), larger stroke volume (19.98 versus $14.70 \mu\text{l}$, respectively) and a leftward shift in ventricular volume. On the contrary, measuring cardiac function with an intact thorax resulted in higher end-systolic pressures (ESP OC 52 versus CC 65 mmHg, with urethane anesthesia) and a higher rate of relaxation as indicated by the dP/dt_{\min} . No differences were found in the PV relationships, i.e. the ESPVR, EDPVR or PRSW. Interestingly, the OC approach did result in a mismatch between arterial afterload and ventricular work. The arterial-ventricular elastance ratio (E_a/E_{es}) was significantly depressed following opening of the chest. In contrast, E_a/E_{es} ratios were normal (i.e. ~ 1.0) in the CC approach under both regimens. This finding is consistently found in open-chest instrumented mice. (8) The arterial-ventricular coupling mismatch was depending on arterial resistance: the slope of the ESPVR

Table 1. Comparison of volume derived by ultrasonography and conductance.

Descriptive statistics of alpha					
	N	Min	Max	Mean	SEM
EDV	13	0.18	0.45	0.30	0.02
ESV	13	0.16	0.94	0.51	0.07
SV	13	0.09	0.58	0.26	0.04

Regression analysis

	N	R	R²	Adjusted R²	SEE
EDV	13	0.82	0.68	0.65	1.79
ESV	13	0.83	0.69	0.66	1.72
SV	13	0.41	0.17	0.09	1.17



Left ventricular volume was measured by both ultrasonography and conductance in adult C57Bl/6 mice. End-diastolic, end-systolic and stroke volume were used to obtain alpha (α). Descriptive analysis shows that α determination at the end-diastolic moment results in the most consistent mean α . Also, the correlation of LV volume values between ultrasonography and conductance is high, as shown by the regression analysis. SEM indicates standard error of the mean; SEE standard error of the estimate.

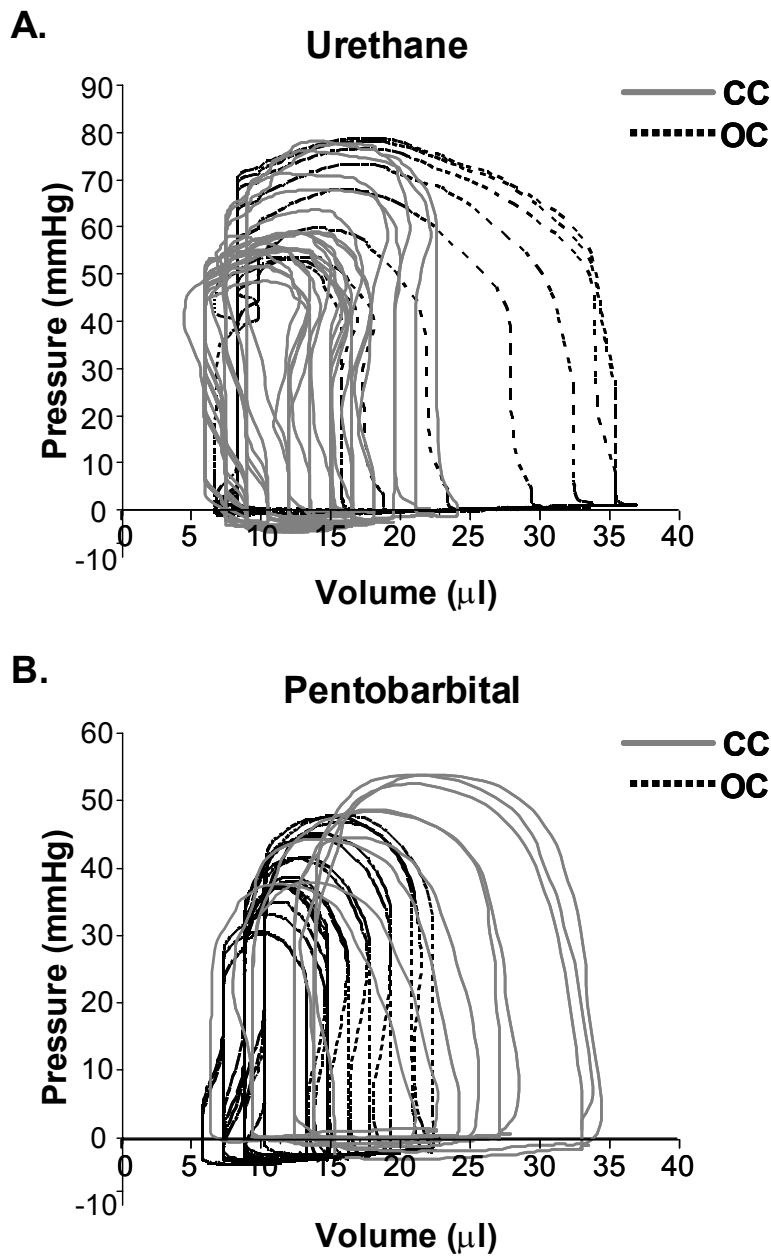
Chapter 3. Murine left ventricular pressure-volume loops

Table 2. Parameters derived by pressure-volume loops

Abbreviations	Definitions
General parameters	
CI (CI = CO/body wt)	Cardiac index
CO	Cardiac output
HR	Heart rate
Pressure	
dP/dt _{max}	Maximum derivative of change in systolic pressure in time
dP/dt _{min}	Maximum derivative of change in diastolic pressure in time
P _{ed}	End-diastolic pressure
P _{es}	End-systolic pressure
τ	Time constant of isovolumic relaxation
Volume	
EF	Ejection fraction
SI (SI = SV/body wt)	Stroke index
SV	Stroke volume
V _{ed}	End-diastolic pressure
V _{es}	End-systolic pressure
Pressure-volume relationships	
β	Slope of the end-diastolic pressure-volume relationship
E _a (E _a = P _{es} /SV)	Arterial elastance
EDPVR	End-diastolic pressure-volume relationship
E _{es}	End-systolic ventricular elastance (slope of the end-systolic pressure-volume relationship)
E _{max}	Maximum chamber elasticity ($\Delta P/\Delta V$)
ESPVR	End-systolic pressure-volume relationship
Pressure-volume area	
Efficiency	EW/PVA
EW	External work = SW
PE	Potential energy
PRSW	Preload-recruitable stroke work
PVA	Pressure-volume area = EW + PE
SW	Stroke work
SWI (SWI = SW/body wt)	Stroke work index

(Ees) proved to be equal in OC and CC instrumented mice. The combination of enlarged stroke volume with attenuated systolic pressures leads to a decrease in arterial elastance. The altered arterial elastance could be explained by the opening of the thorax. A drop in overall peripheral vascular resistance from baseline values has been described during thoracoscopy. (20)

Figure 9



Chapter 3. Murine left ventricular pressure-volume loops

Fig. 9: Left ventricular pressure-volume loops. Pressure presented in mmHg and volume μl .

A. Representative figure of PV loops acquired during urethane anesthesia in closed chest (CC) and open chest (OC) instrumented mice. B. Representative figure of PV loops acquired during pentobarbital anesthesia in CC and OC instrumented mice. Loops are acquired during an occlusion of the inferior caval vein. Venous returns decreases, which is represented in the loops by attenuation of both pressure and volume. The differences in ESP, SW and ESPVR between urethane and pentobarbital anesthesia can be observed by analyzing the loops in A and B. The loops show also the larger stroke volume and depressed systolic pressure in OC instrumented mice.

Figure 9 shows representative PV-loops while venous return was attenuated following inferior caval vein occlusion. Typical pressure and volume effects are depicted, showing the absence of apparent differences in PV relationships. The mentioned differences in ESP, SV and EF are evident in the presented loops, though.

ECG recordings were made during both surgical protocols to detect possible heart rate alterations and arrhythmias. Murine left ventricular PV measurements could be distorted by physiological responses to the catheterization. Heart rate alterations could be anticipated, especially in relation to carotid sinus stimulation while cannulating of the carotid artery.

However, neither bradycardia nor other arrhythmias were observed during either CC or OC procedures (figure 10). This finding indicates that cannulation of the right common carotid artery does not alter heart rate by carotid sinus stimulation.

Table 3. Functional parameters to determine baseline LV functioning in open- and closed-chest protocols during steady-state measurement.

	URETHANE		PENTOBARBITAL	
	OC	CC	OC	CC
	N = 5	N = 5	N = 10	N = 10
	Mean ± SEM	Mean ± SEM	Mean ± SEM	Mean ± SEM
HR*	583 ± 20	658 ± 21	493 ± 25	481 ± 36
SV†	19.58 ± 3.51	15.57 ± 2.54	20.18 ± 1.83	14.26 ± 1.03
CO	12 ± 2	10 ± 2	10 ± 1	7 ± 0
V_{max}*†	17.61 ± 0.53	23.61 ± 2.23	30.89 ± 2.89	38.83 ± 2.30
V_{min}*†	2.15 ± 1.33	6.79 ± 1.80	10.29 ± 1.89	23.73 ± 1.99
EF*†	79 ± 6	66 ± 8	66 ± 4	39 ± 2
ESP*†	52 ± 4	65 ± 5	42 ± 3	47 ± 4
EDP*	1 ± 1	-1 ± 1	-6 ± 2	1 ± 1
dP/dt_{max}*	7200 ± 1349	8252 ± 1685	4004 ± 629	3718 ± 684
dP/dt_{min}*†	-4233 ± 531	-7577 ± 750	-3631 ± 424	-3348 ± 653
Tau*	10 ± 0	7 ± 0	12 ± 1	14 ± 2
SW	1066 ± 245	1147 ± 213	1076 ± 176	666 ± 116
Ea/Ees†	0.65 ± 0.20	0.84 ± 0.16	0.60 ± 0.05	1.03 ± 0.15
ESPVR*	5.70 ± 0.94	5.89 ± 0.74	3.47 ± 0.27	3.18 ± 0.52
EDPVR	0.09 ± 0.09	-0.08 ± 0.15	-0.15 ± 0.14	-0.05 ± 0.15
PRSW	79 ± 14	64 ± 6	68 ± 10	53 ± 3

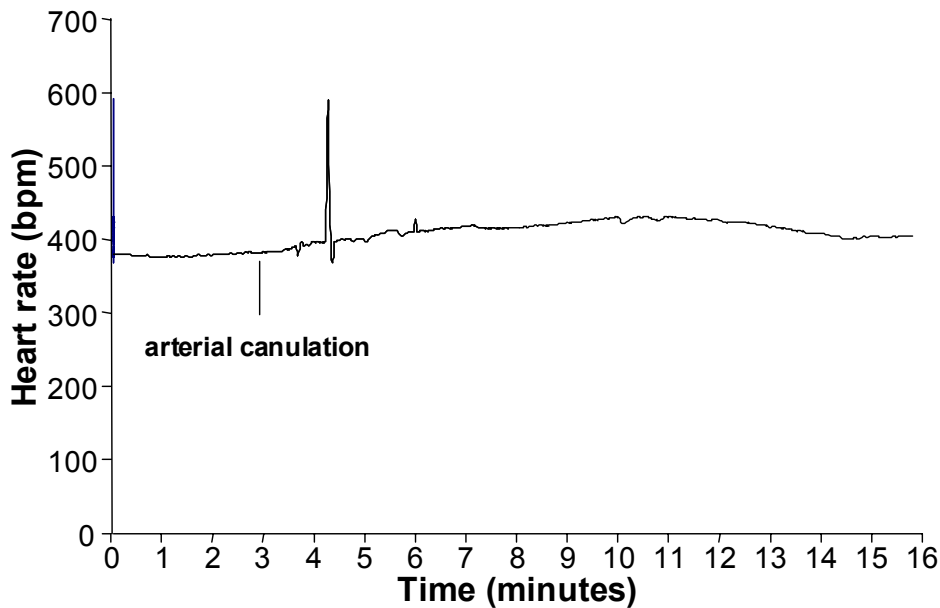
Results from LV pressure-volume measurements in C57Bl/6 mice anesthetized by urethane or pentobarbital. * Urethane versus pentobarbital $P < 0.05$. † OC versus CC $P < 0.05$. ρ Valued 124 $\Omega \cdot \text{cm}$, α 0.30. Open- (OC) and closed-chest (CC) protocols. HR indicates heart rate in bpm; SV left ventricular stroke volume in μl ; CO cardiac output ml/min; V_{min} minimal left ventricular volume in μl ; V_{max} maximal left ventricular volume in μl ; EF ejection fraction in %; ESP left ventricular end-systolic pressure in mmHg; EDP left ventricular end-diastolic pressure in mmHg; dP/dt_{max} maximal first derivative of left ventricular pressure in mmHg/s; dP/dt_{min} minimal first derivative of left ventricular pressure in mmHg/s; Tau time constant of left ventricular relaxation in ms; SW stroke work in mmHg· μl ; Ea arterial elastance / Ees ventricular end-systolic elastance; ESPVR left ventricular end-systolic PV relationship in

mmHg/ μ l; EDPVR left ventricular end-diastolic PV relationship in mmHg/ μ l; PRSW left ventricular preload-recruitable stroke work in mmHg.

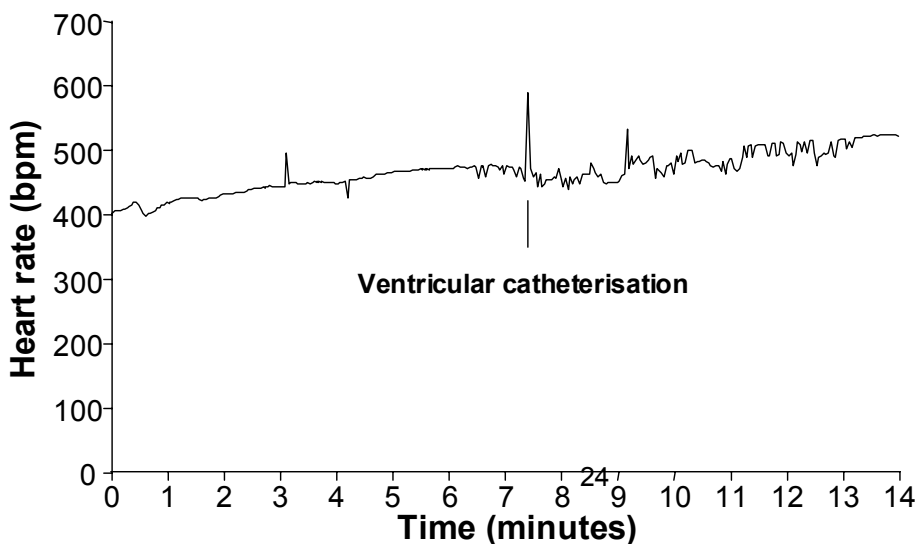
The steady-state functional parameters from OC and CC instrumented mice during either urethane or pentobarbital are also depicted in Table 2. The use of pentobarbital anesthesia had a cardiodepressive effect that was represented by significant function decline in most parameters. EF, dP/dt_{MAX} and ESPVR decreased respectively with 24, 57 and 41% upon pentobarbital use compared to urethane anesthesia. Pentobarbital, therefore, had strong negative chronotropic and inotropic effects.

Figure 10

A. Heart rate trace in closed-chest animal



B. Heart rate trace in open-chest animal



Chapter 3. Murine left ventricular pressure-volume loops

Fig. 10: Heart rate tracings in closed chest and open chest instrumented mice.

A. Representative figure of a heart rate tracing in a closed-chest instrumented mouse. The moment of arterial cannulation is indicated. Some arrhythmias are seen in response to introduction of the catheter into the left ventricle. Arrhythmias are only present in a short time-period that is part of the stabilization period following catheter introduction. Heart rate remains unchanged during the measurements. B. Representative figure of a heart rate tracing in an open-chest instrumented mouse. Somewhat more pronounced chronotropic arrhythmias are seen in response to ventricular introduction of the catheter by apical stab. However, no significant brady- or tachycardias are present during the measurements.

Discussion

In this chapter OC and CC protocols for *in vivo* left ventricular PV relationship measurement are described and discussed. Murine cardiac function determination via these methods is sensitive, reproducible and comparable. The choice for open- or closed-chest PV measurements in mice depends on the aim of the study with regards to the specific cardiac pathology. The OC approach is technically less complicated and less time consuming. Main characteristics of the OC model itself are low systolic pressures and arterial resistance. The OC approach could best be used in studies where myocardial integrity is not at stake. Particularly ischemia/reperfusion studies regarding myocardial integrity are probably better done using the CC approach.

Assessment of cardiac performance in genetically engineered mice is indispensable to understand human cardiovascular pathologies. In general the synergistic features of cardiac diseases, such as hypertrophy and cell death, affect cardiac function negatively. The contractile performance of the heart deteriorates, which is reflected in the attenuation of systolic parameters as ejection fraction, stroke work and PV-relationships. Furthermore, ventricular relaxation prolongs and diastolic filling becomes impaired. The progression of cardiac disease ultimately results in clinical heart failure, which is defined by the inability of the heart to meet hemodynamic demands of the body and is characterized by specific signs and symptoms. (21) The most important parameter of cardiac performance which defines heart failure is cardiac output.

The influence on cardiac performance of specific genes and proteins in the development of cardiac diseases ought to be investigated extensively to assess their clinical relevance. Various techniques have been used to assess cardiac performance in mice. The main techniques will be discussed in brief.

Chapter 3. Murine left ventricular pressure-volume loops

Echocardiography is the most widely used noninvasive technique to determine cardiac performance in mice. High-frequency transthoracic and transesophageal transducers are used as effective tools for two-dimensional and Doppler imaging of ventricular wall structures, dimensions and volumes of cavum, and cardiac function. (22,23) Full-conscious or gas-anesthesia experiments are preferred for echocardiographic assessment of cardiac function in mice. (24,25) There is no limit to the diversity of murine models investigated by this general accepted method of cardiac performance assessment. However, the most questionable aspect of these measurements is the significant inter- and intraobserver variance in the measurements.

Isolated working mouse heart measurements in a Langendorff perfusion setup are a technique for *ex vivo* cardiac function measurements approximating the *in vivo* function level. (5) Cardiac output, developed left ventricular pressure and first derivatives of maximal and minimal pressures are some of the parameters that can be derived. Isolated working heart measurements are especially useful to study the acute effects of ischemic preconditioning and ischemia-induced apoptosis. (26,27) Metabolites of interest can be measured accurately in the perfusion fluid. Disadvantages are the impossibility of chronic studies and the unphysiological situation of *ex vivo* cardiac function measurements.

Aortic flow measurements by means of a flow-probe have been used in several studies. (28,29) Aortic flow acquisition is a validated technique and reveals functional parameters as cardiac output, stroke volume and blood flow velocity. However, several disadvantages oppose against this technique. Firstly, aortic flow measurements are invasive (i.e. thoracotomy or laparotomy) and result solely in aortic derived volume parameters. Integrated ventricular function cannot be assessed. More importantly, the exact localization of the flow probe around the aorta is the critical determinant of the systematic error made by these measurements. Flow probes have been placed around the ascending and descending

Chapter 3. Murine left ventricular pressure-volume loops

thoracic aorta, and the abdominal aorta. The percentage of total cardiac output passing the flow probe on the specific location has to be estimated. Flow probes located at the ascending aorta correct for coronary circulation, and, for instance, bloodvolume passing the descending thoracic aorta has been estimated to be around 75% of total cardiac output. (30) The estimated correction factor provides ‘absolute’ stroke volume instead of absolute LV cavum volumes, and does not correct for cardiophysiological changes. Altered cardiophysiological situations could theoretically influence the relative amount of bloodvolume passing the flow probe. On the other hand, major advances are the possibility of chronic cardiac function measurements and the relative facile manner of data acquirement.(29) Moreover, aortic flow probe measurements are not hampered by deleterious cardiac remodeling in myocardial ischemia or hypertrophy studies.(28,29)

The newly developed method of cardiac performance assessment by *in vivo* left ventricular PV measurements in the CC model is introduced here. Left ventricular PV measurements *in vivo* provide an accurate assessment of murine cardiac function. The method is highly sensitive during open- and closed-chest approaches in determining alterations in left ventricular function as result of cardiac disease or altered hemodynamic stress. The characteristics of *simultaneous* left ventricular pressure and volume measurements enable the researcher to directly investigate pressure-related cardiac diseases, as cardiac hypertrophy and restrictive cardiomyopathy (31), or volume-related diseases, as dilated cardiomyopathy (32). Moreover, the effective influence of both aspects of cardiac disease on each other can be observed in detail. For instance, ventricular dilation and subsequent decrease in ventricular systolic pressure is mapped accurately in PV-loops. *Continuous* measurements provide possibilities to investigate the complete cardiac cycle. Basic aspects of cardiac physiology can be visualized using PV-loops in mice. (8,15,33-35) For instance, increase in ventricular filling is followed by an increase in ejection fraction according to the Frank-Starling mechanism.

Chapter 3. Murine left ventricular pressure-volume loops

The opposite is seen as a result of gradual venous return decrease in the case of transient caval vein occlusion (figure 7 & 9). Moreover, the distinction between systolic and diastolic failure can be made through continuous PV-measurements. (19) Systolic heart failure encompasses mainly an ejection dysfunction with impaired contractility. Both aspects are obtained by and directly visualized through PV-loops. Additionally, the definite diagnosis of diastolic failure is dependent on the observation of an inappropriate upward shift of the (end-)diastolic PV relationship, requiring cardiac catheterization for continuous volume determinations using impedance measurements and high-fidelity measurements of ventricular pressure with a micromanometer. (19) PV-loops are useful determining cardiac performance within the complete continuum of healthy and diseased hearts.

Conclusion

In vivo PV measurements provide an essential tool in the assessment of cardiac function in genetically modified mice. Open- and closed-chest surgical protocols for murine cardiac function determination are sensitive, reproducible and comparable. PV-loops enable the researcher to accurately investigate diverse murine models of cardiac pathology by adequately visualizing the cause-and-effect relationship between genetic modification and their functional outcome. Changes in ventricular contractility are best detected by PV derived parameters in comparison to other methods of cardiac function determination.

References

1. Doevendans PA, Daemen MJ, de Muinck ED, Smits JF. Cardiovascular phenotyping in mice. *Cardiovasc Res* 1998;39:34-49.
2. Hoit BD. New approaches to phenotypic analysis in adult mice. *J Mol Cell Cardiol* 2001;33:27-35.
3. Chacko VP, Aresta F, Chacko SM, Weiss RG. MRI/MRS assessment of in vivo murine cardiac metabolism, morphology, and function at physiological heart rates. *Am J Physiol Heart Circ Physiol* 2000;279:H2218-24.
4. Tanaka N, Dalton N, Mao L, et al. Transthoracic echocardiography in models of cardiac disease in the mouse. *Circulation* 1996;94:1109-17.
5. De Windt LJ, Willems J, Reneman RS, Van der Vusse GJ, Arts T, Van Bilsen M. An improved isolated, left ventricular ejecting, murine heart model. Functional and metabolic evaluation. *Pflugers Arch* 1999;437:182-90.
6. Palmen M, Daemen MJ, Buehler A, et al. Impaired cardiac remodeling and function after myocardial infarction in FGF-1 transgenic mice. *Circulation* 1999;100:250.
7. Rockman HA, Hamilton RA, Jones LR, Milano CA, Mao L, Lefkowitz RJ. Enhanced myocardial relaxation in vivo in transgenic mice overexpressing the beta2-adrenergic receptor is associated with reduced phospholamban protein. *J Clin Invest* 1996;97:1618-23.
8. Georgakopoulos D, Mitzner WA, Chen CH, et al. In vivo murine left ventricular pressure-volume relations by miniaturized conductance micromanometry. *Am J Physiol* 1998;274:H1416-22.
9. Dekker AL, Geskes GG, Cramers AA, et al. Right ventricular support for off-pump coronary artery bypass grafting studied with bi-ventricular pressure-volume loops in sheep. *Eur J Cardiothorac Surg* 2001;19:179-84.
10. Schreuder JJ, Steendijk P, van der Veen FH, et al. Acute and short-term effects of partial left ventriculectomy in dilated cardiomyopathy: assessment by pressure-volume loops. *J Am Coll Cardiol* 2000;36:2104-14.
11. Zimmer HG. Measurement of left ventricular hemodynamic parameters in closed-chest rats under control and various pathophysiologic conditions. *Basic Res Cardiol* 1983;78:77-84.
12. Georgakopoulos D, Kass DA. Estimation of parallel conductance by dual-frequency conductance catheter in mice. *Am J Physiol Heart Circ Physiol* 2000;279:H443-50.
13. Feldman MD, Mao Y, Valvano JW, Pearce JA, Freeman GL. Development of a multifrequency conductance catheter-based system to determine LV function in mice. *Am J Physiol Heart Circ Physiol* 2000;279:H1411-20.
14. Kornet L, Schreuder JJ, Van de Velden ET, Jansen JR. The volume-dependency of parallel conductance throughout the cardiac cycle and its consequence for volume estimation of the left ventricle in patients. *Cardiovasc Res* 2001;51:729-35.
15. Nemoto S, DeFreitas G, Mann DL, Carabello BA. Effects of changes in left ventricular contractility on indexes of contractility in mice. *Am J Physiol Heart Circ Physiol* 2002;283:H2504-10.
16. Baan J, Van de Velden ET, Steendijk P. Ventricular pressure-volume relations in vivo. *Eur Heart J* 1992;13 Suppl:E:2-6.
17. Little WC, Cheng CP. Left ventricular-arterial coupling in conscious dogs. *Am J Physiol* 1991;261:H70-6.
18. Sunagawa K, Maughan WL, Sagawa K. Optimal arterial resistance for the maximal stroke work studied in isolated canine left ventricle. *Circ Res* 1985;56:586-95.

19. Van Kraaij D, Van Pol P, Ruiters AW, et al. Diagnosing diastolic heart failure. *Eur J Heart Fail* 2002;4:419-30.
20. Faunt KK, Cohn LA, Jones BD, Dodam JR. Cardiopulmonary effects of bilateral hemithorax ventilation and diagnostic thoracoscopy in dogs. *Am J Vet Res* 1998;59:1494-8.
21. Lips DJ, Van Kraaij DL, De Windt LJ, Doevendans PA. Molecular determinants of myocardial hypertrophy and failure: alternative pathways for beneficial and maladaptive hypertrophy. *Eur Heart J* 2003;24:883-96.
22. Collins KA, Korcarz CE, Lang RM. Use of echocardiography for the phenotypic assessment of genetically altered mice. *Physiol Genomics* 2003;13:227-39.
23. Scherrer-Crosbie M, Steudel W, Hunziker PR, et al. Determination of right ventricular structure and function in normoxic and hypoxic mice: a transesophageal echocardiographic study. *Circulation* 1998;98:1015-21.
24. Takuma S, Suehiro K, Cardinale C, et al. Anesthetic inhibition in ischemic and nonischemic murine heart: comparison with conscious echocardiographic approach. *Am J Physiol Heart Circ Physiol* 2001;280:H2364-70.
25. Chaves AA, Weinstein DM, Bauer JA. Non-invasive echocardiographic studies in mice: influence of anesthetic regimen. *Life Sci* 2001;69:213-22.
26. Yamaura G, Turoczy T, Yamamoto F, Siddiqui MA, Maulik N, Das DK. STAT signaling in ischemic heart: a role of STAT5A in ischemic preconditioning. *Am J Physiol Heart Circ Physiol* 2003;285:H476-82.
27. Bell RM, Yellon DM. Atorvastatin, administered at the onset of reperfusion, and independent of lipid lowering, protects the myocardium by up-regulating a pro-survival pathway. *J Am Coll Cardiol* 2003;41:508-15.
28. Aartsen WM, Schuijt MP, Danser AH, Daemen MJ, Smits JF. The role of locally expressed angiotensin converting enzyme in cardiac remodeling after myocardial infarction in mice. *Cardiovasc Res* 2002;56:205-13.
29. Janssen B, Debets J, Leenders P, Smits J. Chronic measurement of cardiac output in conscious mice. *Am J Physiol Regul Integr Comp Physiol* 2002;282:R928-35.
30. Georgakopoulos D, Christe ME, Giewat M, Seidman CM, Seidman JG, Kass DA. The pathogenesis of familial hypertrophic cardiomyopathy: early and evolving effects from an alpha-cardiac myosin heavy chain missense mutation. *Nat Med* 1999;5:327-30.
31. Liao P, Georgakopoulos D, Kovacs A, et al. The in vivo role of p38 MAP kinases in cardiac remodeling and restrictive cardiomyopathy. *Proc Natl Acad Sci U S A* 2001;98:12283-8.
32. McConnell BK, Jones KA, Fatkin D, et al. Dilated cardiomyopathy in homozygous myosin-binding protein-C mutant mice. *J Clin Invest* 1999;104:1235-44.
33. Georgakopoulos D, Kass DA. Minimal force-frequency modulation of inotropy and relaxation of in situ murine heart. *J Physiol* 2001;534:535-45.
34. Yang B, Larson DF, Watson R. Age-related left ventricular function in the mouse: analysis based on in vivo pressure-volume relationships. *Am J Physiol* 1999;277:H1906-13.
35. Reyes M, Freeman GL, Escobedo D, Lee S, Steinhilber ME, Feldman MD. Enhancement of contractility with sustained afterload in the intact murine heart: blunting of length-dependent activation. *Circulation* 2003;107:2962-8.

Chapter 4. MEK1-ERK1/2 signaling is cardioprotective.

The MEK1-ERK2 signaling pathway protects the myocardium from ischemic damage in vivo

Daniel J. Lips, Orlando F. Bueno, Benjamin J. Wilkins, Nicole H. Purcell, Robert A. Kaiser, John N. Lorenz, Laure Voisin, Marc K. Saba-El-Leil, Sylvain Meloche, Jacques Pouysségur, Gilles Pagès, Leon J. De Windt, Pieter A. Doevendans, Jeffery D. Molkentin.

In modified version in press *Circulation*.

Abstract.

Myocardial infarction causes a rapid and largely irreversible loss of cardiac myocytes that can lead to sudden death, ventricular dilation, and heart failure. Recent investigation has sought to elucidate the underlying molecular pathways that protect cardiac myocytes from ischemic insults. Members of the mitogen-activated protein kinase (MAPK) signaling cascade have been implicated as important effectors of cardiac myocyte cell death in response to diverse stimuli, including ischemia-reperfusion injury. Specifically, activation of the extracellular signal-regulated kinases 1/2 (ERK1/2) have been associated with cardioprotection, likely through antagonism of apoptotic regulatory pathways. To determine a direct causal relationship between ERK1/2 signaling and cardioprotection, here we analyzed *Erk1* nullizygous gene targeted mice, *Erk2* heterozygous gene targeted mice, and transgenic mice with activated MEK1-ERK1/2 signaling in the heart. This gain- and loss-of-function approach demonstrated a direct cardioprotective role for ERK signaling in the heart following ischemia-reperfusion injury. While MEK1 transgenic mice were largely resistant to myocardial infarction, *Erk2*^{+/-} gene-targeted mice showed enhanced infarction areas, DNA laddering, and TUNEL labeling compared to littermate controls. Enhanced MEK1-ERK1/2 signaling protected hearts from DNA laddering, TUNEL labeling, and preserved hemodynamic function assessed by pressure-volume loop recordings following ischemia reperfusion injury. Collectively, these data are the first to demonstrate that ERK signaling directly participates in mediating cellular protection following ischemic injury in the heart.

Introduction

The mitogen-activated protein kinases (MAPK) constitute an essential signal transduction cascade that occupies a central position in cell growth, differentiation, apoptosis, and transformation (reviewed in Garrington and Johnson, (1)). While it is somewhat oversimplified, the MAPK signaling pathway consists of a sequence of successively acting kinases that ultimately result in the dual phosphorylation and activation of terminal kinases p38, c-Jun N-terminal kinases (JNKs), and extracellular signal-regulated kinases (ERKs) (2). The MAPK signaling cascade is initiated in cardiac myocytes by G-protein coupled receptors, receptor tyrosine kinases, cardiotrophin-1 (gp130 receptor), and by stress stimuli (3). The major upstream activators of ERK1/2 are two MAP kinase kinases (MAPKK), MEK1, and MEK2 which directly phosphorylate the dual site in ERK kinases (Thr-Glu-Tyr) (2). Once activated, p38, JNKs, and ERKs each phosphorylate a wide array of intracellular targets that directly influence cell growth, acute alterations in cellular physiology, or cellular apoptosis.

Within the heart, members of the MAPK cascade have been implicated in regulating myocyte survival following ischemia-reperfusion injury, oxidative stress, and anthracycline exposure. A number of studies support the hypothesis that the MEK-ERK branch of the MAPK pathway is cardioprotective by directly antagonizing myocyte apoptosis. For example, Insulin-like growth factor 1 (IGF-1), catecholamines and cardiotrophin 1 (CT-1) each induce ERK signaling, which is an essential effector of anti-apoptosis in cultured myocytes (4-6). Inhibition of ERK signaling also enhanced daunomycin-induced apoptosis in cultured cardiomyocytes (7) and ERK1/2 activation was associated with reduced apoptosis in a model of ischemia-reperfusion injury (8). More recently, transgenic mice expressing an activated MEK1 protein in the heart were also shown to be partially resistant to ischemia-reperfusion-induced DNA laddering, suggesting a cardioprotective function for ERK1/2 signaling *in vivo* (9).

Chapter 4. MEK1-ERK1/2 signaling is cardioprotective.

While each of the studies discussed above supports the hypothesis that ERK1/2 activation is anti-apoptotic in cardiac myocytes, the direct mechanism of protection is less certain. One potential mechanism involves cyclooxygenase-2 (COX-2) enzyme, which has been implicated as a cardioprotective downstream ERK effector in cardiomyocytes (10). In lymphocytes, ERK1/2 activation enhances expression of FLICE (FADD-like interleukin 1 β -converting enzyme) inhibitory protein, a known inhibitor of the caspase cascade (11). More recently, non-genomic signaling through estrogen was shown to have a myocyte protective effect in association with nitric oxide (NO), ANF, and ERK1/2 signaling (12-16). Finally, ERK1/2 signaling may regulate cardioprotection through a mechanism involving direct interaction with PKC in the mitochondria (17).

While MEK1-ERK1/2 signaling is thought to protect the myocardium from apoptotic insults, definitive genetic data demonstrating a necessary function for MEK1-ERK1/2 signaling have not been reported. Here we analyzed *Erk1*^{-/-} and *Erk2*^{+/-} gene targeted mice, as well as MEK1 transgenic mice to evaluate both gain- and loss-of-function phenotypes associated with this signaling pathway and cardiomyocyte cell survival. *Erk2* heterozygote mice showed enhanced apoptosis following ischemia reperfusion injury, while transgenic mice expressing activated MEK1 in the heart were significantly protected. These results provide definitive genetic data implicating ERKs as beneficial effectors of myocyte survival following myocardial stress stimulation.

Chapter 4. MEK1-ERK1/2 signaling is cardioprotective.

Materials and Methods

Animals

For this study adult *Erk1* nullizygous (*Erk1*^{-/-}), *Erk2* heterozygous (*Erk2*^{+/-}), MEK1 transgenic mice (MEK1 TG) and their wild type littermates (resp. *Erk*^{+/+} and MEK1 wt) were used. All animals were kept under standard housing conditions with an artificial 12h light cycle with free access to standard rodent food and tap water. The animal studies were performed conform the *Guide for the Care and Use of Laboratory Animals* published by the US National Institutes of Health (NIH Publication No. 85-23, revised 1996) and were approved by the animal ethical committee of Cincinnati Children's Hospital Medical Center.

Western Blotting and ERK Kinase Assay

Mice were subjected to *in vivo* PE stimulation to determine total ERK1/2 protein levels and kinase activities. Wild-type, *Erk1*^{-/-}, and *Erk2*^{+/-} mice (average weight = 20 grams) were injected subcutaneously with 10 mg kg⁻¹ PE or PBS vehicle. Animals were sacrificed 15 minutes later, and hearts were quickly excised, rinsed in PBS, and snap-frozen in liquid nitrogen. For all experiments, one-quarter of each heart was homogenized in 400 μ L Triton lysis buffer (TLB): Tris-HCl (pH 7.5) 40 mM, NaCl 137 mM, sodium b-phosphoglycerate 25 mM, sodium pyrophosphate 2 mM, EDTA 2 mM, sodium orthovanadate 1 mM, PMSF 1 mM, with 10% (v/v) glycerol, 1% (v/v) Triton X-100, 5 mg mL⁻¹ leupeptin, and 5 mg mL⁻¹ aprotinin. Lysates were cleared by centrifugation and stored at -80 C until use.

For ERK immunoprecipitation (IP) kinase assays, total ERK protein was immunoprecipitated from 100 μ g of lysate by 1 μ g each of agarose-conjugated anti-ERK1 and anti-ERK2 antibodies (Santa Cruz Biotechnology). Samples were rocked overnight at 4° Celsius in 400 μ L TLB; beads were then washed three times in TLB and twice with kinase buffer (KB):

Chapter 4. MEK1-ERK1/2 signaling is cardioprotective.

HEPES (pH 7.4) 25 mM, sodium b-phosphoglycerate 25 mM, MgCl₂ 25 mM, sodium orthovanadate 0.1 mM, and DTT 0.5 mM. ERK kinase activity was determined by incubating beads with 10 mg dephosphorylated myelin basic protein (MBP) (Upstate Biotechnology), 1.25 nmole ATP, and 15 mCi [³²P] ATP in 25 mL KB at 30 C for 30 minutes. Samples were then mixed with SDS loading buffer, boiled 5 minutes, and electrophoresed on 14% SDS-PAGE gels. Gels were dried, exposed overnight to a PhosphorImager screen (Molecular Dynamics), and ³²P-MBP levels were quantitated using a Storm 820 scanner (Molecular Dynamics) and ImageQuant software (v.1.2).

For Western blotting, 100 mg of lysate was electrophoresed by SDS-PAGE and transferred to PVDF membranes. Membranes were blocked in 10% nonfat milk/TBS-T, washed in TBS-T, and probed in 5% milk/TBS-T with antibodies against phospho-ERK1/2 (Cell Signaling) or ERK1/2 (Cell Signaling). Detection was accomplished using alkaline phosphatase-conjugated secondary antibodies, ECF reagent, and a Storm 860 scanner.

Murine in vivo ischemia reperfusion

Adult mice (8-10 weeks) were anesthetized with isoflurane, 2% in O₂ (500 ml/min). The anterior thorax was shaved and disinfected with betadine solution. Mice were placed on a heating plate and body temperature was kept constant. A 20-gauge tube was positioned in the trachea and connected to a rodent ventilator (Minivent, Hugo Sachs Electronics, Germany) for mechanical ventilation (200 µl, 200 strokes per minute). A left thoracotomy was performed to expose the heart and the left anterior descending artery (LAD). The LAD was ligated with 8-0 prolene (Ethicon, USA) using a slip knot placed approximately 2 mm distal from its origin. Mice were allowed to wake up. The LAD ligation was removed following 60 or 90 min ischemia time (C57Bl/6 versus FVB/N backgrounds, respectively), after which the mice were reperfused for 24 h or 7 d depending

Chapter 4. MEK1-ERK1/2 signaling is cardioprotective.

on the final analysis chosen. Sham-operations were performed in a similar manner, although actual LAD ligation was not performed.

Left ventricular in vivo pressure-volume measurements

Following 7 days of reperfusion mice were instrumented and anesthetized as described above. The right and left external jugular veins were cannulated with PE-50 catheters for saline and drug infusion. A 1.4 French conductance-micromanometer (Millar Instruments, Houston, TX, USA) was inserted into the right common carotid artery, advanced through the aorta and positioned in the left ventricle (LV). Correct LV placement was controlled by the combination of the online pressure and volume signal. For pressure and volume signal acquisition the MCPU-200 recording unit (Millar Instruments, Houston, TX, USA) and 8S/P Powerlab control unit (AD instruments, Australia) were used, in combination with Chart and Scope software (AD instruments, Australia). Function data analysis was performed with Circlab software (LUMC, the Netherlands).

Staining for infarct size

Following 24 hours of reperfusion mice were anesthetized with 5% Avertin. Upon complete anesthesia the thorax was quickly opened and the 8-0 prolene ligature was retied around the LAD. A 0.5 cc insulin syringe was used to inject 0.3 ml of 2 % Evans Blue dye in the left ventricle, thereby specifically staining the heart except for the LAD perfusion area. The heart was taken out, washed in PBS to rinse off the excess dye and embedded in 2% agarose gel. Short-axis cross sections were cut from the heart and placed in 2% 2,3,5-triphenyl-tetrazodium chloride (TTC) solution (Sigma, St. Louis, USA) at 37° Celsius to stain for viable myocardium. Fifteen minutes later the slices were taken out of the TTC solution. Slices were fixed in 10% buffered formalin phosphate solution (Fisher Scientific, New Jersey, USA). Digital pictures of both sides of the

Chapter 4. MEK1-ERK1/2 signaling is cardioprotective.

sections were made and analyzed for infarct area (IA), area-at-risk (AAR) and left ventricular area (LV) with ImageJ software (Wayne Rasband, National Institutes of Health, USA)

DNA laddering assays

For PCR-based DNA laddering assays samples of heart tissue were utilized following 24 hours of reperfusion. Hearts were removed and rinsed quickly in ice-cold PBS. After removal of the atria and great vessels, heart tissue was frozen in liquid nitrogen, and was stored at 70°C until further analysis. Tissue was ground with a mortar and pestle immersed in liquid nitrogen, and was digested in 1 ml lysis buffer (10 mM Tris [pH 8.0], 100 mM NaCl, 25 mM EDTA, 0.5% SDS, 1.0 mg/ml Proteinase K (Sigma Chemical Co., St. Louis, MO) overnight at 37°C. Protein was removed by precipitation in NaCl at a final concentration of 1.2 M, followed by centrifugation at 10,000 g for 30 min. After extraction of supernatants with phenol-chloroform, genomic DNA was precipitated with isopropanol, washed in 70% ethanol, resuspended in 10 mM Tris (pH 8.0), 1.0 mM EDTA, and treated with RNase A for 30 min at 37°C. 0.5 µg of genomic DNA was mixed with Ligation Buffer (Maxim Biotech Inc., San Francisco, CA), heated to 55°C for 10 min, cooled down to 10°C over approximately 1 hour and incubated with T4 DNA ligase (Maxim Biotech Inc., San Francisco, CA) at 16°C overnight. For PCR-reactions 100 ng of adaptor-ligated DNA was used for each sample. PCR thermocycle profile was set according to manufacturers instructions, and 10 µl samples of the reaction mixture were extracted at cycles 23, 25 and 28. Reaction samples were loaded on a 1.5% agarose/EtBr gel for electrophoresis.

For DNA laddering of cultured cardiomyocytes, three 10 cm plates were utilized under each experimental condition. To isolate genomic DNA cells were trypsinized for 5 min. and collected by a 1 min. spin in a microfuge at 13,000 rpm. Cells were lysed in 10 mM Tris (pH=8.0), 25 mM EDTA, 100 mM NaCl, 0.5% SDS, and 1 mg/ml proteinase K overnight at 37°C. After incubation,

Chapter 4. MEK1-ERK1/2 signaling is cardioprotective.

proteins were precipitated by addition of an equal volume of 2.4 M NaCl and removed by centrifugation. The supernatant was extracted once with phenol:chloroform, the DNA precipitated with isopropanol, washed with 70% ethanol, and resuspended in 10 mM Tris (pH=8.0), 1 mM EDTA, and treated with 100 mg/ml DNase free RNase (Boehringer Mannheim) for 30 min at 37°C. The genomic DNA was precipitated with isopropanol, rewashed with 70% ethanol and dissolved in 10 mM Tris (pH=8.0), 1 mM EDTA and its concentration determined by spectrophotometry. Equal amounts of DNA were loaded on 1.5% agarose gels containing 1 µg/ml ethidium bromide and visualized under UV light.

TUNEL labeling

In situ DNA fragmentation was detected using the terminal deoxyribonucleotide transferase (TdT)-mediated dUTP nick-end labeling (TUNEL) in paraffin-embedded tissue sections. Hearts were collected from genetically modified and wild type littermate mice 24 hours following I/R-injury, rapidly fixed, paraffin embedded and sectioned cross-sectional in 6µm slices. TUNEL labeling was performed using the *In Situ* Cell Death Detection kit (Roche, Penzberg, Germany) using the manufacturer's recommended conditions. Sections were dewaxed and rehydrated, permeabilized with 0.1% Triton X-100, 0.1% sodium citrate solution. Subsequently sections were incubated with TUNEL Labeling solution at 37°C in a humidified climate. Cardiac myofibers were counterstained with 0.05% phalloidin and nuclei with 0.05% bis-benzamide solution. Digital pictures of the sections were made with a fluorescence camera and stored accordingly. TUNEL rates were determined solely in the ischemic area of the mid-myocardium of each heart at various sections.

SDS PAGE and Immunoblot Analysis for PARP cleavage

Chapter 4. MEK1-ERK1/2 signaling is cardioprotective.

Protein samples were separated by SDS-PAGE according to the method described by Laemmli (1970). (18) Protein extracts were prepared from heart tissue using extraction buffer (20 mM NaPO₄, 150 mM NaCl, 2 mM MgCl₂, 0.1% NP-40, 10% glycerol, 10 mM NaF, 0.1 mM sodium orthovanadate, 10 mM sodium pyrophosphate, 10 μM phenylarsine oxide, 10 nM okadaic acid, 1 mM DTT, 10 μg/ml leupeptin, 10 μg/ml aprotinin, 10 μg/ml pepstatin, 10 μg/ml TPCK, and 10 μg/ml TLCK). Samples containing 50-100 μg were thawed on ice, diluted 1:1 with a 2X sample buffer to a final concentration of 2% SDS, 62.5 mM Tris•HCl pH 6.8, 5% 2-mercaptoethanol, 10% glycerol, 0.001% bromophenol blue, and heated at 95°C for 5 min. The samples were then loaded onto 10% acrylamide gels and electrophoresed in the presence of 25 mM Tris pH 8.3, 2 mM glycine and 0.1% SDS at room temperature. Following SDS-PAGE, proteins were transferred electrophoretically onto Hybond-P membranes (Amersham Pharmacia Biotech, Buckinghamshire, UK) with transfer buffer (25 mM Tris, 190 mM glycine, 20% methanol) for 12 hours at 4°C. Membranes were then blocked for 2 hours at room temperature with Tris buffered saline containing 0.1% Tween 20, 10 mM Tris pH 7.5, 150 mM NaCl (TBS-T), 5% non-fat milk, and then incubated either in antiserum (anti-[poly (ADP-ribose) polymerase] PARP) overnight at 4°C. Membranes were then washed three times 10 min each with TBST and incubated for 2 hours with secondary antibody conjugated to horseradish peroxidase with either anti-mouse IgG (dilution 1:2500) or anti-rabbit IgG (dilution 1:2500). After this incubation, membranes were washed three times with TBST and immunoreactivity was detected using the enhanced chemiluminescence system (ECL) (Amersham Pharmacia Biotech, Buckinghamshire, UK) according to kit instructions. Immunoreactive bands on films were digitized and quantified for fluorescence with a Storm 860 PhosphoImager (Molecular Dynamics, Sunnyvale, CA).

Statistical Analysis

Chapter 4. MEK1-ERK1/2 signaling is cardioprotective.

Statistical analyses between the experimental groups were performed using a Student's t-test or one-way ANOVA when comparing multiple groups. Data are reported as mean \pm SEM. *P*-values < 0.05 were considered significant.

Results

A gene targeting approach was employed to evaluate the necessary functions of ERK1 and ERK2 gene products as regulators of cardiac homeostasis and stress responsiveness. *Erk1* and *Erk2* gene targeted mice were each previously described. (19,20) *Erk1* null mice are fully viable as adults, but *Erk2* gene targeted mice could only be analyzed in the heterozygous state, since null mice were not viable. Western blotting from cardiac protein extracts was performed to examine the quantity of ERK1 and ERK2 proteins from each gene targeted mouse (figure 1) and the resulting effect on total cardiac ERK kinase activity following stress stimulation (figure 2). In protein quantification studies through Western blot techniques ERK1/2 proteins were detected using a pan-ERK antibody. Equivalent antibody reactivity was demonstrated with bacterial-generated ERK1 and ERK2 protein standards (GST fusion proteins), from which a standard curve was generated to quantify endogenous ERK1 and ERK2 levels in the heart (figure 1A). Further quantification of cardiomyocyte cellular protein content indicated ERK2 to represent approximately 60-70% of total ERK protein in the heart in wildtype mice (figure 1B). ERK1 protein could not be detected in *Erk1*^{-/-}, while, importantly, ERK2 protein levels were not increased in the hearts of *Erk1* deficient mice. ERK2 protein levels in *Erk2*^{+/-} mice were observed to be downregulated, while ERK1 protein levels were unaffected in these mice. Cardiac ERK activation was assessed by immunoprecipitation kinase assay from hearts of wildtype, *Erk1*^{-/-} and *Erk2*^{+/-} mice following an acute 30 min of ischemia (figure 2B), or acute PE injection (figure 2A & C). The immune kinase assays showed a consistent profile of inhibited total ERK activity from either *Erk1*^{-/-} or *Erk2*^{+/-} hearts by either stimulation. For example, 30 minutes of ischemia induced a 2-fold increase in ERK activity in wildtype hearts, but essentially no increase in *Erk1*^{-/-} or *Erk2*^{+/-} hearts ($P < 0.05$) (figure 2B). In response to PE stimulation, a similar percentage of reduction in ERK kinase activity was observed

Figure 1

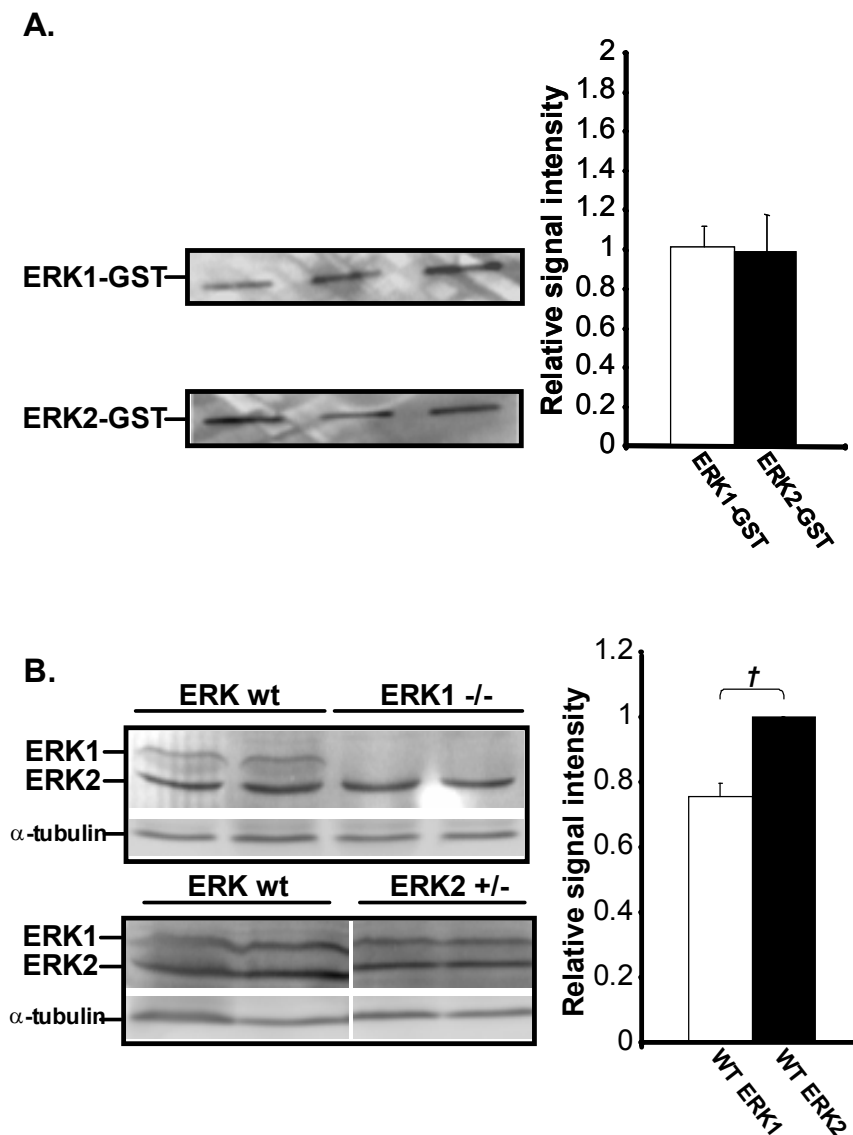


Fig. 1: Analysis of ERK protein expression in wildtype and Erk genetic modified mice. A. Western blot with bacterium-generated ERK1- and ERK2-GST fusion protein standards to verify antibody equivalence. Left panel shows actual Western blots ERK1/2-GST binding by the pan-ERK antibody (Cell Signaling). Right panel shows the quantification of antibody binding affinity, demonstrating equivalent antibody affinity (NS, N = 3). B. Western blot quantification for content of endogenous ERK1 and ERK2 in the heart. Left panels show Western blots from tissue extracts from wild type,

Chapter 4. MEK1-ERK1/2 signaling is cardioprotective.

Erk1^{-/-} and Erk2^{+/-} mice. Quantification of ERK1/2 proteins in wild type mice is visualized in the right panel, demonstrating ERK2 to be the predominant ERK protein in the heart.

Figure 2

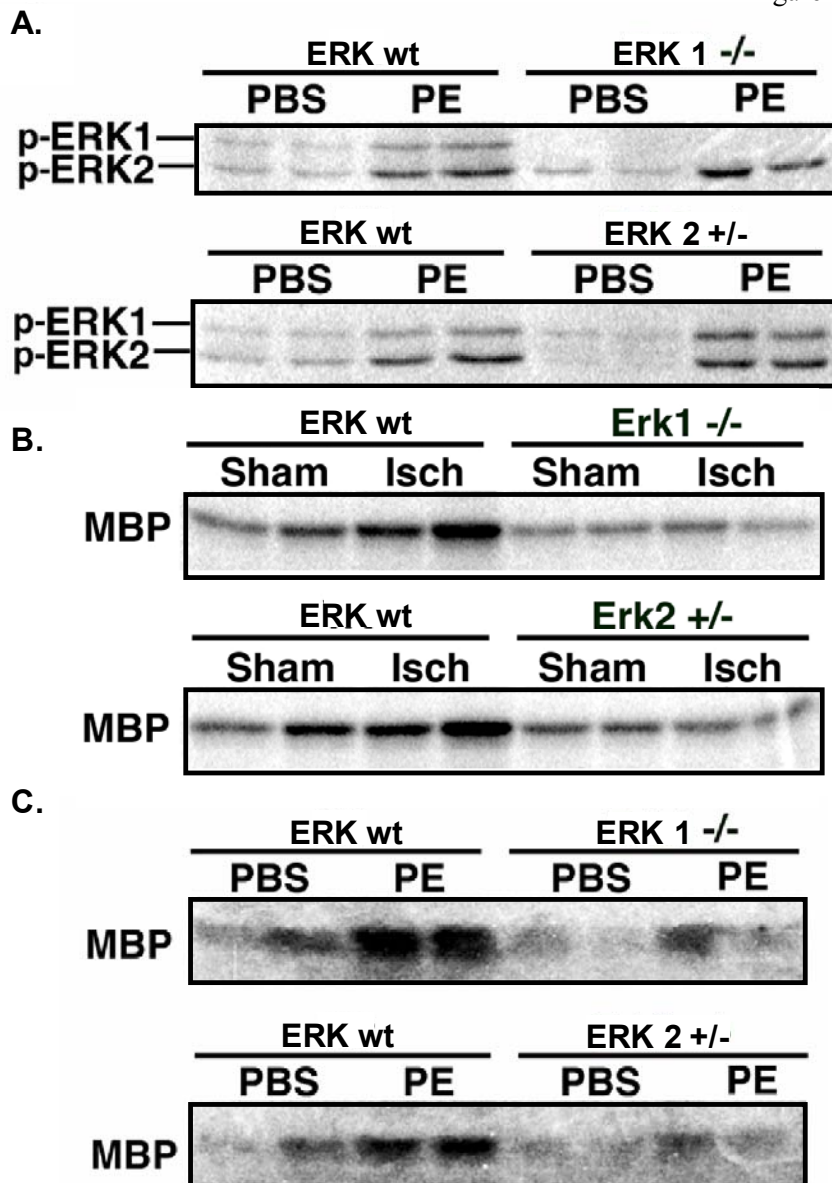


Fig. 2: Analysis of kinase activity in Erk1 and Erk2 gene targeted mice. A. Western blot analysis for phosphorylated ERK1 and ERK2 proteins from cardiac tissue extracts from wild type (wt), Erk1^{-/-}, and Erk2^{+/-} mice at baseline or after PE agonist stimulation. B. Total ERK immune kinase activity against myelin basic protein (MBP) from hearts of wildtype (Wt), Erk1^{-/-}, and Erk2^{+/-}

Chapter 4. MEK1-ERK1/2 signaling is cardioprotective.

mice after 30 min of ischemia *in vivo*, or after sham operation. C. Immune kinase assay for total ERK1/2 activity from wild type, *Erk1*^{-/-}, and *Erk2*^{+/-} hearts at baseline line or 30 minutes after PE stimulation. The kinase substrate was myelin basic protein (MBP). Similar results were observed in 2 independent experiments.

in both *Erk1*^{-/-} or *Erk2*^{+/-} hearts ($P < 0.05$). These results indicate that both *Erk1*^{-/-} and *Erk2*^{+/-} mice show a similar defect in ERK kinase activation in the heart (see discussion).

While previous studies using cell culture-based models have suggested an anti-apoptotic role for ERK MAPK signaling, such results have yet to be definitively extended to an intact animal. Here we analyzed both gain- and loss-of-function phenotypes associated ERK1/2 signaling in the heart following an acute apoptosis provoking insult within the intact heart. Specifically, *Erk1*^{-/-} and *Erk2*^{+/-} gene targeted mice underwent 60 minutes of left ventricular cardiac ischemia followed by 24 h of reperfusion to induce myocardial infarctions and cell death *in vivo*. Remarkably, *Erk2*^{+/-} mice showed a significant increase in total left ventricular infarct area normalized to area-at-risk compared to wild type controls (identical strain) or *Erk1*^{-/-} mice ($P < 0.05$)(figure 3A,C, infarct areas are white, while viable myocardium stains red). No significant difference was measured in the AAR normalized to left ventricular area, indicating that alterations in infarct size were not influenced by variations in the perfused areas between each cohort (figure 3B). These data indicate that a 50% reduction in *Erk2* gene dosage renders the myocardium more susceptible in I/R. However, loss of *Erk1* did not significantly enhance myocardial infarction susceptibility (see discussion).

Figure 3

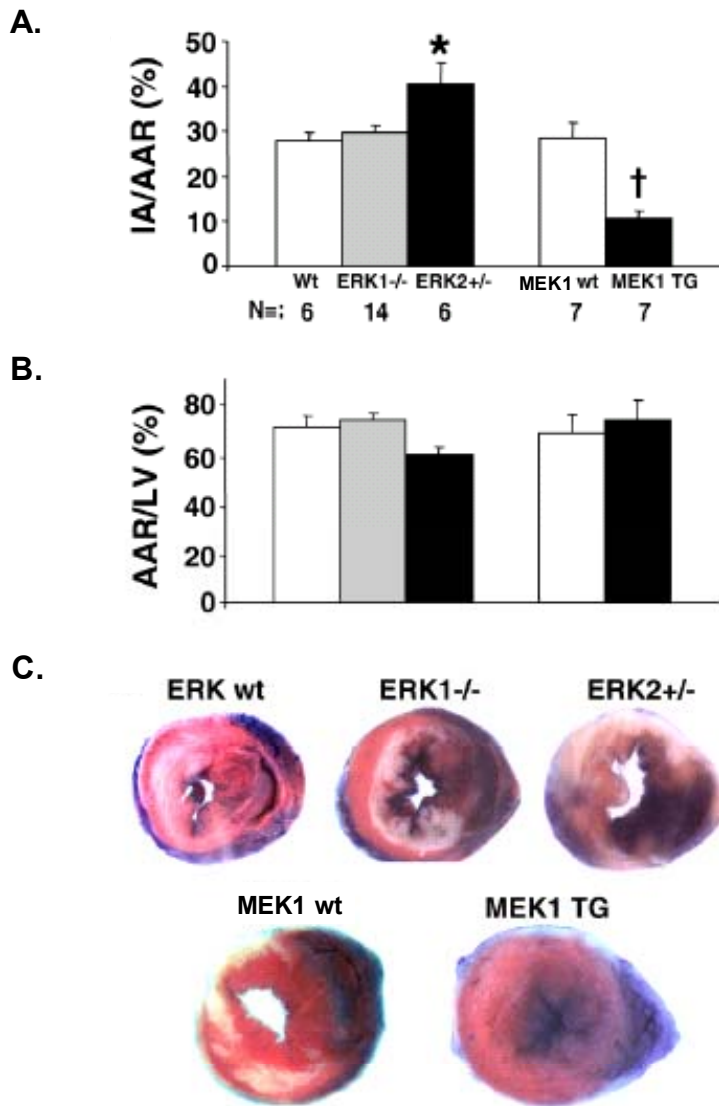


Fig. 3: Ischemia-reperfusion injury in *Erk1*^{-/-}, *Erk2*^{+/-} and MEK1 transgenic mice. A. Infarct area (IA) was normalized to the area-at-risk (AAR) by histological analysis of TTC- and Evans blue-stained heart sections from ischemia/reperfusion (I/R) injury. B. Each of the genetic models showed equivalent AARs normalized to left ventricular (LV) areas. C. Representative TTC- and Evans blue-stained heart cross-sections from each of the cohorts.

To extend the mechanistic implications between alterations in ERK activity and susceptibility to myocardial infarction, cardiac specific transgenic mice with enhanced ERK1/2 activation were analyzed. Transgenic mice expressing an activated MEK1 mutant protein in the

Chapter 4. MEK1-ERK1/2 signaling is cardioprotective.

heart were previously shown to have enhanced ERK1/2 activities, which were associated with the presentation of a mild hypertrophic response (9). MEK1 transgenic mice and non-transgenic littermate controls (FVB strain) were also subjected to ischemia/reperfusion injury and quantification of infarct area by histological staining. The data demonstrate that activated MEK1 transgenic mice, which have greater ERK1/2 activity, were significantly protected (figure 3A,C). These results indicate that enhanced ERK1/2 signaling in the heart is associated with cardioprotection following ischemia/reperfusion damage and are consistent with the observation of greater infarct areas in *Erk2*^{+/-} mice. To extend these analyses of cardiac myocyte cell death and further determine the role of apoptosis in the cardioprotective effect seen, caspase activation was also measured by direct quantification of poly (ADP-ribose) polymerase (PARP) cleavage from I/R injured hearts (figure 4). The data demonstrate that MEK1 transgenic mice were largely protected from PARP cleavage (33% less cleavage) following I/R injury, indicating less caspase activation ($P < 0.05$) (figure 4, quantification was performed from 5 individual hearts in each cohort).

Figure 4

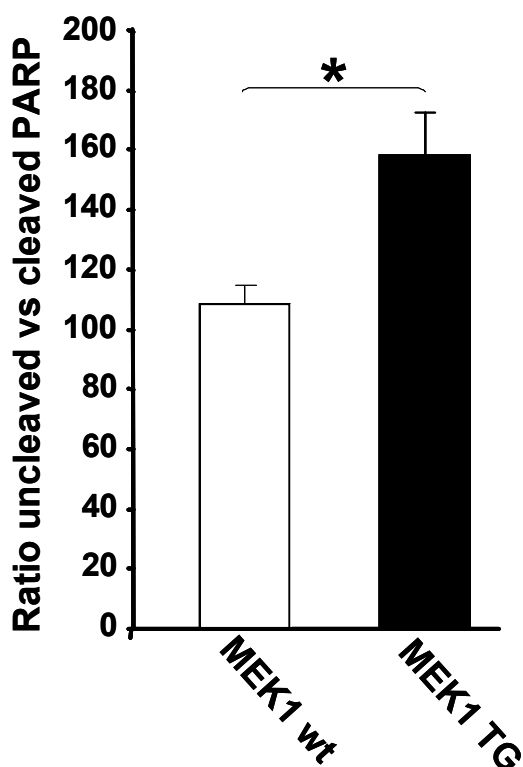


Figure 4

Apoptosis determination in MEK1 transgenic mice by PARP cleavage. Relative apoptosis amounts were investigated by poly (ADP-ribose) polymerase (PARP) cleavage determination in I/R injured hearts. MEK1 transgenic mice were largely protected from PARP cleavage (33% less cleavage) following I/R injury, indicating less caspase activation ($P < 0.05$).

Chapter 4. MEK1-ERK1/2 signaling is cardioprotective.

The role of myocardial cell apoptosis was further investigated using TUNEL and ligation-mediated PCR laddering for DNA fragmentation studies in the infarct susceptibility region of the left ventricle following ischemia and 24 hrs of reperfusion. The data demonstrate significantly reduced TUNEL and DNA laddering in MEK1 transgenic hearts compared with strain-matched controls ($P < 0.05$) (figure 6A,B; figure 8A), and significantly higher TUNEL and DNA laddering in *Erk2*^{+/-} hearts compared to strain-matched controls ($P < 0.05$) (figure 7A,B; figure 8A). These results were extended through the use of neonatal myocytes infected with recombinant adenoviruses expressing various MEK1-ERK1/2 effectors, which were subsequently treated with staurosporine (500 nM) for 18 hours to induce apoptosis. Staurosporine induced significant DNA laddering in control Adβgal-infected myocytes, which was qualitatively antagonized by expression of activated MEK1 (figure 8B). More importantly, inhibition of endogenous ERK1/2 activity with recombinant adenoviruses expressing either dominant negative MEK1 or the ERK-specific dual-specificity phosphatase MKP-3, each noticeably enhanced staurosporine-induced DNA laddering (figure 8B). MEK1 transgenic mice and their littermate controls were also subjected to thorough physiologic analysis following myocardial ischemia-reperfusion injury to correlate infarct susceptibility with functional performance. Each cohort was analyzed 7 days after ischemic injury by invasive hemodynamic assessment of left ventricular pressure and volume collected in the anesthetized mouse (Table 1). Using 90 minutes of ischemia time wild type FVB/N mice demonstrated a significant decrease in physiologic performance (Table 1). For example, cardiac output and ejection fraction were significantly depressed in non-transgenic mice compared to sham operated controls ($P < 0.05$) (figure 8A, table 1). In dramatic contrast, MEK1 transgenic mice (FVB/N) did not show a significant loss in functional performance (figure 9A, Table 1), consistent with the observed reduction in myocardial infarct size assessed by histological methods. This cardioprotective relationship is more dramatically visualized through individual pressure-volume loops collected in

Chapter 4. MEK1-ERK1/2 signaling is cardioprotective.

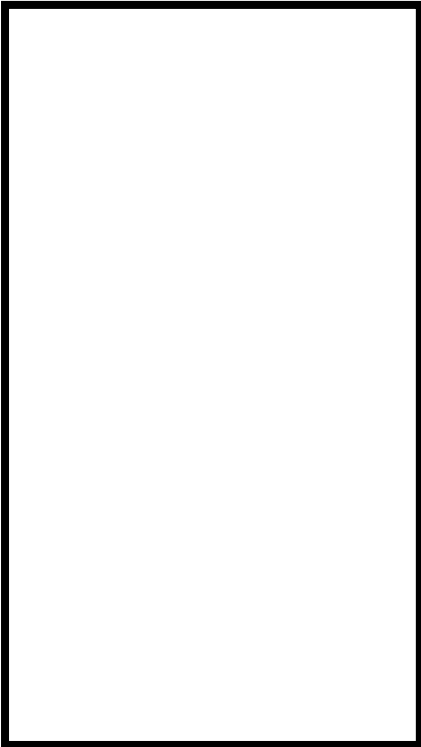


Figure 5

Detailed image of TUNEL labeling in the heart. A representative image of cardiomyocyte apoptosis as detected by TUNEL labeling (i.e. red staining) of myocyte nuclei in myofibers from an *Erk2*^{+/-} mouse.

each of the cohorts (figure 9B). Specifically, wild type mice subjected to ischemia/reperfusion damage show a rightward shift in the pressure-volume relationship during both diastole and systole (figure 9B). However, MEK1 transgenic mice showed essentially no shift in this relationship. Collectively, these data indicate that MEK1-ERK1/2 signaling protects myocardial function following ischemia/reperfusion damage.

Erk1^{-/-} and *Erk2*^{+/-} gene targeted mice were also analyzed for cardioprotection following ischemia/reperfusion injury and compared to C57Bl/6 strain-matched controls. In this series of experiments we induced less ischemia/reperfusion injury to permit evaluation of increased myocardial infarction from a given baseline level of damage. Specifically, C57Bl/6 strain-matched controls were subjected to 60 minutes of ischemia followed by 7 days of reperfusion, which induced a more nominal level of injury and dysfunction compared to the conditions used in FVB/N mice above (Table 1). Under these conditions, *Erk1*^{-/-} mice (C57Bl/6) showed no difference in function

Chapter 4. MEK1-ERK1/2 signaling is cardioprotective.

Figure 6

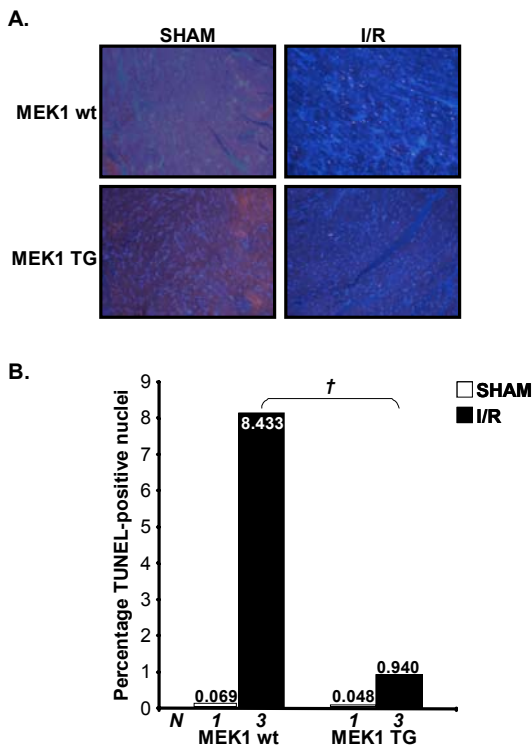


Fig. 6: Apoptosis detection by TUNEL labeling in MEK1 transgenic mice. A. Representative overview images of the apoptosis amount in the ischemic area of the myocardium 24 hours following the ischemic event. The images show the evident lower apoptosis rate in MEK1 transgenic compared to wild type littermate mice. B. Quantification of apoptosis amount shows a significant reduction in MEK1 transgenic mice following I/R injury compared to wild type littermates ($\dagger P < 0.05$). Baseline apoptosis rates in non-ischemic hearts were not different between genotypes.

Figure 7

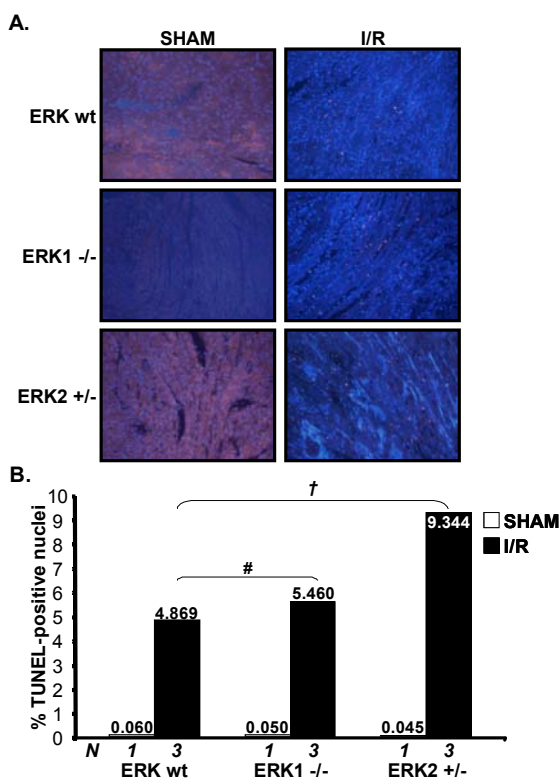


Fig. 7: Apoptosis detection by TUNEL labeling in ERK gene targeted mice. A. Representative overview images of the apoptosis amount in the ischemic area of the myocardium 24 hours following the ischemic event. The images show the evident higher apoptosis rate in *Erk2*^{+/-} compared to wild type littermates and *Erk1*^{-/-} mice. B. Quantification of apoptosis amount shows a significant increase in *Erk2*^{+/-} mice following I/R injury compared to wild type littermates ($\dagger P < 0.05$), while apoptosis amounts were not different between wild type and *Erk1*^{-/-} mice (# NS). Baseline apoptosis rates in non-ischemic hearts were not different between genotypes.

Figure 8

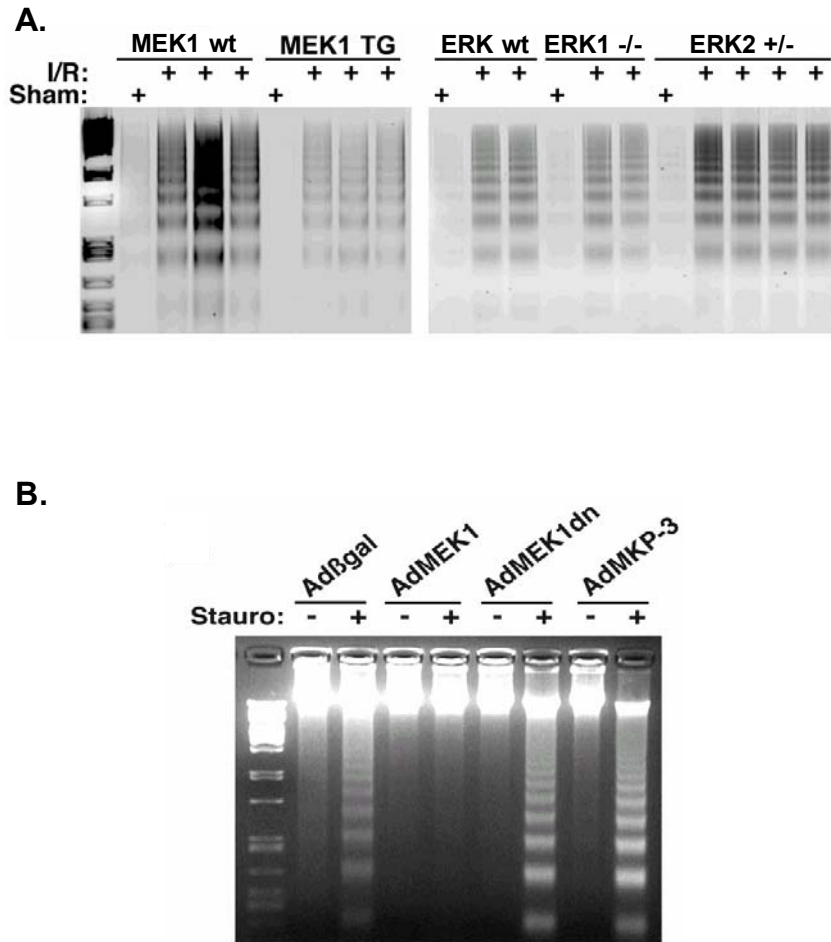


Fig. 8: Assessment of ischemia-reperfusion-induced DNA laddering in *Erk1*^{-/-}, *Erk2*^{+/-}, and MEK1 transgenic mice or cultured cardiomyocytes. A. Representative DNA laddering analysis from the left ventricle of sham mice or *Erk1*^{-/-}, *Erk2*^{+/-}, and MEK1 transgenic mice 24 h after ischemia/reperfusion injury. MEK1 transgenic mice were largely protected against I/R-induced DNA laddering, while *Erk2*^{+/-} showed enhanced DNA laddering compared to wild type mice. B. Representative DNA ladders from +/- staurosporine-treated neonatal cardiomyocytes infected with the indicated adenoviruses. Adenoviral MEK1 overexpression inhibits DNA laddering in cultured cardiomyocytes, while dominant-negative MEK1 overexpression (AdMEK1dn) pronounces apoptotic cell death as demonstrated by DNA laddering. Adenoviral overexpression of the endogenous inhibitor of MEK1 (AdMKP-3) even so pronounced DNA laddering.

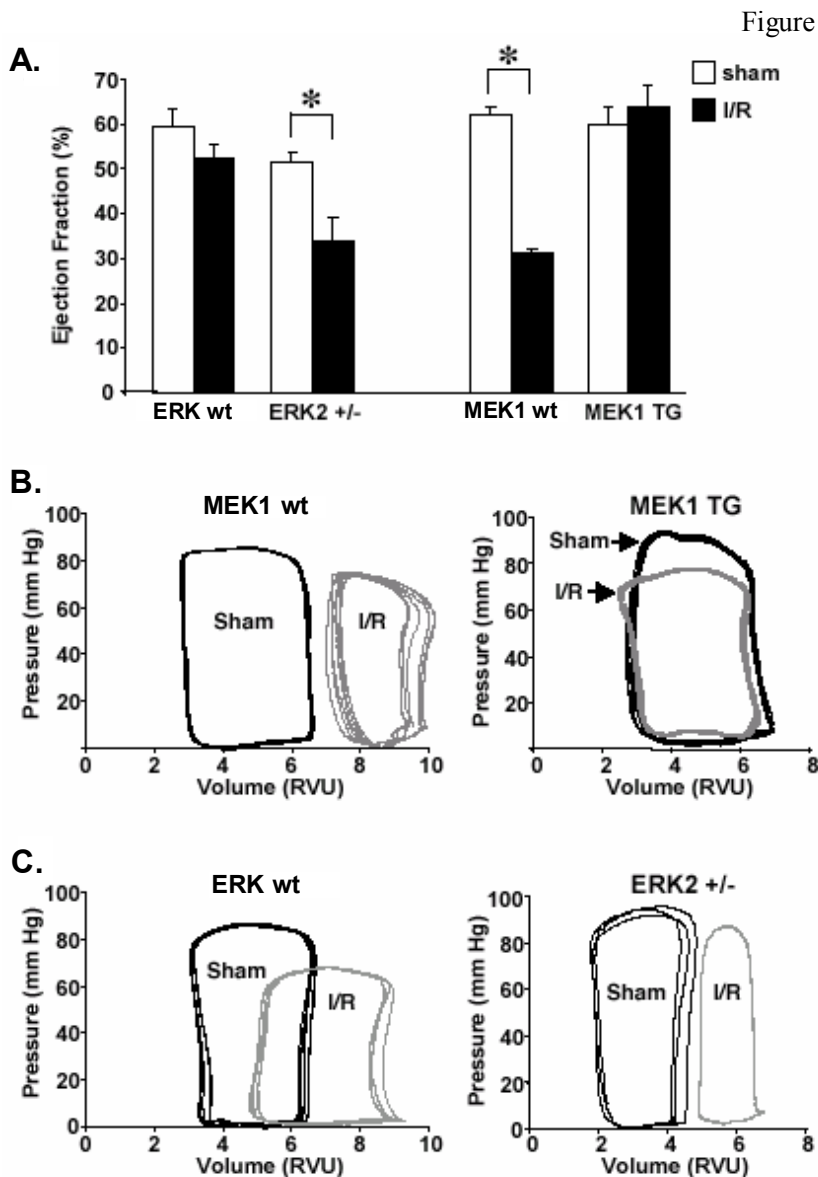


Figure 9 Fig. 9: MEK1 transgenic mice maintain functional performance following I/R injury. (A) Invasive hemodynamic functional assessment of ejection fraction was performed in wildtype versus *Erk2* heterozygous and wild type versus MEK1 transgenic mice 7 days after sham operation or ischemia/reperfusion injury (* $P < 0.05$ versus sham control). (B) Representative pressure-volume loops (PV loops) measured from MEK1 wild type and MEK1 transgenic mice 7 days after sham operation or ischemia/reperfusion injury. (C) Representative PV loops measured from ERK wild type and *Erk2* heterozygous mice.

following ischemia/reperfusion injury compared to strain-matched controls (data not shown). In dramatic contrast, *Erk2*^{+/-} mice (C57Bl/6) showed significant functional deficits following ischemia/reperfusion injury. Specifically, *Erk2*^{+/-} mice showed a greater decrease in ejection fraction and dp/dt_{max} compared to strain-matched controls, consistent with the observed increase in myocardial damage assessed by histological methods ($P < 0.05$) (figure 9A, Table 1). Analysis of individual pressure-volume loops showed a greater rightward shift in *Erk2*^{+/-} mice following ischemia/reperfusion damage compared to sham operated mice (figure 9C). Collectively, these

Chapter 4. MEK1-ERK1/2 signaling is cardioprotective.

results support the hypothesis that ERK factors are normally cytoprotective in the heart and indicate that MEK1-ERK2 signaling antagonizes cell death following acute stress stimulation in cardiac myocytes.

Table. Cardiac function measurements in sham and I/R injured mice.

	<u>MEK1 wt</u>		<u>MEK1 TG</u>	
	<u>Sham</u> n = 12	<u>I/R</u> n = 13	<u>Sham</u> n = 10	<u>I/R</u> n = 13
HR	415 ± 19	416 ± 6	449 ± 43	492 ± 12
SV	4.70 ± 0.35	2.92 ± 0.19 [‡]	3.99 ± 0.49	3.40 ± 0.13
CO	1899 ± 115	1215 ± 81 [‡]	1688 ± 160	1667 ± 66
V_{max}	7.88 ± 0.69	9.95 ± 0.54 [‡]	6.96 ± 0.63	5.59 ± 0.37
V_{min}	3.22 ± 0.42	7.15 ± 0.47 [‡]	2.80 ± 0.42	2.79 ± 0.33
ESP	75 ± 2	74 ± 3	68 ± 5	59 ± 3
EDP	7 ± 2	10 ± 2	10 ± 2	2 ± 0 [§]
dP/dt_{max}	7008 ± 497	4965 ± 329 [‡]	5726 ± 224	5660 ± 199
dP/dt_{min}	-4816 ± 361	-3300 ± 348 [‡]	-3567 ± 198	-4112 ± 160 [§]
SW	305 ± 23	166 ± 15 [‡]	230 ± 30	163 ± 12
TAU	11 ± 1	16 ± 1 [‡]	13 ± 2	9 ± 0 [§]
PHT	6 ± 0	9 ± 1 [‡]	6 ± 1	4 ± 0 [§]
EF	62 ± 2	31 ± 1 [‡]	60 ± 4	64 ± 5

	<u>ERK wt</u>		<u>Erk2 +/-</u>	
	<u>Sham</u> n = 10	<u>I/R</u> n = 9	<u>Sham</u> n = 4	<u>I/R</u> n = 3
HR	650 ± 16	587 ± 28	691 ± 20	565 ± 9 [§]
SV	3.26 ± 0.44	3.81 ± 0.23	2.30 ± 0.18	2.44 ± 0.75
CO	2121 ± 299	2227 ± 141	1595 ± 163	1390 ± 435
V_{max}	5.98 ± 0.56	7.79 ± 0.58 [‡]	4.97 ± 0.31	7.25 ± 1.62
V_{min}	2.19 ± 0.35	3.73 ± 0.58 [‡]	2.14 ± 0.05	4.49 ± 0.77 [§]
ESP	71 ± 3	64 ± 3	76 ± 3	71 ± 8
EDP	2 ± 1	2 ± 0	1 ± 1	5 ± 2
dP/dt_{max}	8176 ± 455	7381 ± 453	9720 ± 447	6366 ± 556 [§]
dP/dt_{min}	-6767 ± 373	-5792 ± 519	-8397 ± 354	-5875 ± 1067
SW	240 ± 27	240 ± 23	195 ± 19	180 ± 78
TAU	7.7 ± 0.3	8.6 ± 0.5	7.3 ± 0.1	8.7 ± 0.5 [§]
PHT	4.0 ± 0.2	4.4 ± 0.3	3.8 ± 0.1	4.8 ± 0.3 [§]
EF	59 ± 4	52 ± 3	52 ± 2	34 ± 5 [§]

Chapter 4. MEK1-ERK1/2 signaling is cardioprotective.

Invasive measurement of hemodynamic function in anesthetized MEK1 wild type mice versus littermate MEK1 transgenic mice and ERK versus littermate *Erk2*^{+/-}. Hemodynamic evaluation performed 7 days after sham and I/R surgery. HR, heart rate per minute; SV, stroke volume in μl ; CO, cardiac output $\mu\text{l}/\text{min}$; V_{max} , maximal left ventricular volume in μl ; V_{min} , minimal left ventricular volume in μl ; ESP, end systolic pressure in mmHg; EDP, end diastolic pressure in mmHg; dP/dt_{max} , maximum derivative of pressure in mmHg/sec; dP/dt_{min} , minimum derivative of pressure in mmHg/sec; SW, stroke work mmHg \cdot μl ; Tau, time constant of relaxation in msec; PHT, pressure half time in msec; EF, ejection fraction (%). $\ddagger P < 0.05$, respective wt I/R vs wt sham. $\S P < 0.05$, respective MEK1 TG sham or *Erk2*^{+/-} I/R vs MEK1 TG or *Erk2*^{+/-} sham.

Discussion

Here we analyzed genetically altered mice with both enhanced and depressed ERK activation to determine the function of this kinase effector pathway in regulating cardiomyocyte apoptosis in vivo. While previous studies have suggested the hypothesis that ERK activation can partially antagonize apoptosis, our present analysis simultaneously employed genetically altered mouse models that both represent enhanced and depressed ERK signaling in vivo. For example, although studies in cultured cardiomyocytes have shown that ERK activation is associated with anti-apoptosis, a direct cause and effect relationship was not established (4-7). Here, a direct relationship is suggested given the observation that *Erk2*^{+/-} mice are more susceptible to ischemia/reperfusion damage while activated MEK1 transgenic mice are protected. While previously MEK1 transgenic mice were shown to be partially resistant to DNA laddering following ischemia/reperfusion injury (9), here we extended these observations to show that MEK1 transgenic have smaller infarcts and maintain cardiac function following ischemia/reperfusion injury. If this analysis of MEK1 transgenic mice is considered in conjunction with the data obtained in *Erk* gene targeted mice a unified hypothesis emerges: that ERK activation regulates myocyte viability following stress stimulation.

An interesting aspect of the present study is that *Erk2* heterozygote gene-targeted mice showed enhanced myocardial injury following I/R stimulation, while *Erk1* null mice showed a level of injury equivalent to wildtype mice. This differential susceptibility to I/R injury documented between *Erk1* null and *Erk2* heterozygote gene targeted mice suggests two possible mechanisms. Quantitative western blotting indicated that ERK2 protein levels are higher than ERK1, as shown in certain other cell-types. (21) However, *Erk2* heterozygote mice showed somewhat similar reduction in total kinase activity in the heart following acute ischemia or PE injection compared with *Erk1* null mice (Fig 1C). Thus, the loss of one allele of *Erk2* appears to alter the net amount of ERK1/2

Chapter 4. MEK1-ERK1/2 signaling is cardioprotective.

activity in the heart similar to loss of both Erk1 alleles. Another more plausible mechanism is that ERK1 and ERK2 have specific functions, as suggested by the lack of compensation by Erk1 in Erk2 null mice, the latter of which die during embryonic development. (19)

Even though ERK1 and ERK2 are highly related, precedent exists for each factor having its own functional characteristics as a second potential mechanism underlying the observed differences in ischemia/reperfusion susceptibility. Indeed, ERK1 and ERK2 can undergo differential activation in response to specific stimuli or upstream effectors (22-27). Moreover, ERK1 and ERK2 proteins also prefer to homodimerize compared to cross dimerization, suggesting structural differences between these two proteins (28). Collectively, these reports suggest that ERK1 and ERK2 proteins could have slightly different intrinsic functions in the heart as an underlying mechanism of regulating cardioprotection.

The contention that ERK1/2 activation promotes cellular protection in response to apoptotic stimuli has been demonstrated in many, but not all cell types (For examples see refs (29-32)). ERK signaling has also been directly associated with cell survival in cultured cardiomyocytes or the intact heart subjected to apoptotic stimuli (7-9,33-35). A number of downstream ERK effectors have been identified including other kinases, transcription factors, and diverse regulatory proteins (21). With respect to potential anti-apoptotic regulatory factors, ERK signaling is associated with cellular protection through the downstream effectors COX-2, FLICE, heat shock protein 27 (HSP27), p90 ribosomal S6 kinase (p90rsk, also referred to as MAPKAP kinase), and Bad phosphorylation (10,11,36-39). For example, ERK1/2 can directly phosphorylate and activate p90rsk which in turn phosphorylates the pro-apoptotic factor Bad in the mitochondria resulting in cellular protection (37). ERK factors were also recently shown to interact with PKC ϵ within the mitochondria facilitating cellular protection within the context of the intact heart (17). While the overall importance of each potential downstream protective mechanism was not evaluated in our

Chapter 4. MEK1-ERK1/2 signaling is cardioprotective.

study, we did observe a prominent increase in p90^{rsk} phosphorylation in MEK1 adenoviral infected cardiomyocytes (data not shown). Regardless of the exact downstream mechanism, this report is the first to unequivocally demonstrate that MEK1-ERK signaling protects the heart from apoptotic insults. A future challenge will be to develop strategies that exploit this function of ERK1/2 signaling in the heart by tightly controlling activation to potentially benefit the myocardium during stress.

Chapter 4. MEK1-ERK1/2 signaling is cardioprotective.

Acknowledgements

D.J.L. was supported by the Journal of Experimental Biology Travelling Fellowship award, the Hein J.J. Wellens Foundation and Foundation 'de Drie Lichten'.

References

1. Garrington TP, Johnson GL. Organization and regulation of mitogen-activated protein kinase signaling pathways. *Curr Opin Cell Biol* 1999;11:211-8.
2. Widmann C, Gibson S, Jarpe MB, Johnson GL. Mitogen-activated protein kinase: conservation of a three-kinase module from yeast to human. *Physiol Rev* 1999;79:143-80.
3. Sugden PH, Clerk A. "Stress-responsive" mitogen-activated protein kinases (c-Jun N-terminal kinases and p38 mitogen-activated protein kinases) in the myocardium. *Circ Res* 1998;83:345-52.
4. Sheng Z, Knowlton K, Chen J, Hoshijima M, Brown JH, Chien KR. Cardiotrophin 1 (CT-1) inhibition of cardiac myocyte apoptosis via a mitogen-activated protein kinase-dependent pathway. Divergence from downstream CT-1 signals for myocardial cell hypertrophy. *J Biol Chem* 1997;272:5783-91.
5. Parrizas M, LeRoith D. Insulin-like growth factor-1 inhibition of apoptosis is associated with increased expression of the bcl-xL gene product. *Endocrinology* 1997;138:1355-8.
6. De Windt LJ, Lim HW, Haq S, Force T, Molkentin JD. Calcineurin promotes protein kinase C and c-Jun NH₂-terminal kinase activation in the heart. Cross-talk between cardiac hypertrophic signaling pathways. *J Biol Chem* 2000;275:13571-9.
7. Zhu W, Zou Y, Aikawa R, et al. MAPK superfamily plays an important role in daunomycin-induced apoptosis of cardiac myocytes. *Circulation* 1999;100:2100-7.
8. Yue TL, Wang C, Gu JL, et al. Inhibition of extracellular signal-regulated kinase enhances Ischemia/Reoxygenation-induced apoptosis in cultured cardiac myocytes and exaggerates reperfusion injury in isolated perfused heart. *Circ Res* 2000;86:692-9.
9. Bueno OF, De Windt LJ, Tymitz KM, et al. The MEK1-ERK1/2 signaling pathway promotes compensated cardiac hypertrophy in transgenic mice. *Embo J* 2000;19:6341-50.
10. Adderley SR, Fitzgerald DJ. Oxidative damage of cardiomyocytes is limited by extracellular regulated kinases 1/2-mediated induction of cyclooxygenase-2. *J Biol Chem* 1999;274:5038-46.
11. Yeh JH, Hsu SC, Han SH, Lai MZ. Mitogen-activated protein kinase kinase antagonized fas-associated death domain protein-mediated apoptosis by induced FLICE-inhibitory protein expression. *J Exp Med* 1998;188:1795-802.
12. Chen Z, Yuhanna IS, Galcheva-Gargova Z, Karas RH, Mendelsohn ME, Shaul PW. Estrogen receptor alpha mediates the nongenomic activation of endothelial nitric oxide synthase by estrogen. *J Clin Invest* 1999;103:401-6.
13. de Jager T, Pelzer T, Muller-Botz S, Imam A, Muck J, Neyses L. Mechanisms of estrogen receptor action in the myocardium. Rapid gene activation via the ERK1/2 pathway and serum response elements. *J Biol Chem* 2001;276:27873-80.
14. Jankowski M, Rachelska G, Donghao W, McCann SM, Gutkowska J. Estrogen receptors activate atrial natriuretic peptide in the rat heart. *Proc Natl Acad Sci U S A* 2001;98:11765-70.
15. van Eickels M, Grohe C, Cleutjens JP, Janssen BJ, Wellens HJ, Doevendans PA. 17beta-estradiol attenuates the development of pressure-overload hypertrophy. *Circulation* 2001;104:1419-23.
16. Palmén M, Daemen MJ, Bronsaer R, et al. Cardiac remodeling after myocardial infarction is impaired in IGF-1 deficient mice. *Cardiovasc Res* 2001;50:516-24.
17. Baines CP, Zhang J, Wang GW, et al. Mitochondrial PKCepsilon and MAPK form signaling modules in the murine heart: enhanced mitochondrial PKCepsilon-MAPK interactions and

Chapter 4. MEK1-ERK1/2 signaling is cardioprotective.

- differential MAPK activation in PKCepsilon-induced cardioprotection. *Circ Res* 2002;90:390-7.
18. Laemmli UK. Cleavage of structural proteins during the assembly of the head of bacteriophage T4. *Nature* 1970;227:680-5.
 19. Saba-El-Leil MK, Vella FD, Vernay B, et al. An essential function of the mitogen-activated protein kinase Erk2 in mouse trophoblast development. *EMBO Rep* 2003;4:964-8.
 20. Pages G, Guerin S, Grall D, et al. Defective thymocyte maturation in p44 MAP kinase (Erk 1) knockout mice. *Science* 1999;286:1374-7.
 21. Pearson G, Robinson F, Beers Gibson T, et al. Mitogen-activated protein (MAP) kinase pathways: regulation and physiological functions. *Endocr Rev* 2001;22:153-83.
 22. Luongo D, Mazzarella G, Della RF, Maurano F, Rossi M. Down-regulation of ERK1 and ERK2 activity during differentiation of the intestinal cell line HT-29. *Mol Cell Biochem* 2002;231:43-50.
 23. Meighan-Mantha RL, Wellstein A, Riegel AT. Differential regulation of extracellular signal-regulated kinase 1 and 2 activity during 12-O-tetradecanoylphorbol 13-acetate-induced differentiation of HL-60 cells. *Exp Cell Res* 1997;234:321-8.
 24. Kortenjann M, Thomae O, Shaw PE. Inhibition of v-raf-dependent c-fos expression and transformation by a kinase-defective mutant of the mitogen-activated protein kinase Erk2. *Mol Cell Biol* 1994;14:4815-24.
 25. Kortenjann M, Shaw PE. Raf-1 kinase and ERK2 uncoupled from mitogenic signals in rat fibroblasts. *Oncogene* 1995;11:2105-12.
 26. Mivechi NF, Giaccia AJ. Mitogen-activated protein kinase acts as a negative regulator of the heat shock response in NIH3T3 cells. *Cancer Res* 1995;55:5512-9.
 27. Schaeffer HJ, Catling AD, Eblen ST, Collier LS, Krauss A, Weber MJ. MP1: a MEK binding partner that enhances enzymatic activation of the MAP kinase cascade. *Science* 1998;281:1668-71.
 28. Hochholdinger F, Baier G, Nogalo A, Bauer B, Grunicke HH, Uberall F. Novel membrane-targeted ERK1 and ERK2 chimeras which act as dominant negative, isotype-specific mitogen-activated protein kinase inhibitors of Ras-Raf-mediated transcriptional activation of c-fos in NIH 3T3 cells. *Mol Cell Biol* 1999;19:8052-65.
 29. Holmstrom TH, Schmitz I, Soderstrom TS, et al. MAPK/ERK signaling in activated T cells inhibits CD95/Fas-mediated apoptosis downstream of DISC assembly. *Embo J* 2000;19:5418-28.
 30. Han BH, Holtzman DM. BDNF protects the neonatal brain from hypoxic-ischemic injury in vivo via the ERK pathway. *J Neurosci* 2000;20:5775-81.
 31. Tran SE, Holmstrom TH, Ahonen M, Kahari VM, Eriksson JE. MAPK/ERK overrides the apoptotic signaling from Fas, TNF, and TRAIL receptors. *J Biol Chem* 2001;276:16484-90.
 32. Shakibaei M, Schulze-Tanzil G, de Souza P, et al. Inhibition of mitogen-activated protein kinase kinase induces apoptosis of human chondrocytes. *J Biol Chem* 2001;276:13289-94.
 33. Heidkamp MC, Bayer AL, Martin JL, Samarel AM. Differential activation of mitogen-activated protein kinase cascades and apoptosis by protein kinase C epsilon and delta in neonatal rat ventricular myocytes. *Circ Res* 2001;89:882-90.
 34. Gu Y, Zou Y, Aikawa R, et al. Growth hormone signalling and apoptosis in neonatal rat cardiomyocytes. *Mol Cell Biochem* 2001;223:35-46.
 35. Mehrhof FB, Muller FU, Bergmann MW, et al. In cardiomyocyte hypoxia, insulin-like growth factor-I-induced antiapoptotic signaling requires phosphatidylinositol-3-OH-kinase-dependent and mitogen-activated protein kinase-dependent activation of the transcription factor cAMP response element-binding protein. *Circulation* 2001;104:2088-94.

Chapter 4. MEK1-ERK1/2 signaling is cardioprotective.

36. Zhu Y, Yang GY, Ahlemeyer B, et al. Transforming growth factor-beta 1 increases bad phosphorylation and protects neurons against damage. *J Neurosci* 2002;22:3898-909.
37. Bonni A, Brunet A, West AE, Datta SR, Takasu MA, Greenberg ME. Cell survival promoted by the Ras-MAPK signaling pathway by transcription-dependent and -independent mechanisms. *Science* 1999;286:1358-62.
38. Scheid MP, Schubert KM, Duronio V. Regulation of bad phosphorylation and association with Bcl-x(L) by the MAPK/Erk kinase. *J Biol Chem* 1999;274:31108-13.
39. Geum D, Son GH, Kim K. Phosphorylation-dependent cellular localization and thermoprotective role of heat shock protein 25 in hippocampal progenitor cells. *J Biol Chem* 2002;277:19913-21.

Chapter 5. The pro-survival role of Calcineurin-NFAT signaling

Calcineurin A β gene targeting predisposes the myocardium to acute stress-induced apoptosis and dysfunction

Orlando F. Bueno, Daniel J. Lips, Robert A. Kaiser, Benjamin, J. Wilkins, Yan-Shan Dai, Betty J. Glascock, Raisa Klevitsky, Timothy E. Hewett, Thomas R. Kimball, Bruce J. Aronow, Pieter A Doevendans, and Jeffery D. Molkentin

Published in *Circulation Research*, volume 94, issue 1, pages 91-9

Abstract

Cardiovascular disease is the leading cause of mortality and morbidity within the industrialized nations of the world, with coronary heart disease (CHD) accounting for as much as 66% of these deaths. Acute myocardial infarction is a typical sequelae associated with long-standing coronary heart disease resulting in large scale loss of ventricular myocardium through both apoptotic and necrotic cell death. In this study, we investigated the role that the calcium calmodulin-activated protein phosphatase calcineurin (PP2B) plays in modulating cardiac apoptosis after acute ischemia-reperfusion injury to the heart. *Calcineurin A β* gene-targeted mice showed a greater loss of viable myocardium, enhanced DNA laddering and TUNEL, and a greater loss in functional performance compared with strain-matched wild-type control mice after ischemia-reperfusion injury. RNA expression profiling was performed to uncover potential mechanisms associated with this loss of cardioprotection. Interestingly, *calcineurin A β* $-/-$ hearts were characterized by a generalized downregulation in gene expression representing approximately 6% of all genes surveyed. Consistent with this observation, nuclear factor of activated T cells (NFAT)-luciferase reporter transgenic mice showed reduced expression in *calcineurin A β* $-/-$ hearts at baseline and after ischemia-reperfusion injury. Finally, expression of an activated NFAT mutant protected cardiac myocytes from apoptotic stimuli, whereas directed inhibition of NFAT augmented cell death. These results represent the first genetic loss-of-function data showing a prosurvival role of calcineurin-NFAT signaling in the heart.

Introduction

Cardiovascular disease is the leading cause of mortality in adults in the United States where it is thought to account for approximately 12 million deaths annually. (1,2) Myocardial infarction, as well as non-ischemic forms of heart failure, are thought to involve an irreversible loss of cardiac myocytes through apoptosis or programmed cell death. (2-4) In recent years, a great body of research has focused on identifying the signaling molecules responsible for myocardial cell death or those molecules that might protect the myocardium from ischemic insults. (5) For example, numerous studies have identified signaling molecules that enhance cardiomyocyte apoptosis such as p38 α , c-Jun N-terminal kinase, tumor necrosis factor- α , p53, β -adrenergic receptors, and nitric oxide. (5-7) In contrast, other signaling pathways have been shown to protect the heart from apoptosis such as cardiotrophin-1 through the gp130 receptor, p38 β , insulin-like growth factor-1 (IGF-1), Akt/protein kinase B, protein kinase C ϵ , nitric oxide, and extracellular signal-regulated kinases 1/2. (5,6,8-12) Another potential regulator of cardiac apoptosis is the calcium-calmodulin-activated protein phosphatase calcineurin (or PP2B). Calcineurin was identified as an important regulator of cardiomyocyte hypertrophy in vivo and in vitro, while more recent investigation has suggested a role for calcineurin in the modulation of cardiomyocyte apoptosis. (13,14) Studies conducted in neurons, lymphocytes, and tumor cell lines have demonstrated either pro- or antiapoptotic effects associated with calcineurin activation. (15-22) Similarly, both pro- and antiapoptotic modulatory roles have been ascribed to calcineurin in cardiomyocytes. For example, calcineurin activation in cultured cardiac myocytes confers protection to H₂O₂- or 2-deoxyglucose-induced apoptosis, suggesting that calcineurin is cytoprotective. (14,23) Moreover, transgenic mice expressing an activated form of calcineurin in the heart are largely protected from ischemia-reperfusion-induced DNA laddering, further suggesting that calcineurin activation antagonizes cardiomyocyte apoptosis in vivo. (14) In contrast,

Chapter 5. The pro-survival role of Calcineurin-NFAT signaling

isoproterenol stimulation of cardiac β -adrenergic receptors promoted myocyte apoptosis, in part, by stimulating calcineurin activity. (24) Part of this disparity potentially stems from the dichotomous actions of the often-employed inhibitory agent cyclosporine A. For example, cyclosporine A not only inhibits calcineurin enzymatic activity, but also inhibits mitochondrial permeability pore transition (MPTP) and apoptosis through its association with cyclophilin D in the inner-mitochondrial membrane. (25) However, use of cyclosporine-independent strategies have also revealed pro- and antiapoptotic regulatory roles for calcineurin, suggesting multiple levels of complexity underlying the biology of calcineurin and cell death. Given these issues, we pursued a genetic approach to evaluate the functional significance of calcineurin as a potential modulator of ischemia-reperfusion-induced apoptosis in vivo.

Materials and Methods

Surgical Procedure and Animal Models

Mice were randomized to receive either ischemia-reperfusion injury or a sham procedure. Mice were anesthetized and placed on a warming pad maintained at 37°C. The trachea was cannulated with a polyethylene tube connected to a respirator (Harvard Apparatus) with a tidal volume of 0.6 mL (110/min). A left lateral thoracotomy was performed between the fourth and fifth ribs, pericardial tissue was removed, and the left anterior descending artery (LAD) was visualized and ligated with a slipknot of 8-0 silk. Reperfusion was initiated 60 minutes after the occlusion. The *calcineurin A β (CnA β)-/-* mouse and the NFAT-dependent luciferase reporter transgenic line (containing nine copies of an NFAT binding site upstream of a minimal promoter) were described previously. (26,27)

Measurements of Ischemic Area at Risk (AAR) and Infarct Size

Twenty-four hours after reperfusion, mice were anesthetized, the individual LADs were re-occluded, and 1 mL of 1.0% Evans blue was injected into the apex of each heart to stain non-ischemic tissue. The hearts were then excised, washed with PBS, embedded in agarose, and cut into five transverse slices for 15 minutes of incubation at room temperature with 1.5% 2,3,5-triphenyltetrazolium chloride (TTC) to measure viable myocardium (red staining). Slices were photo-graphed (each side) under a microscope and left ventricular area, AAR, and infarct area were determined by digital planimetry.

Echocardiography and Working Heart Analyses

CnA β -/- or wild-type mice were anesthetized with 2% isoflurane and hearts were visualized using a Hewlett Packard Sonos 5500 instrument and a 15-MHZ transducer. Cardiac ventricular dimensions were measured on M-mode three times for the number of animals

Chapter 5. The pro-survival role of Calcineurin-NFAT signaling

indicated. The isolated ejecting mouse heart preparation has been described in detail previously. (28)

DNA Laddering and TUNEL

CnA β *-/-* mice or wild-type controls were subjected to 60 minutes LAD occlusion and 24 hours of reperfusion to induce cardiac apoptosis for DNA laddering and 3 weeks of reperfusion for terminal deoxyribonucleotide transferase (TdT)–mediated dUTP nick-end labeling (TUNEL) assessment as previously described. (14)

Assessment of Apoptosis in Cultured Cardiac Myocytes

Conditions for generating and culturing neonatal cardiac myocytes were described previously. (14) The Ad Δ CnA and Ad Δ NFATc4 adenoviruses were described previously, (14) whereas the AdVIVIT NFAT inhibitory adenovirus was composed of the green fluorescent protein (GFP) fused to the VIVIT sequence as described previously(29) (gift of Dr Susan D. Kraner and Chris Norris, University of Kentucky, Lexington). Cardiac myocytes were treated with staurosporine (500 nmol/L) for 18 hours, and all manipulations were performed 24 hours after adenoviral infection to allow adequate protein expression. (14) DNA laddering and measurement of TUNEL were described previously. (14)

Affymetrix Gene Expression Profiling and Bioinformatics

Total RNA samples were prepared from four individual hearts from 8-week-old *CnA* β *-/-* or wild-type control mice. Biotin-labeled target cRNA was prepared from T7-transcribed cDNA made from 10 μ g of the total RNA using the Affymetrix-recommended protocol(30,31) and hybridized for expression analysis to the Affymetrix U74Av2 Gene-Chip using antibody-based fluorescence signal amplification. Data values used for filtering and

Chapter 5. The pro-survival role of Calcineurin-NFAT signaling

clustering were Signal, Signal Confidence, Absolute Call (Absent/Present), and Change (Increase, Decrease, and Unchanged) as implemented in MicroArray Suite 5.0.

Statistical Analysis

Statistical analyses between the experimental groups were performed using a Student's t-test or one-way ANOVA when comparing multiple groups. Data were reported as mean \pm SEM. Values of $P < 0.05$ were considered significant.

Results

Although conclusive evidence has emerged implicating calcineurin as a pivotal regulator of cardiac myocyte hypertrophy, its role in regulating cardiac myocyte survival or apoptosis after ischemic or stress-related injury has engendered some controversy. To more thoroughly evaluate the association between calcineurin signal transduction and cardiac survival/apoptosis, we analyzed *CnA β* ^{-/-} mice for susceptibility to ischemia-reperfusion injury. Null mice and strain-matched wild-type (wt) controls were subjected to 60 minutes of LAD coronary artery occlusion followed by 24 hours of reperfusion. After this 24-hour reperfusion period, hearts were removed and perfused with Evans blue dye, sectioned, and incubated in 1.5% TTC to quantify area at risk and area of infarct normalized to total left ventricular area (AAR/LV). The area at risk normalized to ventricular area was not different between the two groups (wt, $79.8 \pm 3.3\%$; *CnA β* ^{-/-} mice, $76.5 \pm 2.9\%$; Figure 1A). These results indicated that there were no genotype-dependent differences in the perfused areas between the two groups. In contrast, loss of viable myocardium was increased by approximately 30% in *CnA β* ^{-/-} mice compared with wt mice (wt, $31.9 \pm 3.6\%$; *CnA β* ^{-/-} mice, $46.19 \pm 3.6\%$, $N = 8$; $P < 0.05$, Figures 1B and 2C).

Figure 1

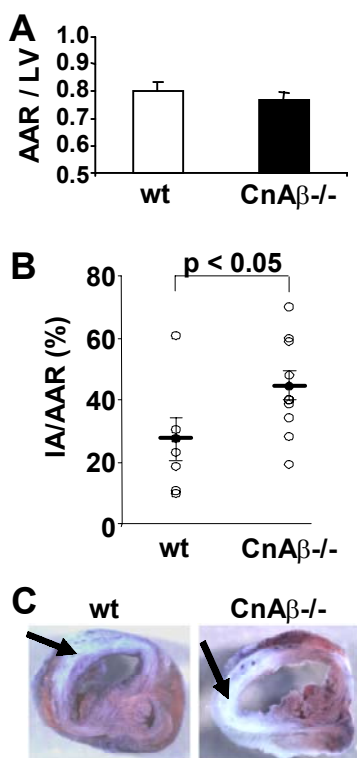
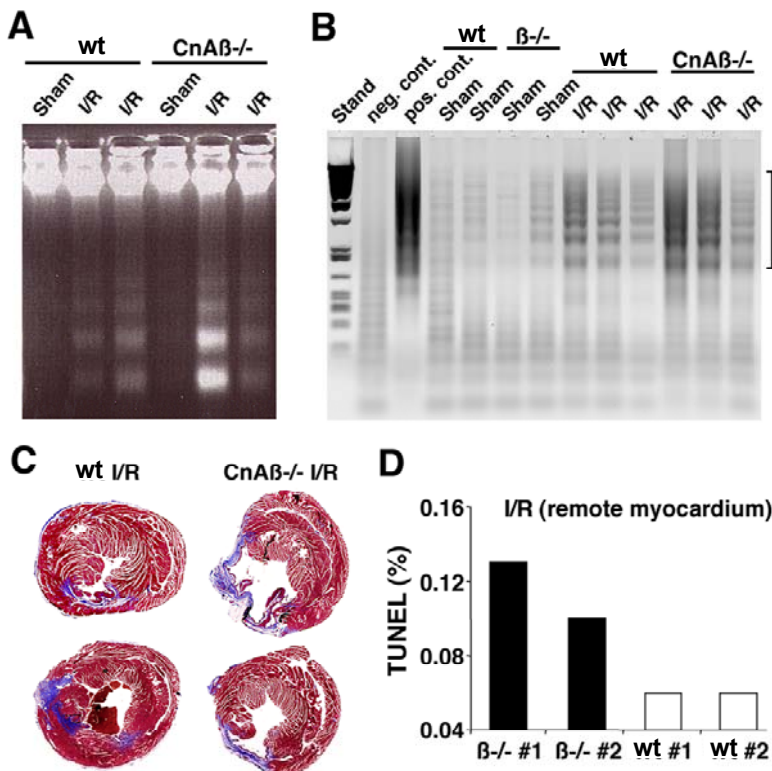


Fig. 1: *CnA β* ^{-/-} mice show greater myocardial injury following ischemia-reperfusion injury. A. Area at risk (AAR) to total left ventricular area ratios. B. Infarcted area (IA) normalized to AAR ($N = 8$; $P < 0.05$). C. Representative injured hearts from wildtype (wt) and *CnA β* ^{-/-} mice stained with Evans blue and TTC.

DNA laddering was examined by agarose gel electrophoresis using hearts from sham operated animals and mice subjected to ischemia-reperfusion injury. *CnAβ*^{-/-} mice showed a qualitative increase in the degree of DNA laddering compared with hearts from wt mice, suggestive of more apoptotic damage (*N* = 6 hearts in each group, although only two each are shown) (Figure 2A). These data were extended through along with independent assessment of DNA fragmentation by ligation-mediated polymerase chain reaction, which also showed significantly greater signal in the *CnAβ*^{-/-} hearts after ischemia-reperfusion injury (Figure 2B). Histological analysis was performed using Masson's trichrome staining (blue color shows fibrosis and scar) on myocardial tissue from wt and *CnAβ*^{-/-} mice subjected to ischemia and 3 weeks of reperfusion. Analysis of six individual hearts in each group revealed greater myocardial damage and increased interstitial fibrosis in *CnAβ*^{-/-} mice compared with wt animals (two representative hearts are shown for each group) (Figure 2C).

Figure 2a-d Figure 2



CnAβ^{-/-} mice show greater myocyte death following ischemia-reperfusion. A. Representative DNA ladder as an indication of apoptosis from wildtype (wt) and *CnAβ*^{-/-} hearts after ischemia-reperfusion injury (*N* = 6). B. Representative DNA fragmentation detection assays by ligation-mediated PCR. C. Representative histological sections showing greater scarring in *CnAβ*^{-/-} hearts after ischemia-reperfusion injury (*N* = 6). D. TUNEL quantification of cardiomyocytes in 2 *CnAβ*^{-/-} and wildtype control hearts 3 weeks after ischemic injury expressed as a percentage of total myocytes in the remaining viable myocardium.

As a more quantifiable measure of cell death, TUNEL was performed from histological sections, 3 weeks after ischemia-reperfusion injury. Rates of TUNEL in cardiac myocytes were assessed within the remaining region of viable left ventricle and septum, which demonstrated approximately twice the rate in *CnA β* ^{-/-} hearts compared with wt controls (Figure 2D). Basal TUNEL rates did not vary between wt and *CnA β* ^{-/-} hearts from sham animals (data not shown). Collectively, these results indicate that *CnA β* ^{-/-} mice undergo enhanced cell death after ischemia-reperfusion injury, suggesting that calcineurin is normally cytoprotective in the heart.

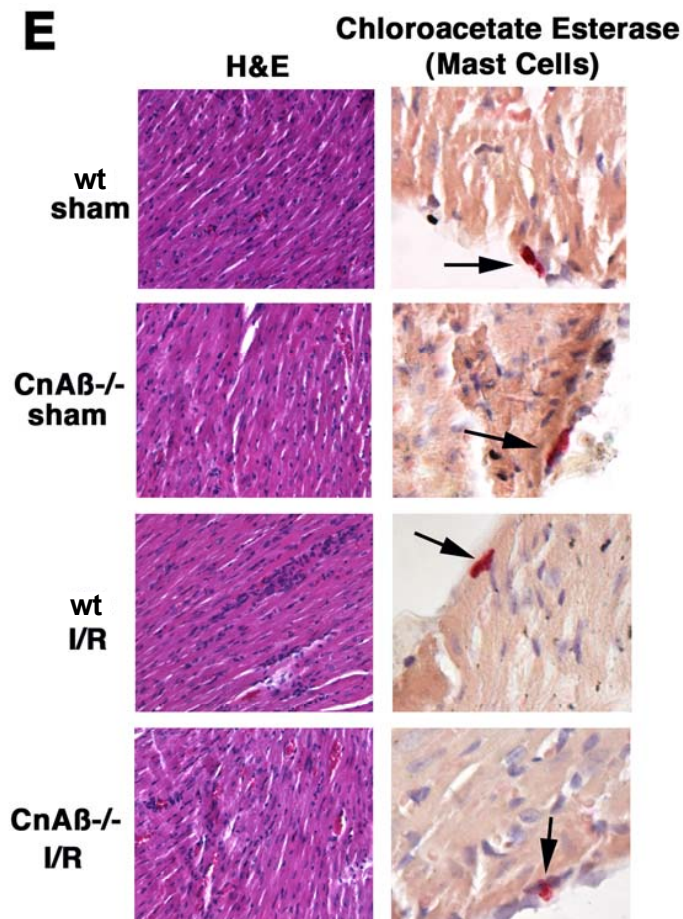


Figure 2e E. Hematoxylin and eosin- and chloroacetate esterase-stained cardiac histological sections from the indicated mice (24 hours of reperfusion; arrows show mast cells).

CnA β ^{-/-} mice have a partially compromised immune response, (26) an effect that might secondarily lessen the degree of myocardial injury, ventricular remodeling, and the inflammatory response after ischemia-reperfusion injury. In attempt to control for such

variables, cardiac histological sections were subjected to immunohistochemical analysis for CD45 (total leukocytes), CD3 (T-lymphocytes), and B220 (B-lymphocytes), which showed no differences in cellular recruitment 24 hours after ischemia-reperfusion in either group (data not shown). Histological sections were also stained with hematoxylin and eosin (H&E) and chloroacetate esterase (for mast cells) (Figure 2E). The data show similar degrees of cellularity augmentation in both groups 24 hours after ischemia-reperfusion injury (H&E sections), as well as equivalent levels of mast cells in the pericardium (Figure 2E).

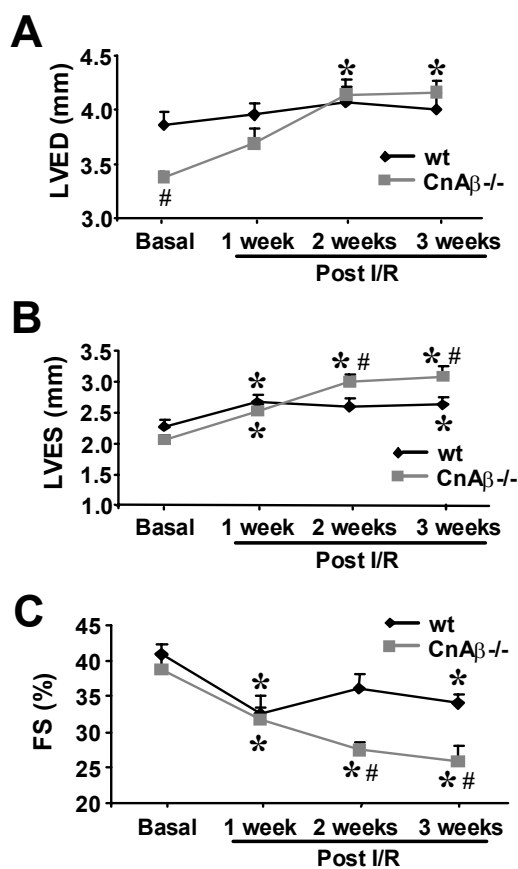


Figure 3

Figure 3

Cardiac morphology and function as determined by echocardiography. A and B. Left ventricular end-diastolic dimensions (LVED) and left ventricular end-systolic dimensions (LVES) in *CnAβ^{-/-}* mice compared to wildtype (wt) mice (*, $P < 0.05$ versus baseline; #, $P < 0.05$ versus wt after ischemia-reperfusion). Data are expressed in millimeters, average \pm SEM, $N = 9$. C. Fractional shortening assessed by echocardiography in *CnAβ^{-/-}* and wt mice (*, $P < 0.05$ versus baseline; #, $P < 0.05$ versus wt post-ischemia/reperfusion, $N = 9$). Fractional shortening was calculated as $(LVED - LVES)/LVED \times 100$ and expressed as percentage, average \pm SEM, $N = 9$.

Chapter 5. The pro-survival role of Calcineurin-NFAT signaling

At baseline, hearts from *CnA β -/-* mice functioned equivalent to wt control hearts with respect to +dP/dt, maximal left ventricular pressure developed, and time to peak pressure, each assessed by working heart preparation (Table). These results indicate that loss of *calcineurin A β* does not obviously alter cardiac function in the unstimulated state. To further evaluate the functional ramifications of enhanced cell death after ischemia-reperfusion injury, transthoracic echocardiography was performed in *CnA β -/-* mice and wt animals.

Echocardiography was performed at baseline and 1, 2, and 3 weeks after ischemia-reperfusion injury to serially evaluate function non-invasively. As shown in Figures 3A and 3B, left ventricular end-diastolic dimensions (LVED) and left ventricular end-systolic dimensions (LVES) increased to a larger extent in *CnA β -/-* mice compared with wt mice ($P < 0.05$).

These results indicate greater left ventricular dilation in the heart, presumably due to enhanced cell death in the absence of *CnA β* . More importantly, fractional shortening, which approximates cardiac contractile performance, was reduced to a greater extent in *CnA β -/-* mice compared with wt mice 2 and 3 weeks after the ischemic event ($P < 0.05$, $N = 9$; Figure 3C). These results indicate that *CnA β -/-* mice had reduced cardiac function after ischemia-reperfusion injury compared with wt controls, consistent with the notion that *CnA β -/-* hearts are more susceptible to a cell death-promoting stimulus. However, it is possible that *CnA β -/-* mice could also show alterations in function due to differences in ventricular remodeling that typifies post-infarction injury. To address this possibility, heart weight to body weight ratio assessments were performed after the final 3-week echocardiographic measurement in both groups. Neither wt nor *CnA β -/-* mice underwent significant cardiac hypertrophy over this time period under the conditions used, suggesting that the difference in functional performance likely reflects the degree of injury (data not shown).

Figure 4

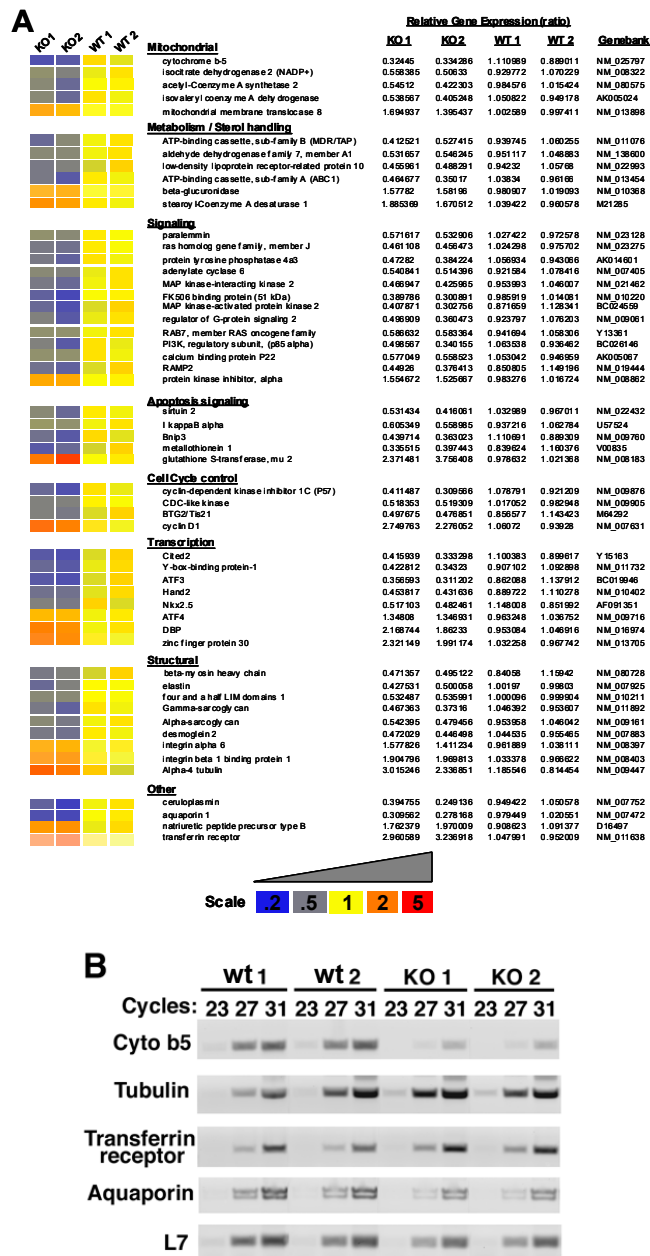


Fig. 4: Relative expression ratios of selected functional gene groups assessed from microarray screening. Cardiac RNA was collected from 2 *Cnab^{-/-}* mice (KO) and two wildtype mice (wt) and subjected to expression profiling using the Affymetrix U74Av2 array. The left panels show a color scale representation of gene expression levels, with yellow equal to 1 (no change), blue equal to 0.2 (reduced expression), and red equal to 5 (increased expression). Absolute normalized expression data are shown for each sample in the right-hand columns along with the Genebank accession number. B. Select group of genes showing altered

Chapter 5. The pro-survival role of Calcineurin-NFAT signaling

expression in the array screen was subject to a confirmatory RT-PCR analysis of expression levels at varying cycles (to show the most linear point in amplification).

The enhanced myocardial damage observed after ischemia-reperfusion injury in *CnAβ*^{-/-} mice suggested an alteration in one or more molecular pathway(s) that influences cell survival. Given the vast number of effectors that might potentially influence the survival versus apoptotic decision of myocardial cells after ischemia-reperfusion injury, we performed a large scale, unbiased screen for altered gene expression. Specifically, hearts from 8-week-old *CnAβ*^{-/-} and strain-matched wt mice (2 each) were harvested and RNA was purified for gene expression profiling using the Affymetrix U74Av2 array. This array contains all genes in the murine Unigene database that have been functionally characterized (approximately 6000) as well as an additional 6000 expressed sequence tags (ESTs). Duplicate heart samples were cross-compared between wt and *CnAβ*^{-/-} mice resulting in 5735 genes being significantly detected in one or more groups after internal normalization. Of these genes, 437 were significantly altered in expression between *CnAβ*^{-/-} and wt hearts ($P < 0.05$). The raw data shown in Figure 4 represent the 2ⁿ relationship of expression between wt and *CnAβ*^{-/-} hearts. For example, a wt value of 1.0 and a null value of 0.33 or 3.0 translates into an 8-fold change in gene expression either way. The data are also depicted on a colorimetric scale for simplicity (Figure 4A). Remarkably, 383 genes showed downregulated expression in *CnAβ*^{-/-} hearts, whereas only 54 genes showed upregulated expression. This general profile suggests that the loss of *CnAβ* reduces the expression of a subset of cardiac genes, implicating calcineurin as an important positive transcriptional effector pathway in the heart.

Expression signatures were further analyzed in *CnAβ*^{-/-} hearts to potentially implicate individual genes as phenotypic modulators. The most significantly altered genes within seven functional categories were assembled and annotated; any one of which might affect the

Chapter 5. The pro-survival role of Calcineurin-NFAT signaling

viability of cardiac myocytes after injury. An interesting alteration was identified in a select group of genes that regulate sterol/cholesterol metabolism such as ATP-binding cassette transporter ABC1, the low-density lipoprotein receptor-related protein 10, and the stearyl-coenzyme A desaturase 1 (Figure 4A). Also of interest, four cell cycle regulatory genes were significantly altered in *CnA β* *-/-* hearts, as well as five genes encoding mitochondrial-localized proteins (Figure 4A). Within the transcription category, the DNA binding factors Nkx2.5, Hand2, YB-1, and ATF-3 were each downregulated in *CnA β* *-/-* hearts, whereas ATF4 and DBP were upregulated. The observed reduction in Nkx2.5 and Hand2 expression, which themselves are important regulators of cardiac gene expression, is consistent with the proposed paradigm whereby calcineurin-NFAT signaling directly and indirectly augments expression of a subset of cardiac genes. Another intriguing pathway alteration was observed in structural genes that facilitate cellular adhesion and/or intracellular support. For example, four and a half LIM domains 1, γ -sarcoglycan, α -sarcoglycan, desmoglein-2, α -6-integrin, and α -4-tubulin each showed altered expression in the *CnA β* *-/-* heart (Figure 4A). A large number of genes that participate in cellular signaling, apoptosis signaling, or stress-responsive signaling were also identified as significantly altered in the absence of *CnA β* . Finally, a group of genes showing altered expression in the array screen were selected for reverse transcriptase polymerase chain reaction (RT-PCR) analysis at varying cycles to confirm the observed relationships (Figure 4B). The data obtained by RT-PCR showed the same profile of increased or decrease expression, confirming the reliability of the array screen (normalized to L7 expression) (Figure 4B).

The large number of candidate genes showing altered expression made it difficult to mechanistically establish which factors or pathways might ultimately underlie the observed profile of greater stress-induced cell death in the absence of *CnA β* . Despite this qualification, the overall observation that large subsets of genes are reduced in expression suggests that

Chapter 5. The pro-survival role of Calcineurin-NFAT signaling

calcineurin functions as a general transcriptional regulator in the heart, which might predispose the heart to cell death. Indeed, NFAT transcription factors are primary effectors of calcineurin signaling that could fulfill such a role (see next section).

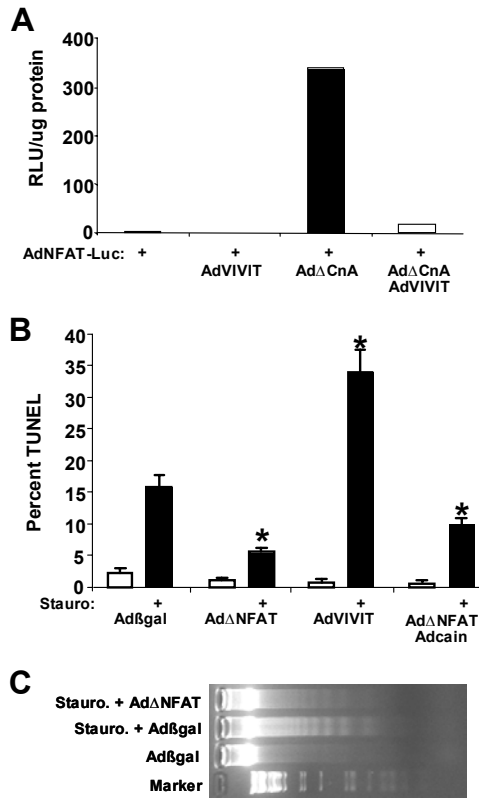


Figure 5 Fig. 5: NFAT mediates cytoprotection in the heart. A. Relative luciferase activity (RLU) derived from cultured neonatal cardiomyocytes infected with an NFAT-dependent reporter adenovirus (AdNFAT-luc) alone or in combination with AdΔCnA and/or AdVIVIT. B. TUNEL quantization in neonatal cardiomyocytes infected with the indicated adenoviruses for 24 hours, followed by staurosporine treatment for 18 hours. (* $P < 0.05$ versus Adβgal with staurosporine; $N = 3$). C. Representative DNA ladder analysis following adenoviral infection then staurosporine treatment ($N = 4$ each).

Fig. 6: Relative luciferase activity from the hearts of NFAT-luciferase reporter transgenic mice at baseline or after ischemia-reperfusion injury. These reporter mice were crossed into the $CnA\beta^{-/-}$ or $CnA\beta^{+/+}$ background ($N = 6$ and 5, respectively). Activity is shown from the whole heart (control), right ventricle (RV), non-ischemic region of the LV and septum (LV-non), and the LAD-perfused area of the LV subject to ischemia (LV-injured).

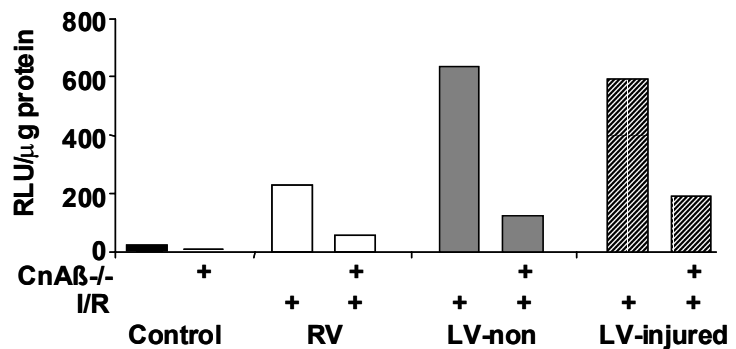


Figure 6

Chapter 5. The pro-survival role of Calcineurin-NFAT signaling

To determine the potential involvement of NFAT factors as regulators of cardiac myocyte cell survival, a neonatal cardiac myocyte culture-based model was employed. Whereas we have previously shown that calcineurin activation protects cultured myocytes from staurosporine- or 2-deoxyglucose-induced apoptosis, the necessity of NFAT factors as downstream mediators was not determined.¹⁴ To this end an NFAT-specific inhibitory adenovirus was used that expresses the VIVIT peptide as a GFP fusion. (28) The specificity of this inhibitory virus was demonstrated by co-infection with an NFAT-dependent reporter adenovirus in cultured neonatal myocytes (Figure 5A). AdVIVIT dramatically inhibited Ad Δ CnA-induced activation of the NFAT-dependent luciferase reporter. More importantly, AdVIVIT infection in neonatal cardiac myocytes augmented staurosporine-induced TUNEL, whereas expression of an activated NFATc4 truncation mutant antagonized TUNEL ($P < 0.05$; Figure 5B). Moreover, Ad Δ NFATc4 partially reduced enhanced TUNEL associated with calcineurin inhibition through Adcain infection (also see De Windt et al(14))($P < 0.05$, Figure 5B). Expression of Ad Δ NFATc4 infection also antagonized staurosporine-induced DNA laddering, further implicating NFAT factors as modulators of apoptosis itself in cardiac myocytes (Figure 5C).

The results discussed above indicate that NFAT factors can function as regulators of apoptosis in cultured cardiac myocytes. However, it was uncertain whether NFAT factors might play a similar role within the intact adult heart, downstream of calcineurin signaling. To address this issue, NFAT-luciferase reporter transgenic mice were crossed into the *CnA β* $-/-$ background and subjected to ischemia-reperfusion injury. NFAT-luciferase transgenic mice, wt for *CnA β* , were also generated from the same parental cross for direct comparison. Six *CnA β* $-/-$ and five wt controls were subjected to 60 minutes of ischemia followed by 48 hours of reperfusion injury, at which time the hearts were removed and parsed into three components for measurement of luciferase activity: right ventricle (RV), non-ischemic left

Chapter 5. The pro-survival role of Calcineurin-NFAT signaling

ventricle and septum (LV-non), and the injured area of the LV (LV-injured). The RV was analyzed to measure NFAT activity as a secondary consequence of ischemia-reperfusion injury–induced remodeling/hypertrophy. Ischemia-reperfusion injury dramatically enhanced NFAT luciferase activity in each of the assayed ventricular compartments in wt controls (Figure 6). More importantly, *CnAβ* ^{-/-} mice consistently showed less NFAT activation after injury (Figure 6). These results suggest an association between reduced NFAT transcriptional activity and diminished cardioprotection in *CnAβ* ^{-/-} mice.

Discussion

In this study, we investigated the association between the calcineurin-NFAT signaling pathway and cell death in the myocardium after stress stimulation. Loss of *CnA β* rendered the myocardium more susceptible to ischemia-reperfusion injury, suggesting that calcineurin signaling helps maintain myocyte viability in vivo. Part of the mechanism responsible for increased ischemic damage in *CnA β* $-/-$ mice is likely a secondary consequence of altered gene expression due to reduced NFAT activity.

Although calcineurin has been recognized as a central regulator of the hypertrophic growth of the myocardium, its role as an effector of myocardial cell death is more controversial. In other tissues or cell-types, calcineurin has been shown to either agonize or antagonize apoptosis after stress stimulation. Studies conducted in neurons, lymphocytes, and tumor cell lines have shown both pro- and antiapoptotic effects of calcineurin activation. (15-22) The exact decision of cytoprotection versus apoptosis is likely regulated by coordinated signals from other co-stimulated signaling pathways or depends on cell-type specific calcineurin effector/docking proteins. Indeed, calcineurin activation was shown to either induce apoptosis or to antagonize apoptosis depending on the status of p38 activation. (32) More recently, calcineurin was shown to localize to the mitochondria in fibroblasts through docking with the inhibitory protein FKBP38, resulting in Bcl-2 and Bcl-xl redistribution. (33) Calcineurin has also been implicated as a direct inducer of apoptosis in primary hippocampal neurons through dephosphorylating the proapoptotic factor Bad. (15) In addition to cell-type specific regulatory considerations, the pro- or antiapoptotic effects attributed to calcineurin have been obscured by the use of cyclosporine A, which can modulate apoptosis independent of calcineurin through direct effects on mitochondrial permeability transition pore (MPTP) formation within the inner mitochondrial membrane. (25) Given the calcineurin-independent effects associated with cyclosporine A and FK506, the use of calcineurin gene-targeted mice

Chapter 5. The pro-survival role of Calcineurin-NFAT signaling

and/or null cells derived from these mice should help elucidate the direct role that calcineurin plays in modulating cellular apoptosis in diverse tissues.

In the present study, we demonstrated that genetic disruption of the *CnA β* gene in the mouse enhanced cardiac damage induced by ischemia-reperfusion injury. This result indicates that calcineurin signaling imparts a degree of protection against cell death in the heart. Consistent with this notion, we have previously shown that transgenic mice expressing a constitutively active mutant of calcineurin in the heart are significantly protected from ischemia-reperfusion-induced cell death. (14) In cultured cardiomyocytes, adenoviral-mediated gene transfer of activated calcineurin reduced 2-deoxyglucose-induced TUNEL, whereas calcineurin inhibition with a Cain-expressing adenovirus increased TUNEL. (14) In contrast, a subsequent study reported that isoproterenol stimulation of neonatal cardiomyocytes promoted apoptosis, in part, by stimulating calcineurin activity. (24) These authors demonstrated that cyclosporine A and FK506 blocked the increase in cardiomyocyte apoptosis induced by isoproterenol stimulation and, more significantly, that transgenic mice expressing dominant-negative calcineurin in the heart were refractory to isoproterenol-induced TUNEL reactivity in vivo. These results suggest that calcineurin activation is associated with enhanced apoptosis in cardiomyocytes, in contrast to our original and subsequent observations. It is likely that the nature of the stimulus (isoproterenol) partially underlies the disparity between the two studies discussed above. For example, isoproterenol induces a prominent elevation in cAMP, which induces protein kinase A signaling and secondary alterations in inotropy, events not typically associated with ischemic injury or staurosporine stimulation.

By comparison, Kakita et al(23) recently identified an anti-apoptotic role for calcineurin activation in cardiomyocytes after endothelin-1 stimulation. Specifically, endothelin-1 stimulation protected cardiac myocytes in culture from H₂O₂-induced TUNEL

Chapter 5. The pro-survival role of Calcineurin-NFAT signaling

reactivity, DNA laddering, caspase-3 cleavage, and loss of mitochondrial membrane potential. This endothelin-1-mediated cytoprotection from H₂O₂-induced apoptosis was blocked by inhibition of calcineurin with either cyclosporine A or FK506. Collectively, these disparate accounts underscore the complexity of intracellular signaling networks within mammalian cells, such that seemingly related stress stimuli can elicit fundamentally different responses depending on the nature of the stimulus (mitochondrial- versus death receptor-mediated), the status of other parallel signaling pathways, and the context of cell-type specific calcineurin modulatory factors.

Although a large number of studies have implicated calcineurin as a modulator of cell death in varied cell types, only a few downstream mechanisms responsible for death or protection have been identified. As discussed above, calcineurin was reported to directly dephosphorylate Bad in neurons, thus enhancing apoptosis. (15) Careful evaluation of Bad phosphorylation at serine 112, 136, and 128 from the hearts of calcineurin transgenic mice or *CnAβ*^{-/-} mice failed to show any difference from controls (data not shown). Kakita et al(23) reported that calcineurin-mediated protection from H₂O₂-induced apoptosis was associated with an increase in Bcl-2 expression in cultured neonatal cardiac myocytes. However, expression levels of Bcl-2 did not change in the hearts of either calcineurin TG mice or *CnAβ*^{-/-} mice, nor was expression altered for Bcl-xl, Bad, caspase-1, -3, -8, -9, or FKBP38 (data not shown). Previously, we identified a minor but significant increase in Akt phosphorylation in the hearts of calcineurin transgenic mice. (14) However, *CnAβ*^{-/-} mice showed no difference in basal or stimulated Akt phosphorylation in the heart, ruling out this potential mechanism (data not shown). Collectively, these negative findings suggest that the classical effectors of the apoptotic response are not directly linked to calcineurin signaling in the heart.

To investigate other potential mechanisms, an unbiased array screen was performed from the hearts of *CnAβ*^{-/-} and matched wt mice. Although a number of potential regulatory

Chapter 5. The pro-survival role of Calcineurin-NFAT signaling

proteins were altered in expression, the most significant observation was the dramatic downregulation in expression of large subsets of unrelated genes (about 6% of detectable genes in the heart). This observation suggested a defect in the transcriptional potency underlying a group of genes in the hearts of *CnA β -/-* mice. This interpretation is consistent with known role of NFAT transcription factors as important effectors of calcineurin-regulated gene expression in most cell types. (34) Indeed, the full potency of calcineurin-induced hypertrophy in the heart was shown to require NFATc3 using gene-targeted mice. (35)

With respect to apoptosis signaling, we previously observed that overexpression of an activated NFATc4 in cultured neonatal cardiomyocytes partially antagonized 2-deoxyglucose-induced apoptosis. (14) Furthermore, Kakita et al (23) showed that endothelin-1-mediated protection from H₂O₂-induced apoptosis also promoted NFAT dephosphorylation. In this study, we showed that specific inhibition of NFAT with AdVIVIT augmented cardiomyocyte cell death after staurosporine treatment. More importantly, *CnA β -/-* mice showed reduced NFAT transcriptional activity in vivo after ischemia-reperfusion injury. These results are also consistent with a recent report by Izumo and colleagues (36) in which NFAT inhibition augmented cardiac myocyte apoptosis after phenylephrine stimulation in culture.

Collectively, these results discussed suggest that the homeostatic transcriptional activity of NFAT provides the necessary framework of basal gene expression that affords cardiac “health” and resistance to apoptotic stimuli. However, the exact array of downstream effectors that are regulated by NFAT factors in providing protection is not known. Despite this, the results of this study provide the first genetic data indicating that calcineurin signaling is necessary for cardiac protection and suggests that strategies to acutely agonize calcineurin might be of therapeutic benefit during or after myocardial infarction. However, this notion is in dramatic contrast to the function of calcineurin as a mediator of cardiac hypertrophy, which itself can lead to cardiomyopathy and heart failure if constitutively activated (although it is

Chapter 5. The pro-survival role of Calcineurin-NFAT signaling

apoptosis-independent). These observations suggest that calcineurin may function as a “double-edge sword,” such that transient activation antagonizes myocyte apoptosis, but long-standing activation induces cardiac hypertrophy and deleterious ventricular remodeling associated with heart failure.

Acknowledgements

This work was supported by the NIH (to J.D.M. and B.J.A.) and the Pew Charitable Trusts (J.D.M). O.F.B was supported by Post-Doctoral Fellowships from the NIH (HL10336). B.J.W. was supported by an MD/PhD scholar award from the University of Cincinnati Physician Scientist Training Program and the Albert J. Ryan Foundation.

References

1. Kannel WB. Overview of Atherosclerosis. *Clinical Ther* 1998;20:B2-17.
2. Gill C, Menstril R, Samali A. Losing heart: the role of apoptosis in heart disease-a novel therapeutic target? *FASEB J* 2002;16:135-46.
3. Guerra S, Leri A, Wang X, et al. Myocyte death in the failing human heart is gender dependent. *Circ Res* 1999;85:856-66.
4. Kang PM, Izumo S. Apoptosis and heart failure: a critical review of the literature. *Circ Res* 2000;86:1107-13.
5. Bishopric NH, Andreka P, Slepak T, Webster KA. Molecular mechanisms of apoptosis in the cardiac myocyte. *Curr Opin Pharm* 2001;1:141-50.
6. Dawn B, Bolli R. Role of nitric oxide in myocardial preconditioning. *Ann NY Acad Sci* 2002;962:18-41.
7. Aoki H, Kang PM, Hampe J, et al. Direct activation of mitochondrial apoptosis machinery by c-Jun N-terminal kinase in adult cardiac myocytes. *J Biol Chem* 2002;277:10244-50.
8. Bueno OF, Molkentin JD. Involvement of extracellular signal-regulated kinases 1/2 in cardiac hypertrophy and cell death. *Circ Res* 2002;91:776-81.
9. Matsui T, Li L, Wu JC, et al. Phenotypic spectrum caused by transgenic overexpression of activated Akt in the heart. *J Biol Chem* 2002;277:22896-901.
10. Miao W, Luo Z, Kitsis RN, Walsh K. Intracoronary, adenovirus-mediated Akt gene transfer in heart limits infarct size following ischemia-reperfusion injury in vivo. *J Mol Cell Cardiol* 2000;32:2397-402.
11. Yamashita K, Kajstura J, Discher DJ, et al. Reperfusion-activated Akt kinase prevents apoptosis in transgenic mouse hearts overexpressing insulin-like growth factor-1. *Circ Res* 2001;88:609-14.
12. Brar BK, Stephanou A, Pennica D, Latchman DS. CT-1 mediated cardioprotection against ischemic re-oxygenation injury is mediated by PI3 kinase, Akt and MEK1/2 pathways. *Cytokine* 2001;16:93-6.
13. Molkentin JD, Lu JR, Antos CL, et al. A calcineurin-dependent transcriptional pathway for cardiac hypertrophy. *Cell* 1998;93:215-28.
14. De Windt LJ, Lim HW, Taigen T, et al. Calcineurin-mediated hypertrophy protects cardiomyocytes from apoptosis in vitro and in vivo: An apoptosis-independent model of dilated heart failure. *Circ Res* 2000;86:255-63.
15. Wang HG, Pathan N, Ethell IM, et al. Ca²⁺-induced apoptosis through calcineurin dephosphorylation of BAD. *Science* 1999;284:339-43.
16. Tombal B, Weeraratna AT, Denmeade SR, Isaacs JT. Thapsigargin induces a calmodulin/calcineurin-dependent apoptotic cascade responsible for the death of prostatic cancer cells. *Prostate* 2000;43:303-17.
17. Jayaraman T, Marks AR. Calcineurin is downstream of the inositol 1,4,5-trisphosphate receptor in the apoptotic and cell growth pathways. *J Biol Chem* 2000;275:6417-20.
18. Shibasaki F, McKeon F. Calcineurin functions in Ca(2+)-activated cell death in mammalian cells. *J Cell Biol* 1995;131:735-43.
19. Zhao Y, Tozawa Y, Iseki R, Mukai M, Iwata M. Calcineurin activation protects T cells from glucocorticoid-induced apoptosis. *J Immunol* 1995;154:6346-54.
20. Asada A, Zhao Y, Kondo S, Iwata M. Induction of thymocyte apoptosis by Ca²⁺-independent protein kinase C (nPKC) activation and its regulation by calcineurin activation. *J Biol Chem* 1998;273:28392-98.
21. Ankarcrona M, Dypbukt JM, Orrenius S, Nicotera P. Calcineurin and mitochondrial function in glutamate-induced neuronal cell death. *FEBS Lett* 1996;394:321-4.

Chapter 5. The pro-survival role of Calcineurin-NFAT signaling

22. Wood AM, Bristow DR. N-methyl-D-aspartate receptor desensitisation is neuroprotective by inhibiting glutamate-induced apoptotic-like death. *J Neurochem* 1998;70:677-87.
23. Kakita T, Hasegawa K, Iwai-Kanai E, et al. Calcineurin pathway is required for endothelin-1-mediated protection against oxidant stress-induced apoptosis in cardiac myocytes. *Circ Res* 2001;88:1239-46.
24. Saito S, Hiroi Y, Zou Y, et al. beta-Adrenergic pathway induces apoptosis through calcineurin activation in cardiac myocytes. *J Biol Chem* 2000;275:34528-33.
25. Crompton M. Mitochondrial intermembrane junctional complexes and their role in cell death. *J Physiol* 2000;529.
26. Bueno OF, Brandt EB, Rothenberg ME, Molkentin JD. Defective T cell development and function in calcineurin Abeta-deficient mice. *Proc Natl Acad Sci USA* 2002;99:9398-403.
27. Braz JC, Bueno OF, Liang Q, et al. Targeted inhibition of p38 MAPK promotes hypertrophic cardiomyopathy through upregulation of calcineurin NFAT signaling. *J Clin Invest* 2003;111:1475-86.
28. Gulick J, Hewett TE, Klevitsky R, Buck SH, Moss RL, Robbins J. Transgenic remodeling of the regulatory myosin light chains in the mammalian heart. *Circ Res* 1997;80:655-64.
29. Aramburu J, Yaffe MB, Lopez-Rodriguez C, Cantley LC, Hogan PG, Rao A. Affinity driven peptide selection of an NFAT inhibitor more selective than cyclosporin A. *Science* 1999;285:2129-33.
30. Cho RJ, Huang M, Campbell MJ, et al. Transcriptional regulation and function during the human cell cycle. *Nat Genet* 2001;27:48-54.
31. Notterman DA, Alon U, Sierk AJ, Levine AJ. Transcriptional gene expression profiles of colorectal adenoma, adenocarcinoma, and normal tissue examined by oligonucleotide arrays. *Cancer Res* 2001;61:3124-30.
32. Lotem J, Kama R, Sachs L. Suppression or induction of apoptosis by opposing pathways downstream from calcium-activated calcineurin. *Proc Natl Acad Sci USA* 1999;96:12016-20.
33. Shirane M, Nakayama KI. Inherent calcineurin inhibitor FKBP38 targets Bcl-2 to mitochondria and inhibits apoptosis. *Nat Cell Biol* 2003;5:28-37.
34. Crabtree GR, Olson EN. NFAT signaling: choreographing the social lives of cells. *Cell* 2002;109:S67-79.
35. Wilkins BJ, De Windt LJ, Bueno OF, et al. Targeted disruption of NFATc3, but not NFATc4 reveals an intrinsic defect in calcineurin-mediated cardiac hypertrophic growth. *Mol Cell Biol* 2002;22:7603-13.
36. Pu WT, Ma Q, Izumo S. NFAT transcription factors are critical survival factors that inhibit cardiomyocyte apoptosis during phenylephrine stimulation in vitro. *Circ Res* 2003;92:725-31.

Chapter 6. GSK-3 β augments the apoptotic response

GSK-3 β overexpression attenuates hypertrophy and sensitizes the heart to ischemic damage and dysfunction

Daniel J. Lips, Christopher L. Antos, Rutger J. Hassink, Leon J. de Windt, Pieter A. Doevendans, Eric N. Olson.

In preparation for publication

Abstract

GSK-3 β acts as an anti-hypertrophic kinase that can interfere with calcineurin mediated signaling pathways evoked by diverse hypertrophic stimuli *in vivo*. Previously, transgenic mice overexpressing a signal resistant form of GSK-3 β (serine 9 mutated to alanine) in the heart have been generated and characterized to have a blunted hypertrophic response in response to calcineurin activation, adrenergic stimulation and pressure overload, suggesting that GSK-3 β functions as an inhibitor of hypertrophy *in vivo*. The present study was designed to elucidate the role of GSK-3 β following ischemia-reperfusion. Ischemia-reperfusion induces immediate cardiac damage through apoptotic and necrotic processes, followed by hypertrophic remodeling of the non-infarcted, viable myocardium. In transgenic animals, ischemia led to a significantly larger infarct area and subsequent worsened cardiac performance, while post-ischemic hypertrophic remodeling was blunted. Conclusively, these findings point towards a role for GSK-3 β as a dualistic signal molecule transducing both anti-hypertrophic as well as cell death promoting pathways.

Introduction

The adult myocardium responds to a variety of pathologic stimuli by hypertrophic growth that frequently progresses to heart failure. (1) In contrast to other kinases, glycogen synthase kinase-3 β (GSK-3 β) is highly active in unstimulated cells and becomes inactivated in response to mitogenic stimulation. (2,3) The activity of GSK-3 is controlled by the phosphorylation status of serine-9. Phosphorylation of this residue leads to inactivation of GSK-3 β activity by creating an inhibitory pseudosubstrate for the enzyme. (4) Conversely, dephosphorylation of this site, or mutations that prevent phosphorylation, result in activation of the kinase. Several protein kinases, including Akt/protein kinase B (PKB), have been shown to phosphorylate serine-9 of GSK-3 β in response to mitogenic signaling, thereby inactivating the enzyme. (5) GSK-3 β is also inhibited by Wntless/Wnt signaling through a mechanism independent of serine-9 phosphorylation. (6)

Cardiac-specific expression of a signal resistant form of GSK-3 β (GSK-3 β S9A) diminished hypertrophy in response to chronic β -adrenergic stimulation and pressure overload. (7) The calcium/calmodulin-dependent protein phosphatase calcineurin is a potent transducer of hypertrophic stimuli. (8) Calcineurin dephosphorylates members of the nuclear factor of activated T cell (NFAT) family of transcription factors, which results in their translocation to the nucleus and activation of calcium-dependent genes. GSK-3 β phosphorylates NFAT proteins and stimulates NFAT nuclear export leading to a diminished DNA binding ability and prevention of transcription activation (figure 1). (9) Cross-breeding of transgenic mouse lines with cardiac specific α -myosin-heavy-chain (MHC) driven overexpression of constitutively active calcineurin and GSK-3 β S9A gave significant reductions in cardiac size, prevented β -MHC expression and reduced immunostaining for nuclear NFAT. Moreover, left ventricular failure did not arise following surgical constriction of the thoracic aorta in GSK-3 β transgenic mice.

Several molecules involved in cardiac hypertrophic signaling have been implicated to promote cell survival. For instance, the MEK1-ERK1/2 signaling pathway stimulates cardiac hypertrophic growth associated with augmented cardiac function (i.e. beneficial adaptive hypertrophy) combined with partial resistance to apoptosis.(10,11) Another potent cardiac survival factor, cardiotrophin-1 (CT-1) initiates cardiac hypertrophy and is capable of inhibiting cardiomyocyte apoptosis too.(12,13) To date, the role of the calcineurin-NFAT pathway in pro- or anti-apoptotic responses is not clear. For instance, adrenergic stimulation led to calcineurin-mediated cardiomyocyte apoptosis (14), while other *in vitro* and *in vivo* studies found calcineurin mediated myocardial protection against ischemia-induced apoptosis. (15,16) It seems that NFAT nuclear import is the critical component in the regulation whether calcineurin stimulation results in the activation of pro- or antiapoptotic pathways in cardiomyocytes. (16,17) Selective NFAT inhibition during phenylephrine stimulation prevented calcineurin mediated hypertrophy but resulted in increased cardiomyocyte apoptosis. (17)

Figure 1

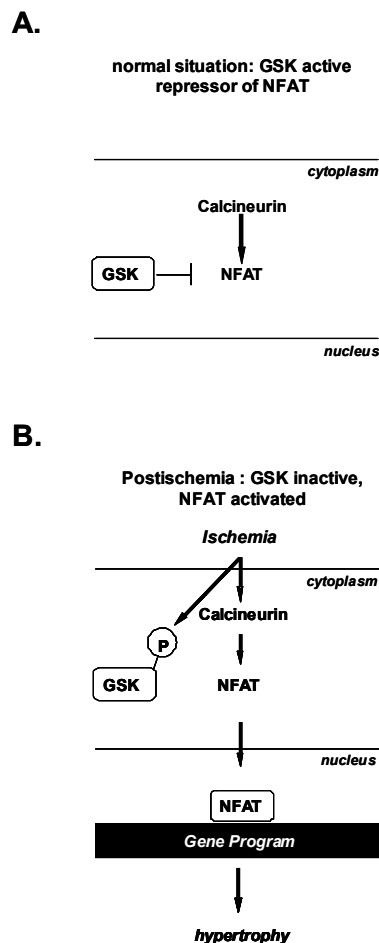


Fig. 1: Inhibition of NFAT nuclear transport by GSK-3 β . GSK-3 β is an endogenous inhibitor of the calcineurin pathway. In unstimulated cells active GSK-3 β is present. GSK-3 β phosphorylates NFAT thereby inhibiting its nuclear transport. During ischemia GSK-3 β is inactivated, and is the transcription factor NFAT able to exert its effects in the nucleus.

Chapter 6. GSK-3 β augments the apoptotic response

Previous studies have demonstrated that GSK-3 β can act as an anti-hypertrophic kinase capable of interfering with calcineurin mediated hypertrophic signals *in vivo*. (7) The present study addressed whether GSK-3 β is also involved in the acute cell death process and later hypertrophic remodeling associated with ischemia-reperfusion-induced damage of the myocardium. In addition, cardiac function was monitored by non-invasive echocardiography and invasive pressure-volume determinations. It was observed that, ischemia led to a significantly larger infarct area and subsequent worsened cardiac performance, while post-ischemic hypertrophic remodeling was blunted.

Materials and methods

Animals

For this study adult transgenic mice (GSK-3 β TG) that expressed a signal resistant form of GSK-3 β (GSK-3 β S9A) under control of the α -MHC promoter (7) and their wild type littermates (GSK-3 β wt) were used. All animals were kept under standard housing conditions with an artificial 12h light cycle with free access to standard rodent food and tap water. The animal studies were performed conform the *Guide for the Care and Use of Laboratory Animals* published by the US National Institutes of Health (NIH Publication No. 85-23, revised 1996) and were approved by the animal ethical committee of the University of Texas Southwestern Medical Center.

Murine heart ischemia- reperfusion in vivo

Adult mice (8-10 weeks) were anesthetized with isoflurane, 2% in O₂ (500 ml/min). The anterior thorax was shaved and disinfected with betadine solution. Mice were placed on a heating pad and body temperature was kept constant at 37° Celsius. A 20-gauge tube was positioned in the trachea and connected to a rodent ventilator (Minivent, Hugo Sachs Electronics, Germany) for mechanical ventilation (200 μ l, 150 strokes per minute). A left thoracotomy was performed to expose the heart and the left anterior descending artery (LAD). The LAD was ligated with 8-0 prolene (Ethicon, USA) using a slip knot placed approximately 2 mm distal from its origin. Mice were allowed to wake up. The LAD ligation was removed following 45 minutes of ischemia time, after which the hearts were allowed to reperfuse for either 24 hours or 4 weeks. Sham-operations were performed in a similar manner, but the LAD was not ligated. Myocardial infarction (MI) operation comprised of an irreversible LAD ligation.

Chapter 6. GSK-3 β augments the apoptotic response

Staining for infarct size

Following 24 hours of reperfusion mice were anesthetized with 2% isoflurane. Upon complete anesthesia the thorax was quickly opened and the 8-0 prolene ligature was retied around the LAD. A 0.5 cc insulin syringe was used to inject 0.3 ml of 2 % Evans Blue dye in the left ventricle, thereby specifically staining all of the myocardial regions except for the perfusion area distal to the LAD. The heart was removed, washed in PBS to rinse off the excess dye and embedded in 2% agarose gel. Short-axis cross sections were cut from the heart and placed in 2% 2,3,5-triphenyl-tetrazodium chloride (TTC) solution (Sigma, St. Louis, USA) at 37° Celsius for 15 minutes to stain for viable myocardium. Slices were fixed in 10% buffered formalin phosphate solution (Fisher Scientific, New Jersey, USA). The infarct area (IA) is marked by a white color and represents the actual infarcted (i.e. dead) myocardial tissue. The area-at risk (AAR) is the total area of the myocardium perfused by the LAD, which was ischemic upon LAD occlusion. The AAR has a red color in the TTC/Evans blue staining. The AAR is normalized for left ventricular area (LV) to control for measurement localization. The LV area is colored blue. Digital pictures of both sides of the sections were made and analyzed by computerized planimetry for infarct area (IA), area-at-risk (AAR) and left ventricular area (LV) with ImageJ software (Wayne Rasband, National Institutes of Health, USA).

Echocardiographic measurements

Left ventricular short-axis measurements were made with a Hewlett Packard Sonos 5500 ultra-sound machine and a 13 MHz transducer (Hewlett Packard Company, Palo Alto, USA) 3 weeks following surgery. A standoff of 0.5-1.0 cm through the use of gel-filled glove finger was used for recordings. Mice were anaesthetized with ketamine (100 mg/kg, intramuscular) and xylazine (5 mg/kg, subcutaneous). The anterior thorax was shaved

Chapter 6. GSK-3 β augments the apoptotic response

following complete anesthesia. Body temperature was maintained constant at 37° Celsius with a heating lamp.

Left ventricular in vivo pressure-volume measurements

Following 4 weeks of reperfusion mice were instrumented and anesthetized according to the ischemia-reperfusion procedure described above. The right and left external jugular veins were cannulated with PE-50 catheters for saline and drug infusion. A 1.4 French conductance-micromanometer (Millar Instruments, Houston, TX, USA) was inserted into the right common carotid artery, advanced through the aorta and positioned in the left ventricle. Correct LV placement was controlled by the combination of the online pressure and volume signal. For pressure and volume signal acquisition the MCPU-200 recording unit (Millar Instruments, Houston, TX, USA) and 8S/P Powerlab control unit (AD instruments, Australia) were used, in combination with Chart and Scope software (AD instruments, Australia). Function data analysis was performed with Circlab software (LUMC, the Netherlands).

Statistical analysis

Results are presented as means \pm SEM. Data were statistically analyzed by two-way ANOVA using SPSS 8 software (SPSS Inc., Chicago, Illinois, USA). A *P*-value < 0.05 was considered statistically significant.

Results

The amount of cell death, either necrosis or apoptosis, was assessed by the TTC/Evans Blue staining, where viable and dead tissue are distinguished (figure 2). *GSK-3 β* wt mice ($N = 3$) showed a mean IA/AAR ration of $35 \pm 9\%$, while *GSK-3 β* TG mice ($N = 3$) had an infarct area of $65 \pm 19\%$ following ischemia-reperfusion injury (figure 2). The AAR/LV ratios for both groups were similar, meaning that the localization of the area measurements could not account for differences detected. These findings indicate that GSK-3 β activity exaggerates cardiac damage following acute I/R injury.

Figure 2

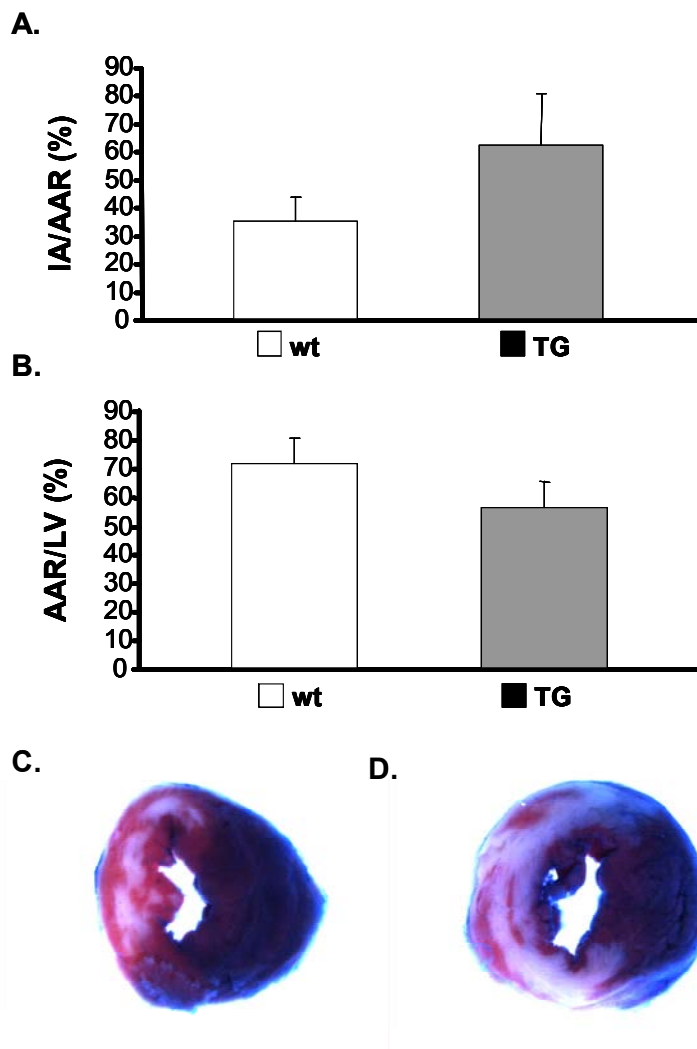


Fig. 2: Cell death following ischemia-reperfusion injury. (A) Infarct area (IA) normalized to the area-at-risk (AAR) by histological analysis of TTC- and Evans blue-stained heart sections

from ischemia-reperfusion (I/R) injury. The IA/AAR for the GSK-3 β wt ($N = 3$) and TG ($N = 3$) mice was respectively 35 and 65% ($P = 0.28$). (B) AAR was normalized to the area of the left ventricle (LV) to control for localization of measurement. Each of the genetic models showed equivalent AAR to LV ratios (wt vs TG, resp. 72 vs 56 %, not significant). (C) Representative picture of a TTC- and Evans blue -stained heart from a GSK-3 β wt mouse. (D) Representative picture of a stained heart from a GSK-3 β TG mouse.

GSK-3 β TG mice showed blunted hypertrophic growth in response to several hypertrophic stimuli in previous investigations. (7) In the present study the GSK-3 β TG mice showed attenuated hypertrophic growth compared to wildtype littermates two weeks following I/R (figure 3). Both ischemia-reperfusion (*) and myocardial infarction (†) stimulated cardiomyocyte hypertrophic growth in wildtype animals (resp. 26 and 19% growth vs sham; $P < 0.05$). GSK-3 β transgenic animals showed diminished growth (resp. 8 and 12%). No significant differences were found between sham operated GSK-3 β wt and TG animals however.

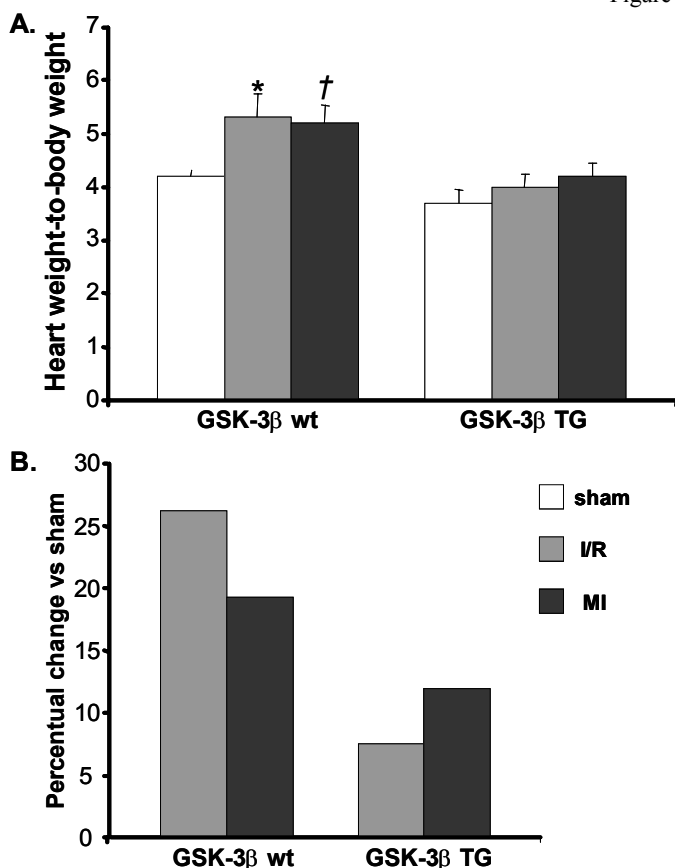


Figure 3

Fig. 3: GSK-3 β transgenic mice are resistant to hypertrophy induced by ischemia. (A) Heart weight-to-body weight analysis showed in the wildtype mice ratios for sham, ischemia-reperfusion and myocardial infarction groups of 4.2 ± 0.1 , 5.3 ± 0.5 and 5.2 ± 0.3 mg/g, respectively. In the transgenic animals values were 3.7 ± 0.2 , 4.0 ± 0.2 and 4.2 ± 0.2 mg/g. * Indicates I/R vs sham $P < 0.05$. † Indicates MI vs sham $P < 0.05$. (B) The hypertrophic growth in percentages is larger in wildtype compared to transgenic animals following both ischemia-reperfusion (26 vs 8%) and myocardial infarction (19 vs 12%).

Chapter 6. GSK-3 β augments the apoptotic response

Echocardiography was used at 2-3 weeks following the ischemic event to investigate cardiac geometry and function (figure 4). *GSK-3 β* overexpression was characterized by a HR depression in TG animals, averaging 678 ± 14 beats per minute (bpm) in the wildtype group compared to 620 ± 11 bpm in the transgenic group ($P < 0.05$). Cardiac function, defined by fractional shortening (FS) was significantly different between wt and TG mice (resp., wt $48 \pm 4\%$ vs TG $39 \pm 3\%$; $P < 0.05$). Ischemia induced several geometrical and functional alterations. Wall diameters were thicker in wildtype compared to transgenic mice (anterior wall diameter, wt 0.85 ± 0.00 mm vs TG 0.75 ± 0.00 mm; $P < 0.05$). I/R led to the most pronounced hypertrophic response as indicated by wall thickness in both wt and TG mice (posterior wall diameter, sham 0.89 ± 0.00 mm vs I/R 0.98 ± 0.00 mm vs MI 0.78 ± 0.00 mm; $P < 0.05$). In addition, the performed procedure resulted in significant differences in FS (resp., sham $53 \pm 2\%$ vs I/R $47 \pm 4\%$ vs MI $31 \pm 3\%$; $P < 0.05$). Transgenic *GSK-3 β* mice subjected to MI showed the most deteriorated cardiac function as assessed by FS, i.e. $28 \pm 4\%$.

Cardiac function by *in vivo* pressure-volume measurements was performed 4 weeks following the ischemic event (table 1). The depression in HR was also evident with this technique: HR averaged 628 ± 13 bpm in wildtype mice and 562 ± 14 bpm in transgenic *GSK-3 β* mice ($P < 0.05$). Several other statistical differences between the two genotypes were found. Cardiac output was lower in *GSK-3 β* transgenic mice (wt 1657 ± 166 rvu/min vs TG 1210 ± 88 rvu/min; $P < 0.05$), without significant differences in stroke volume (figure 5). Left ventricular relaxation was prolonged in *GSK-3 β* transgenic mice as shown by the time constant of left ventricular relaxation (Tau, τ , wt 8.9 ± 0.4 ms vs TG 10.7 ± 0.6 ms; $P < 0.05$) and pressure halftime (PHT, wt 4.7 ± 0.2 ms vs TG 6.0 ± 0.4 ms; $P < 0.05$). Analysis of the pressure-volume relationships did not reveal striking differences between genotypes (table 2).

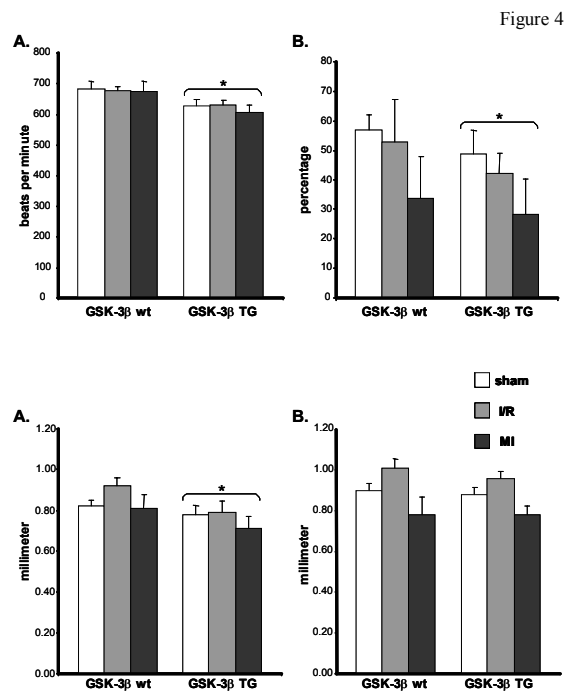


Fig. 4: Echocardiographic analysis three weeks following the ischemic event. (A) Heart rate in beats per minute (bpm). Heart rate averaged 687 bpm within the wildtype group versus 620 bpm in the transgenic group ($P < 0.05$). No differences were found between sham, I/R or MI procedures. (B) Fractional shortening in percentage. Fractional shortening averaged 48% in the wildtype group versus 39% in the transgenic group, which was statistically different ($P < 0.05$). A decline in fractional shortening is seen depending on the severity of the ischemic event (resp., sham 53% vs I/R 47% vs MI 31%; $P < 0.05$). (C) Anterior wall diameter in millimeters. Differences were seen in left ventricular anterior wall diameter three weeks after the ischemic event by echocardiographic analysis between the wildtype and transgenic groups (resp., wt 0.85 mm vs 0.75; $P < 0.05$). (D) Posterior wall diameter in centimeters. No differences were seen between the wildtype and transgenic mice groups. Statistically significant differences were found between procedures, with the largest wall diameters in I/R mice (0.98 mm) compared to the smallest diameters in MI mice (0.78 mm; $P < 0.05$).

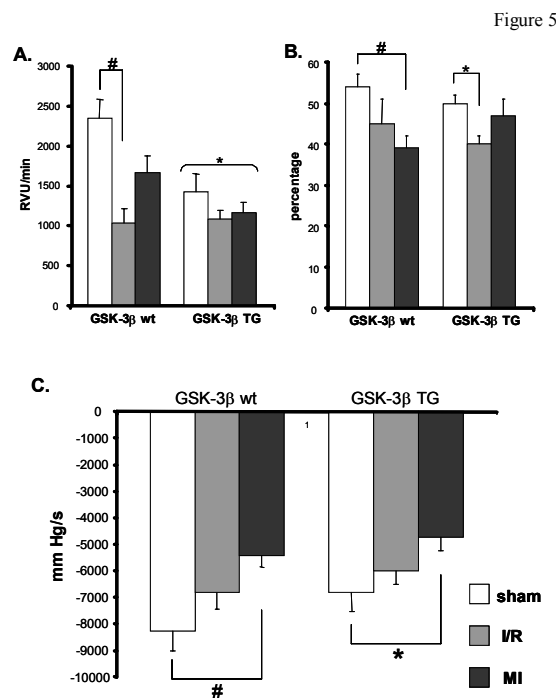


Fig. 5.: Deterioration in cardiac function following ischemia. (A) Cardiac output in relative volume units (RVU) per minute. Cardiac output decreased significantly following ischemia as determined by the *in vivo* catheterization method. # $P < 0.05$ GSK-3 β wt sham versus I/R. Also, cardiac output was lower in GSK-3 β transgenic compared to wildtype mice (resp., 1210 RVU/min vs 1657 RVU/min). (B) Ejection fraction in percentage. Ejection fraction deteriorated following ischemia. # $P < 0.05$ GSK-3 β wt sham versus MI, * $P < 0.05$ GSK-3 β TG sham versus I/R. (C) Minimal first derivative of left ventricular pressure in mm Hg/s. The functional parameter dP/dt_{MIN} deteriorated significantly depending on the severity of the ischemic event. # $P < 0.05$ GSK-3 β wt sham versus MI, * $P < 0.05$ GSK-3 β TG sham versus MI.

Several parameters of cardiac function were significantly altered depending on the performed surgical procedure (table 1, figure 5). Stroke volume (SV) and cardiac output (CO), for instance, were highest in sham animals and lowest in I/R mice (sham 3.18 ± 0.29 rvu vs I/R

1.87 \pm 0.20 rvu vs MI 2.39 \pm 0.20 rvu; $P < 0.05$). Moreover, ischemia-reperfusion groups consistently showed low cardiac performance as assessed by stroke work, ejection fraction and pressure-volume area. Pressure-volume analysis revealed similar differences in preload-recruitable stroke work (PRSW, sham 59 \pm 5 mm Hg/rvu vs 36 \pm 3 mm Hg/rvu vs 37 \pm 4 mm Hg/rvu; $P < 0.05$). The minimal first derivative of left ventricular pressure (dP/dt_{MIN}) was the only parameter completely depending on the severity of the ischemic event (sham -7635 \pm 533 mm Hg/s vs I/R -6432 \pm 416 mm Hg/s vs MI -4981 \pm 373 mm Hg/s; $P < 0.05$; figure 5). The arterial-ventricular coupling ratios (Ea/Ees) equaled 1 in both sham groups reflecting maximal performed left ventricular stroke work (SW). However, upon ischemic damage the coupling ratios deviated from 1, rising up to 1.70 (figure 6). The rise of the coupling ratios depended on the increase of arterial elastance (Ea) in the ischemia study groups, because the slope of the ESPVR lines remained on sham level. Left ventricular mechanical efficiency was found to be depressed also upon ischemia. Left ventricular mechanical efficiency, defined by the ratio between SW and pressure-volume area (PVA), was 0.74 \pm 0.02 in sham, 0.61 \pm 0.02 in ischemia-reperfusion and 0.71 \pm 0.02 in MI mice ($P < 0.05$).

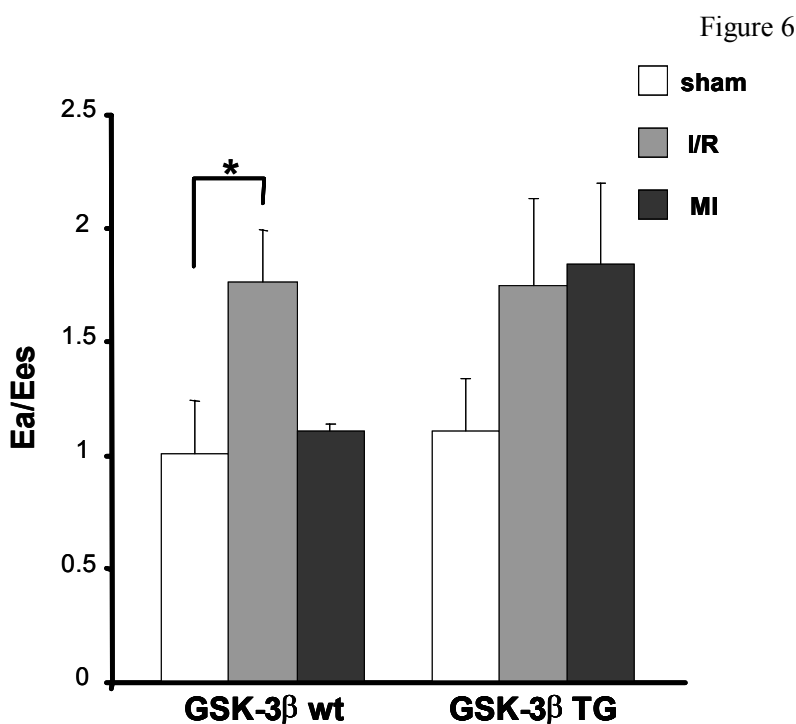


Fig. 6: Arterial-ventricular coupling mismatch following ischemia. The Ea/Ees ratio deviates from 1 following ischemia, indicating a mismatch between arterial and ventricular elastance which results in submaximal left ventricular stroke work. In contrast to the GSK-3 β transgenic mice, the Ea/Ees ratio is significantly augmented between sham and I/R GSK-3 β wildtype mice. The myocardial infarction groups are not incorporated in the analysis because of the low number of animals ($N = 2$) in the studygroups. * $P < 0.05$ GSK-3 β wt sham versus I/R.

Representative pressure-volume loops for all experimental groups are depicted in figure 7. Ischemia led to a decline in cardiac function reflected by a rightward shift of the PV-loops, decreased stroke volume and ejection fraction, and attenuated pressure in both genotypes.

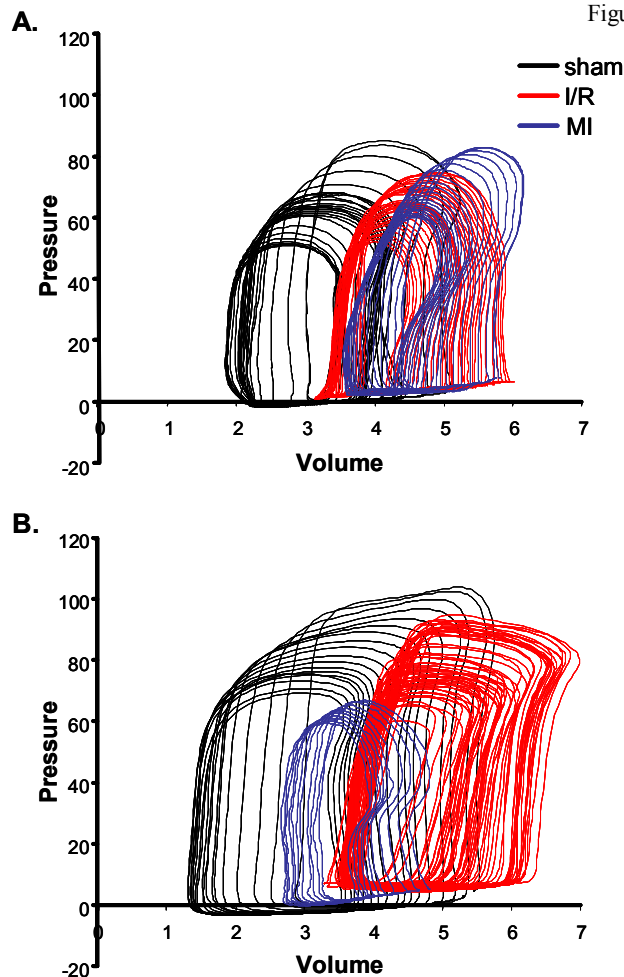


Figure 7

Fig. 7: Cardiac function expressed by pressure-volume loops. (A) PV-loops measured in sham (black line), ischemia-reperfusion (red line) and myocardial infarction (blue line) GSK-3 β wildtype mice. Ischemia leads to a rightward shift of the PV-loops, decreased stroke volume and ejection fraction, and diminished pressure. (B) PV-loops measured in GSK-3 β transgenic mice. Function decline following ischemia is detected by the rightward shift on the volume-axis, the decreased stroke volume and ejection fraction, and lower pressure.

Discussion

In *GSK-3 β* mice ischemia-reperfusion led to an 85% enlargement of the infarct areas compared to wildtype littermates. Hypertrophic growth was attenuated in transgenic animals following I/R. Finally, following ischemia cardiac functional deterioration was more pronounced in *GSK-3 β* transgenic mice than in wildtype mice.

GSK-3 β acts as an antihypertrophic kinase known to interfere with hypertrophic stimuli, such as chronic β -adrenergic stimulation and pressure-overload. The present paper demonstrates the antihypertrophic effect of GSK-3 β overexpression following myocardial ischemia. Several cellular targets of GSK-3 β have been associated with hypertrophic growth. For instance, GSK-3 β is capable of inhibiting c-jun, a prohypertrophic transcription factor and target of the mitogen-activated protein kinase JNK. (18,19) Other targets as c-myc, cyclin D1, glycogen synthase and eukaryotic initiation factor 2B could all be involved in the process of cardiomyocyte hypertrophy. (20,21) However, GSK-3 β prevents hypertrophic growth predominantly by inhibiting NFAT nuclear transport, as NFAT nuclear transport is sufficient to provoke hypertrophic cell growth. (7,8)

The pro-apoptotic effect of GSK-3 β in response to ischemia-reperfusion injury could be explained by the inhibitory effect of GSK-3 β on the cell-survival calcineurin-NFAT pathway. NFAT nuclear transport appears to be the critical determinant in the anti-apoptotic effect of the calcineurin pathway. (16,17) The direct effect of GSK-3 β overexpression on NFAT activity could be the explanation for the myocardial infarction enlargement following ischemia in the studied transgenic mice. However, as shown by the study of De Windt et al. is the calcineurin-NFAT pathway only partly capable of inhibiting apoptosis. (15)

The mechanism whereby calcineurin affords protection from apoptosis is partially mediated by calcineurin-NFAT signaling and partially by phosphatidylinositol 3-kinase

Chapter 6. GSK-3 β augments the apoptotic response

(PI3K) signaling. (15) PIK3 is involved in both hypertrophic (22,23) and anti-apoptotic processes (24,25). Downstream target for PI3K is Akt/protein kinase B (PKB.) Akt/PKB is capable of phosphorylating BAD and thereby inhibiting the cytochrome C mediated apoptosis pathway. (26,27) Another downstream target of Akt/PKB is GSK-3 β . Many stimuli that activate PI3K inhibit GSK-3 β through Akt/PKB. (3,28) GSK-3 β is inactivated by Akt/PKB through phosphorylation. Inhibition of Akt/PKB and subsequent activation of GSK-3 β leads to the promotion of apoptosis (29), while on the other hand activation of Akt/PKB prevents GSK-3 β mediated apoptosis (30).

Another cellular target of Akt/PKB and active GSK-3 β is NF- κ B. (31) Activation of the transcription factor NF- κ B induces gene transcription programs involved in the myocardial protection against ischemia. (32) GSK-3 β acts as a negative regulator of NF- κ B activity during apoptosis suggesting that the pro-apoptotic effects of active GSK-3 β may be mediated at least in part through the inhibition of NF- κ B pathway. (33,34) Interestingly, NF- κ B activity is partly under the control of calcineurin. Stress-induced activation of NF- κ B involves inactivation of I- κ B β through calcineurin-mediated dephosphorylation. (35,36)

Most other transcription factors that are negatively regulated by active GSK-3 β , thoroughly reviewed by Hardt (3), are involved in processes of apoptosis prevention and cell proliferation.

Overexpression of a constitutively active GSK-3 β protein would theoretically result in the stimulation of apoptosis because of the fact that the protein is catalytically active in cells even under unstimulated conditions as was found in astrocytes. (34) However, unstimulated rates of apoptosis were not found to be augmented in the hearts of the *GSK-3 β* transgenic mice.

Until now, a hemodynamic assessment to elucidate the effects of GSK-3 β activity on plain cardiac function had not been performed. Cardiac performance was assessed by echocardiography and *in vivo* pressure-volume measurements to evaluate the differences in genotype. Cardiac function in the *GSK-3 β* transgenic mice was characterized by attenuated heart rate and cardiac output in comparison to wildtype mice at baseline in both echocardiographic and pressure-volume measurements without a known cause. Although a decrease in cardiac output could reflect the pathological state of heart failure, the survival curve of unstimulated *GSK-3 β* transgenic mice is not significantly different compared to their wildtype littermates. Mice overexpressing Akt specifically in the heart demonstrated enhanced contractile parameters. (37) Those mice showed heightened levels of inactive phosphorylated GSK-3 β . Left ventricular catheterization revealed furthermore a relatively slower diastolic relaxation in unstimulated transgenic animals as assessed by the time constant τ and pressure halftime. Ischemia or other causes of myocardial depression are frequently the cause of attenuation in the rate of left ventricular pressure decline. However, without the presence of other indications of cardiac dysfunction at baseline, for instance within the pressure-volume relationships, the prolongation of τ is probably purely depending on the low heart rate in *GSK-3 β* transgenic mice.

Cardiac performance was also analyzed for the effects of ischemia-reperfusion and myocardial infarction on specific parameters. Comparable functional decrements were seen in wildtype and transgenic animals. Ischemia-reperfusion and myocardial infarction showed alternatively the worst attenuation in cardiac performance. Cardiac output and left ventricular ejection fraction decreased significantly indicating worsening of cardiac performance. No differences were seen in the pressure-volume relationships. However, ischemia led to an arterial-ventricular coupling mismatch and attenuation of left ventricular mechanical

efficiency. Augmented vascular resistance associated with altered arterial compliance is the consequence of these effects. (38)

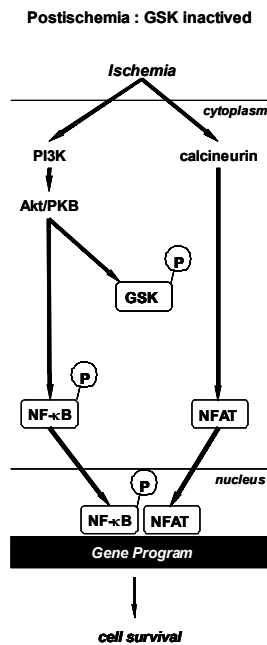


Figure 8

Fig. 8: Proposed mechanisms of the pro-apoptotic effects of GSK-3 β . Active GSK-3 β inhibits the anti-apoptotic effects of the transcription factors NFAT and NF- κ B (dashed lines). Upon stimulation of PI3K by an ischemic stimulus GSK-3 β is inactivated through phosphorylation by Akt/PKB (straight lines). Akt/PKB itself stimulates NF- κ B activity and concomitantly cell survival gene programs. Inactive GSK-3 β has no inhibitory effect on the calcineurin-NFAT pathway, also promoting cell survival.

The present study evidently showed the ischemia-induced proapoptotic effect of GSK-3 β in cardiomyocytes. Ischemia led to an enlargement of the infarct area and subsequent decrease in cardiac performance in transgenic animals, while the hypertrophic response following ischemia was blunted. GSK-3 β acts as a central modifier in antihypertrophic and proapoptotic signaling pathways. Future research should be performed to elucidate the possible clinical value of GSK-3 β in cardiac hypertrophy and ischemia.

Chapter 6. GSK-3 β augments the apoptotic response

Acknowledgements

D.J.L was supported by the Hein JJ Wellens Foundation, Maastricht, The Netherlands.

References

1. Lips DJ, Van Kraaij DL, De Windt LJ, Doevendans PA. Molecular determinants of myocardial hypertrophy and failure: alternative pathways for beneficial and maladaptive hypertrophy. *Eur Heart J* 2003;24:883-896.
2. Cohen P, Frame S. The renaissance of GSK3. *Nat Rev Mol Cell Biol* 2001;2:769-76.
3. Hardt SE, Sadoshima J. Glycogen synthase kinase-3 β : a novel regulator of cardiac hypertrophy and development. *Circ Res* 2002;90:1055-63.
4. Dajani R, Fraser E, Roe SM, et al. Crystal structure of glycogen synthase kinase 3 β : structural basis for phosphate-primed substrate specificity and autoinhibition. *Cell* 2001;105:721-32.
5. Cross DA, Alessi DR, Cohen P, Andjelkovich M, Hemmings BA. Inhibition of glycogen synthase kinase-3 by insulin mediated by protein kinase B. *Nature* 1995;378:785-9.
6. van Es JH, Barker N, Clevers H. You Wnt some, you lose some: oncogenes in the Wnt signaling pathway. *Curr Opin Genet Dev* 2003;13:28-33.
7. Antos CL, McKinsey TA, Frey N, et al. Activated glycogen synthase-3 β suppresses cardiac hypertrophy in vivo. *Proc Natl Acad Sci U S A* 2002;99:907-12.
8. Molkentin JD, Lu JR, Antos CL, et al. A calcineurin-dependent transcriptional pathway for cardiac hypertrophy. *Cell* 1998;93:215-28.
9. Neal JW, Clipstone NA. Glycogen synthase kinase-3 inhibits the DNA binding activity of NFATc. *J Biol Chem* 2000;276:3666-73.
10. Lips DJ, Bueno OF, Wilkins BJ, et al. The MEK1-ERK2 signaling pathway protects the myocardium from ischemic damage in vivo. Submitted 2003.
11. Bueno OF, Molkentin JD. Involvement of extracellular signal-regulated kinases 1/2 in cardiac hypertrophy and cell death. *Circ Res* 2002;91:776-81.
12. Pennica D, King KL, Shaw KJ, et al. Expression cloning of cardiotrophin 1, a cytokine that induces cardiac myocyte hypertrophy. *Proc Natl Acad Sci U S A* 1995;92:1142-6.
13. Sheng Z, Knowlton K, Chen J, Hoshijima M, Brown JH, Chien KR. Cardiotrophin 1 (CT-1) inhibition of cardiac myocyte apoptosis via a mitogen-activated protein kinase-dependent pathway. Divergence from downstream CT-1 signals for myocardial cell hypertrophy. *J Biol Chem* 1997;272:5783-91.
14. Saito S, Hiroi Y, Zou Y, et al. beta-Adrenergic pathway induces apoptosis through calcineurin activation in cardiac myocytes. *J Biol Chem* 2000;275:34528-33.
15. De Windt LJ, Lim HW, Taigen T, et al. Calcineurin-mediated hypertrophy protects cardiomyocytes from apoptosis in vitro and in vivo: An apoptosis-independent model of dilated heart failure. *Circ Res* 2000;86:255-63.
16. Bueno OF, Lips DJ, Kaiser RA, et al. Calcineurin Abeta gene targeting predisposes the myocardium to stress-induced apoptosis and dysfunction. *Circ Res*. 2003 Nov 13 [Epub ahead of print] 2003.
17. Pu WT, Ma Q, Izumo S. NFAT transcription factors are critical survival factors that inhibit cardiomyocyte apoptosis during phenylephrine stimulation in vitro. *Circ Res* 2003;92:725-31.

18. Sugden PH, Clerk A. "Stress-responsive" mitogen-activated protein kinases (c-Jun N-terminal kinases and p38 mitogen-activated protein kinases) in the myocardium. *Circ Res* 1998;83:345-52.
19. Boyle WJ, Smeal T, Defize LH, et al. Activation of protein kinase C decreases phosphorylation of c-Jun at sites that negatively regulate its DNA-binding activity. *Cell* 1991;64:573-84.
20. Sadoshima J, Aoki H, Izumo S. Angiotensin II and serum differentially regulate expression of cyclins, activity of cyclin-dependent kinases, and phosphorylation of retinoblastoma gene product in neonatal cardiac myocytes. *Circ Res* 1997;80:228-41.
21. Starksen NF, Simpson PC, Bishopric N, et al. Cardiac myocyte hypertrophy is associated with c-myc protooncogene expression. *Proc Natl Acad Sci U S A* 1986;83:8348-50.
22. Esposito G, Rapacciuolo A, Naga Prasad SV, et al. Genetic alterations that inhibit in vivo pressure-overload hypertrophy prevent cardiac dysfunction despite increased wall stress. *Circulation* 2002;105:85-92.
23. Schluter KD, Goldberg Y, Taimor G, Schafer M, Piper HM. Role of phosphatidylinositol 3-kinase activation in the hypertrophic growth of adult ventricular cardiomyocytes. *Cardiovasc Res* 1998;40(1):174-81:174-81.
24. Kuwahara K, Saito Y, Kishimoto I, et al. Cardiotrophin-1 phosphorylates akt and BAD, and prolongs cell survival via a PI3K-dependent pathway in cardiac myocytes. *J Mol Cell Cardiol* 2000;32(8):1385-94:1385-94.
25. Wu W, Lee WL, Wu YY, et al. Expression of constitutively active phosphatidylinositol 3-kinase inhibits activation of caspase 3 and apoptosis of cardiac muscle cells. *J Biol Chem* 2000;275:40113-9.
26. Datta SR, Dudek H, Tao X, et al. Akt phosphorylation of BAD couples survival signals to the cell-intrinsic death machinery. *Cell* 1997;91:231-41.
27. del Peso L, Gonzalez-Garcia M, Page C, Herrera R, Nunez G. Interleukin-3-induced phosphorylation of BAD through the protein kinase Akt. *Science* 1997;278:687-9.
28. Morisco C, Zebrowski D, Condorelli G, Tschlis P, Vatner SF, Sadoshima J. The Akt-glycogen synthase kinase 3 β pathway regulates transcription of atrial natriuretic factor induced by beta-adrenergic receptor stimulation in cardiac myocytes. *J Biol Chem* 2000;275:14466-75.
29. Troussard AA, Mawji NM, Ong C, Mui A, St -Arnaud R, Dedhar S. Conditional knock-out of integrin-linked kinase demonstrates an essential role in protein kinase B/Akt activation. *J Biol Chem* 2003;278:22374-8.
30. Zhang HM, Yuan J, Cheung P, et al. Over-expression of interferon-gamma -inducible GTPase inhibits coxsackievirus B3-induced apoptosis Through the activation of the PI3-K/Akt pathway and inhibition of viral replication. *J Biol Chem* 2003;Epub ahead of print.
31. Hoeflich KP, Luo J, Rubie EA, Tsao MS, Jin O, Woodgett JR. Requirement for glycogen synthase kinase-3 β in cell survival and NF-kappaB activation. *Nature* 2000;406:86-90.
32. Valen G, Yan ZQ, Hansson GK. Nuclear factor kappa-B and the heart. *J Am Coll Cardiol* 2001;38:307-14.

Chapter 6. GSK-3 β augments the apoptotic response

33. Bournat JC, Brown AM, Soler AP. Wnt-1 dependent activation of the survival factor NF-kappaB in PC12 cells. *J Neurosci Res* 2000;61:21-32.
34. Sanchez JF, Sniderhan LF, Williamson AL, Fan S, Chakraborty-Sett S, Maggirwar SB. Glycogen synthase kinase 3beta-mediated apoptosis of primary cortical astrocytes involves inhibition of nuclear factor kappaB signaling. *Mol Cell Biol* 2003;23(13):4649-62.
35. Alzuherri H, Chang KC. Calcineurin activates NF-kappaB in skeletal muscle C2C12 cells. *Cell Signal* 2003;15:471-8.
36. Biswas G, Anandatheerthavarada HK, Zaidi M, Avadhani NG. Mitochondria to nucleus stress signaling: a distinctive mechanism of NFkappaB/Rel activation through calcineurin-mediated inactivation of IkappaBbeta. *J Cell Biol* 2003;161:507-19.
37. Condorelli G, Drusco A, Stassi G, et al. Akt induces enhanced myocardial contractility and cell size in vivo in transgenic mice. *Proc Natl Acad Sci U S A* 2002;99:12333-8.
38. Kolh P, Lambermont B, Ghuysen A, et al. Alteration of left ventriculo-arterial coupling and mechanical efficiency during acute myocardial ischemia. *Int Angiol* 2003;22(2):148-58:148-58.

Table 1. LV cardiac function derived by *in vivo* pressure-volume analysis in wildtype and GSK3- β transgenic mice four weeks following the initial ischemic insult.

	GSK3- β wt						GSK3- β TG					
	<u>Sham</u>		<u>I/R</u>		<u>MI</u>		<u>Sham</u>		<u>I/R</u>		<u>MI</u>	
	MEAN	SEM	MEAN	SEM	MEAN	SEM	MEAN	SEM	MEAN	SEM	MEAN	SEM
	N = 9		N = 10		N = 6		N = 7		N = 9		N = 10	
HR*	624	± 22	627	± 21	638	± 25	609	± 17	550	± 28	540	± 21
SV[†]	3.77	± 0.30	1.66	± 0.27	2.64	± 0.37	2.30	± 0.33	2.13	± 0.30	2.17	± 0.19
CO*[†]	2348	± 237	1032	± 180	1662	± 214	1429	± 223	1091	± 106	1159	± 130
V_{MAX}	7.56	± 0.60	4.13	± 0.54	6.91	± 0.78	5.38	± 0.81	5.82	± 0.60	5.03	± 0.39
V_{MIN}	3.42	± 0.45	2.07	± 0.29	4.08	± 0.51	2.72	± 0.49	3.26	± 0.41	2.63	± 0.27
ESP	86	± 6	80	± 5	71	± 4	78	± 6	78	± 7	72	± 5
EDP	4	± 1	5	± 1	6	± 2	7	± 3	6	± 1	10	± 1
dP/dt_{MAX}	10263	± 1055	8205	± 999	6828	± 705	7916	± 714	8340	± 1430	6470	± 659
dP/dt_{MIN}[†]	-8253	± 753	-6826	± 635	-5419	± 442	-6840	± 683	-5994	± 523	-4719	± 535
SW*[†]	321	± 37	135	± 27	167	± 19	175	± 27	153	± 28	149	± 12
Tau*	8.33	± 0.43	9.13	± 0.72	9.41	± 1.04	9.99	± 1.08	9.29	± 0.50	12.51	± 1.08
PHT*	4.49	± 0.35	4.74	± 0.36	5.03	± 0.48	5.40	± 0.74	5.18	± 0.30	7.04	± 0.65
EF[†]	54	± 3	45	± 6	39	± 3	50	± 2	40	± 2	47	± 4
PVA*[†]	432	± 46	217	± 40	235	± 23	237	± 35	223	± 37	211	± 21

* Genotype $P < 0.05$ wt vs TG. [†] Procedure $P < 0.05$ sham vs I/R vs MI. HR indicates heart rate; SV stroke volume; CO cardiac output; V_{MAX} maximal left ventricular volume; V_{MIN} minimal left ventricular volume; ESP end-systolic pressure; EDP end-diastolic pressure; dP/dt_{MAX} maximal first derivative of left ventricular pressure; dP/dt_{MIN} minimal first derivative of left ventricular pressure; SW stroke work; Tau time constant of relaxation; PHT pressure half-time; EF ejection fraction; PVA pressure-volume area.

Table 2. Pressure-volume relationships at baseline cardiac function

	GSK3- β wt						GSK3- β TG					
	<u>Sham</u>		<u>I/R</u>		<u>MI</u>		<u>Sham</u>		<u>I/R</u>		<u>MI</u>	
	MEAN	SEM	MEAN	SEM	MEAN	SEM	MEAN	SEM	MEAN	SEM	MEAN	SEM
	N = 6		N = 6		N = 2		N = 6		N = 6		N = 7	
ESPVR	19	± 5	20	± 1	24	± 9	25	± 4	18	± 2	24	± 4
PRSW[†]	65	± 9	31	± 3	43	± 0	52	± 6	40	± 5	35	± 5
dP/dt_{MAX} – Ved	1352	± 221	1187	± 274	1152	± 224	1420	± 331	1015	± 136	1049	± 192
EDPVR	1.26	± 0.59	3.43	± 0.79	2.39	± 0.74	3.14	± 0.56	3.16	± 0.30	2.89	± 0.82
Ea	15	± 2	35	± 7	27	± 10	27	± 6	30	± 5	39	± 7
Ea/Ees	1.01	± 0.23	1.76	± 0.23	1.11	± 0.03	1.11	± 0.23	1.75	± 0.38	1.84	± 0.36

[†] Procedure $P < 0.05$ sham vs I/R vs MI. ESPVR indicates end-systolic pressure-volume relationship; PRSW preload-recruitable stroke work; dP/dt_{MAX}-Ved maximal first derivative of left ventricular pressure-to-end – diastolic volume relationship; EDPVR end-diastolic pressure-volume relationship; Ea arterial elastance; Ea/Ees arterial-ventricular coupling.

Molecular survival pathways in cardiomyocytes

The concept of cardiomyocyte resuscitative survival pathways

Intracellular signaling pathways mediate cellular adaptation upon stimulation by external or internal factors. These intracellular signaling pathways are cascades of enzymes, kinases, phosphatases and/or peptides. They (in)activate the target protein downstream from itself, thereby forming communication-chains of molecular switches between stimulus and cellular response. Specific stimuli or situations induce (in)activation of specific signaling pathways. The eventual cellular response could be of non-genomic or genomic character. Non-genomic effects develop within seconds and circumvent DNA transcription. The direct modulation by estrogens of L-type Ca^{2+} -channels via cardiac guanine monophosphate (cGMP)-pathways decreasing the cellular Ca^{2+} -influx is one example of a non-genomic cellular response. (1) Initiation of the caspase-cascade by ischemia-injury leading to apoptotic cell death is another non-genomic cellular response. In contrast, genomic effects constitute changes in gene expression, requiring DNA transcription and RNA translation leading to the formation of new or additional proteins. Genomic effects have a delay in the range of minutes to hours. The well-known estrogen-induced expression of atrial natriuretic factor (ANF), which is known to possess anti-hypertrophic effects, is one example of a genomic cellular response. (1) Another example of genomic cellular responses characterizes pressure-induced hypertrophic growth. The mechanical stress induces a fetal-like gene-expression profile that promotes the assembly of additional motor units and cytoplasmic protein content to alleviate the heart from its hemodynamic burden. The adaptation of cells via genomic and non-genomic responses upon stimulation is tightly controlled by multiple signaling pathways in close relationship with each other (Figure 1).

Cardiomyocyte resuscitative survival pathways mediate the response of the cardiomyocyte upon stimulation by deleterious situations as ischemia-reperfusion or pressure-overload. The viability of cells and organs are mainly maintained through the well-conserved

Figure 1

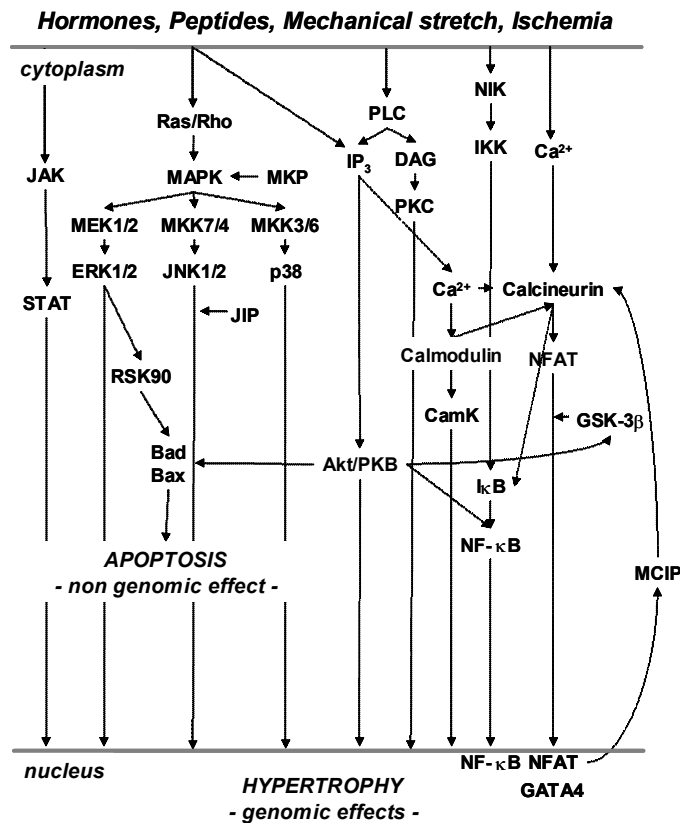


Fig. 1: Intracellular signaling pathways. This figure presents a scheme of some of the signaling pathways involved in cellular hypertrophy and apoptosis. It indicates the multiplicity of signaling pathways involved and their numerous interconnections, making the understanding of precise signaling difficult.

processes of hypertrophy and anti-apoptosis. In general cardiomyocyte hypertrophy augments the capacity of the cell to cope with hemodynamic stress. There is reasonable consensus assuming the cardiomyocyte in the adult heart to be terminally differentiated, although interesting concepts and experimental findings surmise otherwise. (2) Being terminally differentiated the cardiomyocyte is incapable of counteracting augmented wall stress or increased cell loss by cellular self renewal, i.e. regenerating myocardial tissue. It is through the formation of additional sarcomeric motor units and volume-expansion, characteristics of hypertrophy, that cardiomyocytes withstand the hemodynamic burden. Through another mechanism the heart is protected against inefficient, unviable or potentially malignant cells, i.e. by the phenomenon of programmed cell death (apoptosis). Cellular injury, as occurs subsequently to ischemia, negatively influences intracellular activity of structural and functional proteins, and thereby initiates apoptosis. The time- and energy-requiring process of

apoptosis destructs the cells without secondary inflammation and prevents functional deterioration of the heart in time. Both hypertrophy and apoptosis-inhibition provide adequate adaptation of the cardiomyocyte towards detrimental situations, thereby warranting prolonged cellular livelihood.

Cardiomyocyte resuscitative survival pathways can be defined in detail by several characteristics. Firstly, survival pathways are those signaling cascades that *simultaneously* mediate hypertrophic and anti-apoptotic responses in the same response. Another characteristic is their indispensable presence in cellular physiology throughout life. Hypertrophy and apoptosis inhibition are well-conserved cellular adaptation processes that promote cell survival in different situations at distinct life-stages of the organism. Already in the first phase of life, where the struggle for survival begins, the processes of hypertrophy/(proliferation) and apoptosis are crucial for normal development. The region-specific balance between cardiomyocyte proliferation, differentiation and apoptosis sculpts the heart during embryogenesis (Figure 2A). MEK1-ERK1/2 and calcineurin-NFAT pathways are already determining at this time-point in the development of normal cardiogenesis. (3-6) Later in life, in the adult cardiomyocyte, MEK1-ERK1/2 and calcineurin-NFAT pathways promote cellular hypertrophy and protect against apoptosis in response to adverse situations like ischemia. (7-11) Additionally, and interestingly, in an attempt to regain proliferative capacity cardiomyocytes express fetal gene-transcription programs in case of hypertrophic growth.

And finally, the balance between the combination hypertrophy/apoptosis determines the clinical outcome of the heart under pathological conditions (Figure 2). Molecular research in cardiomyocyte hypertrophy led to the concept that specific intracellular signaling could predict the clinical outcome, i.e. *beneficial* or *maladaptive* hypertrophy, which is not depending on the degree of hypertrophy or functional efficiency of the affected

cardiomyocytes. Instead, maladaptive hypertrophy proved to coincide with increased cell death, eventually resulting in the development of heart failure (Figure 2D). (12-16) Heart failure does not develop at a similar rate or to a similar degree, when the occurrence of apoptosis is prevented. (17,18) Interestingly, beneficial hypertrophy is, on the other hand, related to lower degrees of cardiomyocyte apoptosis (Figure 2C). (7) Apparently combined signaling promoting hypertrophy and inhibiting apoptosis simultaneously influences positively the clinical outcome, while the combination of hypertrophy with apoptosis is associated with deterioration of cardiac function.

Figure 2

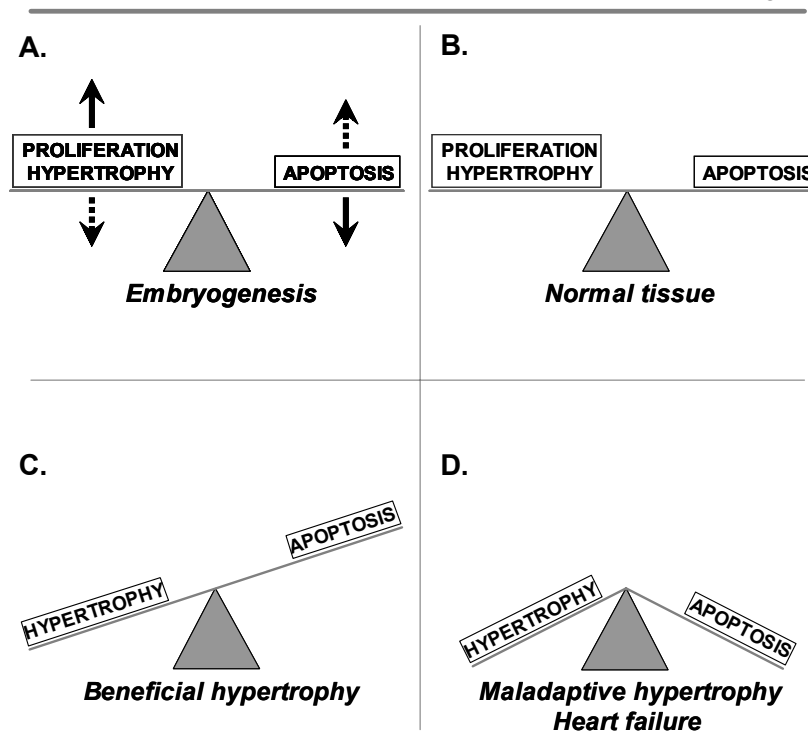


Fig. 2: The balance between hypertrophy and apoptosis. A. During embryogenesis the proliferation/hypertrophy versus apoptosis balance is region-specific. This determines the eventual form of organs and limbs in the growing fetus. In general augmented apoptosis rates coincide with attenuated hypertrophy or proliferation levels (straight arrows). The opposite is true for attenuated apoptosis rates (dotted arrows). B. In normal adult mammal tissue are proliferation/hypertrophy and cell death/apoptosis in balance. C. In the heart the combination of cellular hypertrophy with attenuated apoptosis rates is beneficial for cardiac function and

clinical outcome. This combination is designated beneficial hypertrophy. D. Whenever hypertrophy is in dysbalance with augmented apoptosis rates, the functional status of the heart progresses towards clinical heart failure. This form of hypertrophy is therefore named maladaptive hypertrophy.

The present thesis investigated the MEK1-ERK1/2 and calcineurin-NFAT pathways in their role as cardiomyocyte survival pathways in acute ischemic heart disease.

Several studies proved their role to be essential in endogenous cardiomyocyte hypertrophy through genetic engineering. (7,8) Numerous other studies proved their necessary presence in exogenous stimulated hypertrophic growth through pressure-overload and catecholamines. (19-26) In this thesis their protective role against ischemia-reperfusion injury within the myocardium was shown (Chapter 4-6). The anti-apoptotic effect of MEK1-ERK1/2 activation has been observed by others in the past. For instance, MEK1-ERK1/2 activation enhances expression of FLICE (FADD-like interleukin 1 β -converting enzyme) inhibitory protein, a known inhibitor of the caspase cascade. (27) Alternatively, MEK1-ERK1/2 activation confers cellular protection by preventing mitochondrial membrane permeability. (28) MEK1-ERK1/2 activation directly activates p90rsk resulting in inactivity of the pro-apoptotic factor Bad.

The cytoprotective role of calcineurin has been more controversial, because of contradicting results between several cell types (discussed in Chapter 5). However, the genetic loss-of-function study discussed in Chapter 5 clearly showed the detrimental effect of calcineurin loss in the heart during ischemia-reperfusion injury. The cell-survival effect of calcineurin signaling could partially be mediated by NFAT signaling and partially by phosphatidylinositol 3-kinase (PI3K) signaling, and their respective downstream targets. (11,29) The precise role of NFAT molecules in ischemia-induced apoptosis has not been determined yet, but will be elucidated through future research. The role of PI3K in apoptosis,

Chapter 7; General discussion. Molecular survival pathways in cardiomyocytes

though, has been better delineated. In pathological situations such as ischemia PIK3 activates Akt/protein kinase B (PKB). Akt/PKB itself is capable of phosphorylating Bad and thereby inhibiting cytochrome C release and apoptosis. (30,31) Furthermore, Akt/PKB prevents apoptosis by inhibition of GSK-3 β , of which the numerous downstream targets are generally disadvantageous for cell survival. (32,33) As in addition, Akt/PKB has been proven to be involved in cardiomyocyte hypertrophy (34-36), it certainly complies with the definition of a cardiomyocyte survival pathway.

The future challenge will be to develop strategies that exploit cardiomyocyte resuscitative survival signaling in the heart by tightly controlling activation of potentially beneficial mechanisms in the myocardium during ischemic stress in human patients.

Expanding research in cardiomyocyte resuscitative survival pathways

Research into cardiomyocyte resuscitative survival pathways demands explicit conditions. *In vitro* experiments in cultured cardiomyocytes clarify interactions between molecules and provide indications for the direction of signaling pathways. However, reproducibility of *in vitro* results in the living mammal is not guaranteed. Better evidence is provided by *in vivo* experiments in genetically modified animals, most notably transgenic and gene-targeted mice. Frequently used knockout and overexpression techniques give rise to a genetic modification of the cellular response on pathological situations, as the engineered gene-expression alteration is permanently and irreversibly present since conception. This genetic predisposition very often does not match with human disease. New techniques as tamoxifen-induced cardiac-specific and temporally regulated gene-expression approximate reality better, as the confounder genetic predisposition is evaded. (37,38)

As has been described earlier, heart disease occurs whenever survival pathways have been corrupted or disadvantageous signaling patterns predominate. As signaling pathways constitute of proteins it is essential to look at temporal and spatial changes in protein modulation. The method for molecular analysis is proteomics. Some considerations of proteomic studies have to be mentioned as proteins are more difficult to work with than DNA or RNA. Proteins cannot be amplified like DNA; proteins have secondary and tertiary structure; proteins can be denatured or otherwise altered during the process of purification of intracellular proteins. Purification demands excessive processing and some proteins are difficult to analyze due to their poor solubility. Proteomic studies are performed at the level of protein-protein interactions, frequently using molecular imaging as the investigative tool. Multiple techniques have been developed in the past for *in vitro* molecular imaging, like mass spectrometry and two-hybrid assays. However, *in vitro* investigations miss the theoretic

systemic influences of pathology on cellular processes. New imaging techniques have been developed equipped for studies in the living animal.

Initial reports of real-time molecular imaging were reported by Dumont et al. (39) Fluorescent labeled proteins were infused for visualization of apoptotic membrane changes of single cardiomyocytes during myocardial ischemia in the living mouse. The authors state that this technology could enhance knowledge of intracellular signaling pathways in the process of apoptosis and strategies to manipulate these pathways for therapeutic effect in humans. Human *in vivo* visualization and quantification of apoptotic signaling following myocardial ischemia has been reported using similar techniques. (40) The fluorescence labeling of binding molecules as performed in these studies is feasible for a multitude of target proteins and DNA molecules and results in temporal and spatial information of the various processes involved. Other molecular techniques in development include for instance two-hybrid systems for positron-emission tomography (microPET) and fluorescence imaging in the living animal, involving the creation and intracorporeal implementation of hybrid proteins (i.e. fusion of proteins of interest with DNA binding or transcription activation domains) and resulting expression of a reporter gene. (41,42) Another *in vivo* noninvasive visualization technique uses magnetic resonance molecular imaging combined with exogenous contrast agents directed towards specific molecular entities of most notably the cellular outer membrane. (43) (44) This is not a detailed enumeration of all techniques in development, but does delineate the process of *in vivo* molecular imaging. As the examples from above show, at this moment molecular imaging is confined to the visualization of single molecules in extensive signaling cascades. Focusing on single molecules blindfolds the investigator for the role of other proteins, peptides and signaling cascades. Making molecular imaging more dynamic through incorporating the possibility for visualization of single pathways at distinct levels within the cascade, or simultaneously multiple pathways, would increase its value in molecular

Chapter 7; General discussion. Molecular survival pathways in cardiomyocytes

biological research: dynamic molecular imaging (DMI). Powerful data would arise from detailed exploration of real-time intracellular signal transduction in different heart disease conditions. DMI derived information could clarify and visualize intracellular signaling activity (ISA) patterns in the course of disease development like hypertrophy and heart failure in a temporal and spatial manner. Moreover, changes in ISA patterns could be adequately followed. Detailed knowledge about the relationship between ISA patterns and concurrent disease condition enables scientists and clinicians to predict prognosis. Moreover, therapy could be provided in a tailored manner. As DMI could prove to be indispensable in cardiovascular research and clinical practice and current techniques are not yet insufficient, new developments have to be initiated.

Clinical relevance

This thesis points to the anti-apoptotic effect of genetic activation of MEK1-ERK1/2 and calcineurin-NFAT pathways in ischemia-reperfusion injury. The extent of ischemia-induced apoptotic injury in cardiomyocytes is diminished compared to normal protein activation. In addition, attenuated ischemia-induced injury forms a risk for the maintenance of cardiac function, a determinant of clinical prognosis.

The results reported in this thesis provide in the first place valuable additive basic scientific knowledge about intracellular signaling pathways in ischemia-induced apoptosis. They provide important handles for future therapeutic options in clinical care for mainly acute ischemic heart diseases. Main limitation is the fact that the presented experiments were performed in genetically modified mice. Results derived from murine studies are not necessarily suited for direct translation to the human population, despite the major comparability in DNA composition between the two species. Another important limitation is the use of genetically modified mice, as genetic engineering is not an option in human patients. Nevertheless, the derived results concerning cardiomyocyte survival pathways could have implications for clinical practice.

Activation of MEK1-ERK1/2 and/or calcineurin-NFAT pathways in acute myocardial infarction could protect affected cardiomyocytes against apoptotic cell death resulting in favorably diminished infarction-lesions. Development of methods to inhibit apoptotic cell death could result in a realistic alternative for exogenous tissue engineering. Exogenous tissue engineering using skeletal myoblasts and embryonic or bone marrow stem cells has undergone promising substantial progress, but did not yet reach clinical practice. (45) The treatment procedure with survival pathway activation in acute myocardial ischemia requires specific considerations. The therapeutic signaling activation needs to be cardiac-specific targeted, most preferably cardiomyocyte-specific. As MEK1-ERK1/2 and calcineurin-NFAT

Chapter 7; General discussion. Molecular survival pathways in cardiomyocytes

pathways mediate important processes in other cell types, systemic infusion of a signaling active substance could result in important side effects. (46) Moreover, both pathways have been implicated in carcinogenesis. (47,48) Cardiac-specific targeting could be accomplished by linking the therapeutic agent to smart-binding molecules. These smart-binding molecules, for example cardiomyocyte anti-lineage-specific antibodies or cytokines, are able to target cardiomyocytes specifically and concomitantly deliver the therapeutic agent at the site where it is needed. However, during continuing ischemia the target cells for therapeutic signaling activation cannot be reached through systemic administration unless the coronary occlusion is removed by an intracoronary intervention. Retrograde administration is a possible option, but it constitutes more risks for the patient. Another important aspect of therapy is the timing of administration. With regard to the most optimal clinical outcome therapeutic signaling activation is preferably accomplished before myocardial ischemia occurs. Theoretically that would involve large-scale primary prevention studies, which are costly and not without danger. Most practical would be therapy administration subsequent to myocardial reperfusion. Clinical trials are needed to reveal the range of gain that can be obtained concerning infarct size and maintenance of cardiac function. Another possible moment for therapeutic administration could be during recovery after an acute myocardial infarction, as deleterious cardiac remodeling and heart failure development could be prevented by apoptosis inhibition.

As murine studies have been performed, a new step in the near future concerning the study of cardiomyocyte survival pathways in apoptotic cell death protection could be pig or canine models of acute myocardial ischemia. In these large mammals different therapeutic agents in distinct administration modalities and varying infusion time-schemes could be the subject of investigation. Infarct size, apoptosis rates and cardiac remodeling could be relevant parameters. This step could be a bridge to clinical trials in patients.

Conclusion

Closed-chest left ventricular pressure-volume acquisition is a sensitive, reproducible and adequate method for *in vivo* cardiac function assessment in mice.

MEK1-ERK1/2 activation regulates cardiomyocyte viability following stress stimulation *in vivo*. Calcineurin signaling helps to maintain cardiomyocyte viability *in vivo*, mediated by specific NFAT activity. GSK-3 β sensitizes the cardiomyocyte for stress-induced apoptosis and antagonizes hypertrophic growth *in vivo*.

Cardiomyocyte survival pathways, such as the MEK-ERK1/2 and calcineurin-NFAT pathways, protect the cardiomyocyte against deleterious stimuli by antagonizing apoptosis and promoting hypertrophic growth through (in)activation of specific pathways.

MEK1-ERK1/2 and calcineurin-NFAT activation is cardioprotective in acute myocardial ischemia-reperfusion injury as apoptotic cell death is prevented and follow-up cardiac function maintained. These pathways are part of the concept of well-preserved cardiomyocyte resuscitative survival pathways. New investigative strategies like dynamic molecular imaging could significantly increase our knowledge about intracellular signaling activation patterns in the course of disease. Therapeutic options with regard to intracellular signaling activation in acute myocardial ischemia are at an early stage of investigation. The next step would be the systemic administration of signaling specific therapeutic agents in large mammal models to assess therapeutic potential and important side effects of treatment. This interesting challenge in molecular cardiovascular science lies ahead of us.

References

1. Babiker FA, De Windt LJ, van Eickels M, Grohe C, Meyer R, Doevendans PA. Estrogenic hormone action in the heart: regulatory network and function. *Cardiovasc Res* 2002;53:709-719.
2. Quaini F, Urbanek K, Beltrami AP, et al. Chimerism of the transplanted heart. *N Engl J Med* 2002;346:5-15.
3. Corson LB, Yamanaka Y, Lai KM, Rossant J. Spatial and temporal patterns of ERK signaling during mouse embryogenesis. *Development* 2003;130:4527-37.
4. de la Pompa JL, Timmerman LA, Takimoto H, et al. Role of the NF-ATc transcription factor in morphogenesis of cardiac valves and septum. *Nature* 1998;392:182-6.
5. Ranger AM, Grusby MJ, Hodge MR, et al. The transcription factor NF-ATc is essential for cardiac valve formation. *Nature* 1998;392:186-90.
6. Bennett AM, Tonks NK. Regulation of distinct stages of skeletal muscle differentiation by mitogen-activated protein kinases. *Science* 1997;278:1288-91.
7. Bueno OF, De Windt LJ, Tymitz KM, et al. The MEK1-ERK1/2 signaling pathway promotes compensated cardiac hypertrophy in transgenic mice. *Embo J* 2000;19:6341-50.
8. Molkenin JD, Lu JR, Antos CL, et al. A calcineurin-dependent transcriptional pathway for cardiac hypertrophy. *Cell* 1998;93:215-28.
9. Lips DJ, Antos CL, Hassink RJ, De Windt LJ, Doevendans PA, Olson EN. GSK-3beta overexpression attenuates hypertrophy and sensitizes the heart to ischemic damage and dysfunction. In preparation 2003.
10. Lips DJ, Bueno OF, Wilkins BJ, et al. The MEK1-ERK2 signaling pathway protects the myocardium from ischemic damage in vivo. Submitted 2003.
11. Bueno OF, Lips DJ, Kaiser RA, et al. Calcineurin Abeta gene targeting predisposes the myocardium to stress-induced apoptosis and dysfunction. *Circ Res*. 2003 Nov 13 [Epub ahead of print] 2003.
12. Anversa P, Kajstura J, Olivetti G. Myocyte death in heart failure. *Curr Opin Cardiol* 1996;11:245-51.
13. Hein S, Arnon E, Kostin S, et al. Progression from compensated hypertrophy to failure in the pressure-overloaded human heart: structural deterioration and compensatory mechanisms. *Circulation* 2003;107:984-91.
14. Leri A, Franco S, Zacheo A, et al. Ablation of telomerase and telomere loss leads to cardiac dilatation and heart failure associated with p53 upregulation. *EMBO J* 2003;22:131-9.
15. Oh H, Wang SC, Prahash A, et al. Telomere attrition and Chk2 activation in human heart failure. *Proc Natl Acad Sci U S A* 2003;100:5378-83.
16. Lips DJ, Van Kraaij DL, De Windt LJ, Doevendans PA. Molecular determinants of myocardial hypertrophy and failure: alternative pathways for beneficial and maladaptive hypertrophy. *Eur Heart J* 2003;24:883-896.
17. Wencker D, Chandra M, Nguyen K, et al. A mechanistic role for cardiac myocyte apoptosis in heart failure. *J Clin Invest* 2003;111:1497-504.
18. Abbate A, Biondi-Zoccai GG, Bussani R, et al. Increased myocardial apoptosis in patients with unfavorable left ventricular remodeling and early symptomatic post-infarction heart failure. *J Am Coll Cardiol* 2003;41:753-60.
19. Esposito G, Prasad SV, Rapacciuolo A, Mao L, Koch WJ, Rockman HA. Cardiac overexpression of a G(q) inhibitor blocks induction of extracellular signal-regulated kinase and c-Jun NH(2)-terminal kinase activity in in vivo pressure overload. *Circulation* 2001;103:1453-8.

20. Wilkins BJ, De Windt LJ, Bueno OF, et al. Targeted disruption of NFATc3, but not NFATc4, reveals an intrinsic defect in calcineurin-mediated cardiac hypertrophic growth. *Mol Cell Biol* 2002;22:7603-13.
21. De Windt LJ, Lim HW, Bueno OF, et al. Targeted inhibition of calcineurin attenuates cardiac hypertrophy in vivo. *Proc Natl Acad Sci U S A* 2001;98:3322-7.
22. Zou Y, Hiroi Y, Uozumi H, et al. Calcineurin plays a critical role in the development of pressure overload-induced cardiac hypertrophy. *Circulation* 2001;104:97-101.
23. Antos CL, McKinsey TA, Frey N, et al. Activated glycogen synthase-3 beta suppresses cardiac hypertrophy in vivo. *Proc Natl Acad Sci U S A* 2002;99:907-12.
24. Hill JA, Rothermel B, Yoo KD, et al. Targeted inhibition of calcineurin in pressure-overload cardiac hypertrophy. Preservation of systolic function. *J Biol Chem* 2002;277:10251-5.
25. Bueno OF, Wilkins BJ, Tymitz KM, et al. Impaired cardiac hypertrophic response in Calcineurin Abeta -deficient mice. *Proc Natl Acad Sci U S A* 2002;99:4586-91.
26. Bueno OF, De Windt LJ, Lim HW, et al. The dual-specificity phosphatase MKP-1 limits the cardiac hypertrophic response in vitro and in vivo. *Circ Res* 2001;88:88-96.
27. Yeh JH, Hsu SC, Han SH, Lai MZ. Mitogen-activated protein kinase kinase antagonized fas-associated death domain protein-mediated apoptosis by induced FLICE-inhibitory protein expression. *J Exp Med* 1998;188:1795-802.
28. Bonni A, Brunet A, West AE, Datta SR, Takasu MA, Greenberg ME. Cell survival promoted by the Ras-MAPK signaling pathway by transcription-dependent and -independent mechanisms. *Science* 1999;286:1358-62.
29. De Windt LJ, Lim HW, Taigen T, et al. Calcineurin-mediated hypertrophy protects cardiomyocytes from apoptosis in vitro and in vivo: An apoptosis-independent model of dilated heart failure. *Circ Res* 2000;86:255-63.
30. Datta SR, Dudek H, Tao X, et al. Akt phosphorylation of BAD couples survival signals to the cell-intrinsic death machinery. *Cell* 1997;91:231-41.
31. del Peso L, Gonzalez-Garcia M, Page C, Herrera R, Nunez G. Interleukin-3-induced phosphorylation of BAD through the protein kinase Akt. *Science* 1997;278:687-9.
32. Zhang HM, Yuan J, Cheung P, et al. Over-expression of interferon-gamma -inducible GTPase inhibits coxsackievirus B3-induced apoptosis through the activation of the PI3-K/Akt pathway and inhibition of viral replication. *J Biol Chem* 2003;Epub ahead of print.
33. Hardt SE, Sadoshima J. Glycogen synthase kinase-3beta: a novel regulator of cardiac hypertrophy and development. *Circ Res* 2002;90:1055-63.
34. Matsui T, Li L, Wu JC, et al. Phenotypic spectrum caused by transgenic overexpression of activated Akt in the heart. *J Biol Chem* 2002;277:22896-901.
35. Condorelli G, Drusco A, Stassi G, et al. Akt induces enhanced myocardial contractility and cell size in vivo in transgenic mice. *Proc Natl Acad Sci U S A* 2002;99:12333-8.
36. Shioi T, McMullen JR, Kang PM, et al. Akt/protein kinase B promotes organ growth in transgenic mice. *Mol Cell Biol* 2002;22:2799-809.
37. Rajewsky K, Gu H, Kühn R, et al. Conditional gene targeting. *J Clin Invest* 1996;98:600-3.
38. Petrich BG, Molkentin JD, Wang Y. Temporal activation of c-Jun N-terminal kinase in adult transgenic heart via cre-loxP-mediated DNA recombination. *FASEB J* 2003;17:749-51.
39. Dumont E, Reutelingsperger CP, Smits JF, et al. Real-time imaging of apoptotic cell-membrane changes at the single-cell level in the beating murine heart. *Nat Med* 2001;7:1352-5.

40. Hofstra L, Liem IH, Dumont EA, et al. Visualisation of cell death in vivo in patients with acute myocardial infarction. *Lancet* 2000;356:209-12.
41. Luker GD, Sharma V, Pica CM, Prior JL, Li W, Piwnica-Worms D. Molecular imaging of protein-protein interactions: controlled expression of p53 and large T-antigen fusion proteins in vivo. *Cancer Res* 2003;63:1780-8.
42. Luker GD, Pica CM, Song J, Luker KE, Piwnica-Worms D. Imaging 26S proteasome activity and inhibition in living mice. *Nat Med* 2003;9:969-73.
43. Artemov D. Molecular magnetic resonance imaging with targeted contrast agents. *J Cell Biochem* 2003;90:518-24.
44. Artemov D, Mori N, Ravi R, Bhujwalla ZM. Magnetic resonance molecular imaging of the HER-2/neu receptor. *Cancer Res* 2003;63:2723-7.
45. Hassink RJ, Brutel de la Riviere A, Mummery CL, Doevendans PA. Transplantation of cells for cardiac repair. *J Am Coll Cardiol* 2003;41:711-7.
46. Bueno OF, Brandt EB, Rothenberg ME, Molkentin JD. Defective T cell development and function in calcineurin A beta -deficient mice. *Proc Natl Acad Sci U S A* 2002;99:9398-403.
47. Goto S, Matsukado Y, Mihara Y, Inoue N, Miyamoto E. An immunocytochemical demonstration of calcineurin in human nerve cell tumors. A comparison with neuron-specific enolase and glial fibrillary acidic protein. *Cancer* 1987;60:2948-57.
48. Oka H, Chatani Y, Hoshino R, et al. Constitutive activation of mitogen-activated protein (MAP) kinases in human renal cell carcinoma. *Cancer Res* 1995;55:4182-7.

Summary

The use of genetically engineered mice renders vital information about the precise roles proteins play in the diversity of intracellular signaling pathways associated with the events of cardiomyocyte hypertrophy or apoptosis. In the present thesis, the link between the genotype of the mouse and the concurrent phenotype is investigated employing sophisticated molecular and cellular techniques combined with *in vivo* cardiac performance measurements. In chapter 1 we focus on the characteristics of *cardiac remodeling* following an ischemic event in man. The characteristics of remodeling - such as cell death, deposition of collagen and myocardial hypertrophy - are thoroughly discussed through the results solely derived from studies in genetically modified mice. The use of genetically modified murine models in ischemia (-reperfusion) studies has led to a wealth of knowledge about the molecular pathways involved in these processes. Despite the data available, intracellular signaling is still a mystery as we lack the tools to study several pathways simultaneously and maybe even more important the temporal changes in signaling cascade interactions.

In chapter 2 the molecular processes involved in cardiac hypertrophy are discussed. The concept of *beneficial* and *maladaptive* pathways is introduced and related to the detrimental transition of hypertrophy towards heart failure.

Open-chest and closed-chest protocols for *in vivo* left ventricular *pressure-volume measurement* are illustrated in chapter 3. Murine cardiac function determination via both methods is sensitive, reproducible and comparable. We have chosen for closed-chest cardiac function assessment protocol in our ischemia-reperfusion studies, because of better systolic and diastolic performance, normal arterial-ventricular coupling and preservation of myocardial integrity.

To unravel the importance of specific signaling pathways (e.g. *MEK1-ERK1/2* and *calcineurin-NFAT*) in ischemia-reperfusion-induced cell death techniques of transgenesis (e.g.

MEK1 and GSK-3 β transgenic mice) and gene targeting (e.g. ERK1 homozygous, ERK2 heterozygous and CnA β homozygous knockout mice) have been used. Because single genes were targeted, it was possible to elucidate the specific functions of the corresponding protein in intracellular signaling pathways. In chapter 4 we analyzed ERK1 homozygous knockout mice, ERK2 heterozygous knockout mice, and transgenic mice with activated MEK1-ERK1/2 signaling in the heart to determine a direct causal relationship between ERK1/2 signaling and cardioprotection. A direct cardioprotective role for ERK signaling in the heart following ischemia-reperfusion injury was demonstrated. While MEK1 transgenic mice were largely resistant to myocardial infarction, ERK2 $^{+/-}$ gene targeted mice showed enhanced infarction and cardiomyocyte apoptosis when compared to littermate controls, resulting in concomitant deterioration of cardiac function. Collectively, these data are the first to demonstrate that ERK signaling directly participates in mediating cellular protection following ischemic injury in the heart. In chapter 5 we investigate the role the calcium/calmodulin-activated protein phosphatase calcineurin plays in modulating cardiac apoptosis following acute ischemia-reperfusion injury in the heart. Calcineurin A β (CnA β) gene targeted mice showed a greater loss of viable myocardium, more apoptosis, and a greater loss in functional performance following ischemia-reperfusion injury when compared to strain-matched wildtype control mice. Increased cell death was associated with a reduction of NFAT activity. Indeed, NFAT activation protected cardiac myocytes from apoptotic stimuli, while directed inhibition of NFAT augmented cell death. Collectively, these results represent the first genetic loss-of-function data showing a pro-survival role for calcineurin-NFAT signaling in the heart. The study presented in chapter 6 is designed to elucidate the role of GSK-3 β following ischemia-reperfusion. In GSK-3 β transgenic mice, ischemia led to a larger infarct area and subsequent worsened cardiac performance, while post-ischemic hypertrophic remodeling was blunted.

Conclusively, these findings point towards a role for GSK-3 β as a dualistic signaling molecule transducing both anti-hypertrophic as well as pro-apoptotic pathways.

In previous studies activation of both MEK1-ERK1/2 and calcineurin-NFAT signaling pathways were associated with hypertrophic cellular growth. The present thesis proves their involvement in anti-apoptotic protection against ischemia-reperfusion injury. The dualistic role of both resuscitative survival pathways in distinct pathogenic conditions as cardiomyocyte hypertrophy and apoptosis, is a fascinating observation. To further delineate the specific roles of individual survival pathways and investigate their potential use in clinical practice, future research should focus on studying multiple signaling cascades simultaneously and their interplay. A possible option is to cross-breed different genetically modified mice, thereby creating double knockout or knockout/transgenic mice. Another possibility could come from *dynamic molecular imaging*, through which protein function and interaction could be visualized. The treatment of cardiac ischemia will eventually be improved significantly through new developments in molecular science.

Samenvatting

In de cardiologie worden genetisch gemodificeerde muizenstammen gebruikt voor het wetenschappelijk onderzoek naar pathofysiologische processen zoals hypertrofie en apoptose van de cardiomyocyt. Met deze proefdiermodellen worden de precieze functies van specifieke eiwitten in de diverse intracellulaire processen ontrafeld. Dit proefschrift beschrijft de link tussen het genotype van de muis en het daarbij behorende fenotype door middel van moleculaire en cellulaire laboratoriumtechnieken in combinatie met hartfunctiemetingen in de levende muis.

Hoofdstuk 1 gaat dieper in op de cellulaire en orgaanrespons van het hart op ischemie, een variëteit aan processen die gedefinieerd wordt door de term *remodeling*. Al deze processen worden besproken en verduidelijkt aan de hand van onderzoeksresultaten uitsluitend verkregen in genetisch gemodificeerde muizenstammen. Uit dit hoofdstuk blijkt dat het gebruik van genetisch gemodificeerde muizen onmiskenbaar zijn waarde heeft bewezen in de zoektocht naar determinerende stappen in het remodeleringsproces.

Hoofdstuk 2 bespreekt de moleculaire en cellulaire mechanismen in hypertrofie van het hart. Daarnaast wordt ingegaan op die mechanismen, die de transitie van hypertrofie naar hartfalen lijken te bepalen en versnellen. Het concept van gunstige (*beneficial*) en ongunstige (*maladaptive*) signaalwegen wordt geïntroduceerd en de relevantie besproken voor de dagelijkse klinische praktijk.

In hoofdstuk 3 worden de onderzoeksprotocollen voor drukvolume metingen bij open en gesloten muizenthorax gedetailleerd beschreven en besproken. Hartfunctie metingen in de muis, uitgevoerd volgens deze protocollen, zijn sensitief, reproduceerbaar en vergelijkbaar. In ischemie-reperfusie vervolgstudies werd gekozen voor hartfunctiemeting bij gesloten thorax, vanwege de betere hartfunctie tijdens de systole en diastole, een normale arterial-ventricular coupling en behoud van integriteit van het myocard. De betekenis van specifieke

signaalwegen (MEK1-ERK1/2 en calcineurin-NFAT) in de reactie van de cardiomyocyt op ischemie-reperfusie stress werd onderzocht door middel van transgene (MEK1 en GSK-3 β) en (ERK1 homozygote, ERK2 heterozygote en CnA β homozygote) knockout muizen.

Aangezien deze technieken leiden tot verandering in het enkelvoudige gen is het mogelijk de specifieke functies van het enkelvoudig corresponderend eiwit in de intracellulaire signaalwegen te onderzoeken.

Het onderzoek naar de betekenis van MEK1-ERK1/2 signaalactivatie bij de respons van de cardiomyocyt op schade ten gevolge van ischemie-reperfusie wordt beschreven in hoofdstuk 4. Hierbij werden ERK1 homozygote, ERK2 heterozygote en MEK1 transgene muizen gebruikt. ERK1/2 signaalactivatie blijkt direct gecorreleerd te zijn met bescherming van de cardiomyocyt tegen celdood ten gevolge van myocardischemie. MEK1 transgene muizen blijken vrijwel resistent te zijn voor de ischemische stimulus. ERK2 heterozygote knockout muizen vertonen een groter myocardinfarct met meer apoptose in vergelijking met controle muizen. De hartfunctie blijkt daarbij navenant verslechterd te zijn. Dit zijn de eerste gepubliceerde onderzoeksresultaten waarin bescherming van de cardiomyocyt tegen ischemie-reperfusie schade door MEK1-ERK1/2 signaalactivatie wordt aangetoond.

De rol van het calcium/calmoduline-geactiveerde eiwit fosfatase calcineurine in cardiomyocyt apoptose in respons op ischemie-reperfusie schade is het onderwerp van hoofdstuk 5. Calcineurine A β (CnA β) knockout muizen vertonen een groter myocardinfarct met meer apoptose na myocardischemie dan controle muizen. Het verlies van hartfunctie is lineair degressief in deze muizen in vergelijking met controle muizen. De verhoogde mate van apoptotische celdood is geassocieerd met een reductie in NFAT activiteit. Activatie van NFAT beschermt de cardiomyocyten tegen apoptotische stimuli, terwijl directe inhibitie van NFAT activatie leidt tot meer apoptotische celdood. Deze resultaten leiden tot de conclusie dat de calcineurine-NFAT as bescherming biedt tegen de gevolgen van ischemie.

Het in hoofdstuk 6 beschreven onderzoek is opgezet om de rol van GSK-3 β bij de respons op ischemie-reperfusie te verklaren. Myocardischemie resulteert in grotere myocardinfarcten en verslechtering van de hartfunctie in GSK-3 β transgene muizen, terwijl postischemische hypertrofe remodeling verminderd blijkt. Uit beide observaties komt de duale rol van GSK-3 β naar voren: zowel inhibitie van hypertrofie als promotie van apoptose in de cardiomyocyt.

Eerdere publicaties gingen in op activatie van MEK1-ERK1/2 en calcineurine-NFAT signaalwegen ten tijde van hypertrofe groei van de cardiomyocyt in respons op diverse pathologische situaties. Dit proefschrift beschrijft de rol van beide signaalwegen bij de bescherming van de cardiomyocyt tegen apoptotische celdood in respons op schade door ischemie-reperfusie. De observatie dat beide signaalwegen afzonderlijk een rol van betekenis spelen in zowel prohypertrofe als anti-apoptotische cellulaire processen biedt een fascinerend uitgangspunt voor toekomstig onderzoek. Hierin heeft het simultaan bestuderen van meerdere signaalwegen en de onderlinge interactie prioriteit. Dit kan worden verwezenlijkt door het kruisen van genetisch gemodificeerde muizenstammen waardoor dubbelknockouts of knockout/transgene muizenstammen ontstaan. Ook het bestuderen van meer specifiek proteïne-proteïne interacties is van essentieel belang. Een mogelijkheid zou *dynamic molecular imaging* zijn, dat veranderingen in eiwitfuncties in de tijd visualiseert. De behandeling van myocardischemie in de patiënt zal in de toekomst door moleculaire ontwikkelingen in ieder geval significante verbeteringen ondergaan.

Curriculum vitae

The author of this thesis, *Daniel Jozef Lips*, was born October 15th, 1978 in Hwidiem BA, Ghana. From 1991 he attended Zwijsen College in Veghel, the Netherlands, where he obtained the year prize for Roman language and culture at his graduation in 1997. Subsequently he started his academic career at the Faculty of Health Sciences at Maastricht University. After graduating his first year (i.e. Propedeuse, cf. B.Sc) in Health Sciences, he started in 1998 his medical training at the Faculty of Medicine at Maastricht University. He was founding member of the fraternity *Onafhankelijk Heerendispuut Hyperion Maastricht*, in which he served several years as board member and chairman. During his first year of medical training he began to serve as a research assistant at the Department of Cardiology of the University Hospital Maastricht under supervision of Dr. P.A. Doevendans and Prof. Dr. H.J.J. Wellens. In 2000 he was trained for six weeks at the laboratory of Dr. Howard D. Rockman, Department of Cardiology, Duke University Medical Center, Durham, North Carolina, USA. In 2001 he was awarded the international *Journal of Experimental Biology Travelling Fellowship Award* for his study proposal *Cardiac function in murine genotypes of beneficial and maladaptive myocardial hypertrophy*. In the same year he won the students-science prize at the Maastricht Medical Students Research Conference for the best poster presentation. From 2001 to 2004 he worked with grants from the Hein J.J. Wellens foundation and foundation De Drie Lichten during several periods as a Ph.D. student at the laboratories of Dr. Jeffery D. Molkentin, Children's Hospital Medical Center, Cincinnati, Ohio, USA, and Prof. Dr. Eric N. Olson, University of Texas Southwestern Medical Center, Dallas, Texas, USA. His clinical elective internship was performed at the Department of Cardio-Thoracic Surgery of the University Medical Center Utrecht under supervision of Prof. Dr. A. Brutel de la Rivière in 2003. Currently he is in the last year of medical training and expects to graduate in August 2004.

Full papers

1. Van den Bosch BJC, Doevendans PA, Lips DJ, Geurts JMW, Smeets HJM. Towards elucidation of genetic pathways in cardiac hypertrophy: technique to develop microarrays. In: Doevendans PA, Kaab S. Cardiovascular genomics: new pathophysiological concepts. Dordrecht: Kluwer Academic Publishers, 2002:97-105.
2. Bueno OF, Van Rooij E, Lips DJ, Doevendans PA, De Windt LJ. Cardiac hypertrophic signaling: the good, the bad and the ugly. In: Doevendans PA, Kaab S. Cardiovascular genomics: new pathophysiological concepts. Dordrecht: Kluwer Academic Publishers, 2002:131-155.
3. Mummery C, Ward D, Van den Brink CE, Bird SD, Doevendans PA, Lips DJ, Opthof T, Brutel de la Riviere A, Tertoolen L, Van der Heyden M, Pera M. In: Doevendans PA, Kaab S. Cardiovascular genomics: new pathophysiological concepts. Dordrecht: Kluwer Academic Publishers, 2002:231-243.
4. Van Kraaij D, Van Pol P, Ruiters A, De Swart J, Lips D, Lencer N, Doevendans P. Diagnosing diastolic heart failure. Eur J Heart Fail 2002 Aug;4(4):419.
5. Lips DJ, De Windt LJ, Van Kraaij DVM, Doevendans PA. Molecular determinants of myocardial hypertrophy and failure. Alternative pathways for beneficial and maladaptive hypertrophy. Eur Heart J 2003;24(10):883-96.
6. Bueno OF, Lips DJ, Kaiser RA, Wilkins BJ, Dai YS, Glascock BJ, Klevitsky R, Hewett TE, Kimball TR, Aronow BJ, Doevendans PA, Molkentin JD. Targeted disruption of calcineurin A β indicates a role for calcineurin in cardiac hypertrophy and ischemia-induced injury. Circ Res 2004;94(1):91-9.
7. Eefting F, Rensing B, Wigman J, Pannekoek WJ, Liu WM, Cramer MJ, Lips DJ, Doevendans PA. Role of apoptosis in reperfusion injury. Cardiovasc Res 2004 Feb 15;61(3):414-26.

8. Van Rooij E, Doevendans PA, Crijns HJGM, Heeneman S, Lips DJ, Van Bilsen M, Williams RS, Olson EN, Bassel-Duby R, Rothermel BA, De Windt LJ. MCIP1 overexpression suppresses left ventricular remodeling and sustains cardiac function following myocardial infarction. *Circ Res*. 2004 Feb 20;94(3):e18-26
9. Kaiser RA, Bueno OF, Lips DJ, Doevendans PA, Kimball TF, Molkentin JD. Targeted inhibition of p38 MAPK antagonizes cardiac injury and cell death following ischemia-reperfusion in vivo. *J Biol Chem* 2004 Jan 28 [Epub ahead of print]
10. Lips DJ, Van der Nagel T, De Windt LJ, Van Empel VM, Palmén M, Van Dantzig J-M, Doevendans PA. Left ventricular pressure-volume measurements in mice: A comparative study between a closed-chest versus open-chest approach. In press *Basic Res Cardiol*.
11. Lips DJ, Van Reisen MT, Voigt V, Venekamp W. Pseudomalabsorption of Levothyroxine. In press *Netherlands Journal of Medicine*.
12. Lips DJ, Bueno OF, Wilkins BJ, Purcell NH, Kaiser RA, Lorenz JN, Voisin L, Saba-El-Leil MK, Meloche S, Pouysségur J, Pagès G, De Windt LJ, Doevendans PA, Molkentin JD. The MEK1-ERK2 signaling pathway protects the myocardium from ischemic injury in vivo. In press *Circulation*.
13. Lips DJ, Hassink RJ, Brutel de la Rivière A, Doevendans PA. The use of genetic modified mice in the investigation of cardiac remodeling. In: Greenberg B. *Myocardial remodeling: Mechanisms and treatment*. In press 2004.
14. Palmén M, Daemen MJ, Lips DJ, Buehler A, De Theije C, Zandbergen HR, Bronsaer RJP, Zimmermann R, Van der Zee R, De Muinck ED, Dassen WR, Van Eickels M, Kockx MA, Smits JF, Doevendans PA. Cardiac-specific overexpression of hFGF-1 deteriorates cardiac function and alters remodeling following chronic myocardial infarction in mice. Submitted 2003.

15. Babiker FA, Lips DJ, Delvaux E, Zandberg P, Van Eys G, Van Eickels M, Grohe C, Janssen B, Doevendans PA. Estrogen receptor beta protects the murine heart against left ventricular hypertrophy. Submitted 2004.
16. Lips DJ, Antos CL, Hassink RJ, De Windt LJ, Doevendans PA, Olsen EN. GSK-3 β overexpression attenuates hypertrophy and sensitizes the heart to ischemic damage and dysfunction. In preparation.

Acknowledgements / Dankbetuigingen

Gekomen bij het einde van mijn proefschrift, en daarmee het einde van het wetenschappelijke werk dat aan dit proefschrift vooraf ging, benut ik graag de mogelijkheid om diegenen te bedanken die met hun inzet en enthousiasme in mijn proefschrift en mijn persoon hebben geïnvesteerd. Het proefschrift is dé finale van jaren proefdraaien in de wetenschap; enkele personen hadden daar een bijzonder aandeel in.

De eerste is *Pieter Doevendans*. Pieter bood mij de mogelijkheid kennis te maken met de medische wetenschap. Daarvoor had ik geen betere leermeester kunnen treffen dan Pieter zelf. Persoonskenmerken die ik bewonder in Pieter maken hem tot de meest geschikte begeleider in de afgelopen jaren. Ik heb onze persoonlijke omgang als zeer aangenaam ervaren en hoop die in de toekomst te kunnen voortzetten.

The second person I would like to express my gratitude to is *Jeffery Molkentin*, in whose laboratory, based in Cincinnati USA, I probably spent as much time as I did in the laboratory of Pieter Doevendans. The drive and knowledge of Jeff are like the water stream in Niagara Falls: never ending and with great force, and it greatly influenced my enthusiasm for science. I have not stopped learning from Jeff. I hope I never will.

Een persoon die tevens een significant aandeel heeft gehad in de totstandkoming van mijn proefschrift, is *Leon de Windt*. Ik dank Leon voor de gedetailleerde discussies over de wetenschap, voor de goede ideeën met mij besproken en voor zijn kritische noot op mijn Engelse teksten. Ik betreurde zijn vertrek naar Utrecht, waardoor onze dagelijkse interactie aanzienlijk verminderd werd.

Another person to whom I would like to show my gratitude is *Eric Olson*. I want to thank Eric for making his laboratory and knowledge available for our studies. I enjoyed being in his laboratory in Dallas Texas, where I enormously improved my scientific skills. Even from a distance I will continue to learn from Eric.

Tenslotte wil ik graag mijn grote dank uitspreken jegens *Hein Wellens* en *Aart Brutel de la Rivière*: enerzijds voor hun beider rol als mijn promotor, anderzijds voor hun betekenis als onmiskenbare iconen voor jonge wetenschappers en artsen in de cardiovasculaire wetenschap en geneeskunde. Hun aanwijzingen en correcties waren van fundamenteel belang voor mijn proefschrift.

Een groot aantal mensen heb ik niet genoemd (co-auteurs, adviseurs, technici, etc.), ondanks hun onmisbaar aandeel in dit proefschrift. Weet dat ik jullie zeer erkentelijk ben voor de bijdrage geleverd. Ik zal jullie hier persoonlijk voor bedanken.

De laatste woorden van mijn proefschrift hoopte ik te kunnen vangen in een magisch slotakkoord. Doch, net als magie geen rol heeft in de wetenschap, zo is voor Daan Lips geen rol weggelegd als woordkunstenaar. Daarom zal ik het met het volgende motto moeten doen: *hard werken en daarmee compenseren voor deficiënties in aangeboren talenten.*

Daniel J. Lips